An Ecological Study of Hunting Creek

2018

FINAL REPORT

April 30, 2019

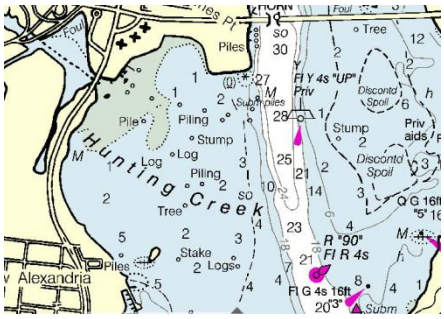

by

R. Christian Jones
Professor, Project Director

Kim de Mutsert
Assistant Professor, Co-Principal Investigator

Benoit Van Aken
Associate Professor, Co-Principal Investigator

Amy Fowler
Assistant Professor, Co-Principal Investigator

Potomac Environmental Research and Education Center
Department of Environmental Science and Policy
Department of Chemistry and Biochemistry
George Mason University

to

Alexandria Renew Enterprises
Alexandria, VA

This page intentionally blank.

Table of Contents

An Ecological Study of Hunting Creek - 2018

Executive Summary

Hunting Creek is an embayment of the tidal Potomac River located just downstream of the City of Alexandria and the I-95/I-495 Woodrow Wilson bridge. This embayment receives treated wastewater from the Alexandria Renew Enterprises wastewater treatment plant and inflow from Cameron Run which drains most of the Cities of Alexandria and Falls Church and much of eastern Fairfax County. The Hunting Creek embayment is bordered on the north by the City of Alexandria and on the west and south by the George Washington Memorial Parkway and associated park land. Due to its tidal nature and shallowness, the embayment does not seasonally stratify vertically, and its water is flushed by rainstorms and may mix readily with the adjacent tidal Potomac River mainstem. Beginning in 2013 the Potomac Environmental Research and Education (PEREC) in collaboration with Alexandria Renew Enterprises (AlexRenew) initiated a program to monitor water quality and biological communities in the Hunting Creek area including stations in the embayment itself, its tributaries, and the adjacent river mainstem. This document presents study findings from 2018 and compares them with that from the previous five years. In addition special studies were continued on anadromous fish usage of Hunting Creek and Cameron Run and *Escherichia coli* levels in Hunting Creek and tributaries. And we completed a second year of benthic macroinvertebrate and water quality sampling on many tributaries of Cameron Run and Hunting Creek.

The Chesapeake Bay, of which the tidal Potomac River is a major subestuary, is the largest and most productive coastal system in the United States. The use of the Bay as a fisheries and recreational resource has been threatened by overenrichment with nutrients which can cause nuisance algal blooms, hypoxia in stratified areas, loss of submersed aquatic vegetation, and declining fisheries. As a major discharger of treated wastewater into Hunting Creek, AlexRenew has been proactive in decreasing nutrient loading since the late 1970's. Also of concern are E. coli and nutrients derived from combined sewer overflows (CSO's) and non point sources within the drainage basin as well as sediments derived from the watershed.

The ecological study reported here provides documentation of the current state of water quality and biological resources in Hunting Creek. The year 2018 was characterized by above normal temperatures from May through September. Precipitation established some new records in 2018 with all months in the study period being above average and May, July and September receiving over twice their annual average rainfall. Flows in the Potomac and in Cameron Run, the major flowing tributary to Hunting Creek, were well over double their long term average on a monthly basis.

Water temperature tracked air temperature on a seasonal basis with little difference among the stations. Specific conductance and chloride were consistently higher at AR1, but showed little seasonal variability. Dissolved oxygen (DO) was generally somewhat below saturation at all stations with little seasonal pattern in percent saturation. Field and lab pH was typically in the 7.3-8.0 range with little seasonal change or pattern. Total

alkalinity exhibited a general upward trend seasonally at most stations dropping back in September.

Water transparency as Secchi depth was generally in the range 0.3-0.8 m. Values were above 0.6 m only during May. These water transparency values were consistently lower than in earlier years and resulted in very poor SAV growth in 2018. Light attenuation coefficient and turbidity followed similar trends and correlation analysis revealed that the three measures of water transparency were indeed correlated.

Ammonia nitrogen followed a seasonal decline at most stations and was consistently low. In contrast to previous years nitrate nitrogen did not follow a seasonal decline, but actually increased seasonally. This can be ascribed to washout and light limitation of both SAV and phytoplankton which normally draw down nitrate as they grow Organic nitrogen values were generally in the range of 0.2-0.6 mg/L and showed a gradual increased from May to September. Total phosphorus responded to storm flows, rising in May and June when flows were high and declining in July. N:P ratio varied greatly through the year, but always remained in a range that was consistent with P limitation of phytoplankton growth. TSS at embayment stations was variable with peaks relating to storm flows. TSS and VSS at AR4, the river station, was quite variable. Significant intercorrelation was observed for TSS, VSS, and total P reflecting the association of P with particles. Total P was also negatively correlated with N:P ratio. Ammonia nitrogen was negatively correlated with pH which may be another product of coincident seasonal changes.

Water quality measurements at tidal stations for 2018 was often different than observed during previous years due to the high flow condition. Specific conductance was markedly lower in 2018 due to the flushing of ions from the frequent storm events. Again, the low DO (percent saturation) and pH values were in a tighter range than normal due to the lack of photosynthesizers like phytoplankton and SAV. Water transparency was markedly different in 2018 due to the input and resuspension of sediments from storms which impeded light penetration and stunted SAV growth. Total P was somewhat higher in 2018 perhaps due to the higher TSS concentrations as P binds to sediments. Nitrate values in 2018 were somewhat higher than in previous years, probably due to lack of uptake in the summer by SAV and phytoplankton.

Water quality was measured in 2018 again at a range of tributary stations. Temperature was quite similar at all stations following a pattern that matched air temperature except at AR13 which was cooler in the summer consistent with underground piped flow. Specific conductance and chloride exhibited a general seasonal decline at all tributary stations. Dissolved oxygen values were generally near saturation at most tributary stations. Exceptions were AR21 that was above saturation and AR23 that was below saturation. Field and lab pH generally remained in the range of 7.0-8.0 in all tributaries. Turbidity was generally quite low in the tributaries except at AR23 which was generally higher. Chlorophyll levels were generally very low except at AR23 which was higher on some dates. AR23 is the one tributary site that is subject to tidal flows and the unusual values of some parameters are probably due to tidal influx of water from the Hunting Creek embayment.

Total alkalinity at the tributary stations were generally in the normal range. Total phosphorus was generally at a low level. Organic nitrogen was low and declined somewhat seasonally except at AR23. Nitrate nitrogen values were consistently elevated at AR13 (Hoffs Run) and AR23 across from the Alex Renew outfall. consistently lower values were found at the other tributary stations. TSS and VSS were generally low except at AR23.

Phytoplankton biomass at the tidal stations was quantified using chlorophyll *a*. Levels were generally quite low (<10 µg/L) due to flushing. Exceptions were significant peaks in mid July and late August, especially at AR2 and AR3. Phytoplankton density (cells/mL) was fairly constant through the year except for a strong peak in late July at both AR2. This peak corresponded to large numbers of cyanobacteria of the genera *Oscillatoria* and *Anabaena*. The lack of correspondence of the chlorophyll peaks and cell density peak is explainable by considering the small size of most cyanobacterial cells. Phytoplankton biovolume (μm^3/mL) is calculated by taking the volumes of individual cells of each species and multiplying by the number of cells per mL for each species giving a size-weighted total. Diatoms, being larger, assumed more importance overall and cyanobacteria, being smaller, assumed a lesser importance. The highest values of phytoplankton biovolume were found in August when discoid centrics and *Melosira* were dominant.

Phytoplankton biomass (as measured by chlorophyll a) continued a gradual decline over the six year monitoring period at all stations. Phytoplankton cell density was in the midrange of previous years as was the levels of each major group of phytoplankters. Median phytoplankton biovolume was the lowest of any year to date at AR4, but relatively high at AR2.

As is typical, the small-bodied rotifers were the most numerous zooplankters, but their dynamics was highly atypical. They were essentially dormant at both stations through the spring and early summer and then increased dramatically to record values on mid-July only to drop back again for the rest of the year. Among the cladocera, all were found at very low levels, presumably due to the effects of storm flushing and turbidity. Copepod nauplii, the immature stage of copepods, showed similar dynamics as the rotifers. They were found at very low levels for most of the year and increased to moderate (not record high) levels in mid-July. The calanoid copepod *Eurytemora affinis*, was also impacted by high flows, but managed two respectable peaks, over 1000/m^3 in early May and mid-July. On the other hand, another calanoid, *Diaptomus pallidus*, was only found in detectable numbers in mid-May at AR2.

Total rotifer density in 2018 was highly reduced on most dates compared to previous years with the record high values showing up as outliers. The individual genera of rotifers tracked all showed a similar pattern. Most of the crustacean zooplankton were also greatly reduced in 2018 as compared to previous years although several had densities similar to 2017. Copepod nauplii were highly reduced in 2018 as compared to previous years, with median values an order of magnitude lower. However, calanoid copepods, notably *Eurytemora* attained values similar to previous years on most dates..

Ichthyoplankton collections were dominated by Gizzard Shad, Blueback Herring, and Alewife, all members of the family Clupeidae. A large number of additional larvae were identifiable to family level as Clupeidae bringing the total of larvae in the family Clupeidae to 88% of all identifiable fish larvae. The rest of the identifiable larvae were mostly *Morone americana*. (White Perch). There were somewhat more larvae collected at AR2 than AR4. White Perch larvae were collected in greater numbers at AR2 and clupeid larvae were collected in large numbers at both stations.

White Perch made up about half of individuals collected by trawling in 2018. Tessellated darter comprised about 16% of the harvest, sunfish about 11%, and Spottail Shiner about 8%. Centrarchids including sunfish and bass comprised about 10%. Total catch via trawling was greatly increased in 2018 over most previous years partially due to the ability to more easily trawl in the absence of SAV. AR3 which is often obstructed by SAV yielded twice as many fish as AR4. Seine sampling was dominated by Banded Killifish which comprised about 52% of the total catch. *Alosa* sp. made up about 25% of the collections and Inland Silverside was about 10% of the seine catch. More fish were seined at AR5 off Jones Point than at AR6 in the Hunting Creek embayment proper. Inland Silverside were almost exclusively collected at AR6 and Banded Killifish were much more common in AR5 samples. A new gear was introduced in 2016 to overcome the drawbacks of trawling in dense SAV, the fyke net. The fyke net is a passive gear that can be deployed in shallow water. The net is static; the natural movement of the fish funnel individuals into the gear and they are generally well retained. This gear was deployed semimonthly starting in May at two locations near trawl site AR3. Catches were limited in 2018 compared to 2016 and 2017.

VIMS was not able to conduct their aerial survey in 2018, but surveys that were made by GMU personnel indicated that SAV was greatly reduced in 2018 compared with previous years. This is most certainly attributable to the very turbid water in 2018 which obstructed light penetration.

Benthic invertebrate data from the tidal stations in 2018 indicated that the river station AR4 had the highest diversity and most samples from that station were distinctly different from the other two stations when compared by multivariate analysis. Annual aggregate taxa richness was 26 at AR4 and only 8 at AR2 and 11 at AR3. The low richness at AR2 and AR3 was at least partially due to the scarcity of SAV which enhances habitat. Oligochaetes, amphipods, and were the most abundant organisms at the tidal benthic stations. Total abundance was somewhat lower than in previous years of the study.

In 2016 a benthic macroinvertebrate sampling program was implemented for the flowing tributary streams starting with six stations. In 2018 two more stations were added with sampling continuing annually in November. Flatworms, chironomids, oligochaetes, baetid mayflies, and philopatamid and hydropsychid caddisflies were the dominant taxa, all of which are taxa tolerant of pollution indicating that the tributaries have been degraded by the impacts of urban development, mostly stormwater pulses and nonpoint pollution. Application of an index of biotic integrity indicated that all streams were categorized as “poor”, but some were approaching “fair”. However, the values of some

individual meterics were “good” indicating that conditions may be improving. The values observed were typical of streams draining urban areas.

Anadromous fish sampling was conducted on a weekly basis from March 30 to May 4 in 2018 at a station just above the head of tide on Cameron Run. Hoop nets were deployed for a 24 hour period each week to collect spawning fish moving upstream and ichthyoplankton nets were deployed to collect fish larvae drifting downstream. Seventy-five individual fish were collected in the hoop nets in 2018. Forty-five of these were 14 adult Alewife, substantial improvement over 2017 and the greatest annual catch to date. A record number of Alewife larvae were also collected in the plankton nets set in the creek. Larvae of several other fish were also collected. Extrapolation from the sample collected to the total period of spawning yielded an estimate 315 adult Alewife spawning in Cameron Run in 2018.

E. coli sampling was expanded to a total of 12 stations in 2016, adding four additional tributary stations as part of the semimonthly sampling program. However, during the 2017 and 2018 field seasons, two of the stations, AR22 and AR11, became inaccessible due to construction. The data continue to support a conclusion that the entire area sampled, including the mainstem of the Potomac River (AR4), is impaired for the bacteriological water quality criterion (*E. coli*) content under Section 9VAC25-260-170 of the Virginia Water Quality Standards that applies to primary contact recreational use surface waters. Although our data showed an increase of the *E. coli* abundance and percent exceedance of the 235 criterion from 2014 to 2016, these numbers seemed to have peaked in 2016 – 2017 and even showed a slight decrease in 2018. It is noteworthy that the large geographical and temporal variability that we observed during the sampling events prevent to draw clear conclusion on the trend of water quality impairment. Finally, the highest counts in 2018 were observed in April and September (the highest counts in 2017 were observed in June and July), revealing no clear seasonal trend in the data. High counts were shown to reflect rainfall data instead of a seasonal trend.

We recommend that:

1. The basic ecosystem monitoring should continue. A range of climatic conditions is needed to effectively establish baseline conditions in Hunting Creek. Interannual, seasonal and spatial patterns are starting to appear, but need validation with future years’s data. With record rainfall and runoff, 2018 provided a glimpse of the vulnerability of the system to flushing and sediment related effects. Continued monitoring will allow us to assess the resiliency of the ecosystem; i.e., how quickly will it recovery from a very wet year.
2. Water quality mapping should be continued. This provides much needed spatial resolution of water quality patterns as well as allowing mapping of SAV distributions.
3. Fyke nets have proven to be a useful new gear to enhance fish collections and should be continued.
4. Anadromous fish sampling is an important part of this monitoring program and has gained interest now that the stock of river herring has collapsed generally, and a moratorium on these taxa has been established in 2012. The discovery and continue presence of river herring spawning in Cameron Run increases the importance of continuing studies of anadromous fish in the study area.

5. We recommend continuing the more intensive *E. coli* sampling plan which seems to be giving better insight into the dynamics of *E. coli* in the study area.
6. We recommend continuing macroinvertebrate studies the tributaries of Hunting Creek to further ascertain overall aquatic biota health and that tidal benthos sampling should continue and the data should be more thoroughly examined.

List of Abbreviations

BOD	Biochemical oxygen demand
cfs	cubic feet per second
DO	Dissolved oxygen
ha	hectare
l	liter
LOWESS	locally weighted sum of squares trend line
m	meter
mg	milligram
MGD	Million gallons per day
NS	not statistically significant
NTU	Nephelometric turbidity units
SAV	Submersed aquatic vegetation
SRP	Soluble reactive phosphorus
TP	Total phosphorus
TSS	Total suspended solids
um	micrometer
VSS	Volatile suspended solids
#	number

This page intentionally left blank.

The Aquatic Monitoring Program for the Hunting Creek Area of the Tidal Freshwater Potomac River 2018

FINAL REPORT
April 30, 2019

by

R. Christian Jones
Professor, Department of Environmental Science and Policy
Director, Potomac Environmental Research and Education Center
George Mason University
Project Director

Kim de Mutsert
Assistant Professor, Department of Environmental Science and Policy
George Mason University
Co-Principal Investigator

Amy Fowler
Assistant Professor, Department of Environmental Science and Policy
George Mason University
Co-Principal Investigator

to

Alexandria Renew Enterprises
Alexandria, VA

ACKNOWLEDGEMENTS

The authors wish to thank the numerous individuals and organizations whose cooperation, hard work, and encouragement have made this project successful. We wish to thank the Alexandria Renew Enterprises especially CEO Karen Pallansch for her vision in initiating the study and to Aster Tekle for her advice and asssitance during the study.

Without a dedicated group of field and laboratory workers this project would not have been possible. Thanks go to Laura Birsa for managing water quality/plankton/benthos field trips and to field/lab workers Kristen Reck, Chelsea Gray, Morgan Collier, Tabitha King, Julia Czarnecki, Michael Cagle, and Steven Chan.

Special thanks go to C.J. Schlick who has put together the figures and tables of the fish section of the report, and to Joris van der Ham, who has operated as the field manager of the fish collections. Others that have helped in the field and in the laboratory to collect and process all fish samples include CJ Schlick, Beverly Bachmann, Sammie Alexander, Jessie Melton, Rachel Kelmartin, Chris Bodner, Tanya Ramseyer, Chris Martin, and Brian Kim.

Claire Buchanan served as a voluntary consultant on plankton identification. Honey Williams and Lisa Bair were vital in handling personnel and procurement functions.

INTRODUCTION

This section reports the results of the sixth year of an aquatic monitoring program conducted for Alexandria Renew Enterprises by the Potomac Environmental Research and Education Center (PEREC) in the College of Science at George Mason University. Two other sections of the report include an anadromous fish study of Cameron Run and a survey of *Escherichia coli* levels in the Hunting Creek area of the tidal Potomac River.

This work was in response to a request from Karen Pallansch, Chief Executive Officer of Alexandria Renew Enterprises (Alex Renew), operator of the wastewater reclamation and reuse facility (WRRF) which serves about 350,000 people in the City of Alexandria and the County of Fairfax in northern Virginia. The study is patterned on the long-running Gunston Cove Study which PEREC has been conducting in partnership with the Fairfax County Department of Public Works and Environmental Services since 1984. The goal of these projects is to provide baseline data and on-going trend analysis of the ecosystems receiving reclaimed water from wastewater treatment facilities with the objective of adaptive management of these valuable freshwater resources. This will facilitate the formulation of well-grounded management strategies for maintenance and improvement of water quality and biotic resources in the tidal Potomac. A secondary but important educational goal is to provide training for Mason graduate and undergraduate students in water quality and biological monitoring and assessment.

Setting of Hunting Creek

Hunting Creek is an embayment of the tidal Potomac River located just downstream of the City of Alexandria and the Woodrow Wilson Bridge. Waters are shallow with the entire embayment having a depth of 2 m or less at mean tide. According to the "Environmental Atlas of the Potomac Estuary" (Lippson et al. 1981), the mean depth of Hunting Creek is 1.0 m, the surface area is 2.26 km^2, and the volume of 2.1 x 10^6 m^3.

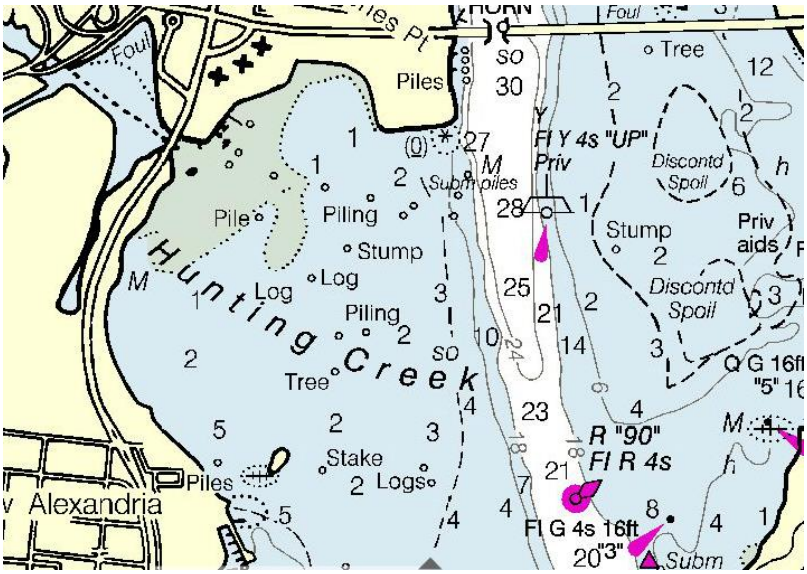

On the left is the Hunting Creek embayment. The Woodrow Wilson Bridge spans the tidal Potomac River at the top of the map. The Potomac River main channel is the whitish area running from north to south through the middle of the map. Soundings (numbers on the map) are in feet at mean low water. For the purposes of this report "Hunting Creek" will extend to the head of tide, roughly to Telegraph Rd.

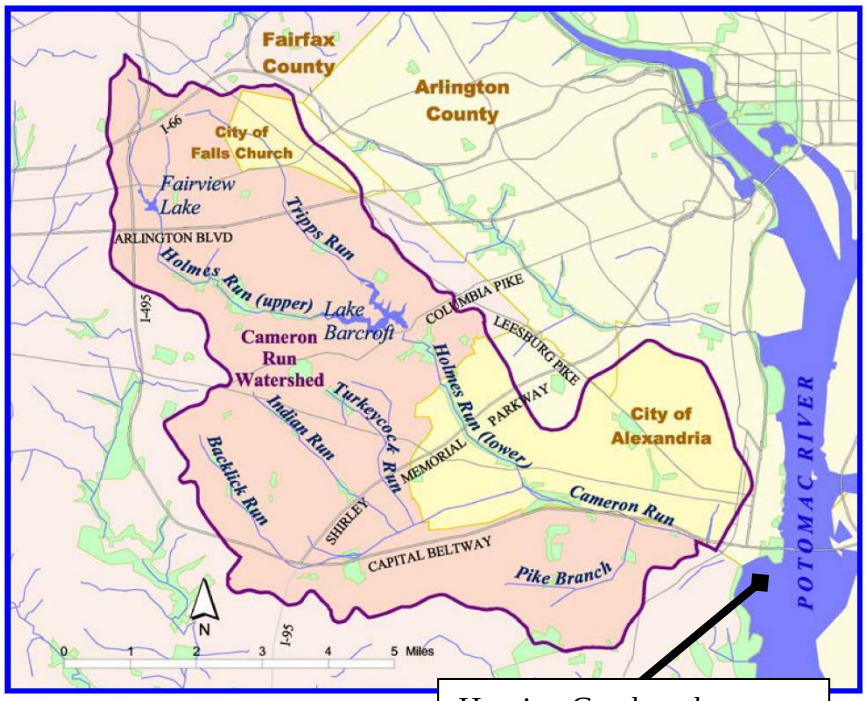

Hunting Creek embayment

On the left is a map of the Hunting Creek watershed. Cameron Run is the freshwater stream which drains the vast majority of the watershed of Hunting Creek. The watershed is predominantly suburban in nature with areas of higher density commercial and residential development. The watershed has an area of 44 square miles and drains most of the Cities of Alexandria and Falls Church and much of east central Fairfax County. A major aquatic feature of the watershed is Lake Barcroft. The suburban land uses in the watershed are a source of nonpoint pollution to Hunting Creek.

The Alex Renew WRRF serves an area similar in extent to the Cameron Run watershed with the addition of some areas along the Potomac shoreline from Four Mile Run to Dyke Marsh. The effluent of the Alexandria Renew Enterprises plant enters the upper tidal reach of Hunting Creek under the Rt 1/I-95 interchange.

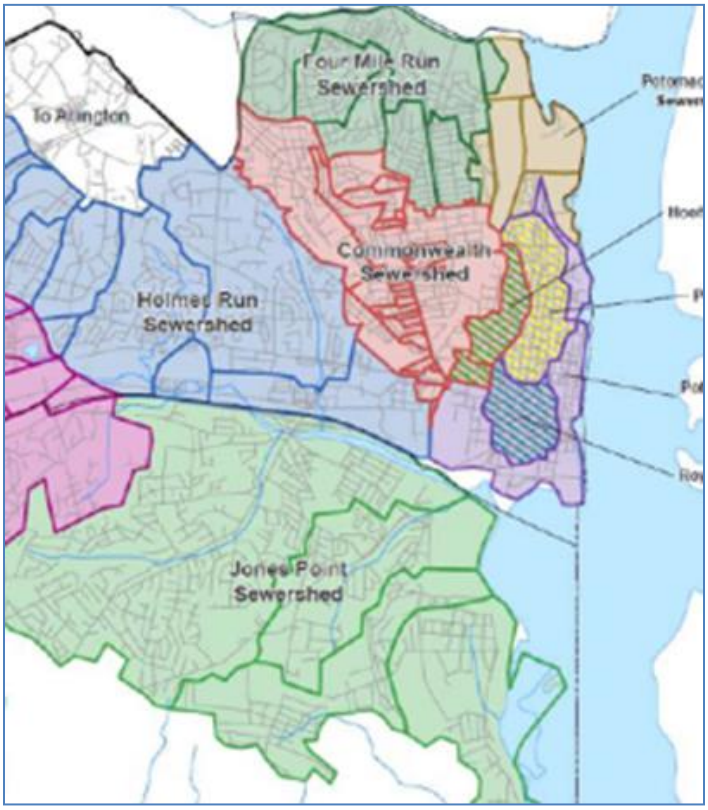

The map at the left shows the sewersheds which contribute to the AlexRenew WRRF. Of particular note are the shaded areas within the City of Alexandria. These sewersheds (Hooff Run, Pendleton, and Royal St.) all contain combined sewers meaning that domestic wastewater is co-mingled with street runoff. Under most conditions, all of this water is directed to the AlexRenew WRRF for treatment. But in extreme runoff conditions (like torrential rains), some may be diverted directly into the tidal Potomac via a Combined Sewer outfall (CSO).

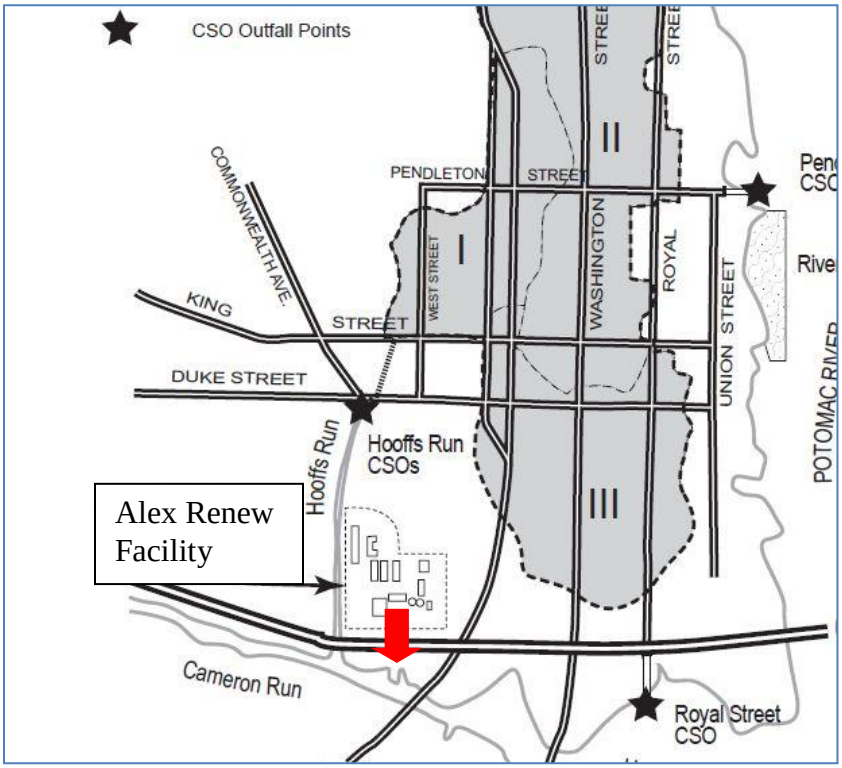

The map at the left is an enlargement of the area where the Alex Renew WRRF is found and where the discharge sites of the CSO's are located. Note the close proximity of two of the CSO's to the Alex Renew WRRF discharge (shown as red arrow).

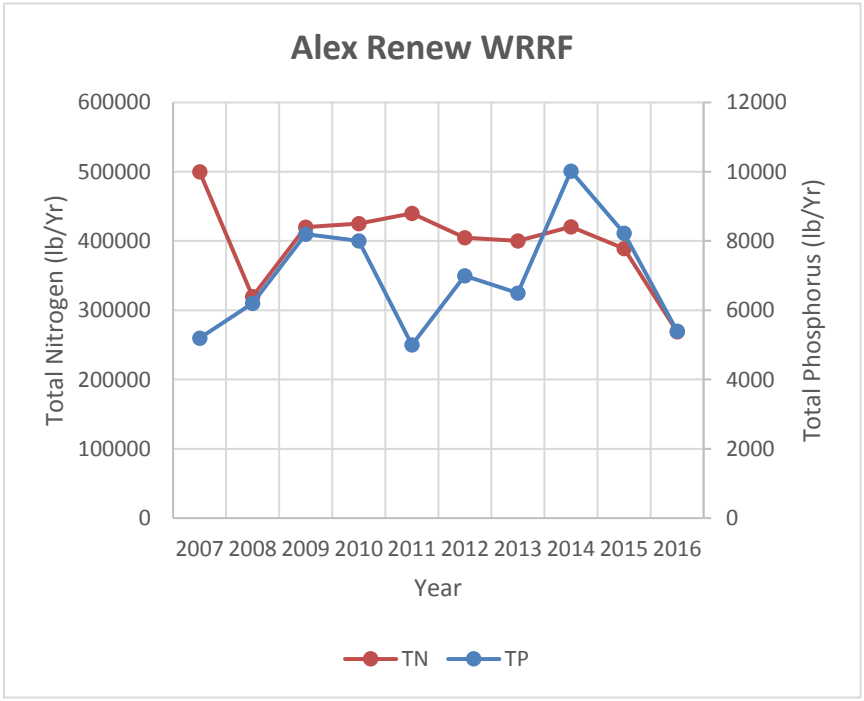

The graph at the left shows the loading of nitrogen and phosphorus from the Alexandria Renew WRRF for the last seven years. Loadings of both nutrient elements were among the lowest in the last decade in 2016: 269,000 lb/yr for nitrogen and 5,400 lb/yr for phosphorus.

Ecology of the Freshwater Tidal Potomac

The tidal Potomac River is an integral part of the Chesapeake Bay tidal system and at its mouth the Potomac is contiguous to the bay proper. The tidal Potomac is often called a subestuary of the Chesapeake Bay and as such it is the largest subestuary of the bay in terms of size and amount of freshwater input. The mixing of freshwater with saltwater is the hallmark of an estuary. While the water elevation in an estuary is "sea level", the water contained in an estuary is not pure sea water such as found in the open ocean. Pure ocean sea water has a salt concentration of about 35 parts per thousand by weight (ppt). Water in Chesapeake Bay ranges from about 30 ppt near its mouth to 0 ppt in the upper reaches where there is substantial freshwater inflow such as in the upper tidal Potomac River. Salinity at a given location is determined by the balance between freshwater input and salt water mixing in from the ocean. It generally varies with season being lower in spring when freshwater inflows are greater and higher in summer when there is less freshwater inflow. In the Hunting Creek study area, the salinity is essentially 0 yearround.

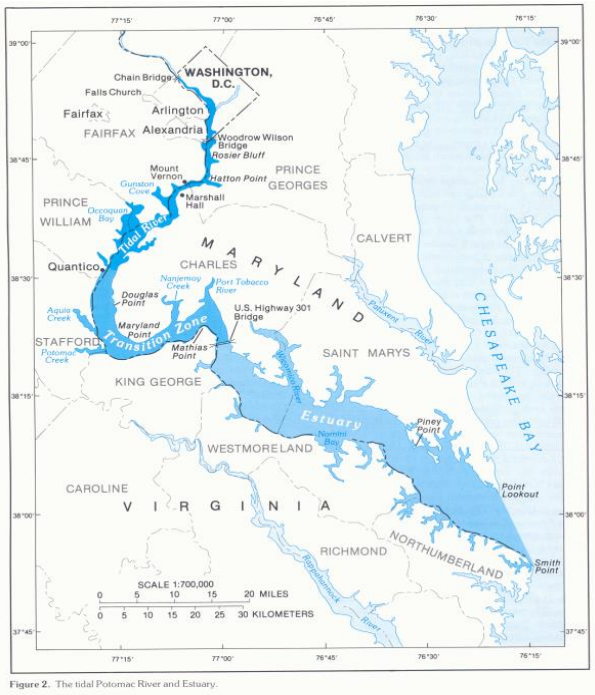

Figure 2. The tidal Potomac River and Estuary.

(map courtesy USGS)

The tidal Potomac is generally divided into three salinity zones as indicated by the map to the left:
-Estuarine or Mesohaline zone (6-14 ppt)
-Transition or Oligohaline zone (0.5-6 ppt)
-Tidal River or Tidal Fresh zone (<0.5 ppt)
Hunting Creek is in the upper part of the Tidal River/Tidal Fresh zone and as such it never experiences detectable salinity

Within the tidal freshwater zone, the flora and fauna are generally characterized by the same species that would occur in a freshwater lake in this area and the food web is similar. Primary producers are freshwater species of submersed aquatic vegetation (SAV) such as native taxa *Vallisneria americana* (water celery), *Potomogeton* spp, (pondweeds), and *Ceratophyllum* (coontail) as well as introduced species such as *Hydrilla verticallata* (hydrilla) and *Myriophyllum spicatum* (water milfoil). Historical accounts indicate that most of the shallow areas of the tidal freshwater Potomac were colonized by SAV when observations were made around 1900 (Carter et al. 1985).

The other group of important primary producers are phytoplankton, a mixed assemblage

of algae and cyanobacteria which may turn over rapidly on a seasonal basis. The dominant groups of phytoplankton in the tidal freshwater Potomac are diatoms (considered a good food source for aquatic consumers) and cyanobacteria (considered a less desirable food source for aquatic consumers). For the latter part of the 20th century, the high nutrient loadings into the river favored cyanobacteria over both diatoms and SAV resulting in large production of undesirable food for consumers. In the last decade or so, as nutrient reductions have become manifest, cyanobacteria have decreased and diatoms and SAV have increased.

The biomass contained in the cells of phytoplankton nourishes the growth of zooplankton and benthic macroinvertebrates which provide an essential food supply for the juvenile and smaller fish. These in turn provide food for the larger fish like striped bass and largemouth bass. The species of zooplankton and benthos found in the tidal fresh zone are similar to those found in lakes in the area, but the fish fauna is augmented by species that migrate in and out from the open interface with the estuary.

Resident fish species include typical lake species such as sunfish (*Lepomis* spp.), bass (*Micropterus* spp.), and crappie (*Pomoxis* spp.) as well as estuarine species such as white perch (*Morone americana*) and killifish (*Fundulus* spp.). Species which spend part of their year in the area include striped bass (*Morone saxitilis*) and river herrings and shad (*Alosa* spp.). Non-native fish species have also become established in the tidal freshwater Potomac such as northern snakehead (*Channa argus*) and blue catfish (*Ictalurus furcatus*).

Larval fishes are transitional stages in the development of juvenile fishes. They range in development from newly hatched, embryonic fish to juvenile fish with morphological features similar to those of an adult. Many fishes such as clupeids (herring family), white perch, striped bass, and yellow perch disperse their eggs and sperm into the open water. The larvae of these species are carried with the current and termed “ichthyoplankton”. Other fish species such as sunfish and bass lay their eggs in “nests” on the bottom and their larvae are rare in the plankton.

After hatching from the egg, the larva draws nutrition from a yolk sack for a few days. When the yolk sack diminishes to nothing, the fish begins a life of feeding on other organisms. This post yolk sack larva feeds on small planktonic organisms (mostly small zooplankton) for a period of several days. It continues to be a fragile, almost transparent larva and suffers high mortality to predatory zooplankton and juvenile and adult fishes of many species, including its own. When it has fed enough, it changes into an opaque juvenile, with greatly enhanced swimming ability. It can no longer be caught with a slow-moving plankton net, but is soon susceptible to capture with the seine or trawl net.

METHODS

A. Profiles and Plankton: Sampling Day

Sampling was conducted on a semimonthly basis at stations representing both Hunting Creek and the Potomac mainstem (Figure 1a). One station (AR 1) was located near the mouth of Cameron Run at the George Washington Parkway bridge. Two stations (AR 2 & 3) were located in the Hunting Creek embayment proper. A fourth station was located in the river channel about 100 m upstream from Buoy 90. Dates for sampling as well as weather conditions on sampling dates and immediately preceding days are shown in Table 1. Note that certain dates such as April 28, June 23, and August 22 had significant rainfall in days preceding sampling which may have impacted conditions in Hunting Creek due to it shallow nature and relatively large watershed contributing runoff.

Figure 1a. Hunting Creek area of the Tidal Potomac River showing water quality, plankton, and benthos sampling stations. AR1, AR2, AR3, AR4, AR22, AR23 represent water quality stations, AR2 and AR4 are the phytoplankton and zooplankton stations and AR2, AR3, and AR4 are benthos stations. Red bar is 0.5 km.

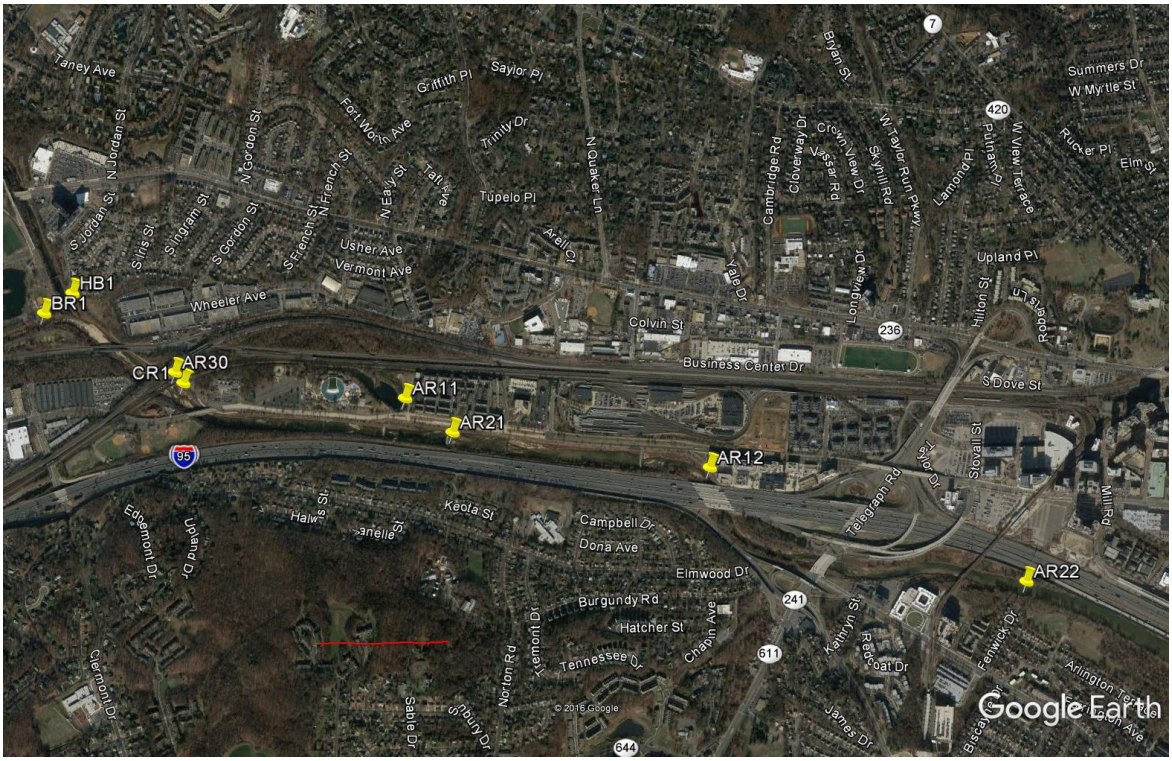

Figure 1b. Cameron Run portion of the study area showing water quality stations.

Figure 1c. Hunting Creek area of the Tidal Potomac River showing fish monitoring stations.

Table 1
Hunting Creek Study: Sampling Dates and Weather Data for 2018

	Type of Sampling						Avg Daily Temp (°C)		Precipitation (cm)	
Date	WP	B	D	T	S	F	1-Day	3-Day	1-Day	3-Day
April 18	X						9.4	9.6	0	4.78
April 24				X	X	X	15.0	15.0	1.17	1.17
May 2	X	X					23.3	18.7	0	0
May 15				X	X	X	25.6	22.6	1.04	6.05
May 16	X						21.7	23.1	2.08	6.91
May 29				X	X	X	24.4	23.1	0	0.04
May 31	X						25.6	24.8	3.35	3.37
June 12				X	X	X	20.6	20.4	0	1.08
June 14	X	X					26.7	24.1	T	0.03
June 26				X	X	X	23.9	25.6	0	0.28
June 28	X	X					27.8	25.6	0	0.01
July 12	X	X					28.3	29.1	0	0
July 16			X				30.6	28.3	0.01	0.03
July 17				X	X	X	28.3	28.7	7.09	7.11
July 31	X			X	X	X	25.6	25/2	0.08	1.37
August 15	X	X					27.8	26.7	0	0.01
August 20				X	X	X	25.0	26.7	T	T
August 28			X				30.0	28.0	0	0
August 30	X						30.0	30.2	0.04	0.10
August 31				X	X	X	28.3	29.7	0.76	0.86
Sept 13	X	X					25.6	25.0	T	0.05
Sept 28				X	X	X	20.6	22.0	0.79	2.77

Type of Sampling: WP: Water quality (samples to AlexRenew Lab), profiles and plankton, B: benthos (station numbers indicated), D: dataflow (water quality mapping), T: fish collected by trawling, S: fish collected by seining. F: fish collected by fyke net. T under Precipitation equals "trace". X indicates full station suite on that date.

Sampling was initiated about 10:00 am. Four types of measurements or samples were obtained at each station: (1) depth profiles of temperature, conductivity, dissolved oxygen, pH, and irradiance (photosynthetically active radiation, PAR) measured directly in the field; (2) water samples for GMU lab determination of chlorophyll *a* and phytoplankton species composition and abundance; (3) water samples for determination of N and P forms, BOD, COD, alkalinity, hardness, suspended solids, chloride, and pH by the Alexandria Renew Enterprises lab; (4) net sampling of zooplankton and ichthyoplankton.

Profiles of temperature, conductivity, and dissolved oxygen were conducted at each station using a YSI 6600 datasonde with temperature, conductivity, dissolved oxygen and pH probes. Measurements were taken at 0.3 m increments from surface to bottom at the embayment stations. In the river measurements were made with the sonde at depths of 0.3 m and 2.0 m increments to the bottom. Meters were checked for calibration before and after sampling. Profiles of irradiance (photosynthetically active radiation, PAR) were collected with a LI-COR underwater flat scalar PAR probe. PAR measurements were taken at 10 cm intervals to a depth of 1.0 m. Simultaneous measurements were made with a terrestrial probe in air during each profile to correct for changes in ambient light if needed. Secchi depth was also determined. The readings of at least two crew members were averaged due to variability in eye sensitivity among individuals. If the Secchi disk was still visible at the bottom or if its path was block by SAV while still visible, a proper reading could not be obtained.

A 1-liter depth-composited sample for GMU lab work was constructed from equal volumes of water collected at each of three depths (0.3 m below the surface, middepth, and 0.3 m off of the bottom) using a submersible bilge pump. A 100-mL aliquot of this sample was preserved immediately with acid Lugol's iodine for later identification and enumeration of phytoplankton at stations AR2 and AR4. The remainder of the sample was placed in an insulated cooler with ice. A separate 1-liter surface sample was collected from 0.3 m using the submersible bilge pump and placed in the insulated cooler with ice for lab analysis of surface chlorophyll *a*.

At embayment and river mainstream sampling stations (AR2, AR3, and AR4), 2-liter samples were collected monthly at each station from just below the surface (0.3 m) and near the bottom (0.3 m off bottom) at each station using the submersible pump. At tributary stations (AR1, AR 10, AR11, AR12, AR13, AR21, AR22, AR23, and AR30), 2-liter samples were collected by hand from just below the surface. This water was promptly delivered to the nearby Alexandria Renew Laboratory for determination of nitrogen, phosphorus, BOD, TSS, VSS, pH, total alkalinity, and chloride.

At stations AR2 and AR4, microzooplankton was collected by pumping 32 liters from each of three depths (0.3 m, middepth, and 0.3 m off the bottom) through a 44 μm mesh sieve. The sieve consisted of a 12-inch long cylinder of 6-inch diameter PVC pipe with a piece of 44 μm nitex net glued to one end. The 44 μm cloth was backed by a larger mesh cloth to protect it. The pumped water was passed through this sieve from each depth and then the collected microzooplankton was backflushed into the sample bottle. The resulting sample was treated with about 50 mL of club soda and then preserved with formalin containing a small amount of rose bengal to a concentration of 5-10%.

At stations AR2 and AR4, macrozooplankton was collected by towing a 202 µm net (0.3 m opening, 2 m long) for 1 minute at each of three depths (near surface, middepth, and near bottom). Ichthyoplankton (larval fish) was sampled by towing a 333 µm net (0.5 m opening, 2 m long) for 2 minutes at each of the same depths at Stations AR2 and AR4. In the embayment, the boat traveled from AR2 toward AR3 during the tow while in the river the net was towed in a linear fashion along the channel. Macrozooplankton tows were about 300 m and ichthyoplankton tows about 600 m. Actual distance depended on specific wind conditions and tidal current intensity and direction, but an attempt was made to maintain a constant slow forward speed (approximately 2 miles per hour) through the water during the tow. The net was not towed directly in the wake of the engine. A General Oceanics flowmeter, fitted into the mouth of each net, was used to establish the exact towing distance. During towing the three depths were attained by playing out rope equivalent to about 1.5-2 times the desired depth. Samples which had obviously scraped bottom were discarded and the tow was repeated. Flowmeter readings taken before and after towing allowed precise determination of the distance towed and when multiplied by the area of the opening produced the total volume of water filtered.

Macrozooplankton were preserved immediately with rose bengal formalin with club soda pretreatment. Ichthyoplankton was preserved in 70% ethanol. Macrozooplankton was collected on each sampling trip; ichthyoplankton collections ended after July because larval fish were normally not found after this time.

Benthic macroinvertebrate samples were collected monthly at stations AR2, AR3, and AR4. Three samples were collected at each station using a petite ponar grab. The bottom material was sieved through a 0.5 mm stainless steel sieve and resulting organisms were preserved in rose bengal formalin for lab analysis.

Samples for water quality determination were maintained on ice and delivered to the Alexandria Renew Enterprises (AlexRenew) Laboratory by 2 pm on sampling day and returned to GMU by 3 pm. At GMU 10-15 mL aliquots of both depth-integrated and surface samples were filtered through 0.45 µm membrane filters (Gelman GN-6 and Millipore MF HAWP) at a vacuum of less than 10 lbs/in^2 for chlorophyll a and pheopigment determination. During the final phases of filtration, 0.1 mL of $MgCO_3$ suspension (1 g/100 mL water) was added to the filter to prevent premature acidification. Filters were stored in 20 mL plastic scintillation vials in the lab freezer for later analysis. Seston dry weight and seston organic weight were measured by filtering 200-400 mL of depth-integrated sample through a pretared glass fiber filter (Whatman 984AH).

Sampling day activities were normally completed by 5:30 pm.

B. Profiles and Plankton: Follow-up Analyses

Chlorophyll *a* samples were extracted in a ground glass tissue grinder to which 4 mL of dimethyl sulfoxide (DMSO) was added. The filter disintegrated in the DMSO and was ground for about 1 minute by rotating the grinder under moderate hand pressure. The ground suspension was transferred back to its scintillation vial by rinsing with 90% acetone. Ground samples were stored in the refrigerator overnight. Samples were removed from the refrigerator and centrifuged

for 5 minutes to remove residual particulates.

Chlorophyll *a* concentration in the extracts was determined fluorometrically using a Turner Designs Model 10 field fluorometer configured for chlorophyll analysis as specified by the manufacturer. The instrument was calibrated using standards obtained from Turner Designs. Fluorescence was determined before and after acidification with 2 drops of 10% HCl. Chlorophyll *a* was calculated from the following equation which corrects for pheophytin interference:

$$\text{Chlorophyll } a\ (\mu g/L) = F_s R_s (R_b - R_a)/(R_s - 1)$$

where F_s=concentration per unit fluorescence for pure chlorophyll *a*
R_s=fluorescence before acid/fluorescence after acid for pure chlorophyll *a*
R_b=fluorescence of sample before acid
R_a=fluorescence of sample after acid

All chlorophyll analyses were completed within one month of sample collection.

Phytoplankton species composition and abundance was determined using the inverted microscope-settling chamber technique (Lund et al. 1958). Ten milliters of well-mixed algal sample were added to a settling chamber and allowed to stand for several hours. The chamber was then placed on an inverted microscope and random fields were enumerated. At least two hundred cells were identified to species and enumerated on each slide. Counts were converted to number per mL by dividing number counted by the volume counted. Biovolume of individual cells of each species was determined by measuring dimensions microscopically and applying volume formulae for appropriate solid shapes.

Microzooplankton and macrozooplankton samples were rinsed by sieving a well-mixed subsample of known volume and resuspending it in tap water. This allowed subsample volume to be adjusted to obtain an appropriate number of organisms for counting and for formalin preservative to be purged to avoid fume inhalation during counting. One mL subsamples were placed in a Sedgewick-Rafter counting cell and whole slides were analyzed until at least 200 animals had been identified and enumerated. A minimum of two slides was examined for each sample. References for identification were: Ward and Whipple (1959), Pennak (1978), and Rutner-Kolisko (1974). Zooplankton counts were converted to number per liter (microzooplankton) or per cubic meter (macrozooplankton) with the following formula:

$$\text{Zooplankton } (\#/L \text{ or } \#/m^3) = NV_s/(V_c V_f)$$

where N = number of individuals counted
V_s = volume of reconstituted sample, (mL)
V_c = volume of reconstituted sample counted, (mL)
V_f = volume of water sieved, (L or m^3)

Larval fish were picked from the ethanol-preserved ichthyoplankton samples with the aid of a stereo dissecting microscope. Identification of ichthyoplankton was made to family and further to genus and species where possible. If the number of animals in the sample exceeded

several hundred, then the sample was split with a plankton splitter and the resulting counts were multiplied by the subsampling factor. The works Hogue et al. (1976), Jones et al. (1978), Lippson and Moran (1974), and Mansueti and Hardy (1967) were used for identification. The number of ichthyoplankton in each sample was expressed as number per 10 m^3 using the following formula:

Ichthyoplankton (#/10m^3) = 10N/V
where N = number ichthyoplankton in the sample
V = volume of water filtered, (m^3)

C. Adult and Juvenile Fish

Fishes were sampled by trawling at stations AR3 and AR4, and seining at stations AR5 and AR6 (Figure 1). For trawling, a try-net bottom trawl with a 15-foot horizontal opening, a ¾ inch square body mesh and a ¼ inch square cod end mesh was used. The otter boards were 12 inches by 24 inches. Towing speed was 2-3 miles per hour and tow length was 5 minutes. The trawls were towed upriver parallel to the channel at AR4, and following the curve away from the channel at AR3. The direction of tow should not be crucial. Dates of sampling and weather conditions are found in Table 1.

Seining was performed with a bag seine that was 50 feet long, 3 feet high, and made of knotted nylon with a ¼ inch square mesh. The bag is located in the middle of the net and measures 3 ft^3. The seining procedure was standardized as much as possible. The net was stretched out perpendicular to the shore with the shore end right at the water line. The net was then pulled parallel to the shore for a distance of 100 feet by a worker at each end moving at a slow walk. Actual distance was recorded if in any circumstance it was lower than 100 feet. At the end of the prescribed distance, the offshore end of the net was swung in an arc to the shore and the net pulled up on the beach to trap the fish. Dates for seine sampling were the same as those for trawl sampling (Table 1).

Due to extensive submerged aquatic vegetation (SAV) cover in Hunting Creek, we adjusted our sampling regime in 2016. The trawl at AR3 has been impeded more frequently each year due to this vegetation, and two fyke nets were set in the area close to AR3 (Figure 1). The fyke net sampling stations are called ‘fyke near’ and ‘fyke far’ in reference to their distance from shore. These fyke nets were set within the SAV to sample the fish community that uses the SAV cover as habitat. Fyke nets were set for 4 hours to passively collect fish. The fyke nets have 5 hoops, a 1/4 inch mesh size, 16 feet wings and a 32 feet lead. Fish enter the net by actively swimming and/or due to tidal motion of the water. The lead increases catch by capturing the fish swimming parallel to the wings. Fyke nets were set each sampling date, and trawling in this location (AR3) became impossible by mid-July (Table 1). Utilizing the fyke nets when trawling is still possible allows for gear comparison.

After the catch from each of these three gear types was hauled in, the fishes were measured for standard length and total length to the nearest mm. Standard length is the distance from the front tip of the snout to the end of the vertebral column and base of the caudal fin. This is evident in a crease perpendicular to the axis of the body when the caudal fin is pulled to the

side. Total length is the distance from the tip of the snout to the tip of the longer lobe of the caudal fin, measured by straightening the longer lobe toward the midline.

If the identification of the fish was not certain in the field, a specimen was preserved in 70% ethanol and identified later in the lab. Fishes kept for chemical analysis were kept on ice wrapped in aluminum foil until frozen in the lab. All fishes retained for laboratory analysis or identification were first euthanized by submerging them in an ice sludge conforming to the AICUC protocol. Identification was based on characteristics in dichotomous keys found in several books and articles, including Jenkins and Burkhead (1983), Hildebrand and Schroeder (1928), Loos et al (1972), Dahlberg (1975), Scott and Crossman (1973), Bigelow and Schroeder (1953), Eddy and Underhill (1978), Page and Burr (1998), and Douglass (1999).

D. Submersed Aquatic Vegetation

Data on coverage and composition of submersed aquatic vegetation (SAV) are generally obtained from the SAV webpage of the Virginia Institute of Marine Science (http://www.vims.edu/bio/sav). Information on this web site is obtained from aerial photographs near the time of peak SAV abundance as well as ground surveys which are used to determine species composition. We also recorded SAV relative abundance on a 0-3 scale at 4 minute intervals using visual observations and rake tow during data mapping cruises.

E. Benthic Macroinvertebrates

Benthic macroinvertebrates were sampled monthly using a petite ponar sampler at embayment stations AR2, AR3, and AR4. Triplicate samples were collected at each station monthly. Bottom samples were sieved on-site through a 0.5 mm stainless steel sieve and preserved with rose bengal formalin. In the laboratory benthic samples were rinsed with tap water through a 0.5 mm sieve to remove formalin preservative and resuspended in tap water. All organisms were picked, sorted, identified and enumerated.

In 2018 for the third year, benthic invertebrates were also sampled at selected flowing tributary stations which possessed natural riffle-run areas. At each site one-minute kick samples were collected at one riffle and one run and composited in a single bottle. The sample was preserved with formalin to a concentration of 5%. In the lab the sample was sieved through a 0.5 mm mesh (same as the kick net) and thoroughly washed with tap water before picking and sorting. Following sorting animals were enumerated by taxon and held in ethanol-glycerin. Sampling sites for tributary macroinvertebrate sampling are shown in Figure 1d. Two additional sites, not shown in Figure 1d, were added in 2018: Taylor Run and Timber Branch.

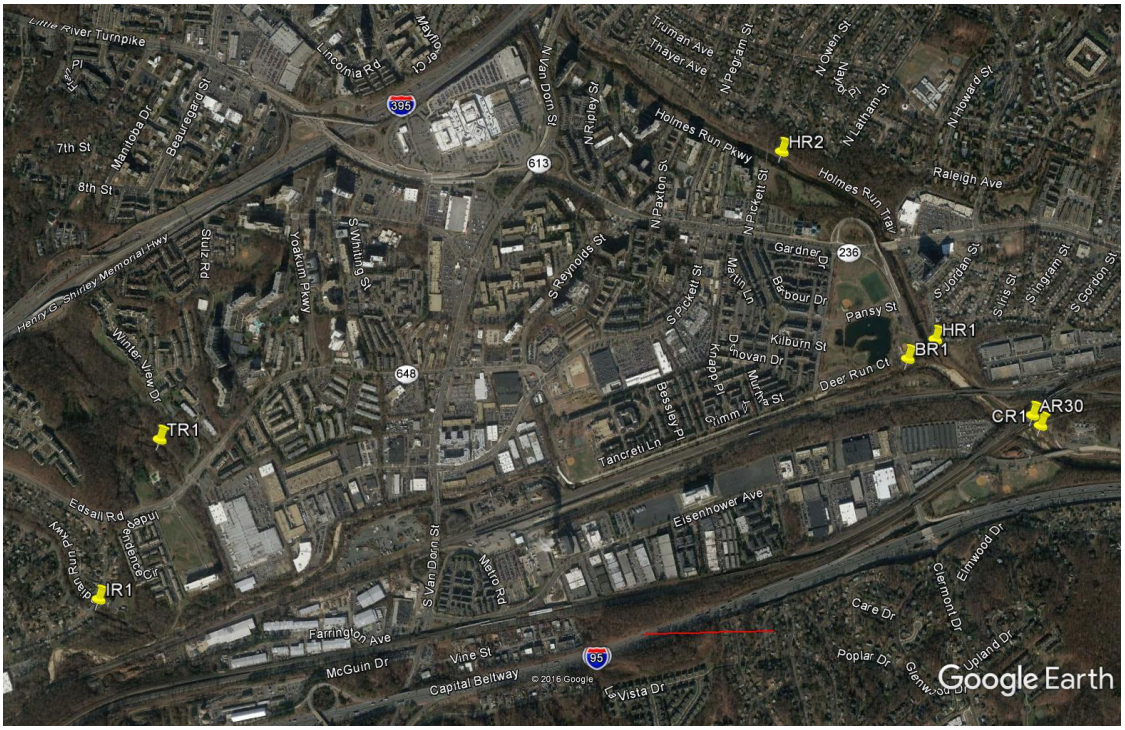

Figure 1d. Western portion of the study area showing benthic sampling stations on flowing tributaries of Cameron Run. CR1: Cameron Run: HR1, HR2: Holmes Run; BR: Backlick Run; IR: Indian Run; TR: Turkeycock Run. Red bar is 0.5 km.

F. Water Quality Mapping (Dataflow)

On two additional dates in 2018 (July 16 and August 28) *in situ* water quality mapping was conducted by slowly transiting through much of the Hunting Creek study area as water was pumped through a chamber containing a YSI 6600 sonde equipped with temperature, specific conductance, dissolved oxygen, pH, turbidity, and chlorophyll probes. Readings were recorded at 15 second intervals along with simultaneous GPS position readings. Every 2 minutes SAV relative abundance by species was recorded and every 4 minutes water samples were collected for extracted chlorophyll and TSS determination. Some areas of the Hunting Creek embayment could not be surveyed due to shallow water or heavy SAV growth. These surveys allowed a much better understanding of spatial patterns in water quality within the Hunting Creek area which facilitated interpretation of data from the fixed stations. This approach is in wide use in the Chesapeake Bay region by both Virginia and Maryland under the name "dataflow".

G. Data Analysis

Data for each parameter were entered into spreadsheets (Excel or SigmaPlot) for graphing of temporal and spatial patterns. SYSTAT was used for statistical calculations and to create illustrations of the water quality mapping cruises. JMP v8.0.1was used for fish graphs. Other data analysis approaches are explained in the text.

RESULTS

A. Climatic and Hydrologic Factors - 2018

In 2018 temperature was below normal in March and April, but well above normal for the period May through September (Table 3). There were 37 days with maximum temperature above 32.2ºC (90ºF) in 2018 which is above the median number over the past decade. August was particularly warm in 2018 being 2°C higher than its normal average. Precipitation established some new records in 2018 with all months in the study period being above average and May, July and September receiving over twice their annual average rainfall. The largest daily rainfall total was 10.2 cm on July 21 which followed a 7.1 cm day on July 17. Another period of heavy precipitation was May 13-19 when substantial rainfall occurred every day and the total amounted to 15.2 cm.

Table 2. Meteorological Data for 2018. National Airport. Monthly Summary.

	Air Temp (ºC)		Precipitation (cm)	
MONTH				
March	6.4	(8.1)	4.9	(9.1)
April	12.7	(13.4)	9.1	(7.0)
May	22.4	(18.7)	22.2	(9.7)
June	24.6	(23.6)	13.2	(8.0)
July	27.1	(26.2)	24.7	(9.3)
August	27.2	(25.2)	13.2	(8.7)
September	24.2	(21.4)	24.7	(9.6)
October	17.0	(14.9)	7.8	(8.2)
November	8.1	(9.3)	19.2	(7.7)
December	6.4	(4.2)	14.8	(7.8)

Note: 2018 monthly averages or totals are shown accompanied by long-term monthly averages (1971-2000). Source: Local Climatological Data. National Climatic Data Center, National Oceanic and Atmospheric Administration.

River and stream flow in 2018 was also well above average for most months in both the Potomac mainstem and in Cameron Run indicating that the effects of the enhanced precipitation translate into higher flows both locally and regionally. Potomac River flow for each month between May and September was over twice the long-term average and in June and August, it was over four times the average. Cameron Run exhibited a similary pattern with May, July, and September experiencing the most atypically high flows.

Table 3. Monthly mean discharge at USGS Stations representing freshwater flow into the study area. (+) 2018 month > 2x Long Term Avg. (-) 2018 month < ½ Long Term Avg.

	Potomac River at Little Falls (cfs)		**Cameron Run at Wheeler Ave (cfs)**	
	2018	**Long Term Average**	**2018**	**Long Term Average**
January	6463 (-)	13700	10.8 (-)	41
February	20282	16600	60.8	45
March	12600	23600	24.4 (-)	55
April	23746	20400	75.3	42
May	33622 (+)	15000	138.5 (+)	41
June	38900 (+)	9030	87.8 (+)	38
July	14833 (+)	4820	183.1 (+)	31
August	21809 (+)	4550	100.0 (+)	28
September	46083 (+)	5040	167.0 (+)	38
October		5930	78.8 (+)	33

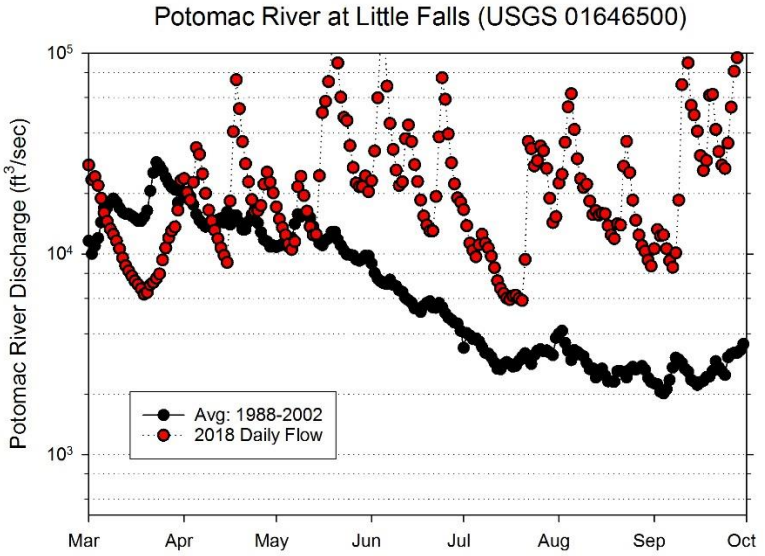

In a tidal freshwater system like the Potomac River, river flow entering from upstream is important in maintaining freshwater conditions and also serves to bring in dissolved and particulate substances from the watershed. High freshwater flows may also flush planktonic organisms downstream and bring in suspended sediments that decrease water clarity. The volume of river flow per unit time is referred to as "river discharge" by hydrologists. Note the general long term seasonal pattern of higher discharges in winter and spring and lower discharges in summer and fall.

Figure 2. Mean Daily Discharge: Potomac River at Little Falls (USGS Data). Month tick is at the beginning of the month.

These same patterns were seen in the graphs of daily river flow when compared to long-term averages. The long term average shows a steadily decreasing trend from April through September. In 2018 this decline was not observed and river flow remained 1-2 orders of magnitude above the long term mean for the entire study period. Of note is the minimum in river flow observed in early and mid-July. Water quality/plankton sampling dates which may have been particularly affected by immediately prior storm events include May 16 and May 31 (Table 1), but other dates were also impacted due to the pervasive nature of rainfall events in 2018.

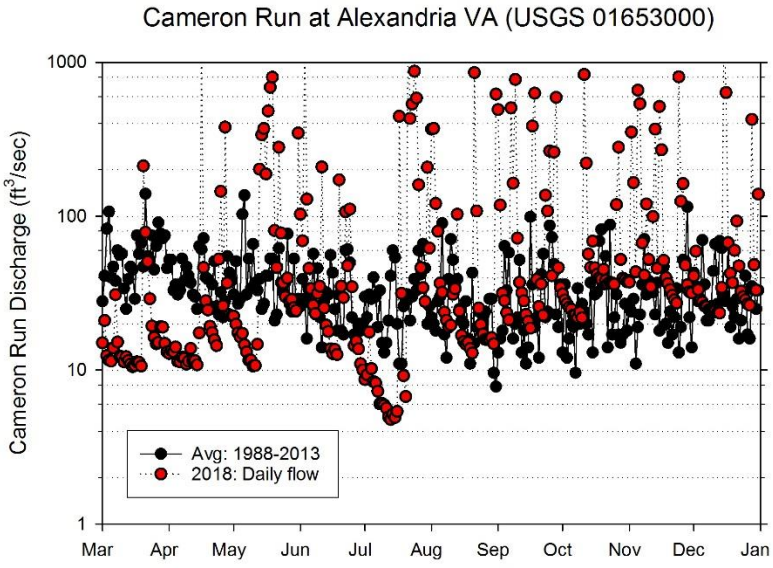

In the Hunting Creek region of the tidal Potomac, freshwater discharge is occurring from both the major Potomac River watershed upstream (measured at Little Falls) and from immediate tributaries, principally Cameron Run which empties directly into Hunting Creek. The gauge on Cameron Run at Wheeler Avenue is located just above the head of tide and covers most area which contributes runoff directly to the Hunting Creek embayment from the watershed. The contributing area to the Wheeler Ave gauge is 33.9 sq mi. (USGS)

Figure 3. Mean Daily Discharge: Cameron Run at Alexandria (Wheeler Ave) (USGS Data).

B. Physico-chemical Parameters: Embayment and River Stations – 2018

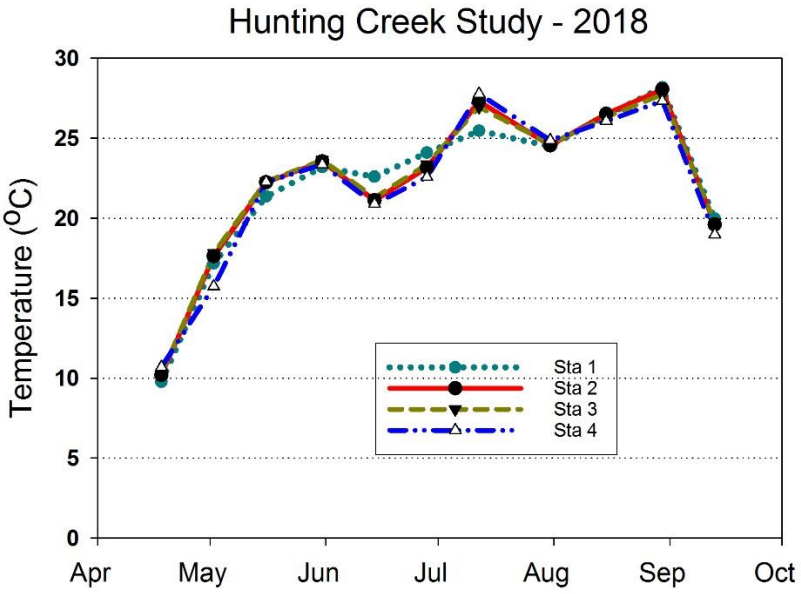

Water temperature is an important factor affecting both water quality and aquatic life. In a well-mixed system like the tidal Potomac, water temperatures are generally fairly uniform with depth. In a shallow mixed system such as the tidal Potomac, water temperature often closely tracks daily changes in air temperature.

Figure 4. Water Temperature (ºC). GMU Field Data. Month tick is at first day of month.

In 2018 water temperature followed the typical seasonal pattern at all station (Figure 4). Temperatures increased rapidly in April and May and dropped back in early June before continuing to increase in July. Maximum temperatures were observed in early July and late August. These were the times of maximum daily air temperature (Figure 5).

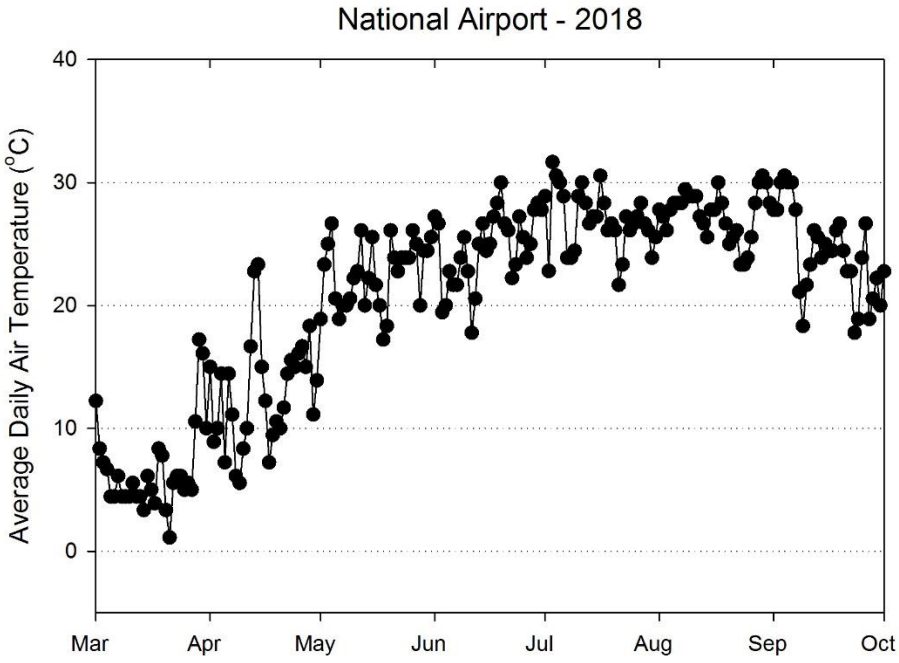

Mean daily air temperature (Figure 5) was a good predictor of water temperature (Figure 4).

Figure 5. Average Daily Air Temperature (ºC) at Reagan National Airport.

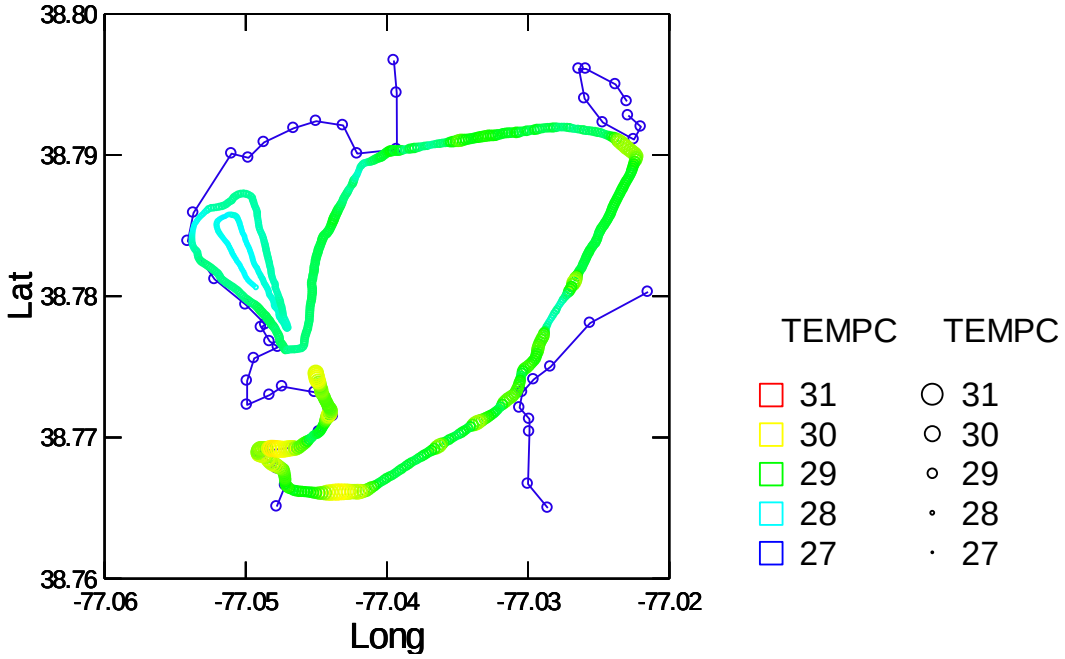

Figure 6a. Water Quality Mapping. July 16, 2018. Temperature (°C).

Mapping of water temperature was conducted on two dates in 2018: July 16 and August 28. In July water temperature in the iver mainstem area was uniformly 29°C while in Hunting Creek it was slightly lower and in a shallow river margin downstream on the Virginia side was slightly higher (Figure 6a). In August the range of temperatures was somewhat lower and there were higher readings both in the river channel and near shore in the Hunting Creek embayment (Figure 6b).

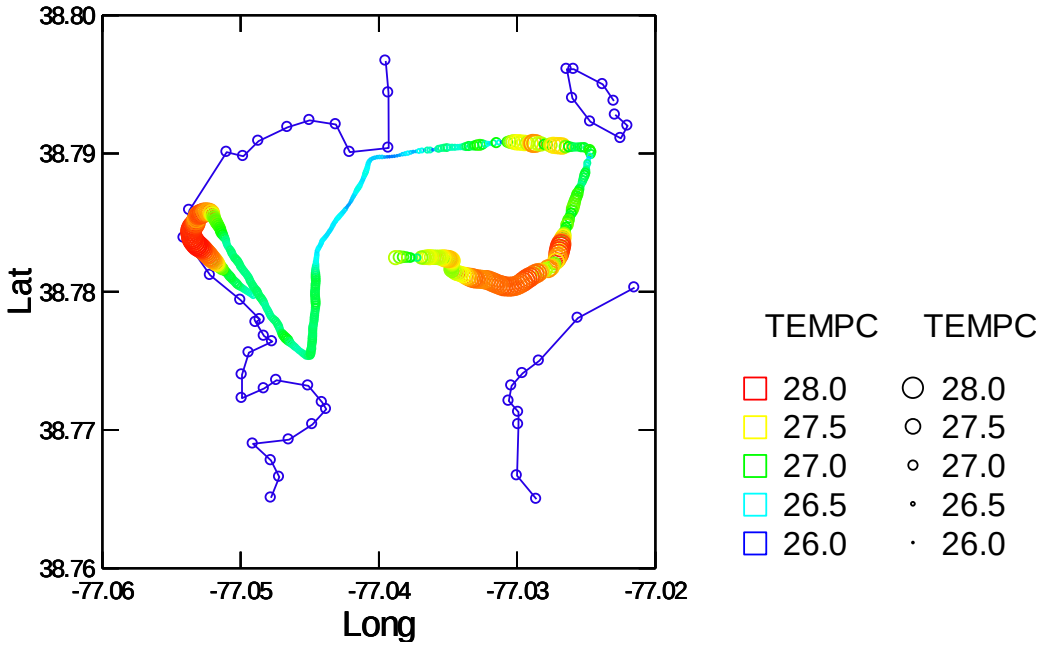

Figure 6b. Water Quality Mapping. August 28, 2018. Temperature (°C).

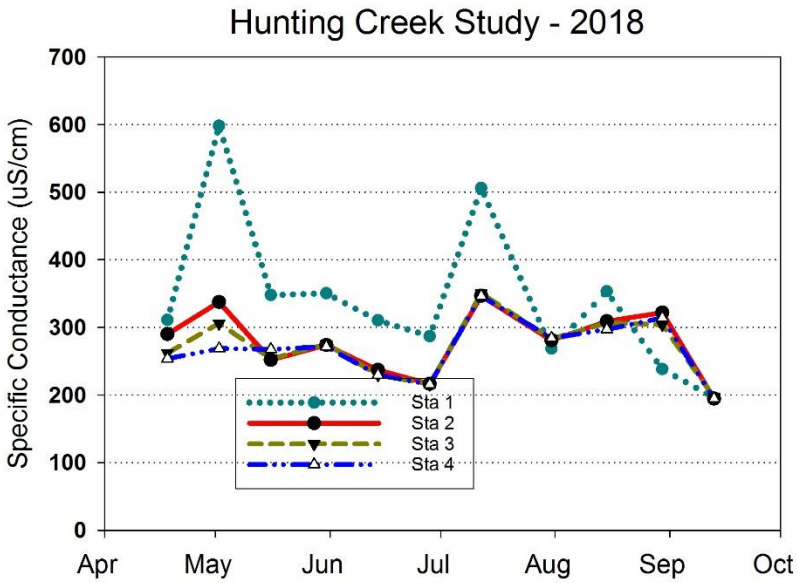

Specific conductance measures the capacity of the water to conduct electricity standardized to 25°C. This is a measure of the concentration of dissolved ions in the water. In freshwater, conductivity is relatively low. Ion concentration generally increases slowly during periods of low freshwater inflow and decreases during periods of high freshwater inflow. Sewage treatment facilities can be a source of elevated conductivity. In winter road salts can be a major source of conductivity in urban streams.

Figure 7. Specific Conductance (µS/cm). GMU Field Data. Month tick is at first day of month.

Specific conductance was generally substantially higher at AR1 than at the other stations reflecting its location just downstream of the Alex Renew outfall (Figure 7). The other stations were very similar to one another and were fairly constant seasonally. As one of the major ions contributing to specific conductance, chloride exhibited much higher values at AR1 than at the other sites (Figure 8). The same seasonal patterns were found for chloride as for specific conductance.

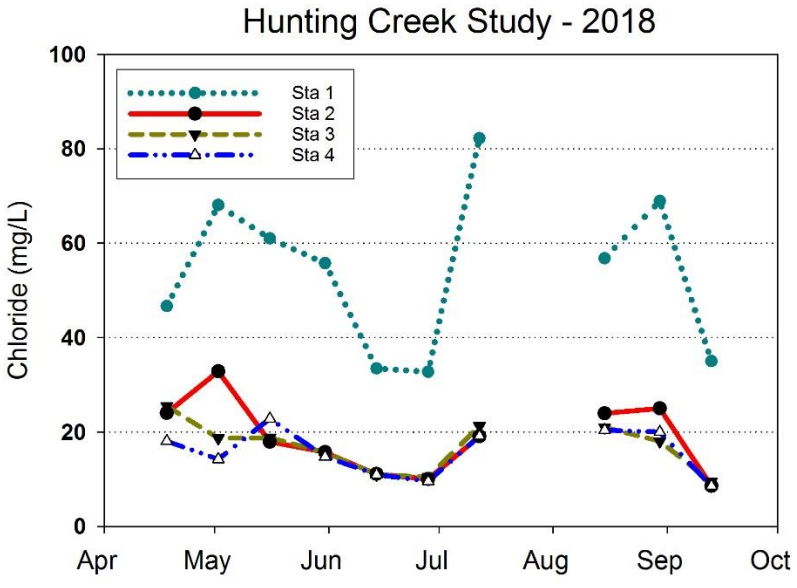

Chloride ion (Cl-) is a principal contributor to conductance. Major sources of chloride in the study area are sewage treatment plant discharges, road salt, and brackish water from the downriver portion of the tidal Potomac. Chloride concentrations observed in the Hunting Creek area are very low relative to those observed in brackish, estuarine, and coastal areas of the Mid-Atlantic region. Chloride may increased slightly in late summer or fall when brackish water from down estuary may reach the area as freshwater discharge declines.

Figure 8. Chloride (mg/L). Alexandria Renew Lab Data. Month tick is at first day of month.

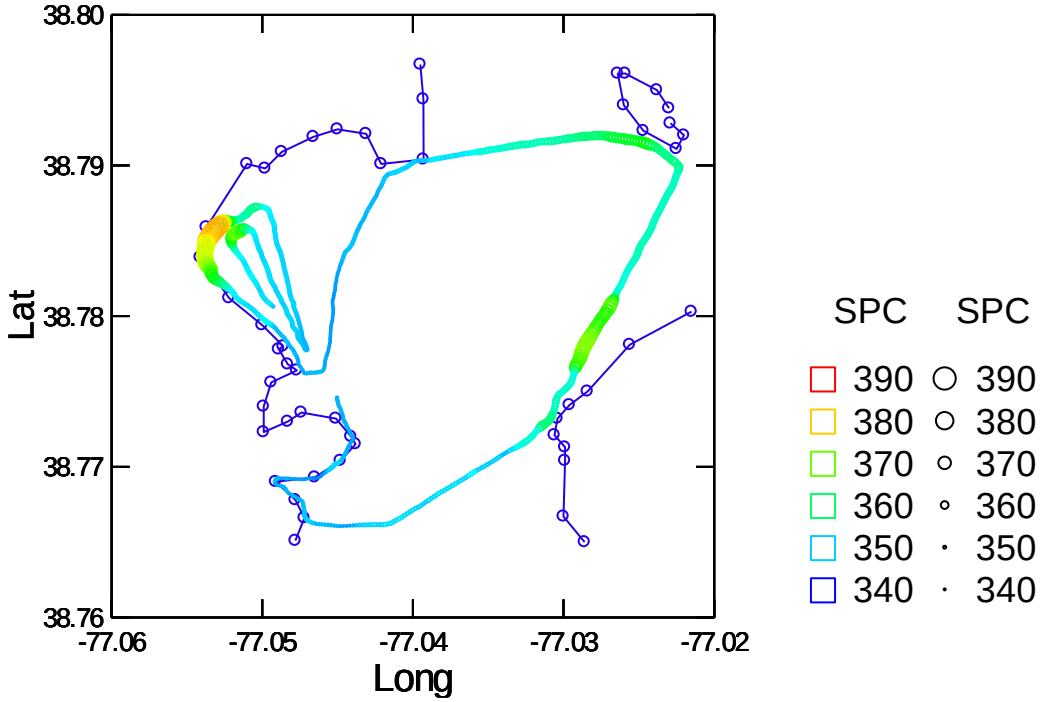

Figure 9a. Water Quality Mapping. July 26, 2018. Specific conductance (µS).

Mapping of specific conductance on July 26 showed that values were generally the lowest in the outer part of Hunting Creek and toward the western side of the mainstem (Figure 9a). The somewhat elevated values found in the neer part of Hunting Creek and the Maryland side of the channel can be explained by proximity to the Alex Renew and Blue Plains discharge sites, respectively. A similar pattern was observed on August 28 with a greater range of values overall (Figure 9b).

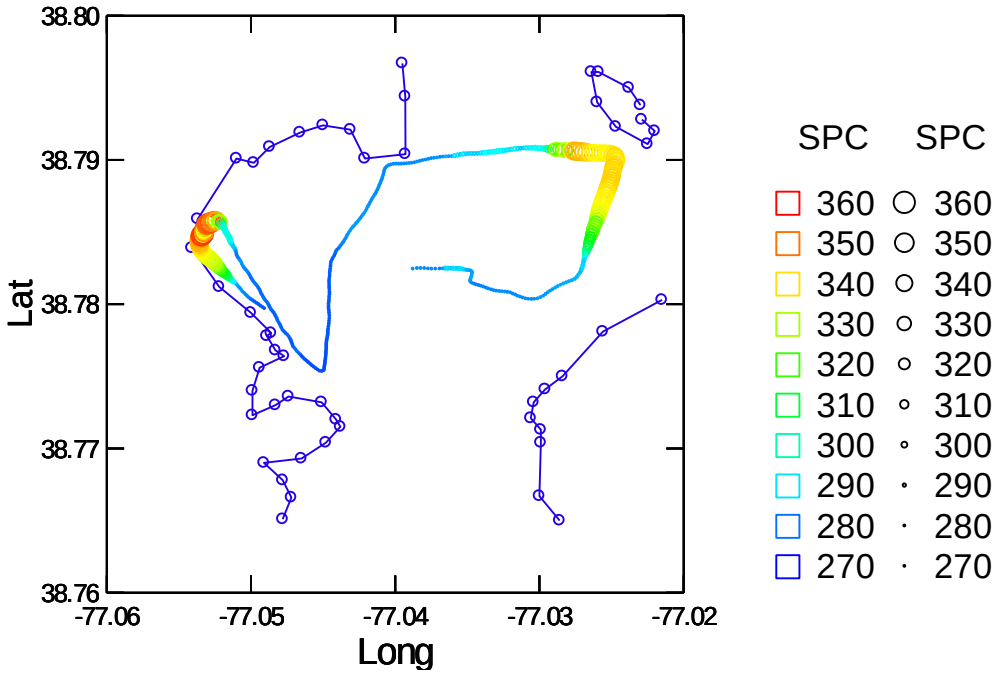

Figure 9b. Water Quality Mapping. August 28, 2018. Specific conductance (µS).

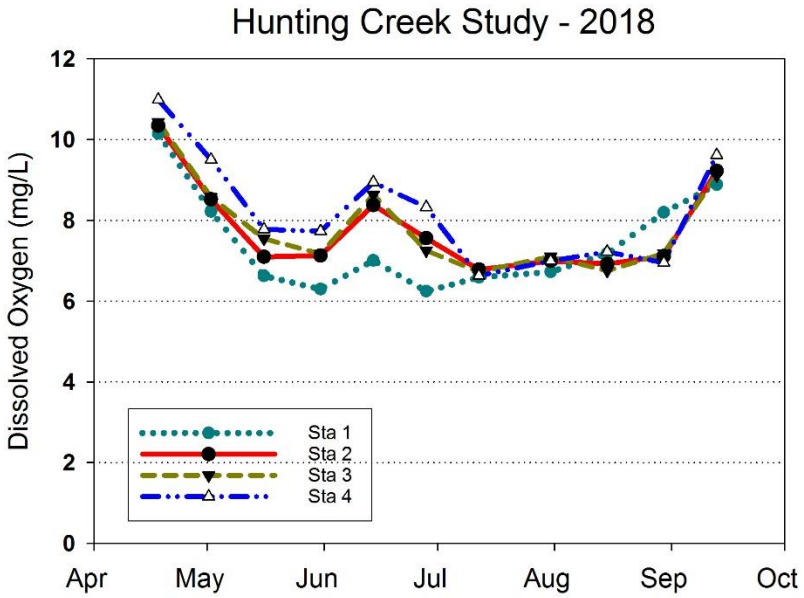

Oxygen dissolved in the water is required by freshwater animals for survival. The standard for dissolved oxygen (DO) in most surface waters is 5 mg/L. Oxygen concentrations in freshwater are in balance with oxygen in the atmosphere, but oxygen is only weakly soluble in water so water contains much less oxygen than air. This solubility is determined by temperature with oxygen more soluble at low temperatures.

Figure 10. Dissolved Oxygen (mg/L). GMU Field Data. Month tick is at first day of month.

The general pattern for dissolved oxygen (mg/L) was a seasonal decline from May through early June and steady values through September (Figure 10). Looking at DO as as percent saturation (Figure 11), the basic seasonal pattern was less pronounced indicating that temperature was the main variable deriving the seasonal pattern in DO as mg/L. Do rarely exceeded 100% and was below 80% indicating that photosynthesis and respiration were not major factors.

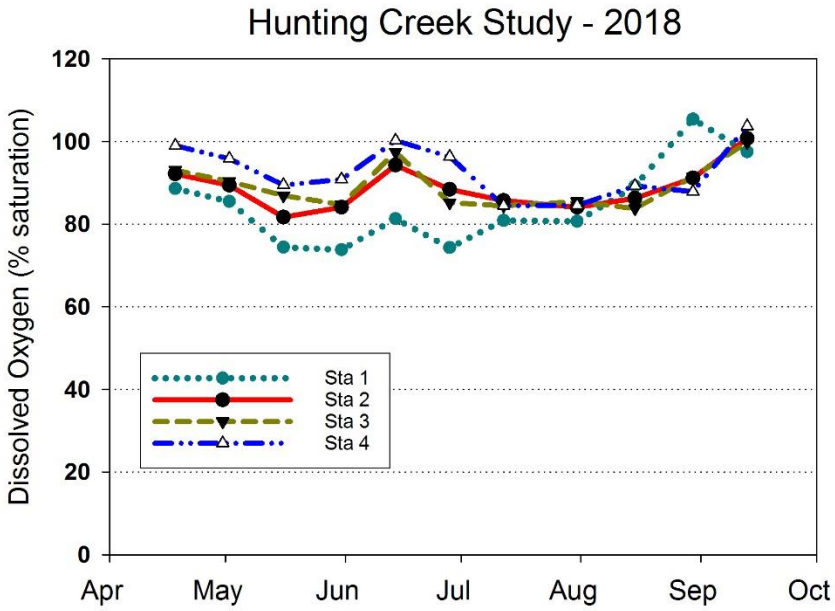

The temperature effect on oxygen concentration can be removed by calculating DO as percent saturation. This allows examination of the balance between photosynthesis and respiration both of which also impact DO. Photosynthesis adds oxygen to the water while respiration removes it. Values above 120% saturation are indicative of intense photosynthesis while values below 80% reflect a preponderance of respiration or decomposition.

Figure 11. Dissolved Oxygen (% saturation). GMU Field Data. Month tick is at first day.

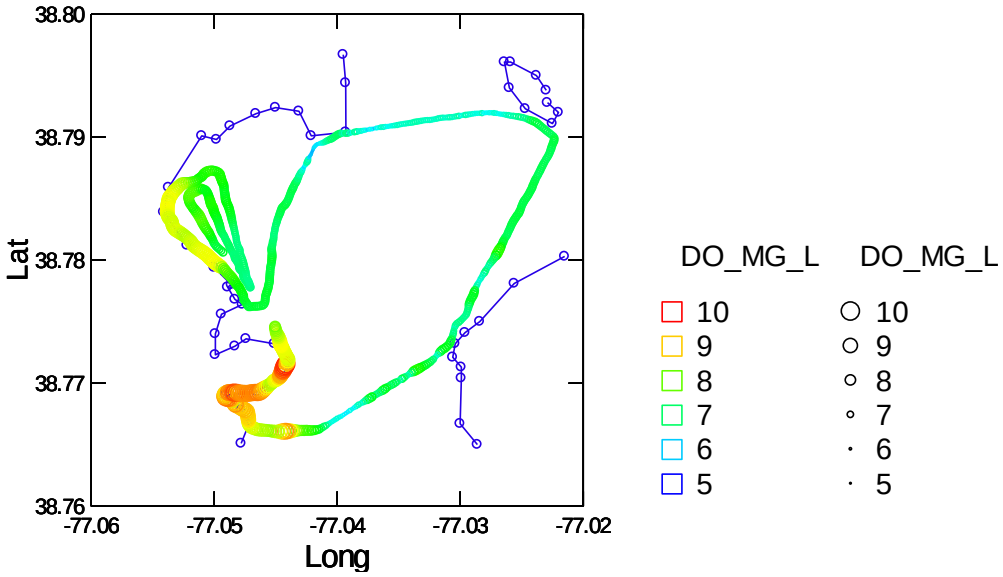

Figure 12a. Water Quality Mapping. July 16, 2018. Dissolved oxygen (mg/L).

On July 16 dissolved oxygen (both mg/L and percent saturation) exhibited clea spatial patterns (Figures 12a&b). Levels were lowest in the river running about 90% saturation and 7-8 mg/L. Higher levels were found in the most westerly part of Hunting Creek and even more so along the Virginia shoreline downstream of Hunting Creek. While SAV was limited in Hunting Creek in 2018, there wer some appreciable growths in the shallows downstream which might expain the spatial pattenr

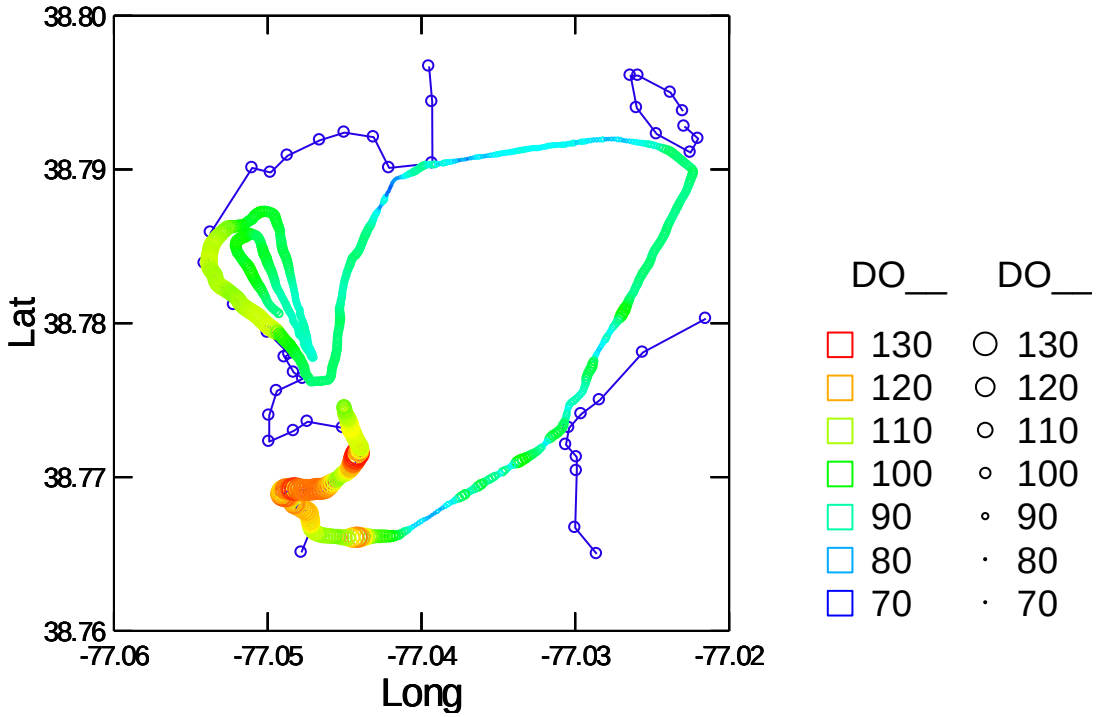

Figure 12b. Water Quality Mapping. July 16, 2018. Dissolved oxygen (percent saturation).

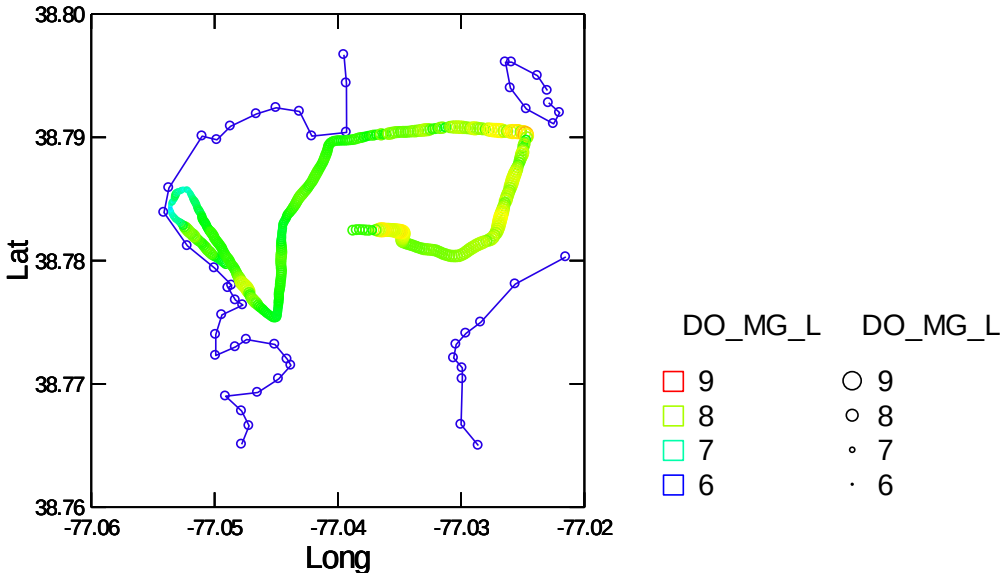

Figure 13a. Water Quality Mapping. August 28, 2018. Dissolved oxygen (mg/L).

On August 28, the spatial patterns weren't quite as strong and the highest levels were seen in the shallows on the Maryland side and in the channel (Figures 13a&b). The causes of this pattern were not readily discernable.

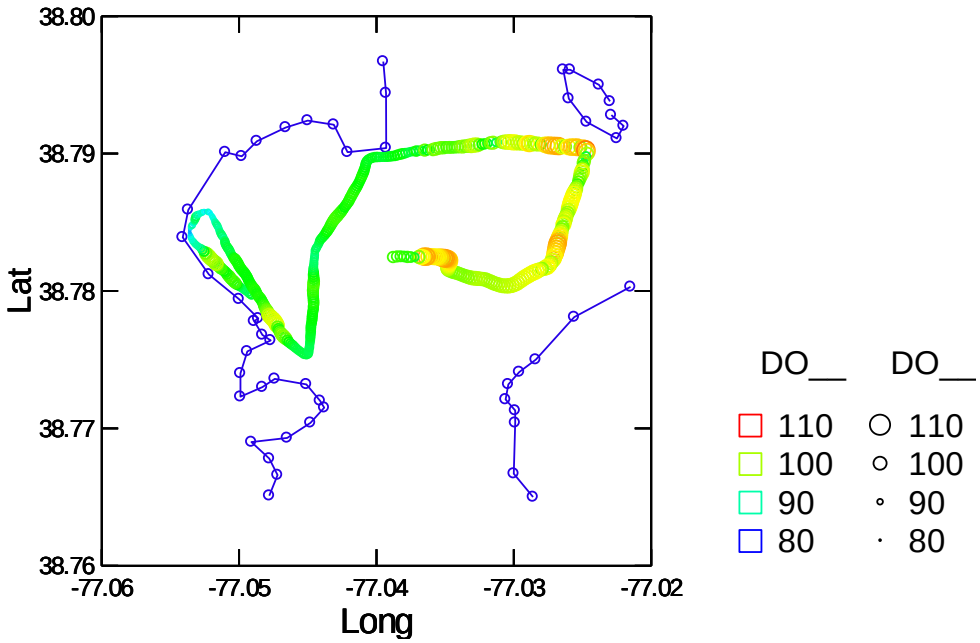

Figure 13b. Water Quality Mapping. August 28, 2018. Dissolved oxygen (percent saturation).

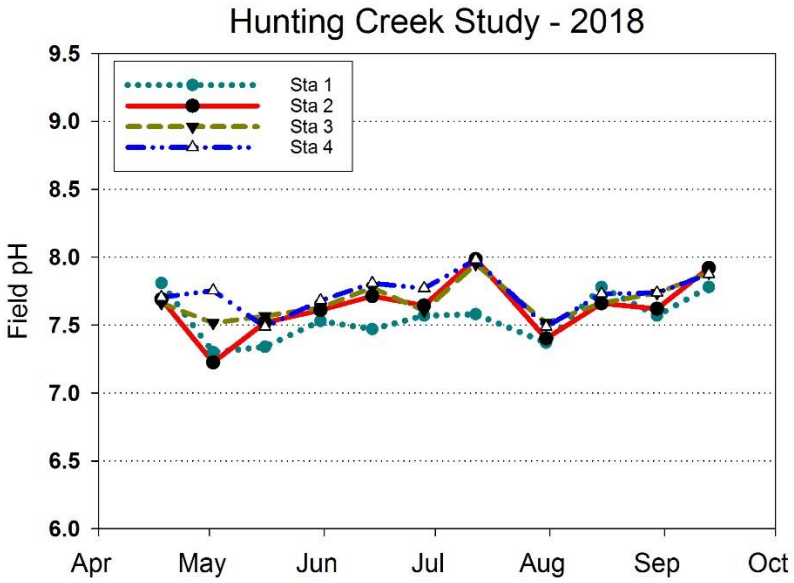

pH is a measure of the concentration of hydrogen ions (H+) in the water. Neutral pH in water is 7. Values between 6 and 8 are often called circumneutral, values below 6 are acidic and values above 8 are termed alkaline. Like DO, pH is affected by photosynthesis and respiration. In the tidal Potomac, pH above 8 indicates active photosynthesis and values above 9 indicate intense photosynthesis. A decrease in pH following a rainfall event may be due to acids in the rain or in the watershed.

Figure 14. pH. GMU Field Data. Month tick is at first day of month.

In 2018 pH values remained in a fairly narrow range (7.2-8.0) with little difference among the sample stations (Figure 14). Lab pH was consistently lower at AR1, but the values at the other stations were very similar and the seasonal differences were minor (Figure 15).

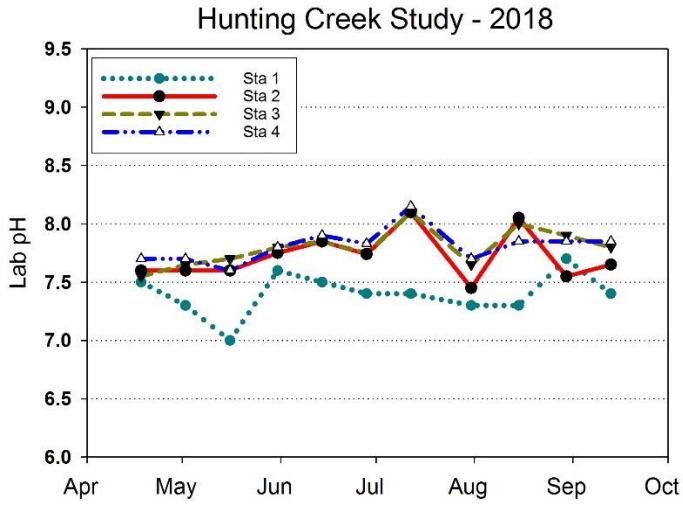

pH may be measured in the field or in the lab. Field pH is more reflective of in situ conditions while lab pH is done under more stable and controlled laboratory conditions and is less subject to error. Newer technologies such as the Hydrolab and YSI sondes used in GMU field data collection are more reliable than previous field pH meters and should give results that are most representative of values actually observed in the river.

Figure 15. pH. AlexRenew Lab Data. Month tick is at first day of month.

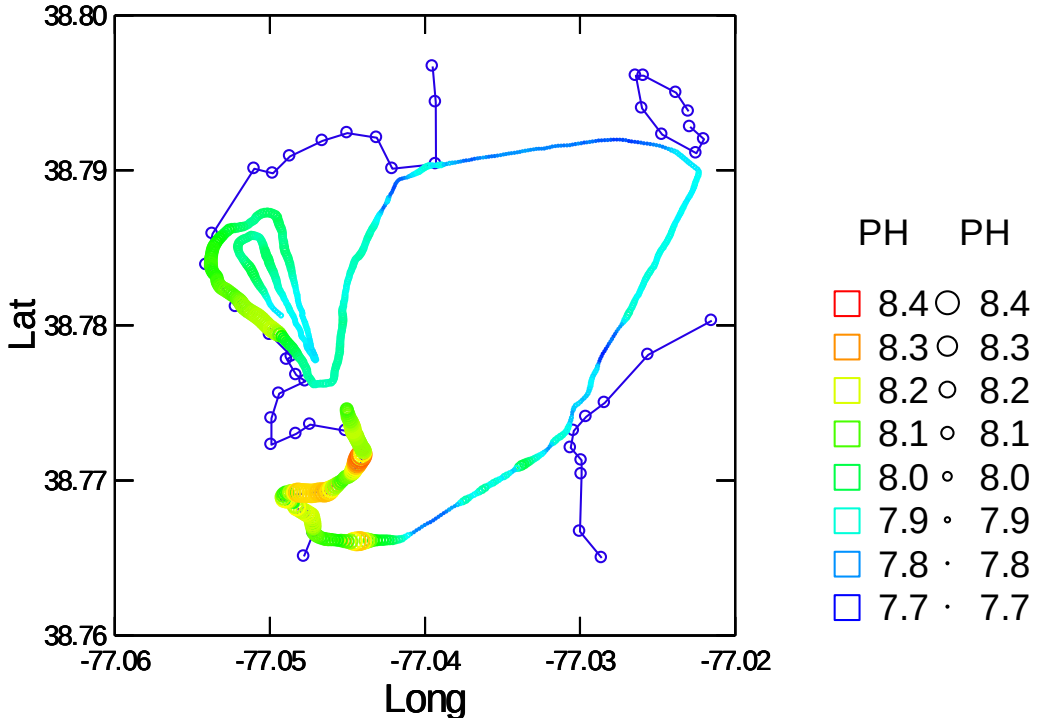

Figure 16a. Water Quality Mapping. July 16, 2018. pH.

Water quality mapping of pH showed very different patterns in July 16 vs. August 28 (Figure 16a&b). Values were substantially higher in July than in August. Values were higher in the river and outer Hunting Creek and lower in inner Hunting Creek and the Maryland shore in July. In August values were generally lower and had a narrower range.

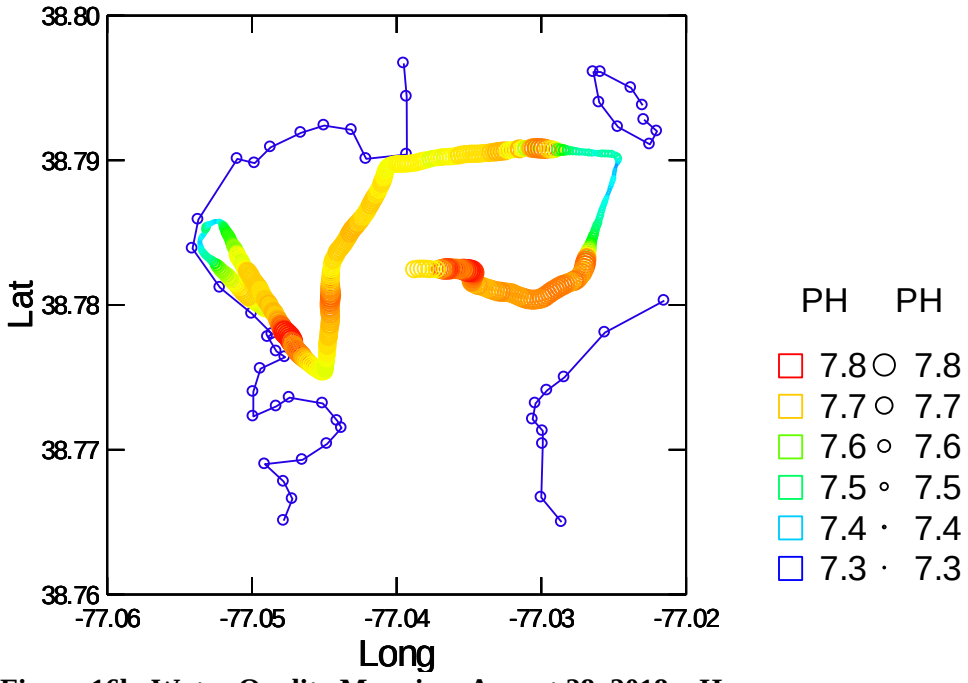

Figure 16b. Water Quality Mapping. August 28, 2018. pH.

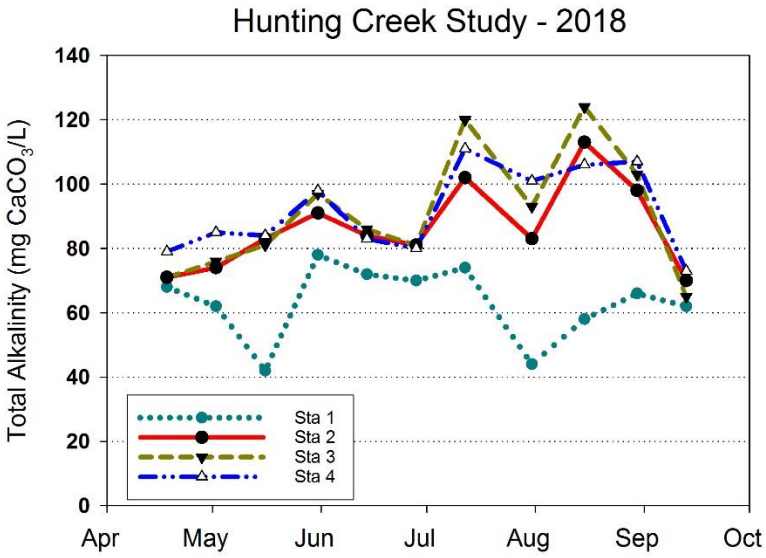

Total alkalinity measures the amount of bicarbonate and carbonate dissolved in the water. In freshwater this corresponds to the ability of the water to absorb hydrogen ions (acid) and still maintain a near neutral pH. Alkalinity in the tidal freshwater Potomac generally falls into the moderate range allowing adequate buffering without carbonate precipitation.

Figure 17. Total Alkalinity (mg/L as $CaCO_3$). AlexRenew Lab data. Month tick is at first day.

Total alkalinity was generally in the range 60-100 mg/L as $CaCO_3$ (Figure 17). There was a gradual trend of increasing values as the year went along. Values were consistently lower at AR1. Water clarity as reflected by Secchi disk exhibited a variable pattern in spring and was uniformly low throughout the summer at all stations (Figure 18). Very low clarity in April was followed in early May by much clearer water which was again reversed in late May at AR4 especially. Another increase in water clarity was observed late May at AR4. At the Hunting Creek stations AR2 and AR3, the clearest water was observed in early July, but even this (at about 55 cm) was well below the typical 1 m values found in summer at these stations.

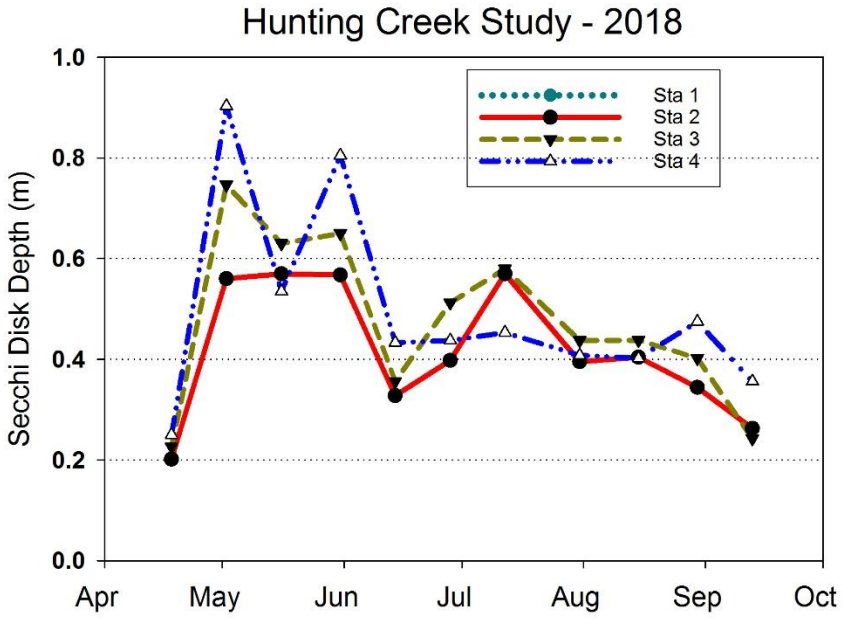

Secchi Depth is a measure of the transparency of the water. The Secchi disk is a flat circle of thick sheet metal or plywood about 6 inches in diameter which is painted into alternate black and white quadrants. It is lowered on a calibrated rope or rod to a depth at which the disk disappears. This depth is termed the Secchi Depth. This is a quick method for determining how far light is penetrating into the water column. Light is necessary for photosynthesis and thereby for growth of aquatic plants and algae.

Figure 18. Secchi Disk Depth (m). GMU Field Data. Month tick is at first day of month.

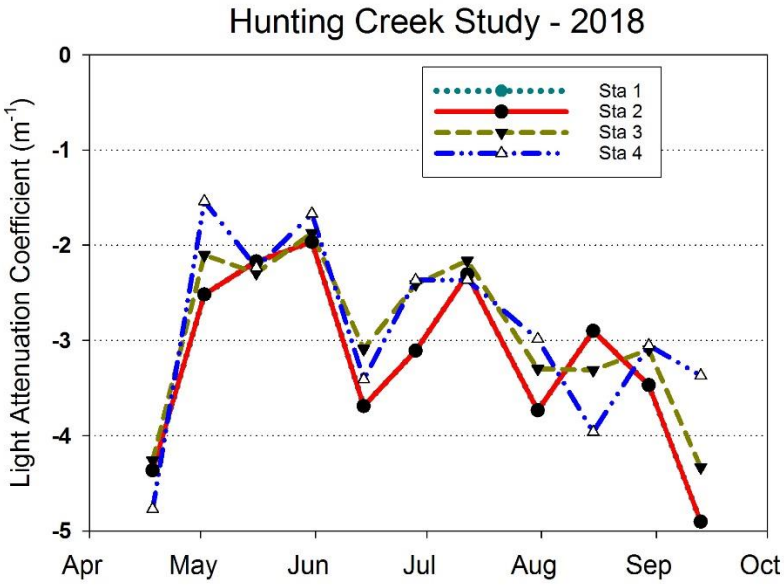

Light Attenuation is another approach to measuring light penetration. This is determined by measuring light levels at a series of depths starting near the surface. The resulting relationship between depth and light is fit to a semi-logarithmic curve and the resulting slope is called the light attenuation coefficient. This relationship is called Beer's Law. It is analogous to absorbance on a spectrophotometer. The greater the light attenuation, the faster light is absorbed with depth. More negative values indicate greater attenuation. Greater attenuation is due to particulate and dissolved material which absorbs and deflects light.

Figure 19. Light Attenuation Coefficient (m^{-1}). GMU Field Data. Month tick is at first day of month.

Light attenuation coefficient data reflected a very similar pattern with peaks and low points occurring on the same dates as Secchi disk values (Figure 19). Again, light attenuation (due primarily to suspended sediment from runoff events) was much greater than normal resulting in more negative values especially in early June and late July through September. Turbidity also showed this effect with values increasing markedly in the aftermath of storms (Figure 20).

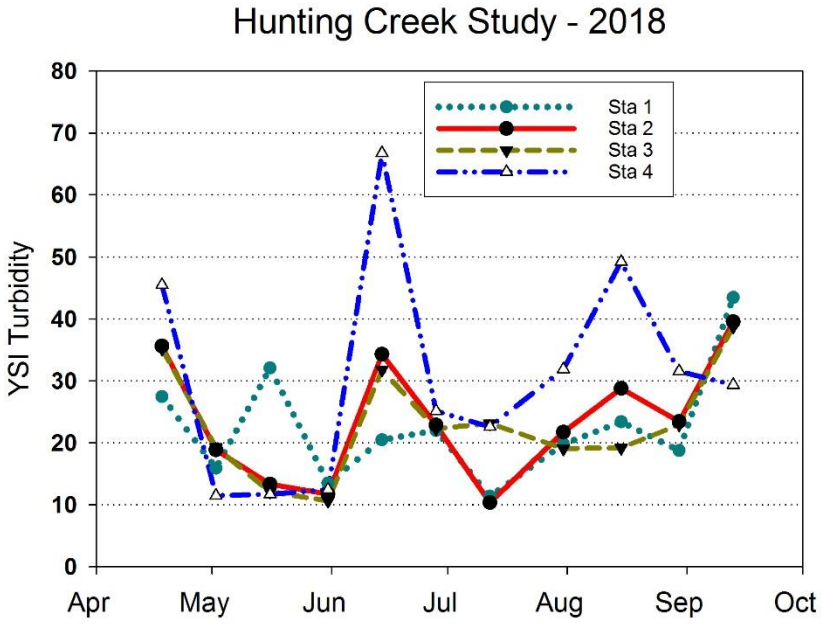

Turbidity is yet a third way of measuring light penetration. Turbidity is a measure of the amount of light scattering by the water column. Light scattering is a function of the concentration and size of particles in the water. Small particles scatter more light than large ones (per unit mass) and more particles result in more light scattering than fewer particles.

Figure 20. Turbidity (NTU). GMU Lab Data. Month tick is at first day of month.

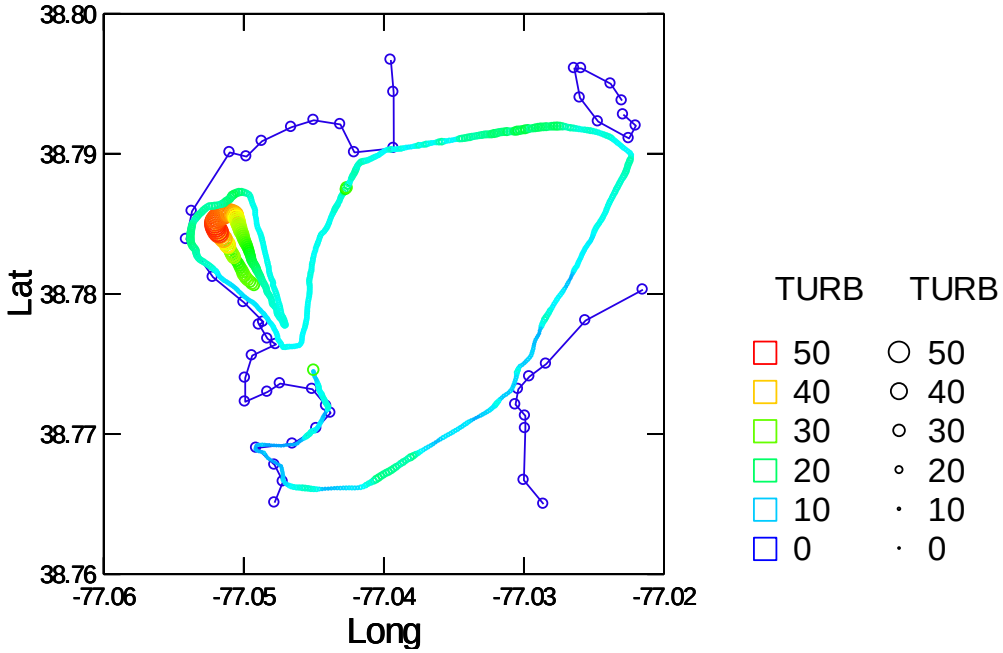

Figure 21a. Water Quality Mapping. July 16, 2018. Turbidity YSI.

On the July 16 mapping, turbidity was generally fairly low throughout the study area with a small hotspot in westernmost Hunting Creek (Figure 21a). Values were generally in the 10-30 NTU range. The cause of the hotspot is not readily apparent; it may have been an artifact caused by sediment resuspension by the boat in this shallow area. In August turbidity was also generally low again throughout the study area (Figure 21b). Of note is the fact that both of these mapping dates were during the periods of relatively clear water not strongly influenced by storm runoff.

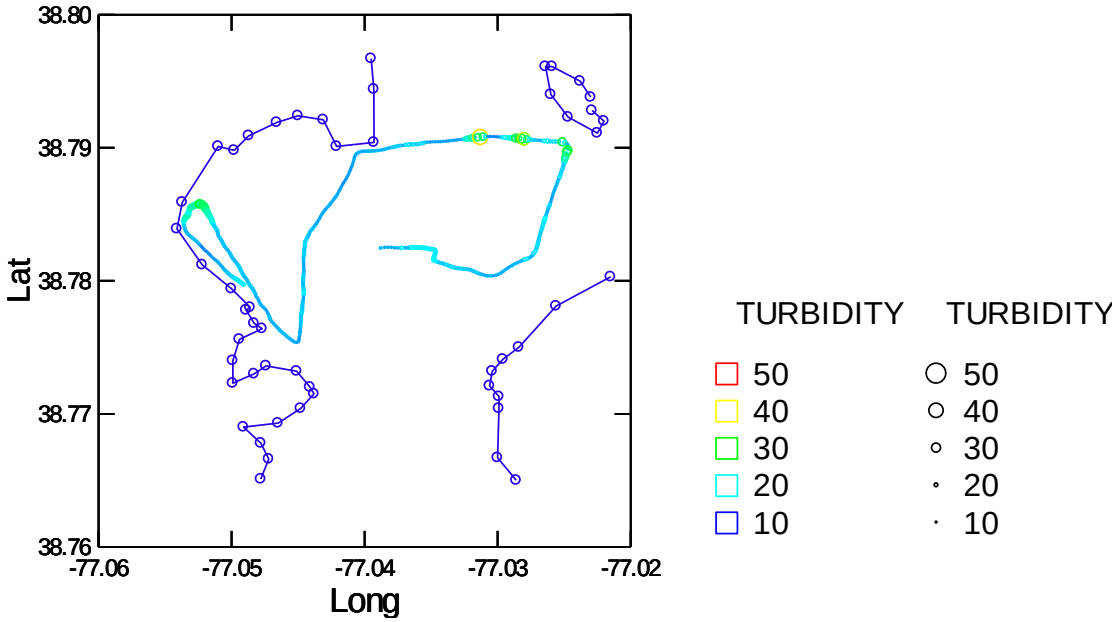

Figure 21b. Water Quality Mapping. August 28, 2018. Turbidity YSI.

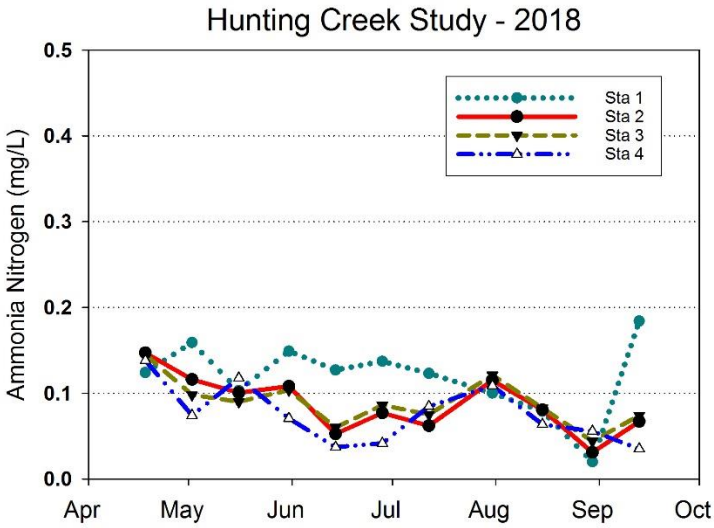

Ammonia nitrogen measures the amount of ammonium ion (NH_4^+) and ammonia gas (NH_3) dissolved in the water. Ammonia nitrogen is readily available to algae and aquatic plants and acts to stimulate their growth. While phosphorus is normally the most limiting nutrient in freshwater, nitrogen is a close second. Ammonia nitrogen is rapidly oxidized to nitrate nitrogen when oxygen is present in the water so high ammonia levels suggest proximity to a source.

Figure 22. Ammonia Nitrogen (mg/L). AlexRenew Lab Data. Month tick is at first day of month.

Ammonia nitrogen was consistently low (<0.2 mg/L) for the entire study period (Figure 22). A slight seasonal pattern was seen at all stations with a general decline. At AR1 an increase was observed on the last date. Nitrate nitrogen levels showed a pattern of gradual increase through the year starting near 1.0 mg/L and ending near 1.5 mg/L (Figure 23). Typically, nitrate has decreased in summer at AR2 and AR3 due to uptake by SAV, but this was not observed in 2018 as SAV was virtually absent, apparently due to poor light conditions.

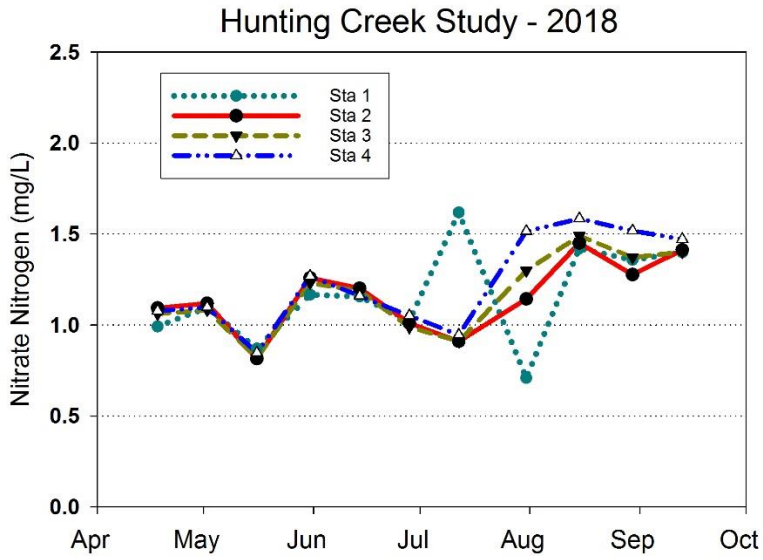

Nitrate Nitrogen refers to the amount of N that is in the form of nitrate ion (NO_3^-). Nitrate ion is the most common form of nitrogen in most well oxidized freshwater systems. Nitrate concentrations are increased by input of wastewater, nonpoint sources, and oxidation of ammonia in the water. Nitrate concentrations decrease when algae and plants are actively growing and removing nitrogen as part of their growth.

Figure 23. Nitrate Nitrogen (mg/L). AlexRenew Lab Data. Month tick is at first day of month.

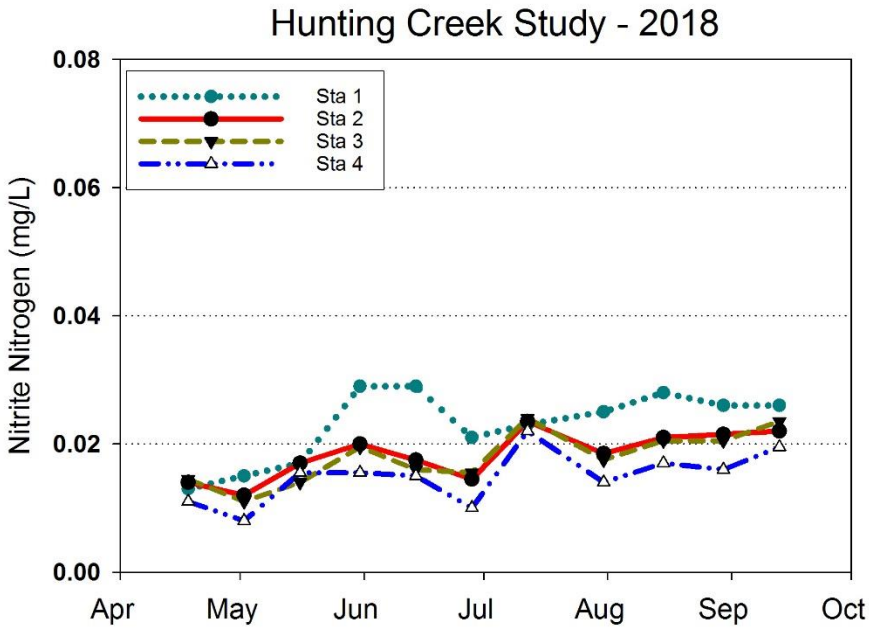

Nitrite nitrogen consists of nitrogen in the form of nitrite ion (NO_2^-). Nitrite is an intermediate in the oxidation of ammonia to nitrate, a process called nitrification. Nitrite is usually in very low concentrations unless there is active nitrification.

Figure 24. Nitrite Nitrogen (mg/L). AlexRenew Lab Data. Month tick is at first day of month.

Nitrite nitrogen was generally low (<0.03 mg/L) throughout the year and showed a slight gradual increase through the year (Figure 24). Organic nitrogen values were generally in the range of 0.2-0.6 mg/L with a gradual increase from May through September (Figure 25). The exception was AR1 which showed more variability and somewhat higher values.

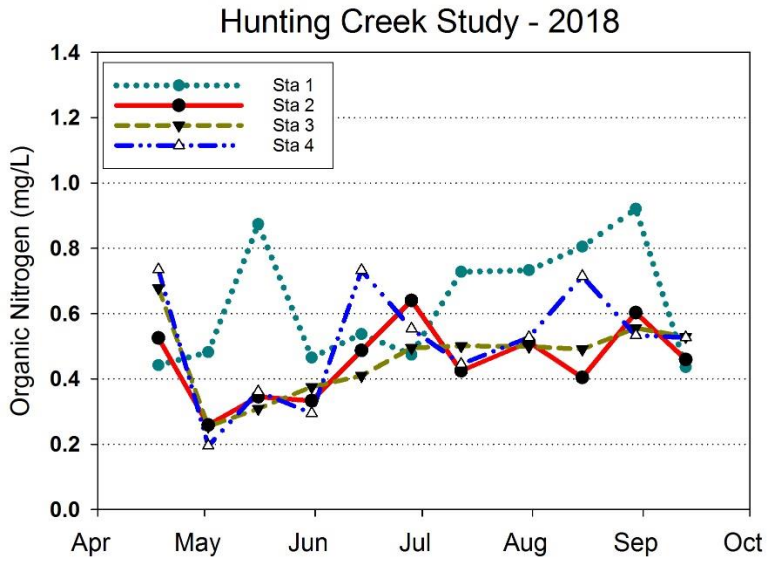

Organic nitrogen measures the nitrogen in dissolved and particulate organic compounds in the water. Organic nitrogen comprises algal and bacterial cells, detritus (particles of decaying plant, microbial, and animal matter), amino acids, urea, and small proteins. When broken down in the environment, organic nitrogen results in ammonia nitrogen. Organic nitrogen is determined as the difference between total Kjeldahl nitrogen and ammonia nitrogen.

Figure 25. Organic Nitrogen (mg/L). AlexRenew Lab Data. Month ti

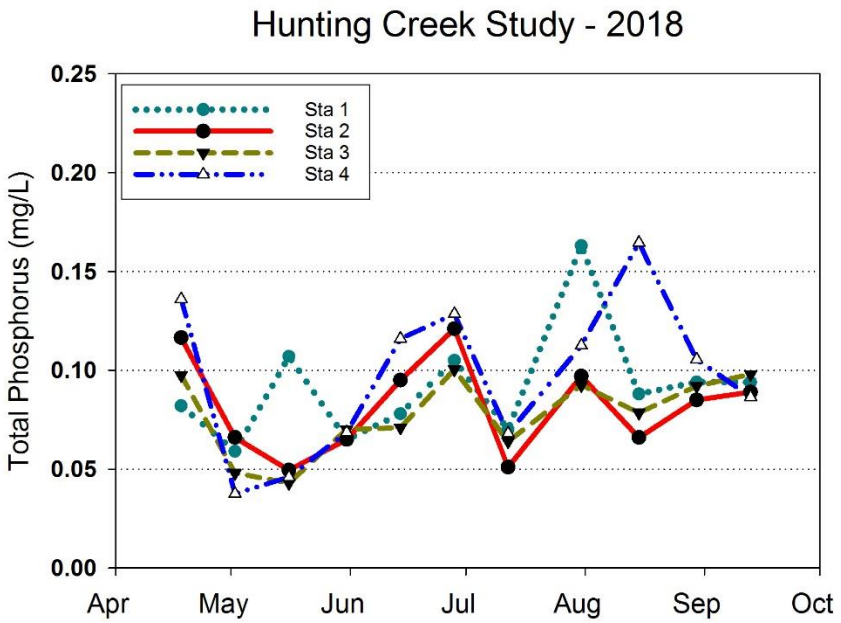

Phosphorus (P) is often the limiting nutrient in freshwater ecosystems. As such the concentration of P can set the upper limit for algal growth. Total phosphorus is the best measure of P availability in freshwater since much of the P is tied up in biological tissue such as algal cells. Total P includes phosphate ion (PO_4^{-3}) as well as phosphate inside cells and phosphate bound to inorganic particles such as clays.

Figure 26. Total Phosphorus (mg/L). AlexRenew Lab Data. Month tick is at first day of month.

Total phosphorus did not exhibit a seasonal pattern in 2018, but rose and fell over the year, probably in response to storm flows (Figure 26). Values were high in April and late June. Values followed similar patterns at all stations. Ortho-phosphorus was generally quite low (<0.04 mg/L) followed similar patterns at AR2, AR3, and AR4 (Figure 27). Values at AR1 were uniformly lower.

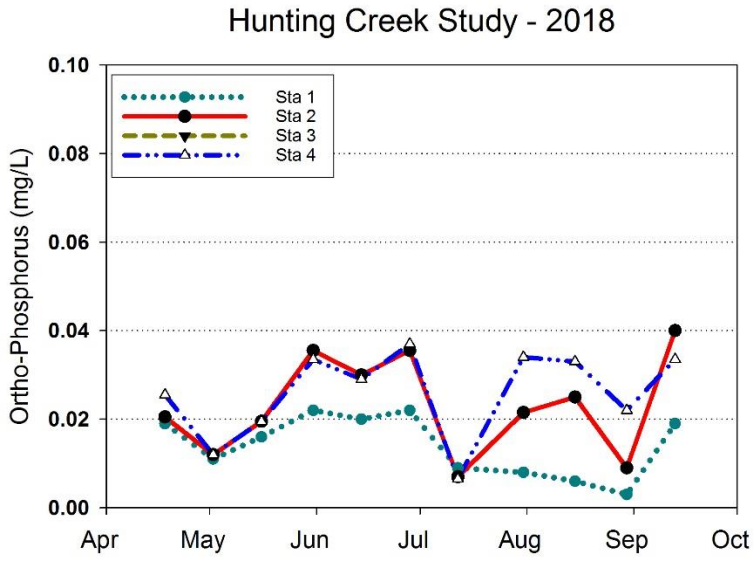

Soluble reactive phosphorus (SRP) is a measure of phosphate ion (PO_4^{-3}). Phosphate ion is the form in which P is most available to primary producers such as algae and aquatic plants in freshwater. However, SRP is often inversely related to the activity of primary producers because they tend to take it up so rapidly. So, higher levels of SRP indicate either a local source of SRP to the waterbody or limitation by a factor other than P.

Figure 27. Soluble Reactive Phosphorus (mg/L). AlexRenew Lab Data. Month tick is at first day of month.

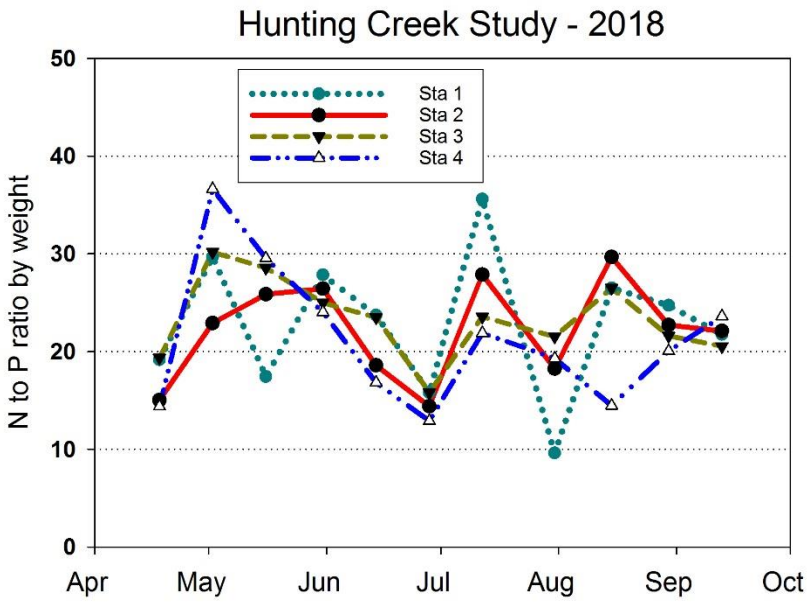

N:P ratio is determined by summing all of the components of N (ammonia, nitrate, nitrite, and organic nitrogen) and dividing by total P. This ratio gives an indication of whether N or P is more likely to be limiting primary production in a given freshwater system. Generally, values above 7.2 are considered indicative of P limitation while values below 7.2 suggest N limitation. N limitation could lead to dominance by cyanobacteria who can fix their own N from the atmosphere.

Figure 28. N/P Ratio (by mass). AlexRenew Lab Data. Month tick is at first day of month.

N/P ratio consistently pointed to P limitation, being greater than 7.2 in all samples (Figure 28). Values were generally in the 15 to 30 range. Biochemical oxygen demand (BOD) could not be graphed as all values were below the detection limit of 2 mg/L (Figure 29).

All data below detection limit…

Biochemical oxygen demand (BOD) measures the amount of decomposable organic matter in the water as a function of how much oxygen it consumes as it breaks down over a given number of days. Most commonly the number of days used is 5. BOD is a good indicator of the potential for oxygen depletion in water. BOD is composed both dissolved organic compounds in the water as well as microbes such as bacteria and algae which will respire and consume oxygen during the period of measurement.

Figure 29. Biochemical Oxygen Demand (mg/L). AlexRenew Lab Data. Month tick is at first day of month.

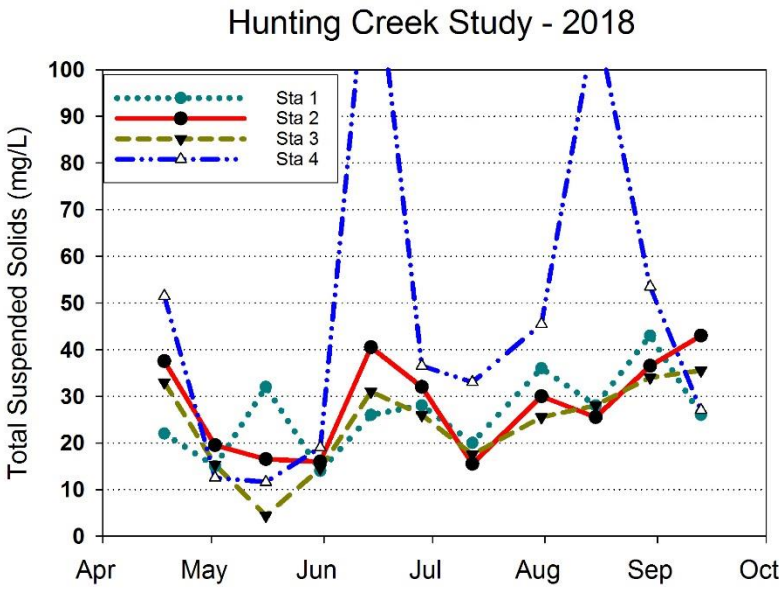

Total suspended solids (TSS) is measured by filtering a known amount of water through a fine filter which retains all or virtually all particles in the water. This filter is then dried and the weight of particles on the filter determined by difference. TSS consists of both organic and inorganic particles. During periods of low river and tributary inflow, organic particles such as algae may dominate. During storm flow periods or heavy winds causing resuspension, inorganic particles may dominate.

Figure 30. Total Suspended Solids (mg/L). AlexRenew Lab Data. Month tick is at first day of month.

Total suspended solids was generally in the range 15-40 mg/L at all stations (Figure 30). A peak was observed in mid June at all stations and a gradual rise was found through August and September. VSS values were generally much lower, but followed similar patterns (Figure 31).

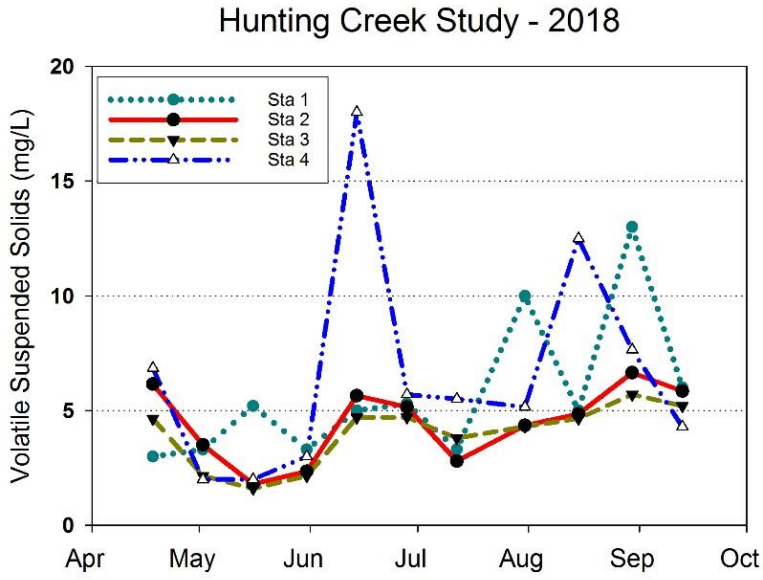

Volatile suspended solids (VSS) is determined by taking the filters used for TSS and then ashing them to combust (volatilize) the organic matter. The organic component is then determined by difference. VSS is a measure of organic solids in a water sample. These organic solids could be bacteria, algae, or detritus. Origins include sewage effluent, algae growth in the water column, or detritus produced within the waterbody or from tributaries. In summer in Gunston Cove a chief source is algal (phytoplankton) growth.

Figure 31. Volatile Suspended Solids (mg/L). AlexRenew Lab Data. Month tick is at first day of month.

C. Physico-chemical Parameters: Tributary Stations – 2018

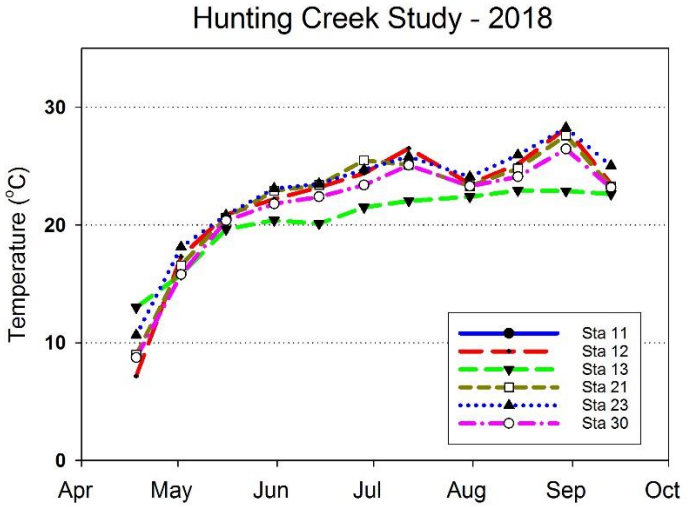

Figure 32. Water Temperature (ºC). GMU Field Data. Month tick is at first day of month.

Water quality data for the tributary stations was combined into a series of graphs by parameter. Temperatures at almost all stations closely followed air temperatures (Figure 32). The most obvious exception was AR13 which exhibited lower temperatures during most of the year. The water at AR13 is just emerging from underground storm sewers and is buffered from the higher air temperatures. Specific conductance was generally in the 200-600 uS/cm range (Figure 33). Values were generally lower than in previous years due to the wet conditions. There was a gradual decline at most stations through the year.

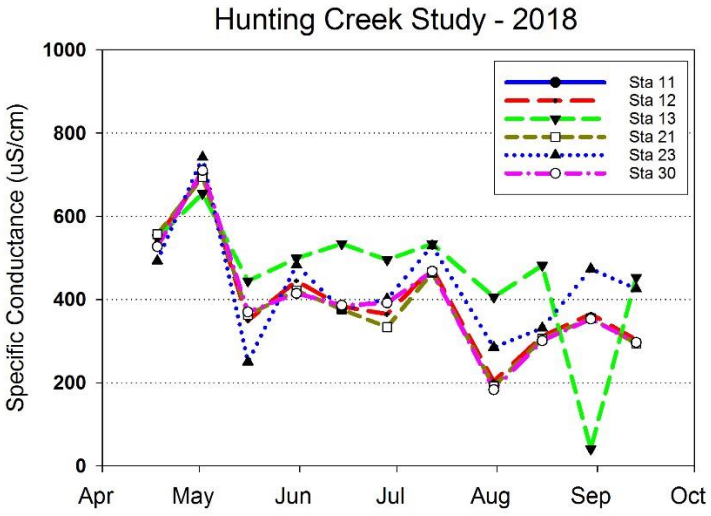

Figure 33. Specific Conductance (uS/cm). GMU Field Data. Month tick is at first day of month.

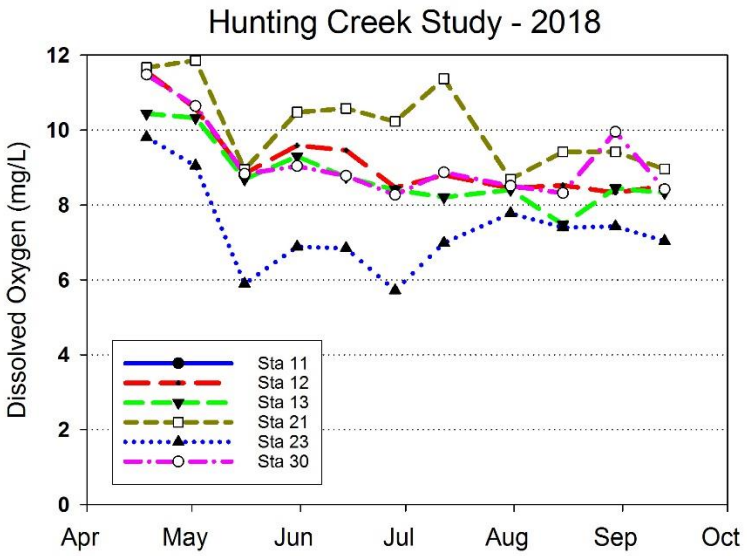

Figure 34. Dissolved Oxygen (mg/L) GMU Field Data. Month tick is at first day of month.

Dissolved oxygen (mg/L) in the tributaries exhibited a clear seasonal pattern that was mainly reflective of changes in DO saturation with temperature (Figure 34). The only station that exhibited concentrations that were substantially below saturation was AR23 which dropped below 6 mg/L on two occasions. This station is directly across from the AR outfall and could be impacted by that. When expressed in percent saturation, most of the seasonal pattern disappeared (Figure 35). Interestingly, AR21 on Cameron Run above Telegraph Rd. consistently exhibited supersaturated DO which does not have an obvious cause.

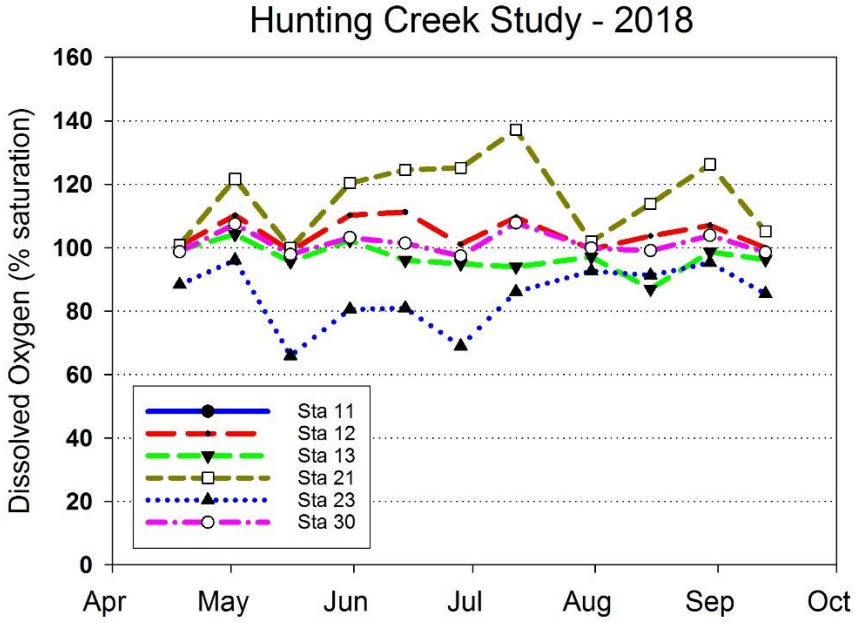

Figure 35. Dissolved Oxygen (% saturation) GMU Field Data. Month tick is at first day of month.

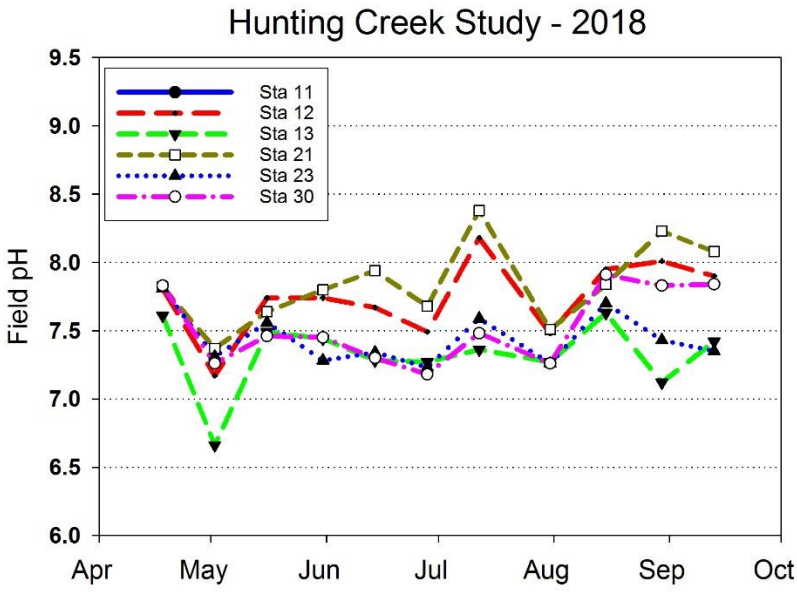

Figure 36. Field pH. GMU Field Data. Month tick is at first day of month.

Field pH was consistently in the 7.2 to 8.0 range at tributary stations (Figures 36 and 37).-AR 12 and 21 exhibited higher values on some occasions which corresponded to the higher DO values noted above. This would suggest that photosynthesis was involved perhaps due to benthic algae which may have developed during this one summer period of relatively low streamflow in Cameron Run. Lab pH displayed similar patterns including the higher values in early July at AR12 and AR 21.

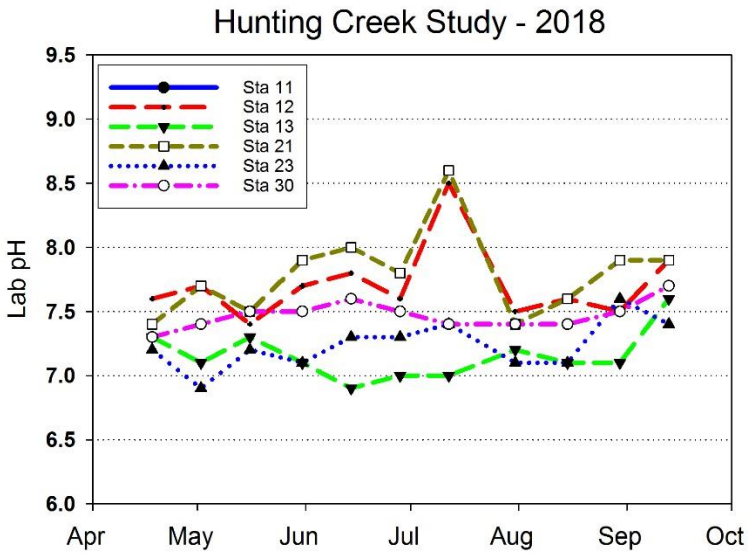

Figure 37. Lab pH. Alex Renew Lab Data. Month tick is at first day of month.

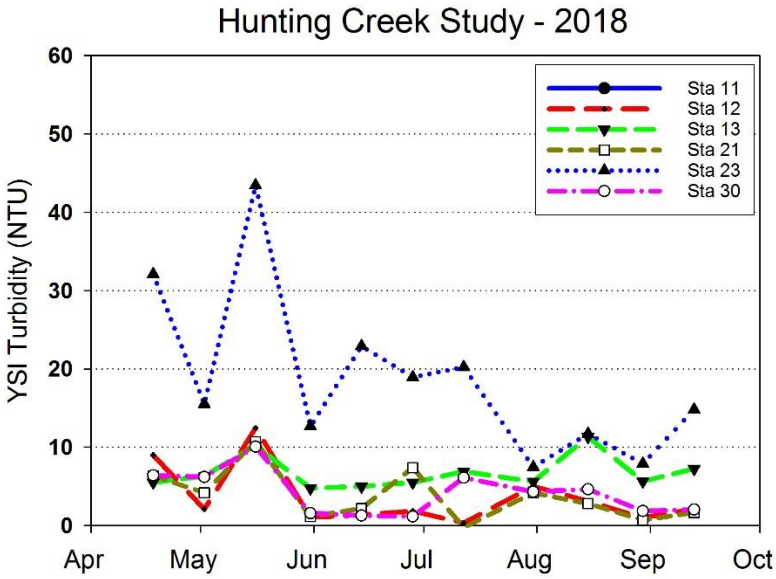

Figure 38. YSI Turbidity. GMU Field Data. Month tick is at first day of month.

Turbidity values were generally quite low (<10 units) at all tributary stations (Figure 38). Given the very wet summer, this was somewhat unexpected as high flows generally mobilize sediments in the watershed resulting in increased turbidity. However, the flows are very flashy and subside quickly. Chlorophyll was generally low in the 1-4 µg/L range (Figure 39). Higher values were observed at AR23 which is influenced by water from the river at high tide. Values also increased in late May and late July at most stations. AR13 which is fed by underground pipe flow was very low in algae and thus chlorophyll *a*.

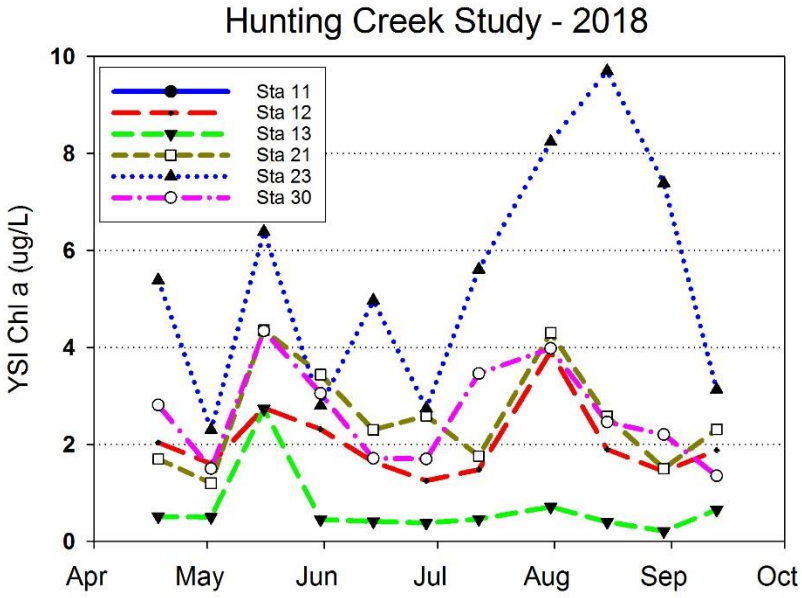

Figure 39. YSI Chlorophyll a. GMU Field Data. Month tick is at first day of month.

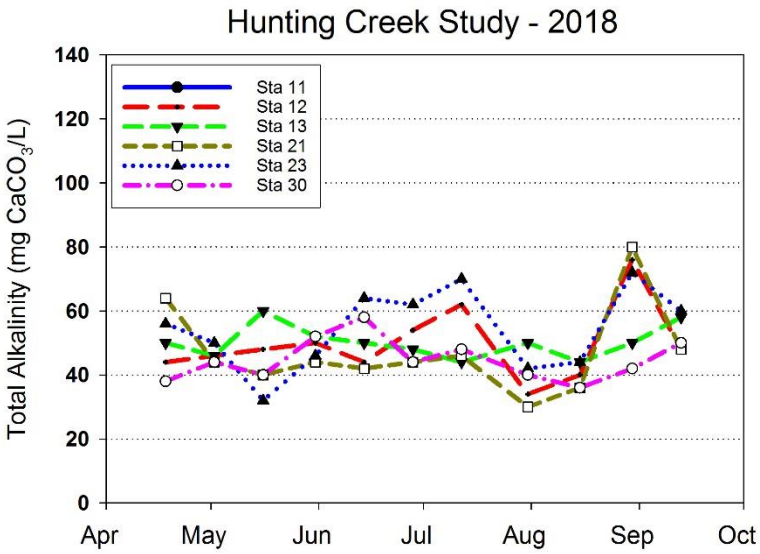

Figure 40. Total Alkalinity (mg/L as $CaCO_3$) AlexRenew Lab Data. Month tick is at first day of month.

Total alkalinity was generally in the 40-60 mg/L range with little seasonal pattern apparent (Figure 40). Somewhat higher values were observed in late August at some stations. Chloride levels showed a general seasonal decline, but varied from date-to-date, probably in response to flow conditions (Figure 41).

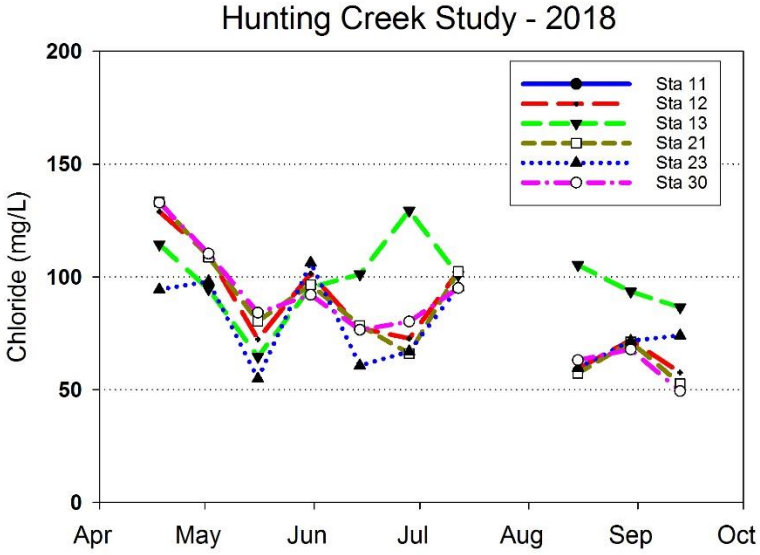

Figure 41. Chloride (mg/L) AlexRenew Lab Data. Month tick is at first day of month.

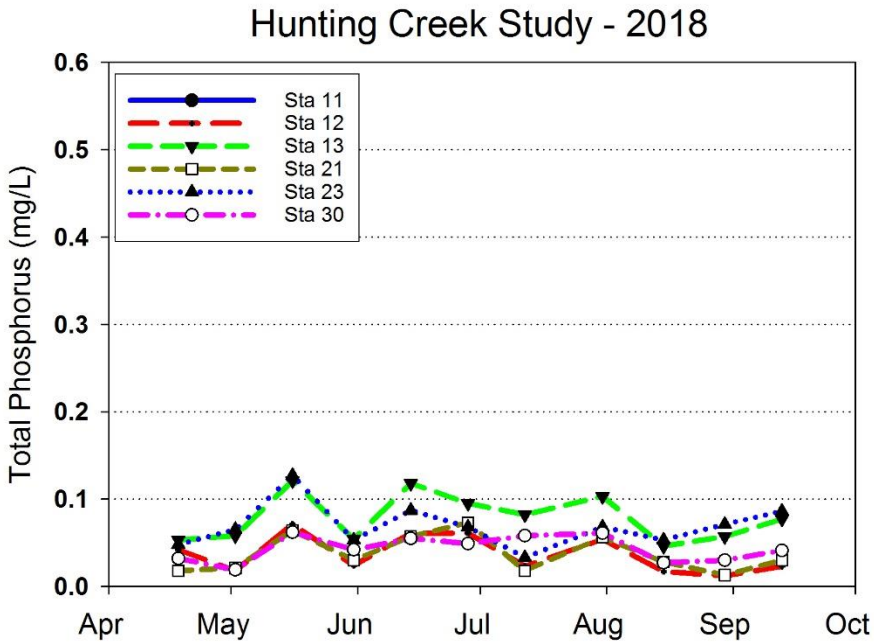

Figure 42. Total Phosphorus (mg/L) AlexRenew Lab Data. Month tick is at first day of month.

Total phosphorus levels were generally relatively low at most tributary stations and did not vary much seasonally (Figure 42). Ortho phosphorus levels hovered around 0.02 mg/L (Figure 43).One high reading was found at AR13.

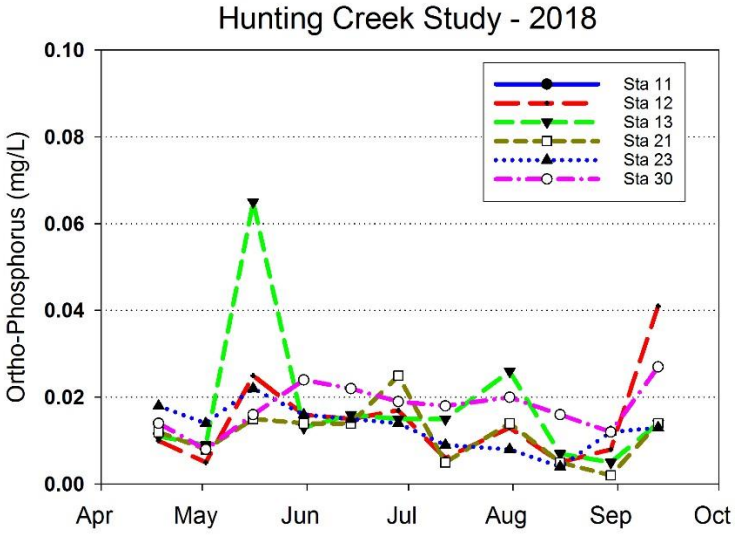

Figure 43. Ortho-Phosphorus (mg/L) AlexRenew Lab Data. Month tick is at first day of month.

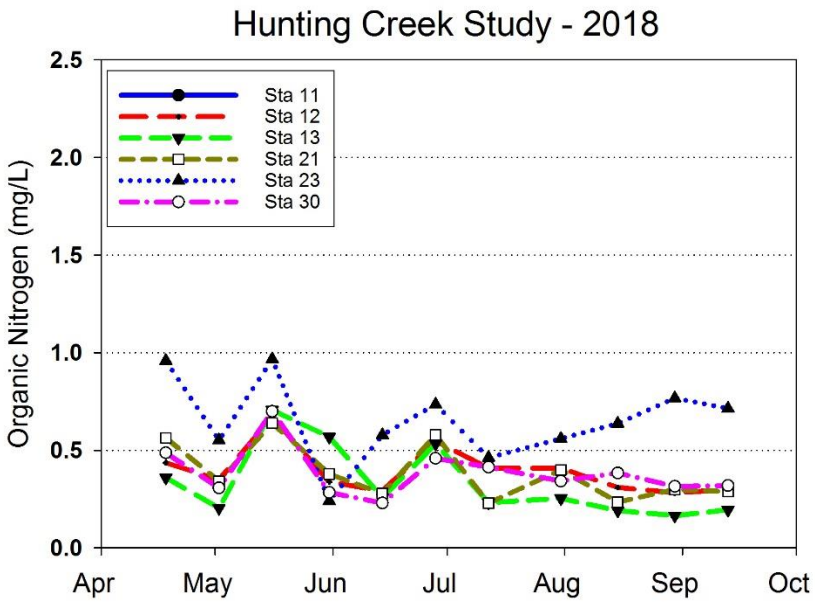

Figure 44. Organic Nitrogen (mg/L) AlexRenew Lab Data. Month tick is at first day of month.

Tributary levels of organic nitrogen are depicted in Figure 44. At AR23 values hovered between 0.5 mg/L and 1.0 mg/L for most of the year whereas at most of the other stations values were 0.2-0.5 mg/L. Ammonia nitrogen values were quite low (<0.2 mg/L) over most of the period at all stations (Figure 45).

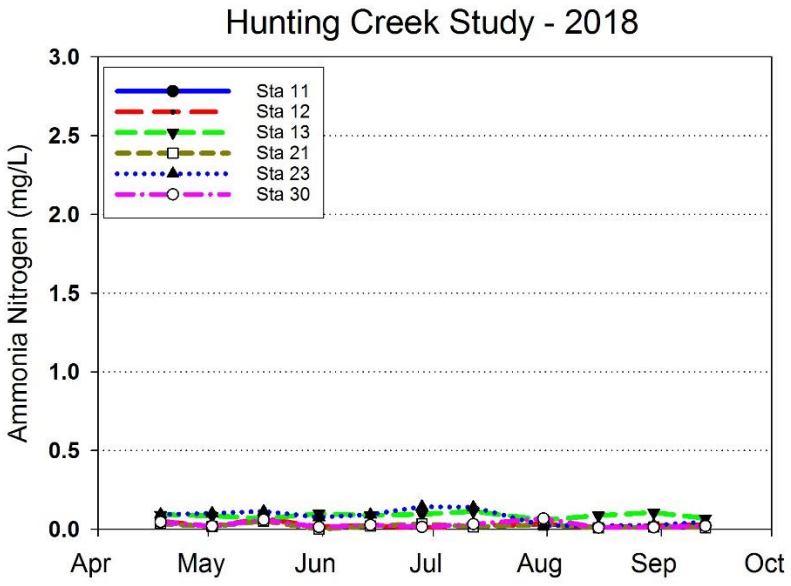

Figure 45. Ammonia Nitrogen (mg/L) AlexRenew Lab Data. Month tick is at first day of month.

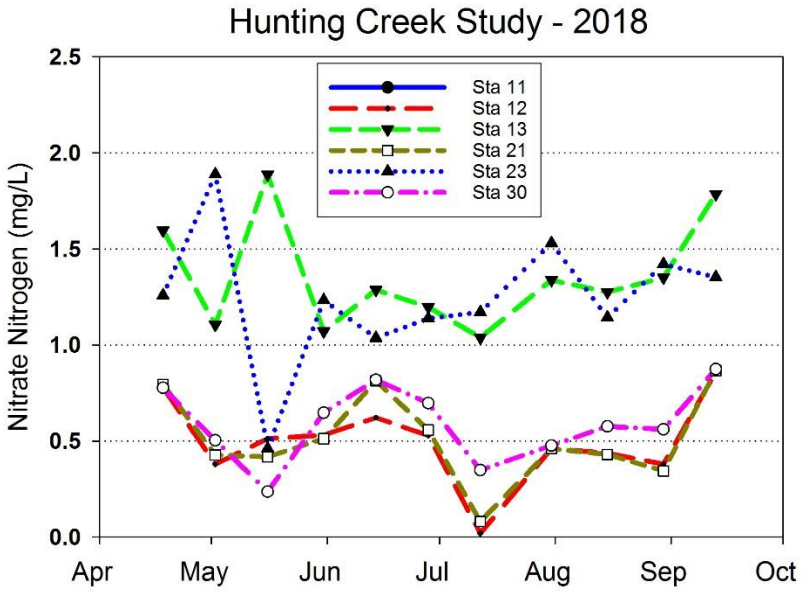

Figure 46. Nitrate Nitrogen (mg/L) AlexRenew Lab Data. Month tick is at first day of month.

Nitrate nitrogen values exhibited clear spatial variation (Figure 46). Values were elevated at AR23 and AR13 but probably for different reasons. AR13, with values hovering around 1 mg/L, is primarily runoff from urbanized areas of Alexandria and so the nitrogen at AR13 probably originates from nonpoint sources. AR23 is downstream from the Alex Renew outfall which probably accounts for the elevated levels there. Nitrite nitrogen was generally quite low at all stations (Figure 47). The exception was a high value at AR30 in late May which may be an error.

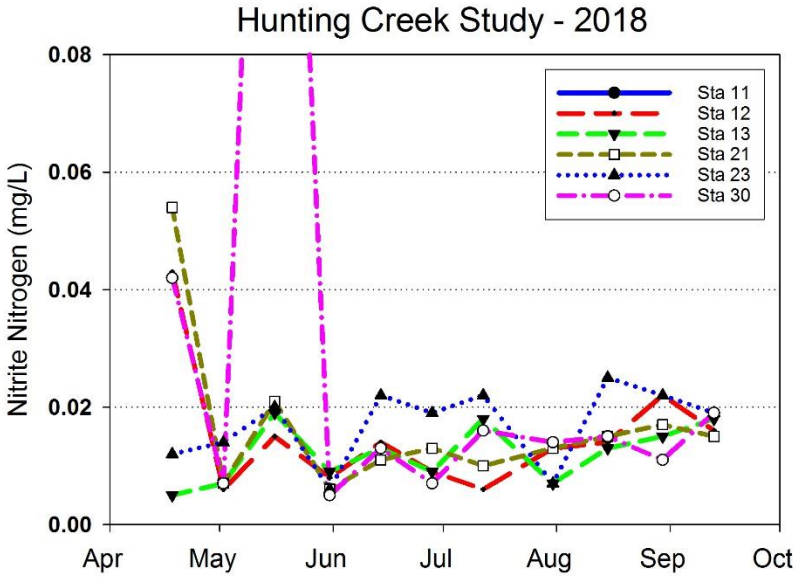

Figure 47. Nitrite Nitrogen (mg/L) AlexRenew Lab Data. Month tick is at first day of month.

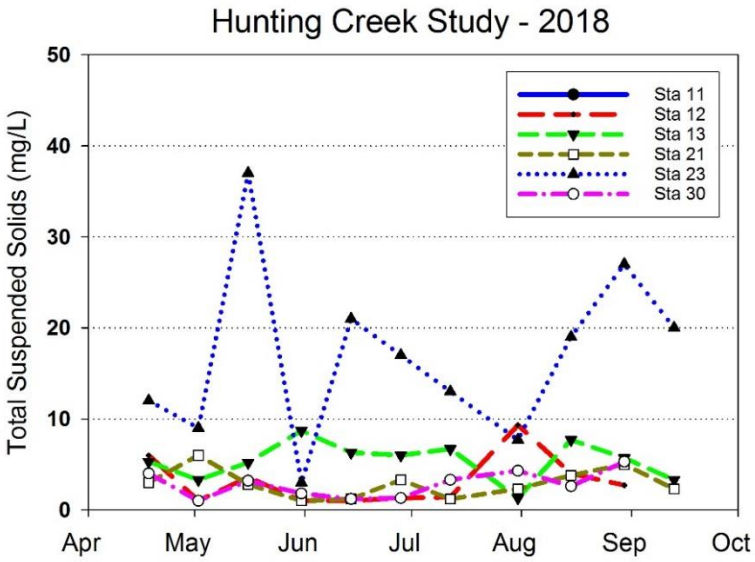

Figure 48. Total Suspended Solids (mg/L) AlexRenew Lab Data. Month tick is at first day of month.

Total suspended solids concentrations at tributary stations are shown in Figure 48. TSS was quite low (<10 mg/L) at most stations for most of the year. The exception was AR 23 which was strongly influenced by Hunting Creek via tidal action. Again, the results are somewhat surprising given the wet summer, but as stated previously, these streams clear quickly after a storm. Similar trends were observed volatile suspended solids (Figure 49) with some higher values also observed at AR23.

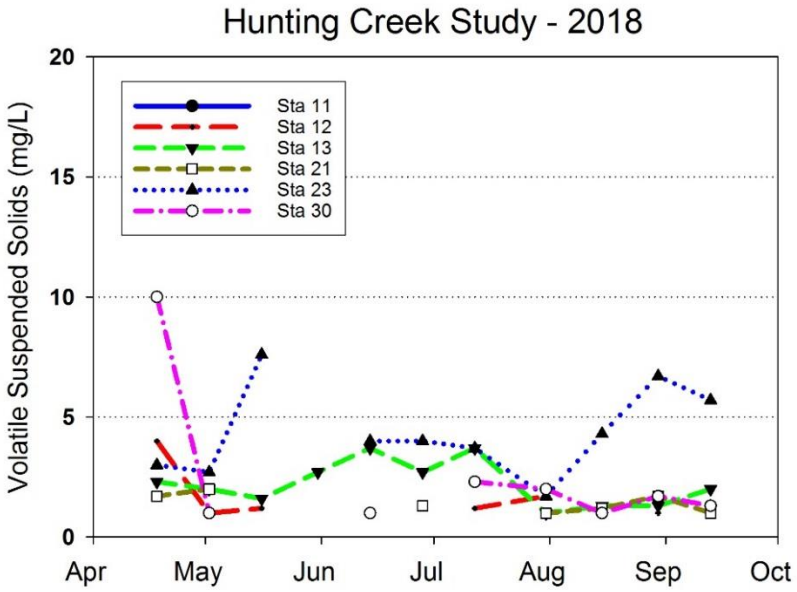

Figure 49. Volatile Suspended Solids (mg/L) AlexRenew Lab Data. Month tick is at first day of month.

D. Phytoplankton - 2018

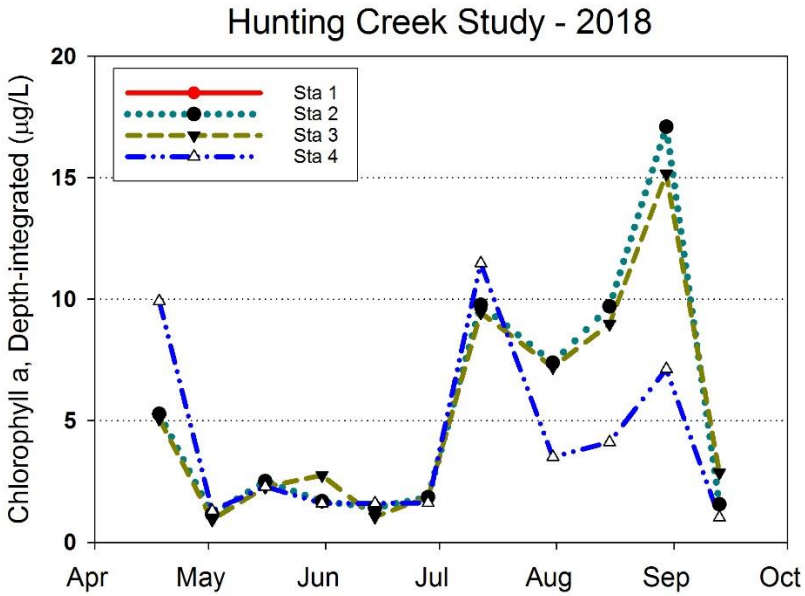

Chlorophyll *a* is a measure of the amount of algae growing in the water column. These suspended algae are called phytoplankton, meaning "plant wanderers". In addition to the true algae (greens, diatoms, cryptophytes, etc.) the term phytoplankton includes cyanobacteria (sometimes known as "blue-green" algae). Both depth-integrated and surface chlorophyll values are measured due to the capacity of phytoplankton to aggregate near the surface under certain conditions.

Figure 50. Chlorophyll *a* (µg/L). Depth-integrated. GMU Lab Data. Month tick is at the first day of month.

Chlorophyll *a* began the year at moderate levels (5-10 µg/L) at all stations in April (Figures 50&51). A major decline occur in early May due to flushing from rain event runoff and these low values continued through the end of June. The system recovered in mid July at all stations reaching levels above 10 µg/L and in late August a second peak was observed at 15-20 µg/L at AR2 and AR3. The August peak was much smaller at river station AR4, but substantially larger at AR1.

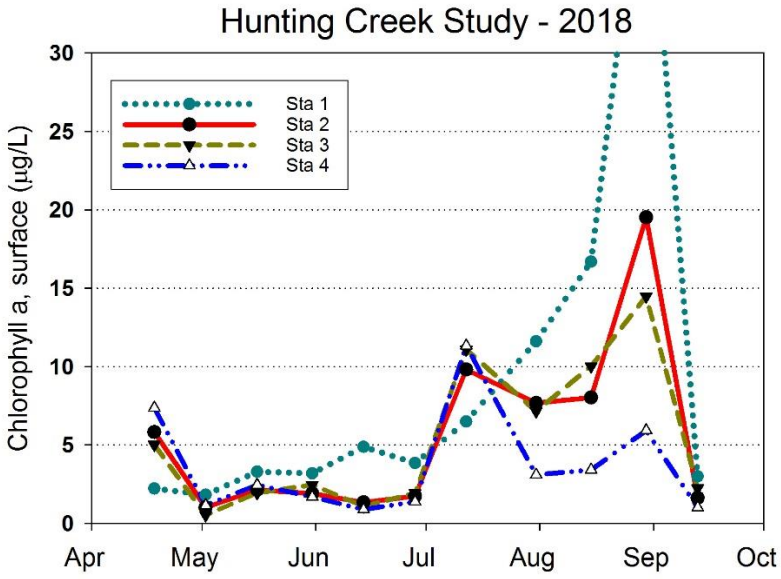

In the tidal freshwater Potomac generally, there is very little difference in surface and depth-integrated chlorophyll levels because tidal action keeps the water well-mixed which overcomes any potential surface aggregation by the phytoplankton. Summer chlorophyll concentrations above 30 ug/L are generally considered characteristic or eutrophic conditions.

Figure 51. Chlorophyll *a* (µg/L). Surface. GMU Lab Data. Month tick is at first day of month.

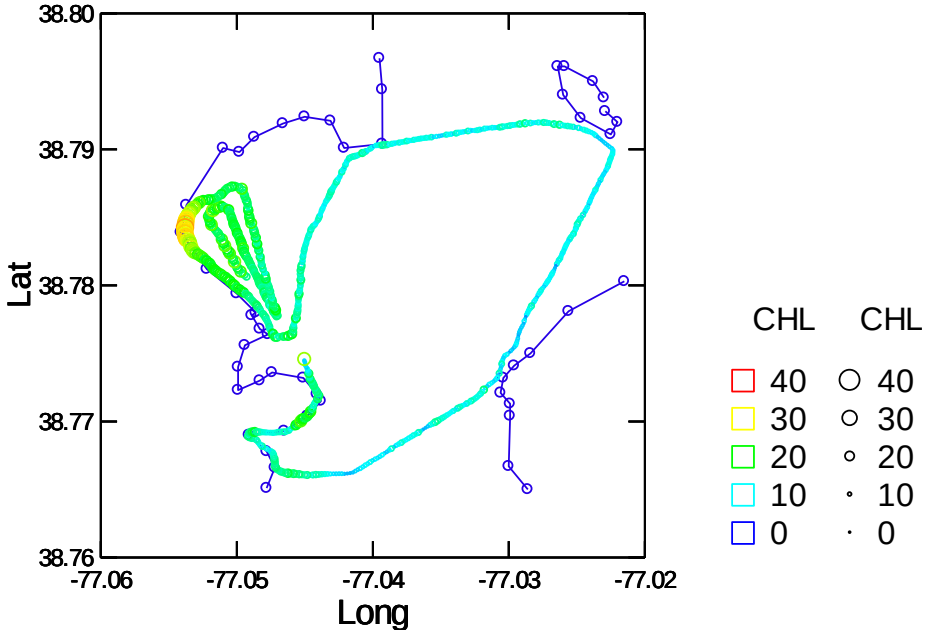

Figure 52a. Water Quality Mapping. July 16, 2018. Chlorophyll YSI (mg/L).

On the July 16 a spatial pattern was observed in chlorophyll with very low values in the river mainstem and somewhat higher values in the Hunting Creek embayment, but not on the Maryland side of the river (Figure 52a). On August 28 Values were even lower in the river mainstem with highest values on the western side of Hunting Creek (Figure 52b).

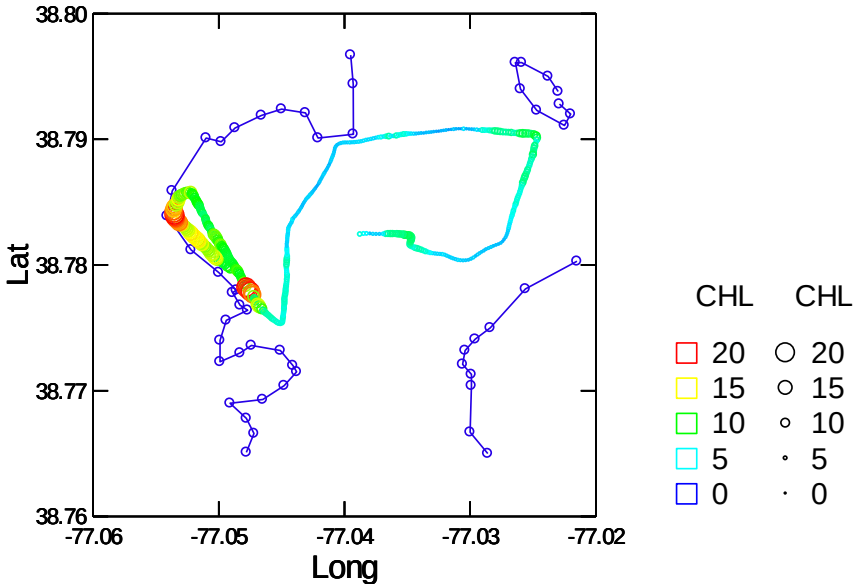

Figure 52b. Water Quality Mapping. August 28, 2018. Chlorophyll YSI (mg/L).

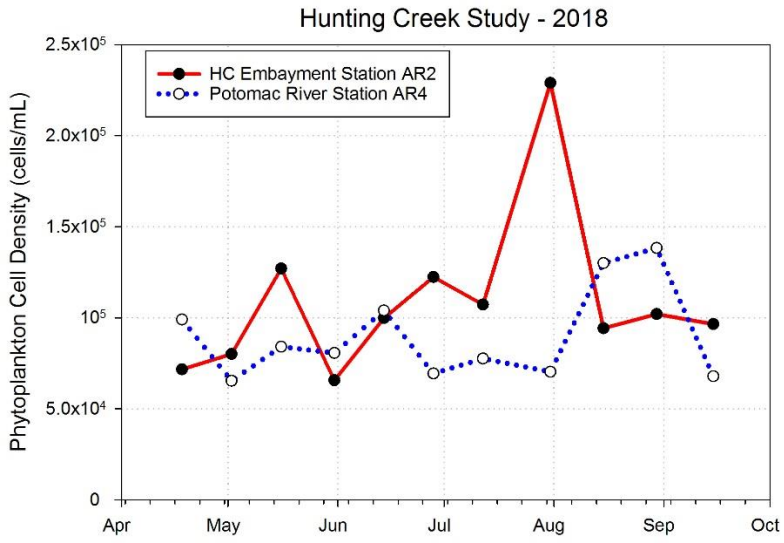

Phytoplankton cell density provides a measure of the number of algal cells per unit volume. This is a rough measure of the abundance of phytoplankton, but does not discriminate between large and small cells. Therefore, a large number of small cells may actually represent less biomass (weight of living tissue) than a smaller number of large cells. However, small cells are typically more active than larger ones so cell density is probably a better indicator of activity than of biomass. The smaller cells are mostly cyanobacteria.

Figure 53. Phytoplankton Cell Density (cells/mL).

Phytoplankton cell density followed different patterns at the two sites (Figure 53). At AR2 in Hunting Creek embayment values were increased through mid May, declined in early June and then increased to a peak in late July before dropping back. At AR4 in the river mainstem there was a peak in mid June and in late August followed by a decline. Total biovolume exhibited similar seasonal ups and downs, but the dates of the peaks were not necessarily the same as those for cell density (Figure 54). In the river mainstem a mid June peak was found in both graphs. However, a mid August peak was found in biovolume in the river compared with a late August peak in cell density. The mid July peaks in chlorophyll *a* peak in the embayment was better reflected in biovolume than in cell density.

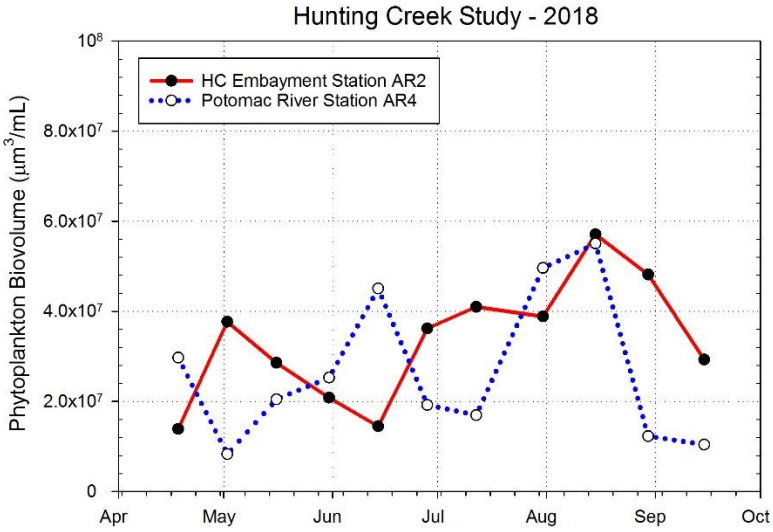

The volume of individual cells of each species is determined by approximating the cells of each species to an appropriate geometric shape (e.g. sphere, cylinder, cone, cube, etc.) and then making the measurements of the appropriate dimensions under the microscope. Total phytoplankton biovolume (shown here) is determined by multiplying the cell density of each species by the biovolume of each cell of that species. Biovolume accounts for the differing size of various phytoplankton cells and is probably a better measure of biomass. However, it does not account for the varying amount of water and other nonliving constituents in cells.

Figure 54. Phytoplankton Biovolume (um^3/mL).

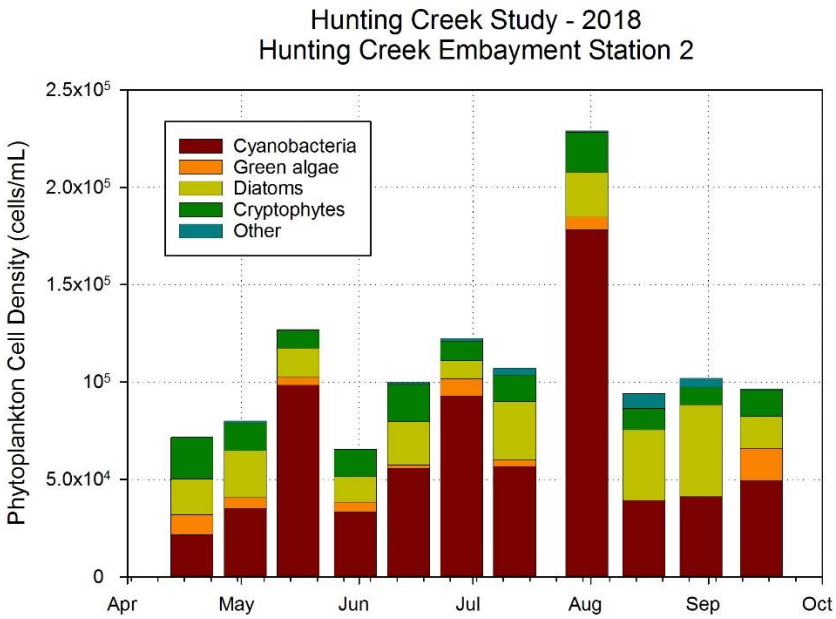

Total phytoplankton cell density can be broken down by major group. **Cyanobacteria** are sometimes called "blue-green algae". **Other** includes euglenoids and dinoflagellates. Due to their small size cyanobacteria typically dominate cell density numbers. Their numbers are typically highest in the late summer reflecting an accumulation of cells during favorable summer growing conditions.

Figure 55. Phytoplankton Density by Major Group (cells/mL). Hunting Creek.

Phytoplankton cell density was distributed fairly evenly among three major groups (cyanobacteria, diatoms, and cryptophytes) at both stations although cyanobacteria were typically the most numerous (Figures 55&56). The major exception to this at the embayment station AR2 was late July when cyanobacteria were strongly dominant at both stations and responsible for the above-normal values on this date. The same was true of the August peaks at the river station AR4.

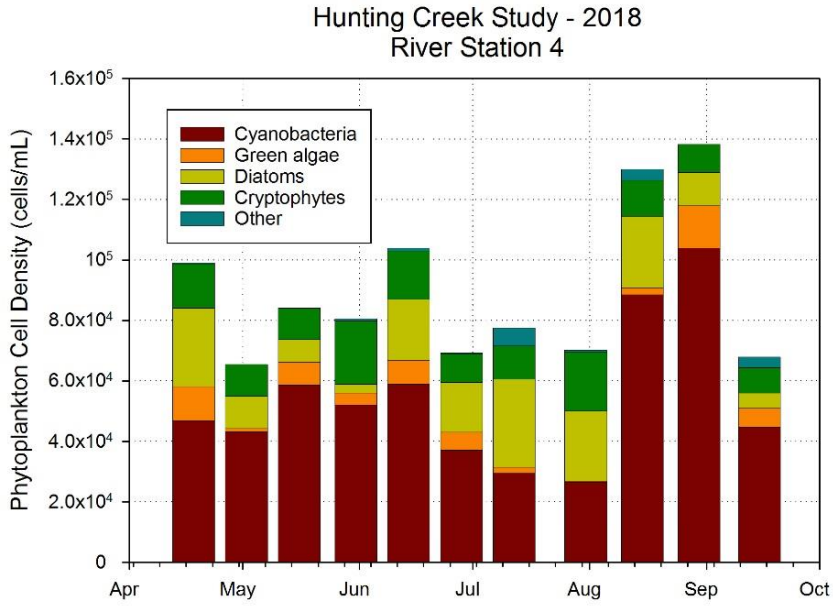

In the river cyanobacteria normally follow similar patterns as in the embayments, but may attain lower abundances. This is probably due to the deeper water column which leads to lower effective light levels and greater mixing. Other groups such as diatoms and green algae tend to be more important on a relative basis than in the embayments.

Figure 56. Phytoplankton Density by Major Group (cells/mL). River.

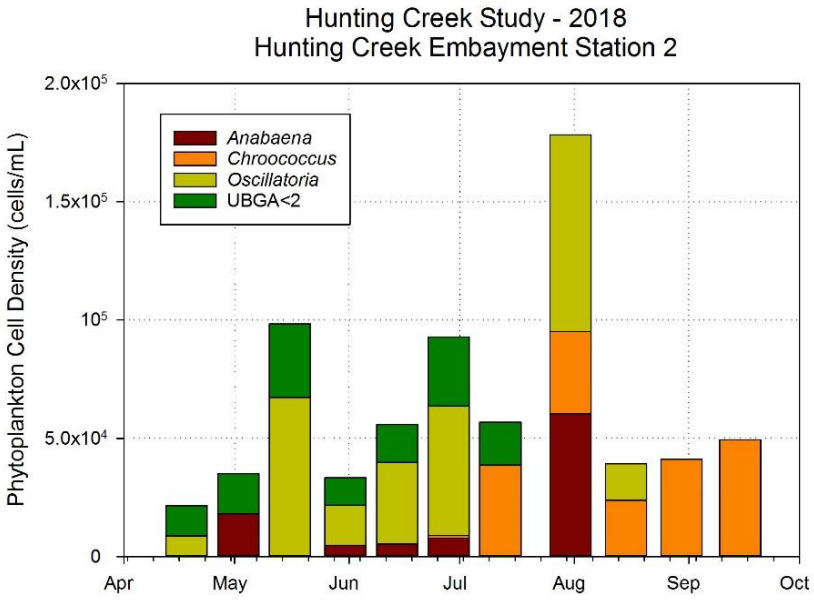

The dominant cyanobacteria on a numerical basis were:
- *Oscillatoria* – a filament with disc-like cells
- *Anabaena* – a filament with bead-like cells & heterocysts
- *Chroococcus* – individual spherical cells
- Unknown cyanobacterium About 2 um

Figure 57. Phytoplankton Density by Dominant Cyanobacteria (cells/mL). Hunting Creek.

Oscillatoria was the most important cyanobacterium at both stations through most of the year (Figure 57&58); *Chroococcus* was mainly a late summer and early fall genus. Anabaena was particularly abundant in lat July and early August while an unknown cyanobacterium (UBGA<2) was mainly found in the spring and early summer.

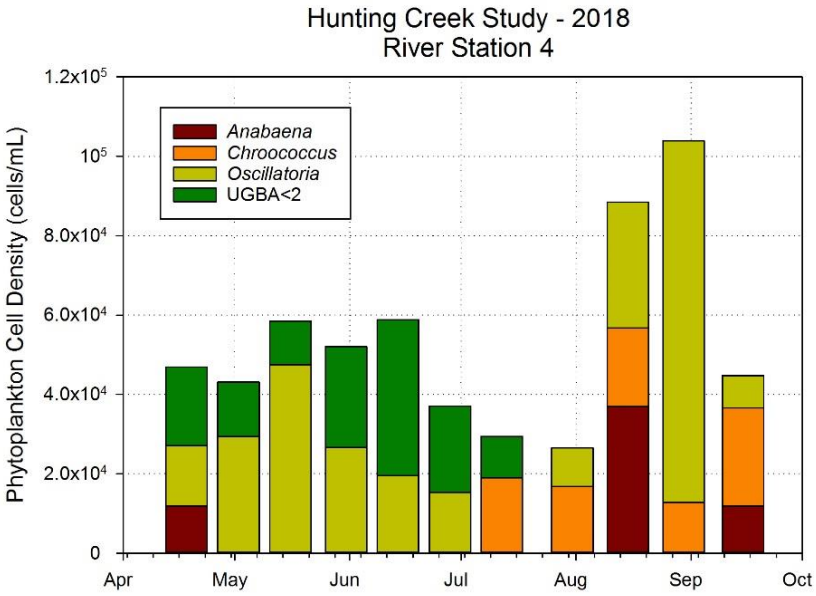

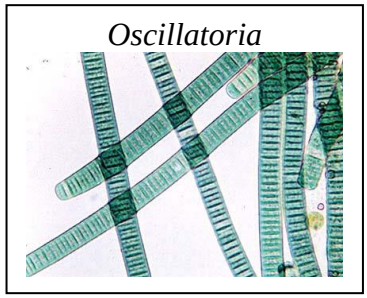

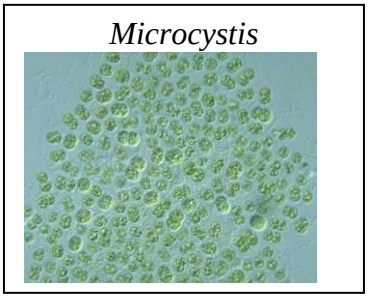

Figure 58. Phytoplankton Density by Dominant Cyanobacteria (cells/mL). River.

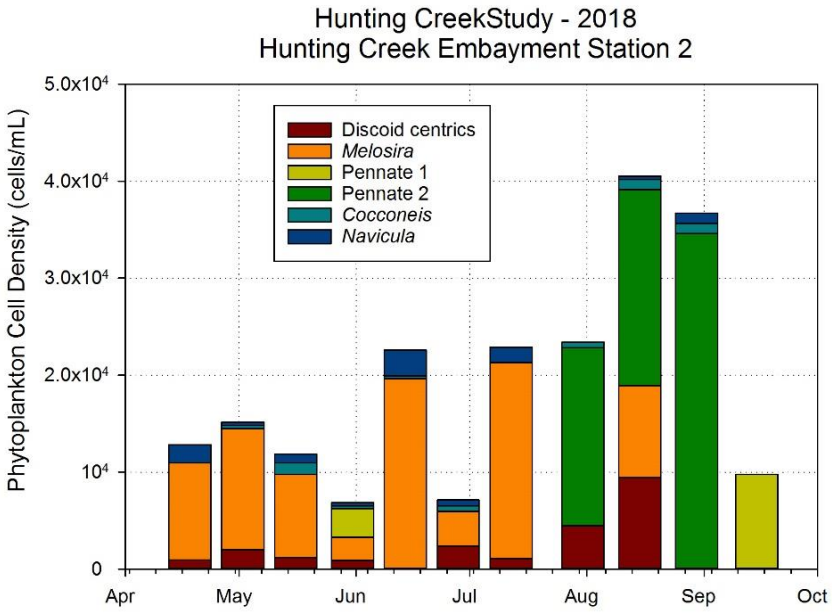

The most numerous non-diatom phytoplankters were:
Discoid centrics – mostly *Cyclotella*
Melosira – a filamentous centric diatom
Pennate 1
Pennate 2
Cocconeis – a pennate
Navicula – a pennate

Figure 59. Phytoplankton Density (#/mL) by Dominant Diatom Taxa. Hunting Creek.

Melosira was the dominant diatom in spring and early summer in at both stations with Pennate 2 taking over in August. (Figure 59&60). Discoid centrics had appreciable numbers in many samples at both stations.

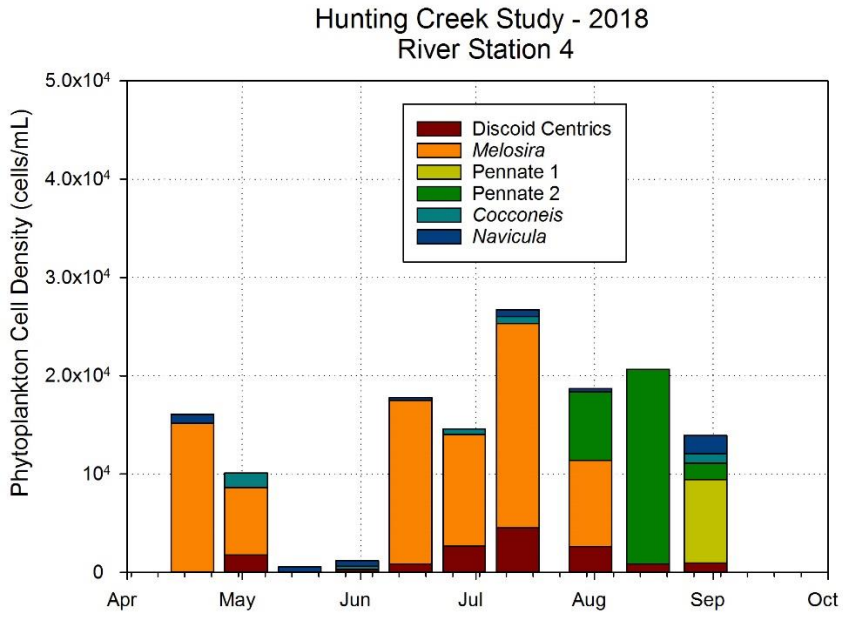

Melosira

Figure 60. Phytoplankton Density (#/mL) by Dominant Diatom Taxa. River.

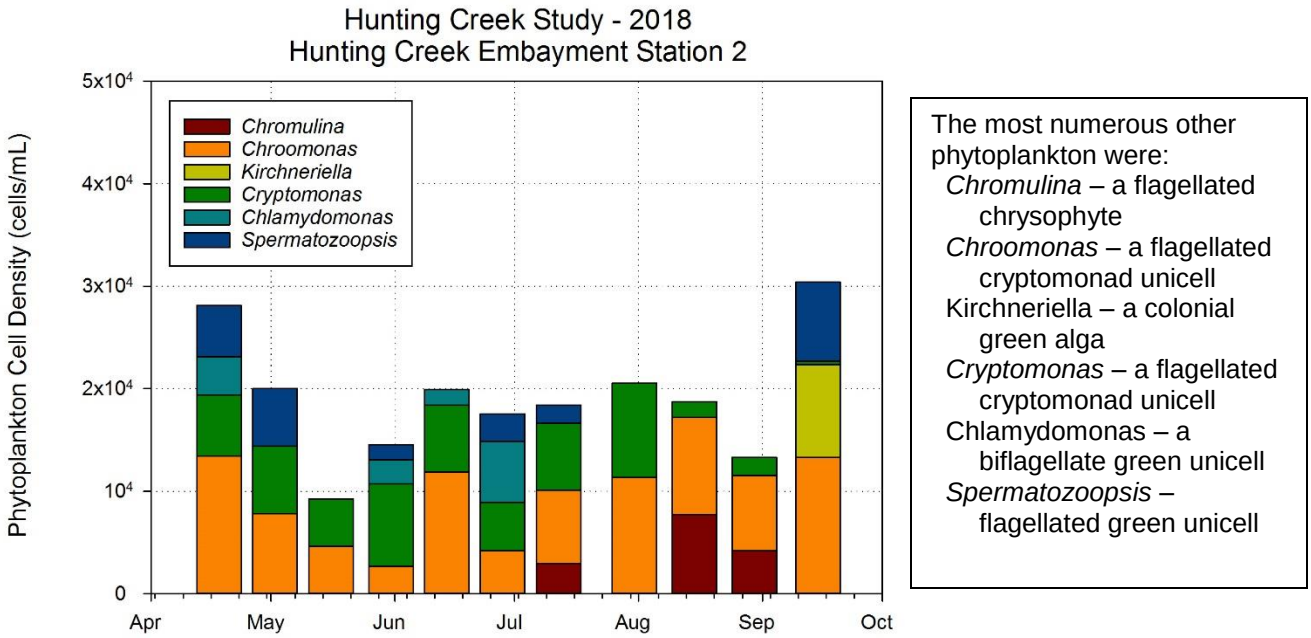

Figure 61. Phytoplankton Density (#/mL) by Dominant Other Taxa. Hunting Creek.

Phytoplankton species that were neither cyanobacteria nor diatoms were grouped together as "other" for these graphs; these included most numerous taxa of green algae, cryptophytes, euglenoids, and dinoflagellates. At both stations the cryptophytes *Cryptomonas* and *Chroomonas* were consistently the most numerous (Figure 61&62). The green algae *Chlamydomonas*, *Spermatozoopsis*, and *Kirchnerella* and the chrysophyte *Chromulina* were important in selected samples.

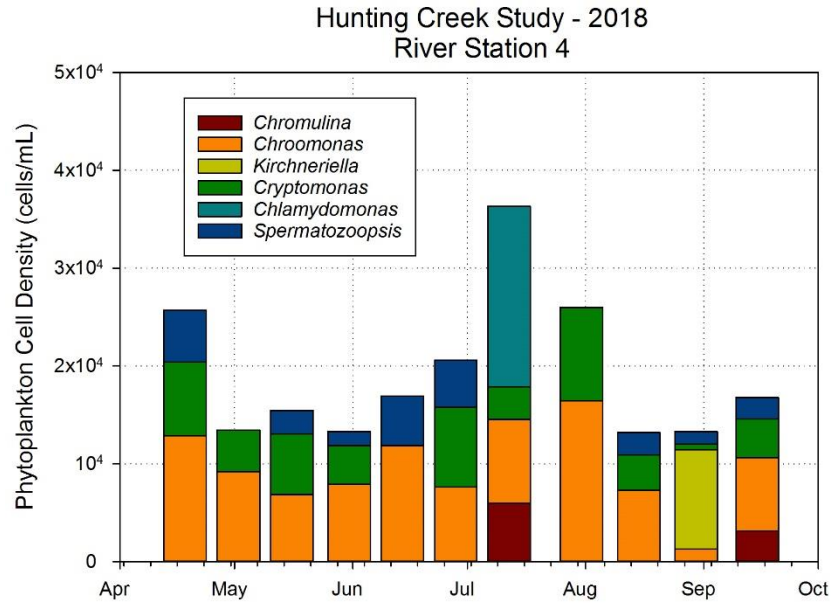

Figure 62. Phytoplankton Density (#/mL) by Dominant Other Taxa. River.

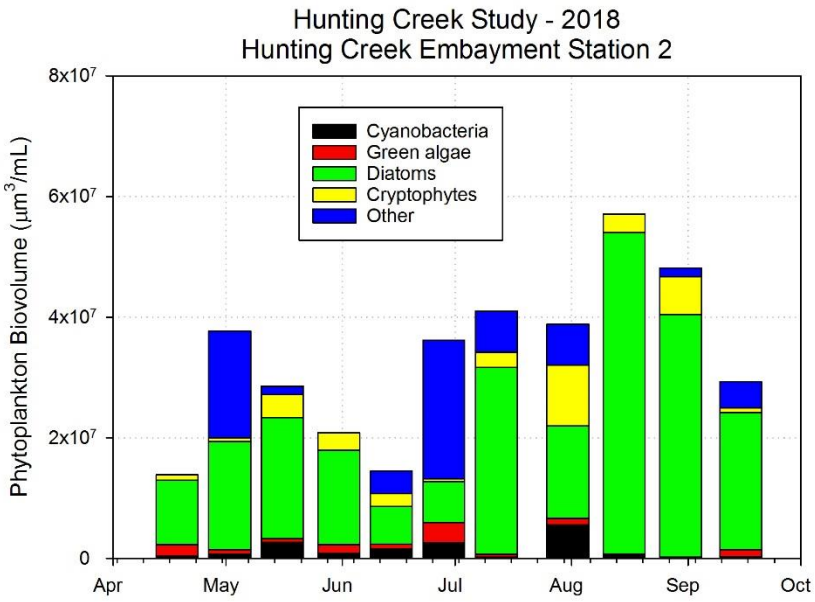

Total phytoplankton biovolume can be broken down into groups:

- **Cyano** – cyanobacteria ("blue-green" algae)
- **Greens** – green algae
- **Diatoms** – includes both centric and pinnate
- **Cryptos** – cryptophytes
- **Other** – includes euglenoids, chrysophytes, and dinoflagellates

Figure 63. Phytoplankton Biovolume (um³/mL) by Major Groups. Hunting Creek.

At AR 2 in Hunting Creek diatoms were dominant in biovolume in most samples (Figure 63). Peak densities were observed in early May, mid July, and mid August. Cryptophytes and Other algae were important on some dates. In the river, diatoms were again dominant on most dates (Figure 64). However, in mid August Other algae were dominant.

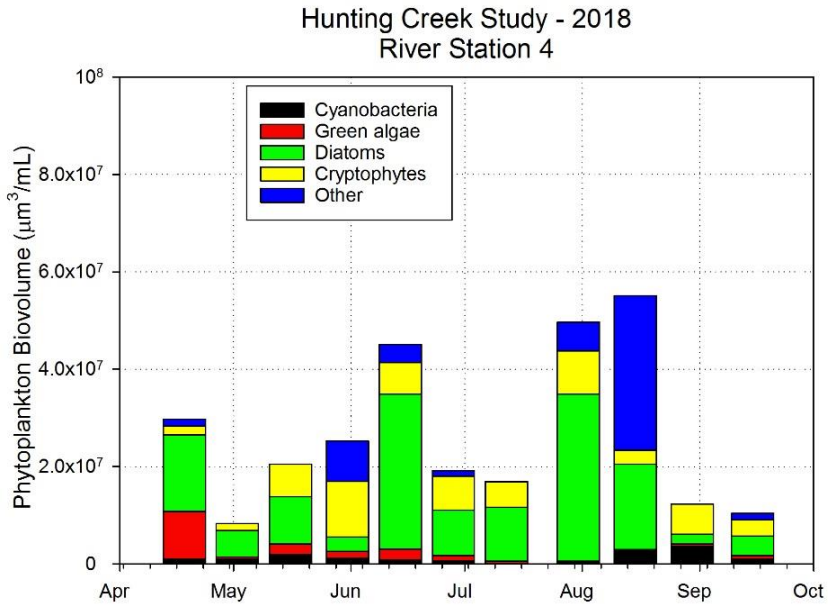

While dominating cell density, cyanobacteria typically make up a much smaller portion of phytoplankton biovolume. Diatoms generally are dominant.

Figure 64. Phytoplankton Biovolume (um³/mL) by Major Groups. River.

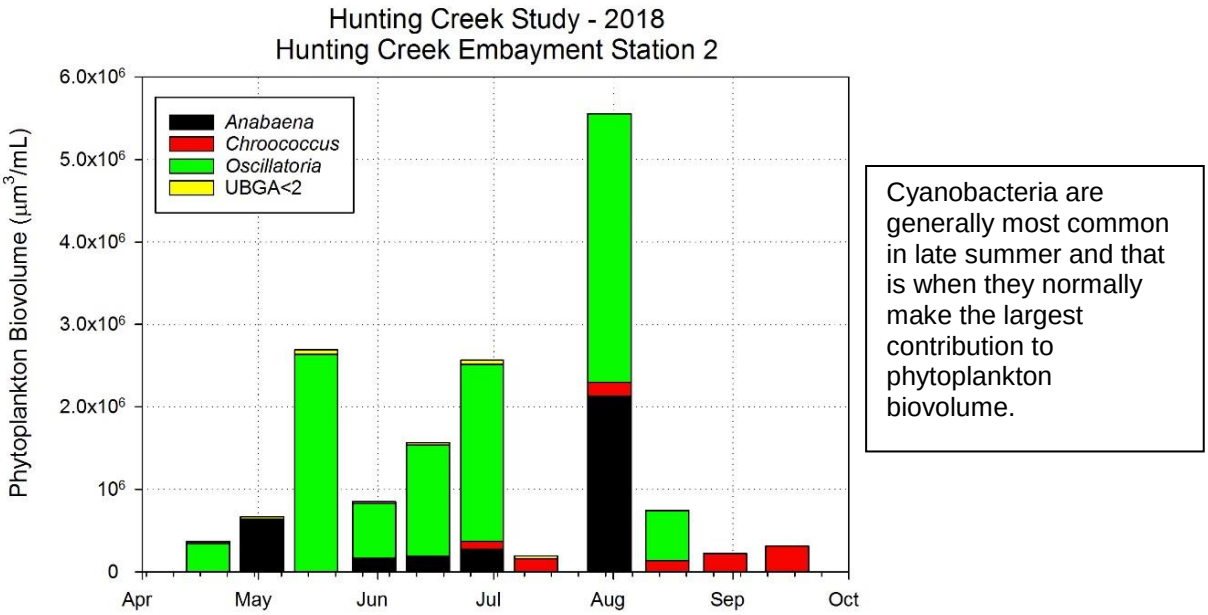

Figure 65. Phytoplankton Biovolume (um^3/mL) by Cyanobacteria Taxa. Hunting Creek.

In Hunting Creek *Oscillatoria* dominant in almost all samples (Figure 65). *Anabaena* was co-dominant in late July. *Oscillatoria* was also the most abundant cyanobacterium at the River mainstem station during the study period, but a large peak of *Anabaena* was observed in mid August and mid September (Figure 66).

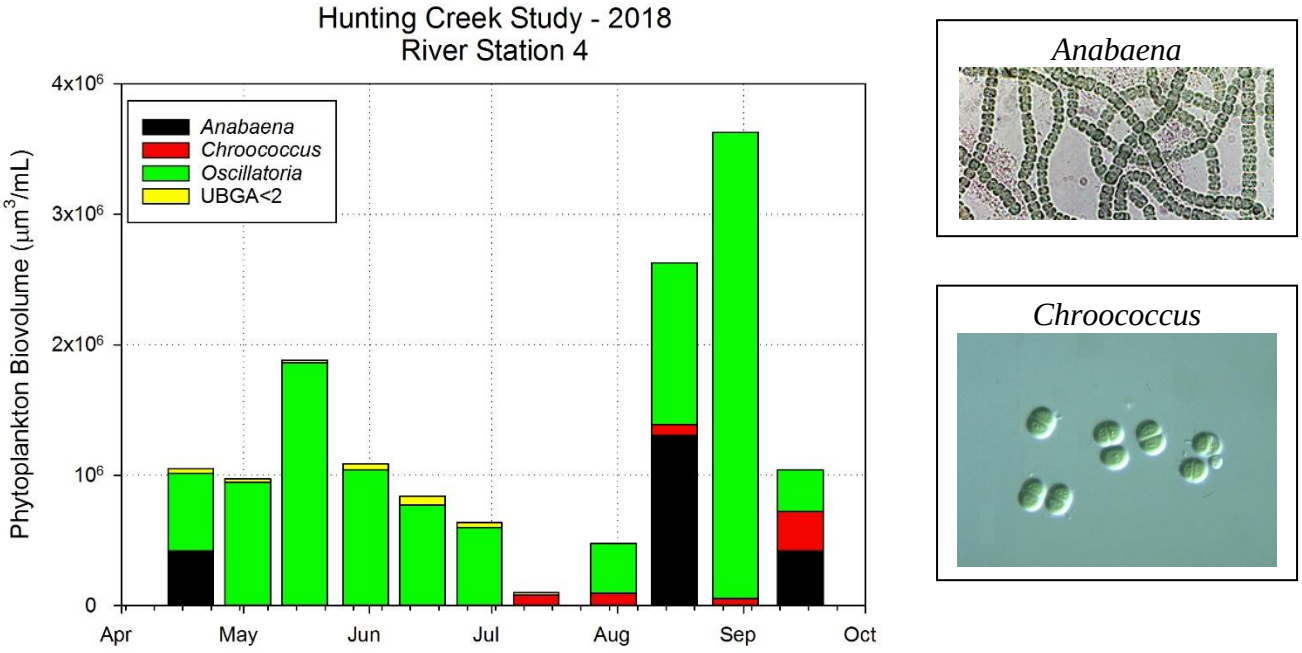

Figure 66. Phytoplankton Biovolume (um^3/mL) by Cyanobacterial Taxa. River.

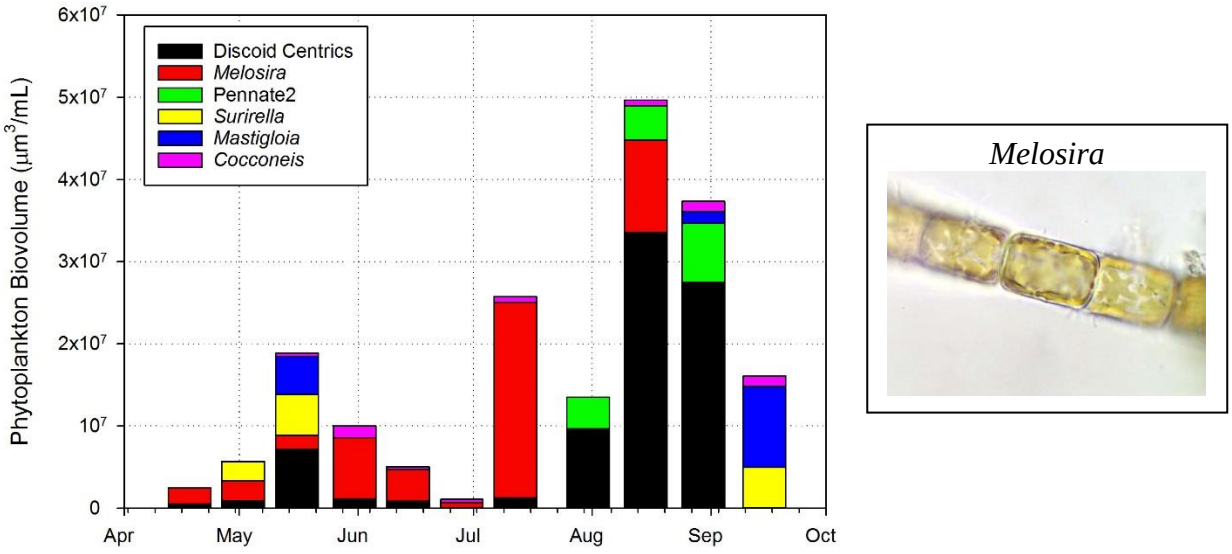

Figure 67. Phytoplankton Biovolume (um^3/mL) by Dominant Diatom Taxa. Hunting Creek.

At the embayment station AR2, *Melosira* was the dominant in biovolume in spring and early summer (Figure 67).In late summer discoid centrics became dominant. In the river, *Melosira* was dominant in early July with discoid centrics being substantial on most dates (Figure 68). Interestingly, none of the dominant diatoms was found in the late May sample.

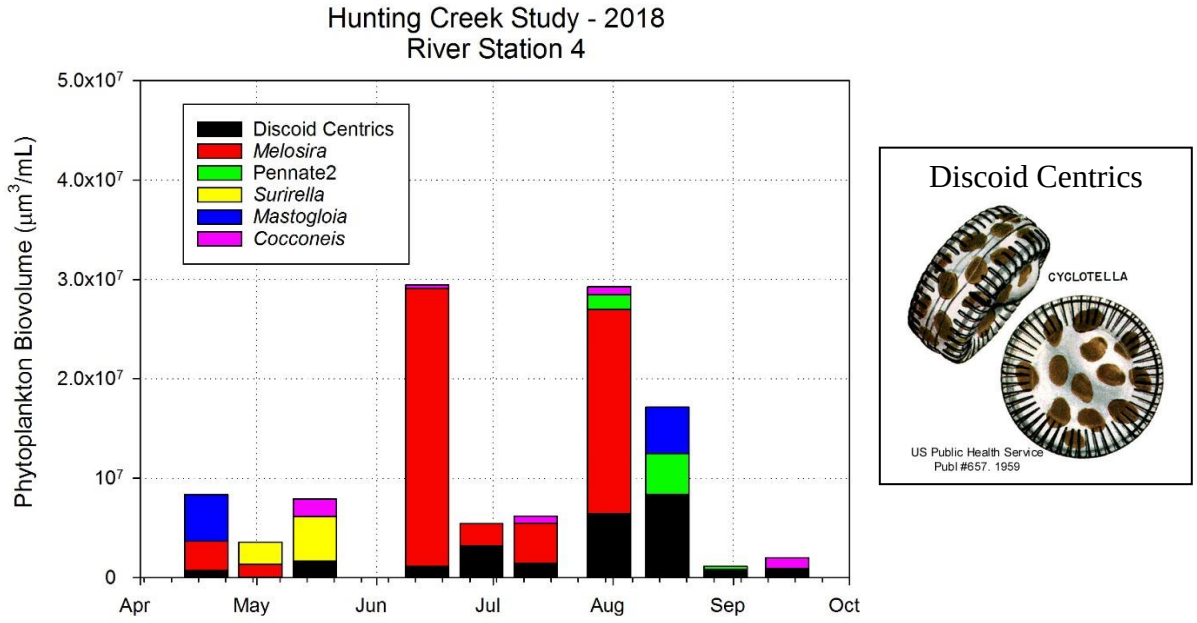

Figure 68. Phytoplankton Biovolume (um^3/mL) by Dominant Diatom Taxon. River.

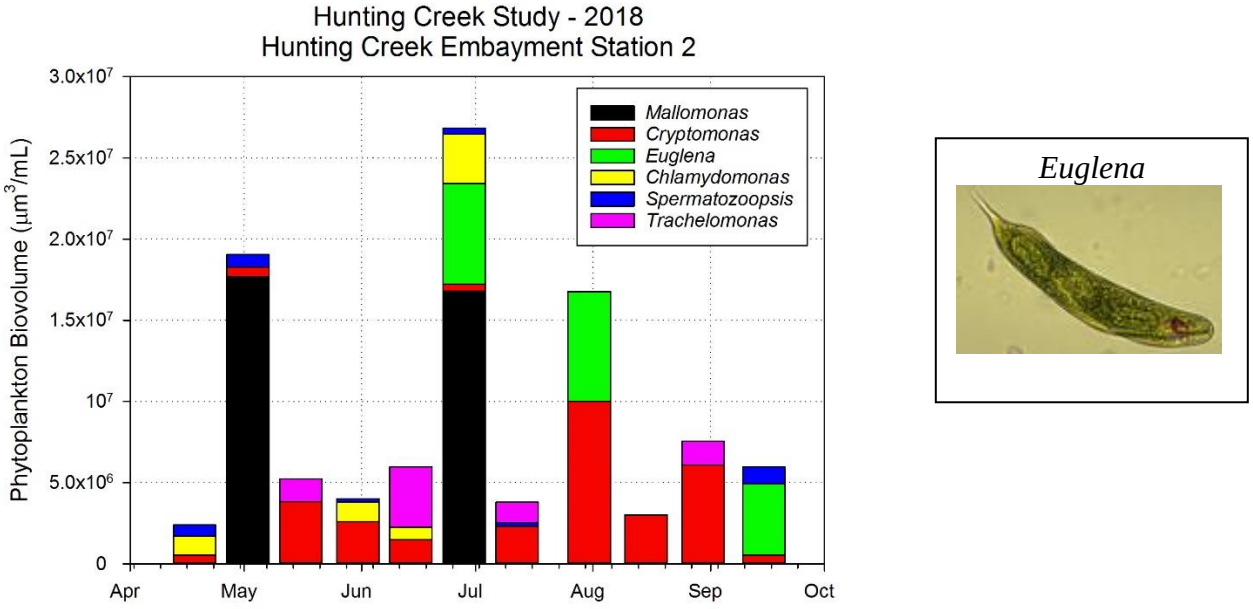

Figure 69. Phytoplankton Biovolume (um³/mL) by Dominant Other Taxa. Hunting Creek.

The large chrysophyte *Mallomonas* was a strong contributor to biovolume in Hunting Creek in early May and late July (Figure 69). Other large taxa such as the euglenoids *Euglena* and *Trachelomonas* was important on certain dates. *Cryptomonas* was most frequently dominant in the river (Figure 70).

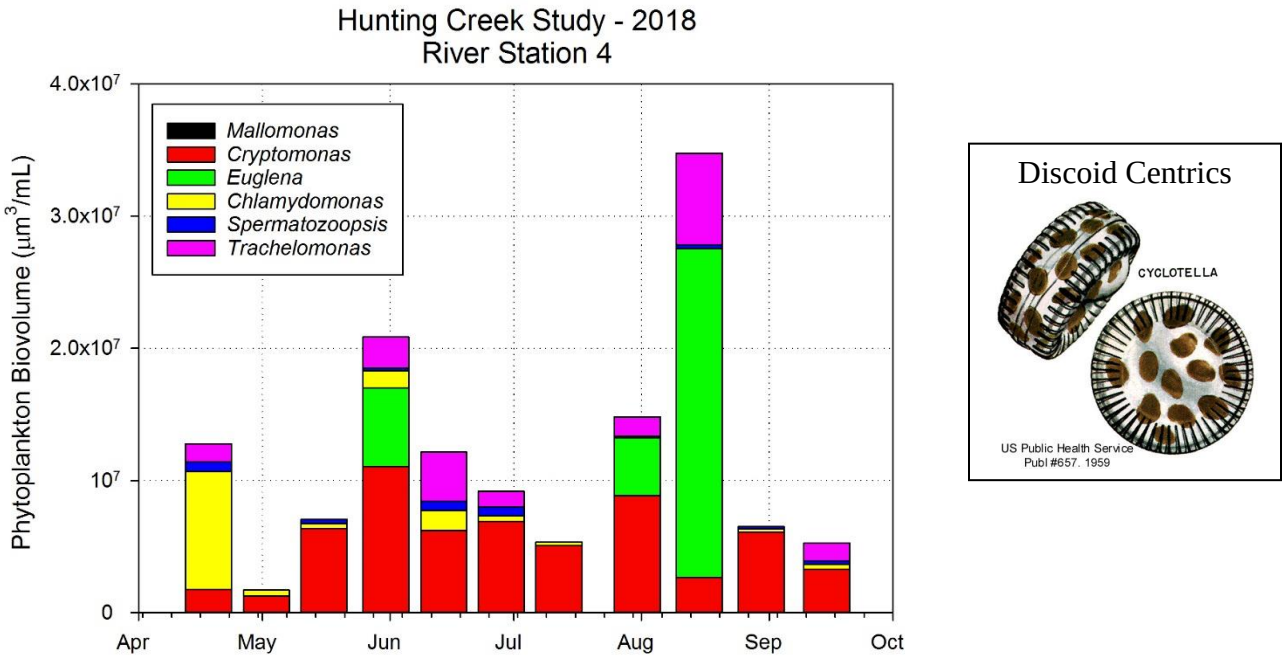

Figure 70. Phytoplankton Biovolume (um³/mL) by Dominant Other Taxon. River.

E. Zooplankton – 2018

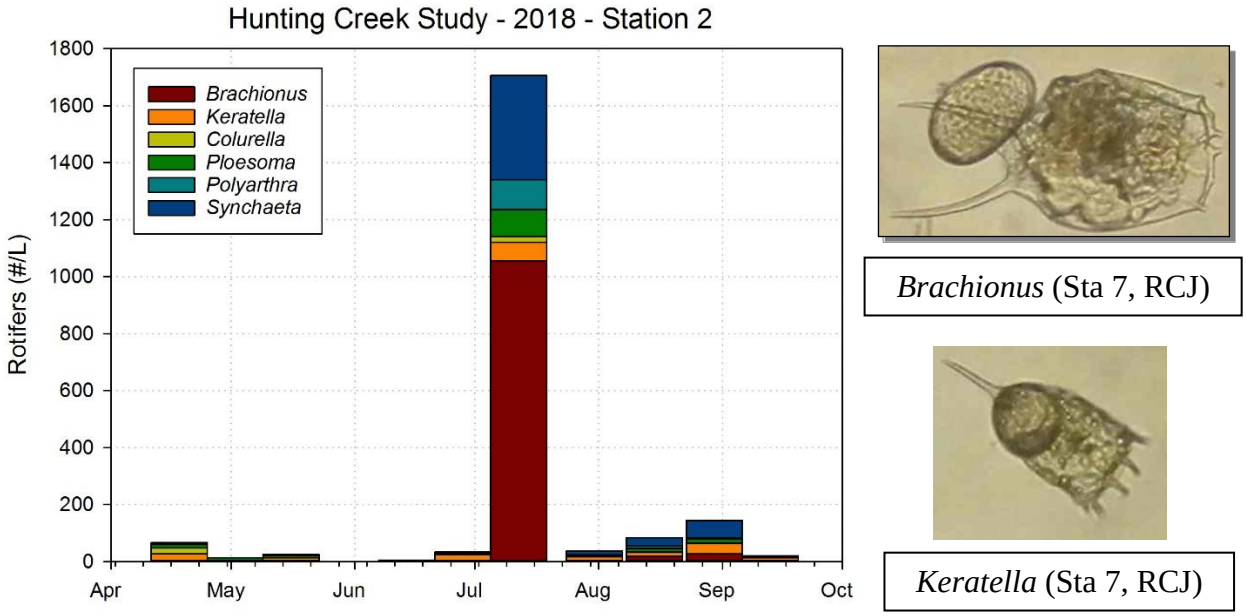

Figure 71. Rotifer Density by Dominant Taxa (#/L). Hunting Creek.

At both stations rotifer populations were very low for most of the year, values of less than 100/L being typical (Figure 71&72). These depressed values are probably attributable to the wet summer and consequent flushing. The one exception to this was July 12 when a large surge of rotifers was observed reaching 1700 – 1900/L at both stations. *Brachionus* made up the majority of the individuals contributing to this peak.

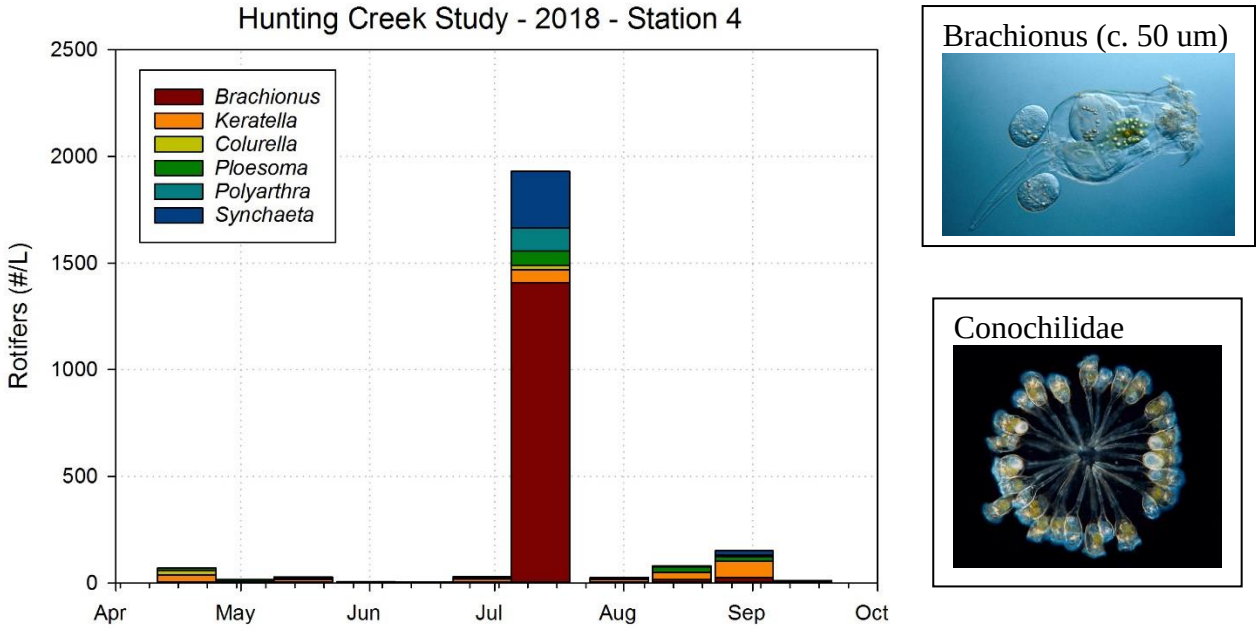

Figure 72. Rotifer Density by Dominant Taxa (#/L). River.

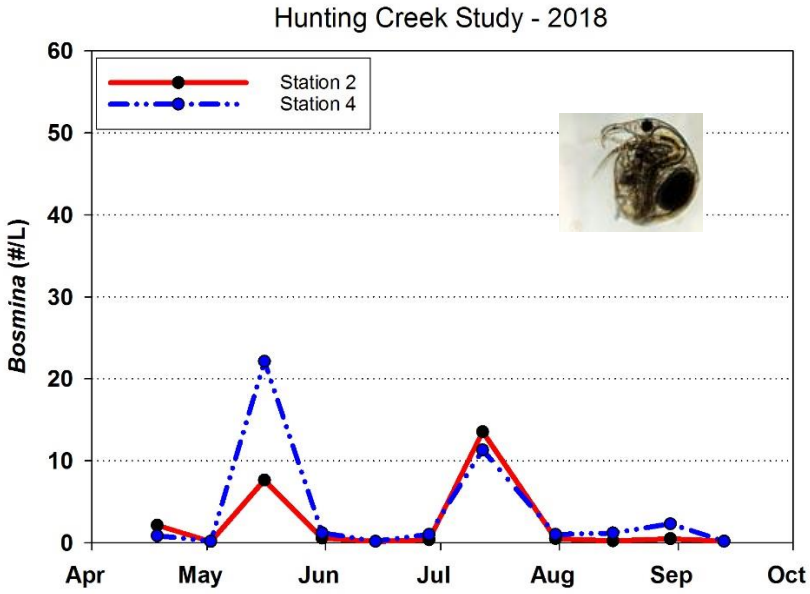

Bosmina is a small-bodied cladoceran, or "waterflea", which is common in lakes and freshwater tidal areas. It is typically the most abundant cladoceran with maximum numbers generally about 100-1000 animals per liter. Due to its small size and relatively high abundances, it is enumerated in the micro-zooplankton samples. *Bosmina* can graze on smaller phytoplankton cells, but can also utilize some cells from colonies by knocking them loose.

Figure 73. *Bosmina* Density by Station (#/L).

In 2018 the small cladoceran *Bosmina* was present only in mid May and mid July at modest densities (Figure 73). Even the highest values here are low for the Potomac. *Diaphanosoma*, typically the most abundant larger cladoceran in Gunston Cove, present but at much reduced values (Figure 74). In 2017 over 1300/L were present in a single AR2 sample.

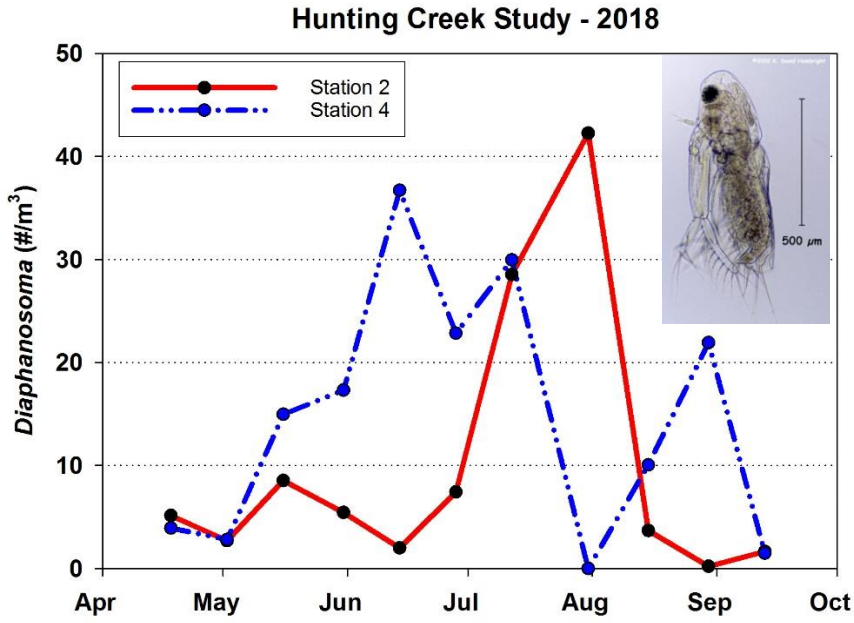

Diaphanosoma is the most abundant larger cladoceran found in the tidal Potomac River. It generally reaches numbers of 1,000-10,000 per m^3 (which would be 1-10 per liter). Due to their larger size and lower abundances, *Diaphanosoma* and the other cladocera are enumerated in the macrozooplankton samples. *Diaphanosoma* prefers warmer temperatures than some cladocera and is often common in the summer.

Figure 74. *Diaphanosoma* Density by Station (#/m^3).

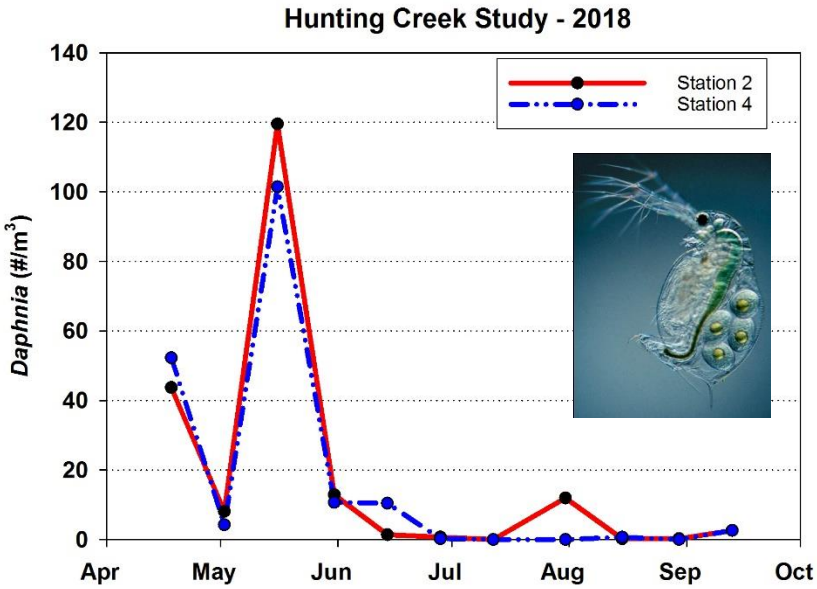

Daphnia, the common waterflea, is one of the most efficient grazers of phytoplankton in freshwater ecosystems. In the tidal Potomac River it is present, but has not generally been as abundant as *Diaphanosoma*. It is typically most common in spring.

Figure 75. *Daphnia* Density by Station (#/m^3).

Daphnia was one of the few plankters that reached higher levels in 2018 than in most years (Figure 75). Peak values of over 100/m^3 were observed a both stations in mid May. *Ceriodaphnia* was observed sporadically at both stations in 2018 (Figure 76).

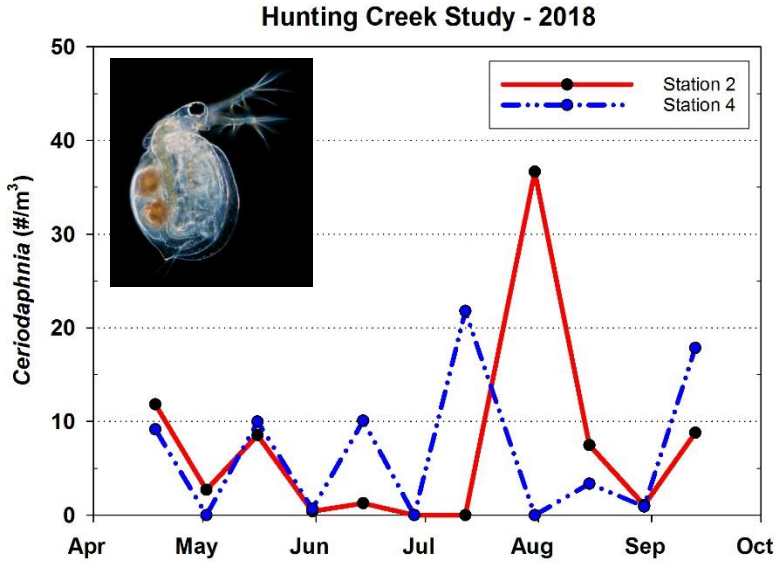

Ceriodaphnia, another common large-bodied cladoceran, is usually present in numbers similar to *Daphnia*. Like all waterfleas, the juveniles look like miniature adults and grow through a series of molts to a larger size and finally reach reproductive maturity. Most reproduction is asexual except during stressful environmental conditions.

Figure 76. *Ceriodaphnia* Density by Station (#/m^3).

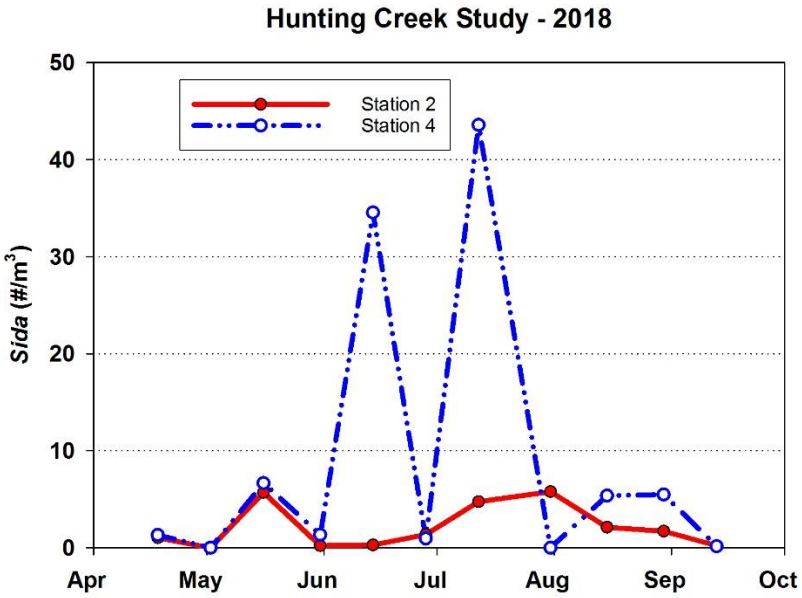

Sida is another waterflea that is often observed in the tidal Potomac River. Like the other cladocera mentioned so far, *Sida* grazes on phytoplankton to obtain its food supply.

Figure 77. *Sida* Density by Station (#/m^3).

Sida was found at moderate levels in mid June and mid July in the river, but otherwise was very scarse (Figure 77). It was also present in very low numbers at the river station. *Leptodora*, the large cladoceran predator, was also quite scares in 2018 (Figure 78).

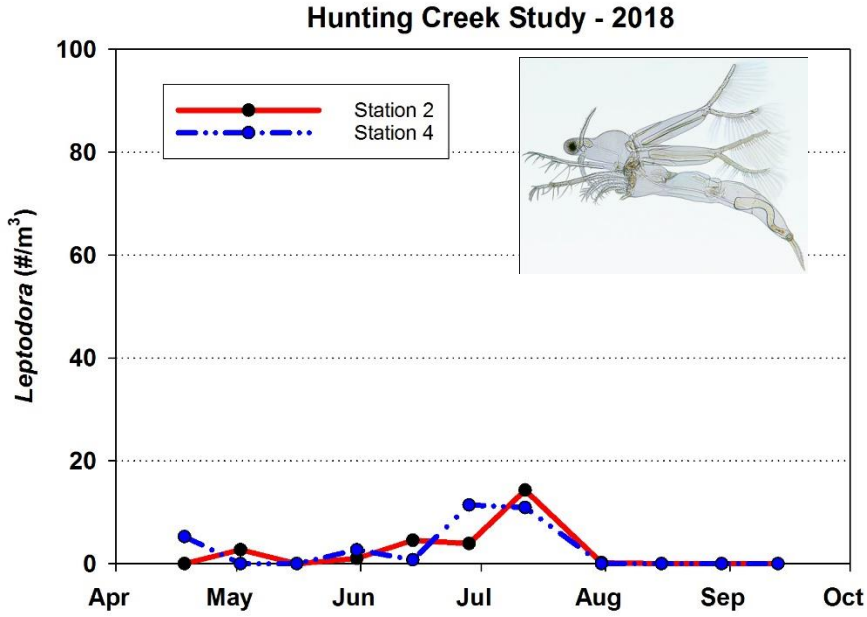

Leptodora is substantially larger than the other cladocera mentioned. Also different is its mode of feeding – it is a predator on other zooplankton. It normally occurs for brief periods in the late spring or early summer.

Figure 78. *Leptodora* Density by Station (#/m^3).

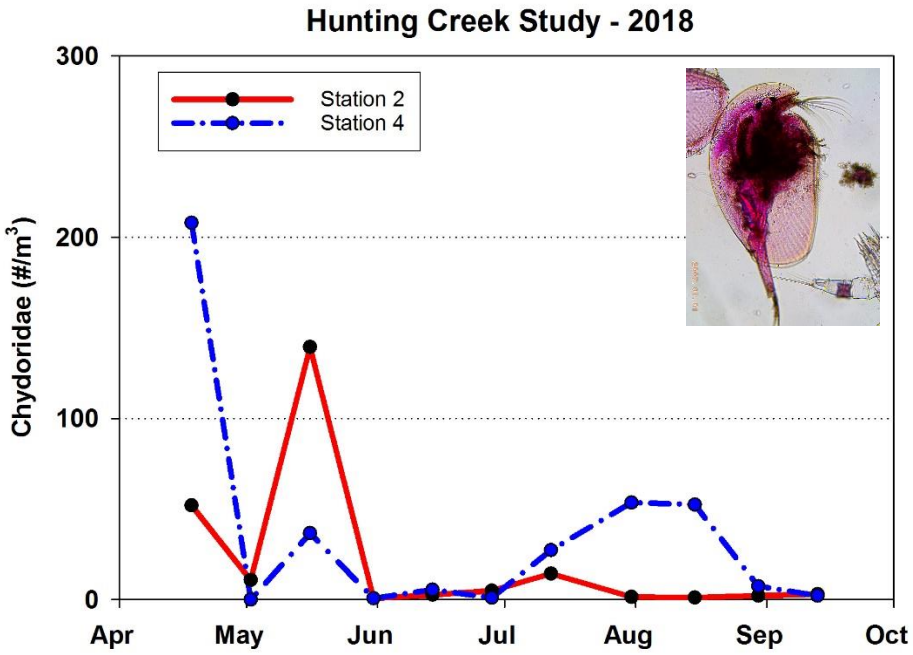

Figure 79. Chydoridae Density by Station (#/m^3). (photo: L. Birsa from HC samples)

Chydoridae is a cladoceran family whose members are associated with SAV (Figure 79). In 2018 members of this family were found at levels less than 10% of those in 2017, probably due to lack of habitat. Macrothricids, another group associated with SAV, were not collected at all in 2018 (Figure 80).

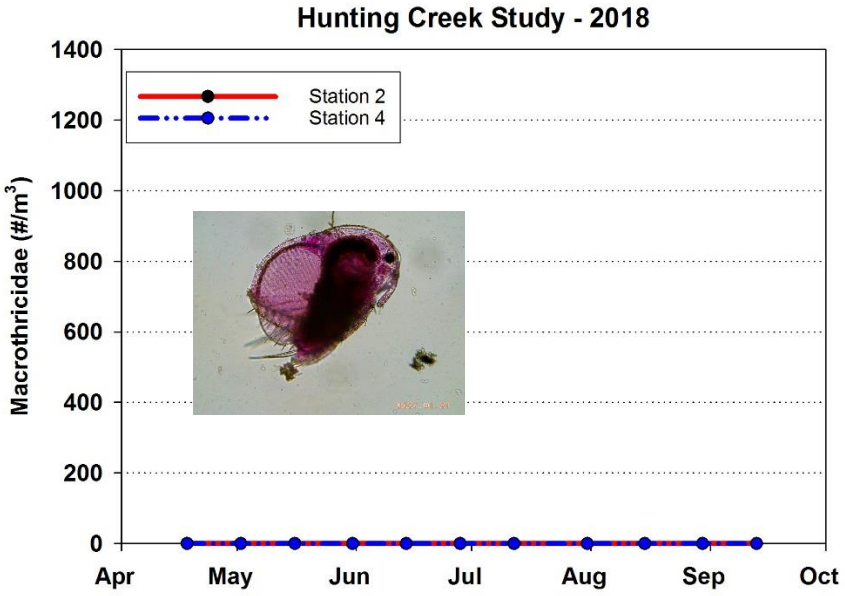

Figure 80. Macrothricid Density by Station (#/m^3). (photo: L. Birsa from HC samples)

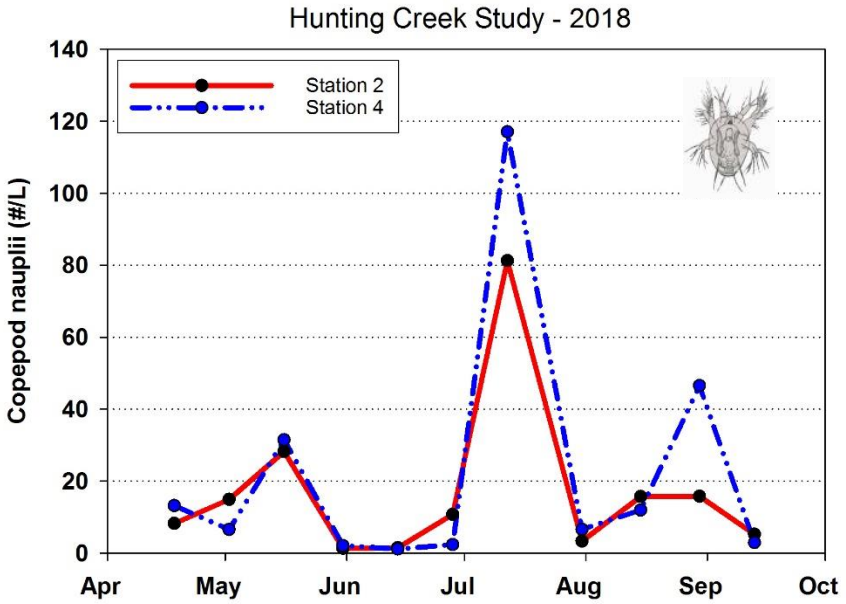

Copepod eggs hatch to form an immature stage called a nauplius. The nauplius is a larval stage that does not closely resemble the adult and the nauplii of different species of copepods are not easily distinguished so they are lumped in this study. Copepods go through 5 naupliar molts before reaching the copepodid stage which is morphologically very similar to the adult. Because of their small size and high abundance, copepod nauplii are enumerated in the micro-zooplankton samples.

Figure 81. Copepod Nauplii Density by Station (#/L).

Copepod nauplii were the most numerous group of crustacean zooplankton. They were present at similar levels at both stations at similar levels in 2018 (Figure 81). Densities increased in early and mid May, but dropped back in late May and June to very low levels. A major increase was found in mid July.followed by a decline in August. At AR4 levels increased again in late August. Maximum densities for nauplii were about half of the normal maxima. *Eurytemora* increased in early May and declined in late May and June followed by a strong rebound in mid July at both stations. At both stations the maximum attained was about 1800/m^3 in mid July (Figure 82).

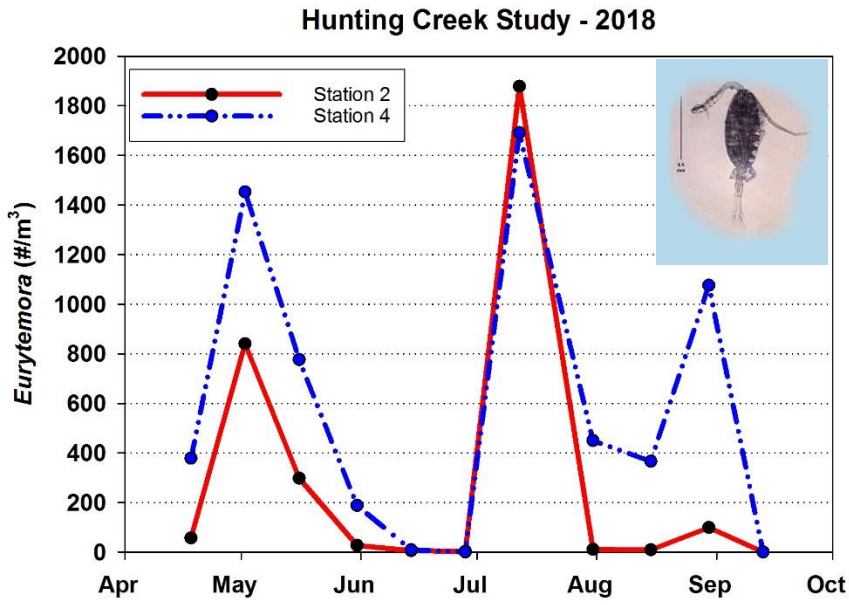

Eurytemora affinis is a large calanoid copepod characteristic of the freshwater and brackish areas of the Chesapeake Bay. *Eurytemora* is a cool water copepod which often reaches maximum abundance in the late winter or early spring. Included in this graph are adults and those copepodids that are recognizable as *Eurytemora*.

Figure 82. *Eurytemora* Density by Station (#/m^3).

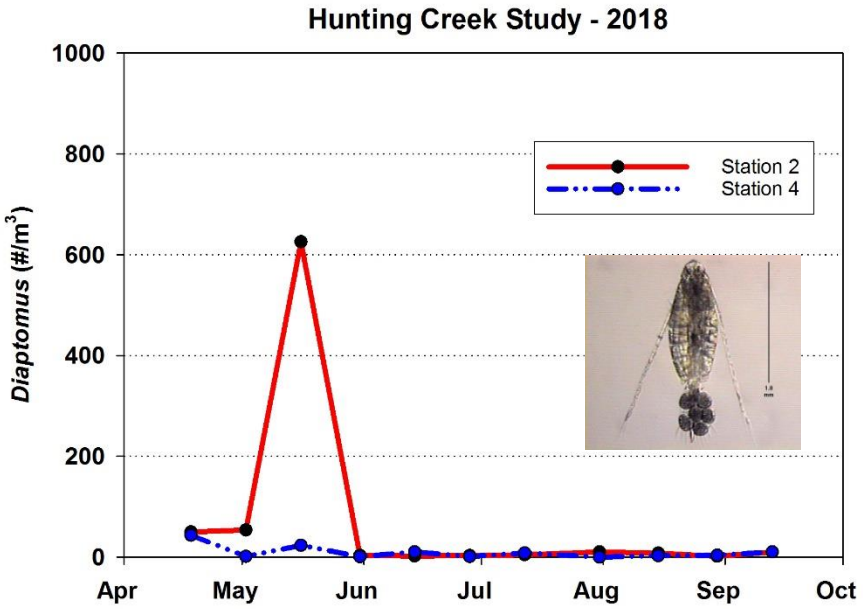

Diaptomus pallidus is a calanoid copepod often found in moderate densities in the Gunston Cove area. *Diaptomus* is an efficient grazer of algae, bacteria, and detrital particles in freshwater ecosystems Included in this graph are adults and those copepodids that are recognizable as *Diaptomus*.

Figure 83. *Diaptomus* Density by Station (#/m^3).

Diaptomus was almost exclusively found in Hunting Creek where it reached a substantial peak of about 600/m^3 in late June which was less than 10% of the maximum attained in 2017 (Figure 83). As in most years *Diaptomus* was very rare in the river mainstem. Cyclopoid copepods were present at generally low levels at both stations with peaks in April, mid May, and mid July (Figure 84).

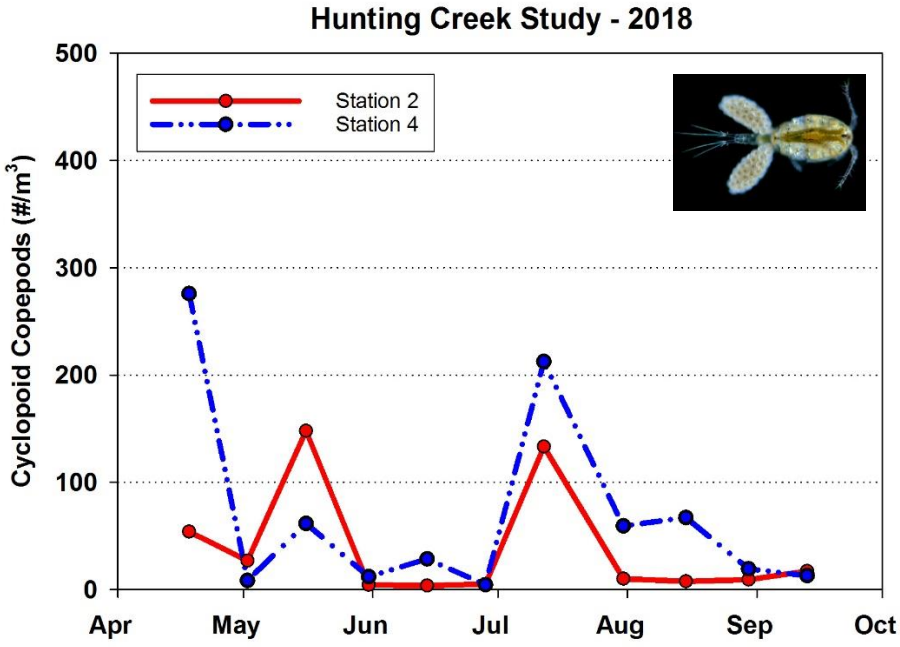

Cyclopoids are the other major group of planktonic copepods. Cyclopoids feed on individual particles suspended in the water including small zooplankton as well as phytoplankton. In this study we have lumped all copepodid and adult cyclopoids together.

Figure 84. Cyclopoid Copepods by Station (#/m^3).

F. Ichthyoplankton – 2018

We collected 14 samples (7 at Station 2 and 7 at Station 4) during the months April through July and found an average total larval density of 175 larvae of at least 11 species per 10 m^3 (Table 4), which is less than the previous years. The dominant family was Clupeidae, of which the species was Gizzard Shad (*Dorosoma cepedianum*) with an average larval density of at least 41.59 larvae per $10m^3$. *Alosa aestivalis* (Blueback Herring) had the second highest density with 28.27 larvae per $10m^3$. *A. pseudoharengus* (Alewife) was present in relative high densities as well: 19.43 larvae per $10m^3$ on average. Other clupeids present that could positively be identified to the species level are Hickory Shad (*A. mediocris*) at an average of 0.79 larvae per $10m^3$, and American Shad (*A. sapidissima*) at 0.08 per $10m^3$. The taxon Clupeidae, which is comprised of clupeids (*Alosa* or *Dorosoma* sp.) that could not be identified to a lower taxonomic level had a density of 64.67 larvae per $10m^3$.

A different taxon with relatively high representation is White Perch (*Morone americana*) with an average of 7.74 larvae per $10m^3$. Spottail Shiner (*Notropis hudsonius*) was relatively abundant as well, with an average of 2.47 larvae per $10m^3$.

Table 4. The larval density (#/$10m^3$) in Hunting Creek (Sta. 2) and the Potomac River (Sta. 4) in 2018.

Scientific Name	Common Name	AR2	AR4	Average
Alosa aestivalis	Blueback Herring	23.55	32.98	28.27
Alosa mediocris	Hickory Shad	0.81	0.77	0.79
Alosa pseudoharengus	Alewife	17.76	21.09	19.43
Alosa sapidissima	American Shad	0.00	0.15	0.08
Carpiodes cyprinus	Quillback	0.41	0.51	0.46
Clupeidae	unk. clupeid species	90.39	38.96	64.67
Dorosoma cepedianum	Gizzard Shad	27.21	55.97	41.59
Eggs	eggs	4.41	6.77	5.59
Lepomis gibbosus	Pumpkinseed	0.00	0.39	0.19
Menidia beryllina	Inland Silverside	0.27	0.39	0.33
Morone americana	White Perch	11.93	3.56	7.74
Notropis hudsonius	Spottail Shiner	1.09	3.86	2.47
Perca flavescens	Yellow Perch	0.00	0.74	0.37
Unidentified	unidentified	4.88	1.55	3.21

The density of clupeid larvae has a clear seasonal pattern as a result of the spring spawning season of most clupeids that occurs higher upstream. Clupeid larvae in Figure 56 include Blueback Herring, Hickory Shad, Alewife, American Shad and Gizzard Shad. These have similar spawning patterns, so they are lumped into one group for this analysis. Clupeids were present in

the sample at the end of April, increased to over 40 larvae per 10 m^3 in late May, and decreased again at the end of June (Figure 56). Of these clupeids, Alewife and Blueback Herring are the two species that make up river herring, of which we describe the spawning population at the end of this report.

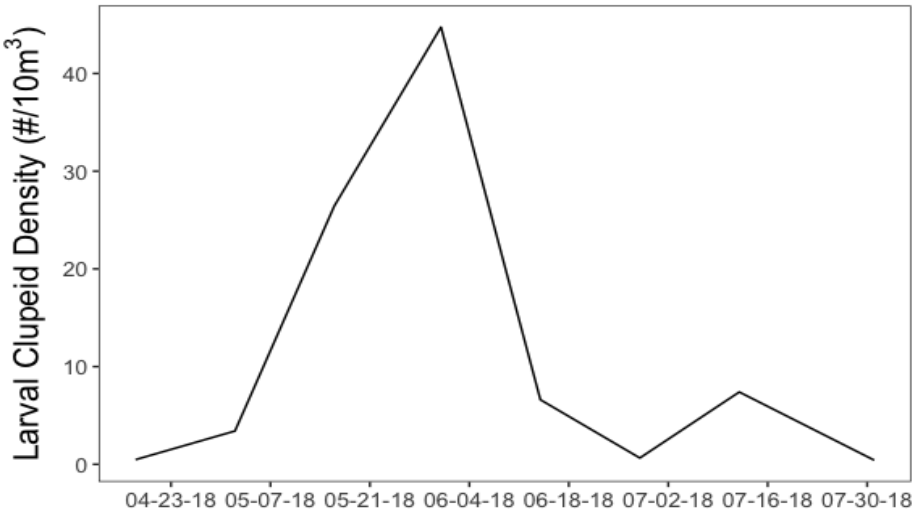

Figure 85. Density of clupeid larvae per $10m^3$.

White Perch larvae attained highest density on average at close to 4 larvae per $10m^3$ at the start of sampling in April (Figure 57), and disappeared from the samples in June. The group of larvae that are not positively identified clupeids or *Morone* species are dominated by unidentified larvae and Spottail Shiner. Highest densities of other larvae were found mid-May. The unidentified larvae were not intact unknown species, but larvae to mangled for proper identification. Because of the high density of clupeid larvae, most unidentified larvae are likely to be clupeids as well.

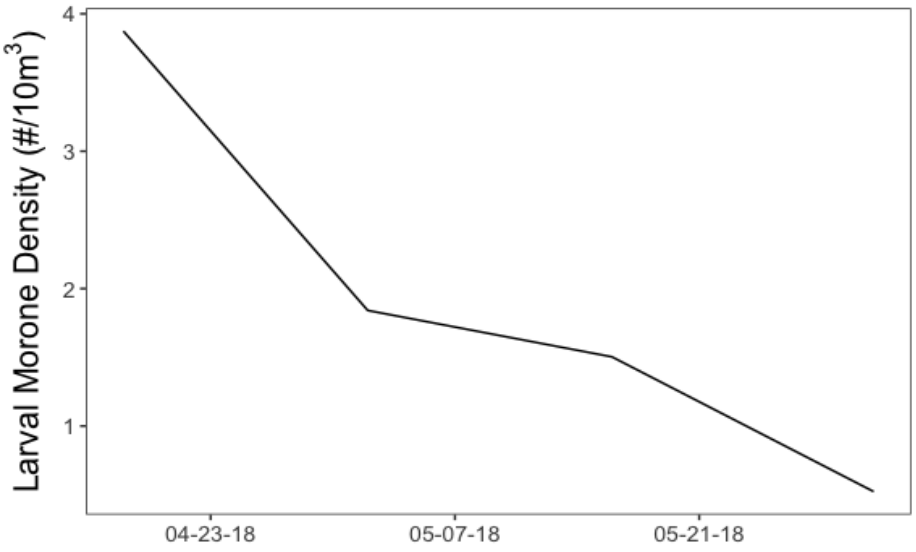

Figure 86. Density of *Morone americana* (White Perch) per $10m^3$.

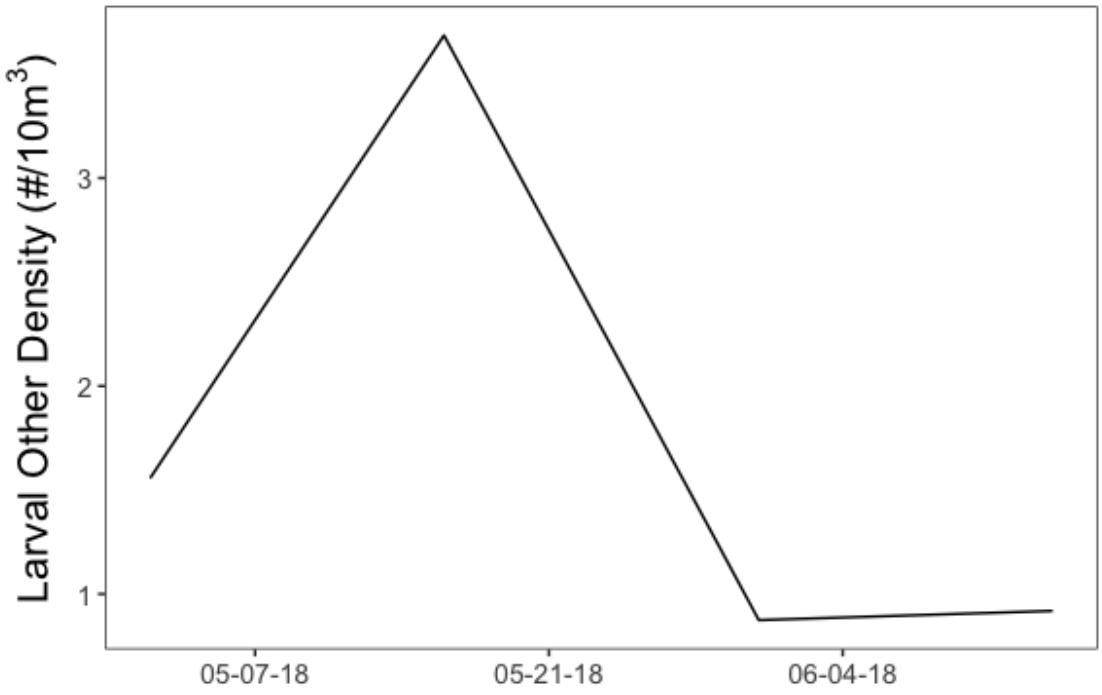

Figure 87. Density of other larvae per $10m^3$.

G. Adult and juvenile fishes – 2018

Trawls

Trawl sampling was conducted between April 24 and September 28 at station 3 and 4. A total of 1287 fishes comprising 21 species were collected with trawls (Table 5). This abundance is about 3 times higher than last year with higher species diversity. Part of the reason is the fact that we could do trawls at all sampling dates in 2018, since there were no dense SAV beds obstructing the trawl this year. Collections were dominated by White Perch (49.03%). The second most abundant species was Tessellated Darter (15.62%). Other relatively abundant species were Spottail Shiner (8%), Pumpkinseed (5.98%), Bluegill (4.74%), species of the Alosa genus (4.66%), Blue Catfish (4.43%), Yellow perch (2.64%), and Banded Killifish (1.48%) (Tables 5 and 6). An interesting find was the collection of native catfishes (Brown Bullhead and White Bullhead), which have seen declining abundances since the invasion of Blue Catfish. We collected Brown Bullhead last year as well.

Table 5. Adult and juvenile fish collected by trawling. Hunting Creek - 2018.

Scientific Name	Common Name	Abundance	Percent
Morone americana	White Perch	631	49.03
Etheostoma olmstedi	Tessellated Darter	201	15.62
Notropis hudsonius	Spottail Shiner	103	8.00
Lepomis gibbosus	Pumpkinseed	77	5.98
Lepomis macrochirus	Bluegill	61	4.74
Alosa species	unk. Alosa species	60	4.66
Ictalurus furcatus	Blue Catfish	57	4.43
Perca flavescens	Yellow Perch	34	2.64
Fundulus diaphanus	Banded Killifish	19	1.48
Ameiurus nebulosus	Brown Bullhead	11	0.85
Ameiurus catus	White Bullhead	8	0.62
Hybognathus regius	Eastern Silvery Minnow	7	0.54
Menidia beryllina	Inland Silverside	7	0.54
Cyprinus carpio	Carp	2	0.16
Ictalurus punctatus	Channel Catfish	2	0.16
Pomoxis nigromaculatus	Black Crappie	2	0.16
Dorosoma cepedianum	Gizzard Shad	1	0.08
Erimyzon oblongus	Creek Chubsucker	1	0.08
Morone saxatilis	Striped Bass	1	0.08
Moxostoma macrolepidotum	Shorthead Redhorse	1	0.08
Sander vitreus	Walleye	1	0.08
Total		**1287**	**100.00**

Table 6. Adult and juvenile fish collected by trawling. Hunting Creek study - 2018.

Scientific Name	Common Name	4/24	5/15	5/29	6/12	6/26	7/17	7/31	8/20	8/31	9/28	Total
Alosa species	unk. Alosa species	0	0	1	0	19	0	0	23	15	2	58
Ameiurus catus	White Bullhead	0	0	0	7	0	0	0	0	1	0	8
Ameiurus nebulosus	Brown Bullhead	0	3	0	1	1	2	0	0	4	0	11
Cyprinus carpio	Carp	0	0	0	0	0	1	0	0	1	0	2
Dorosoma cepedianum	Gizzard Shad	0	0	0	0	0	0	0	0	1	0	1
Erimyzon oblongus	Creek Chubsucker	0	0	1	0	0	0	0	0	0	0	1
Etheostoma olmstedi	Tessellated Darter	21	6	3	20	50	11	1	41	15	33	168
Fundulus diaphanus	Banded Killifish	1	4	2	6	2	2	0	0	2	0	19
Hybognathus regius	Eastern Silvery Minnow	6	0	0	0	1	0	0	0	0	0	7
Ictalurus furcatus	Blue Catfish	0	0	1	16	7	11	9	3	8	2	55
Ictalurus punctatus	Channel Catfish	0	0	0	2	0	0	0	0	0	0	2
Lepomis gibbosus	Pumpkinseed	9	7	9	11	8	1	1	3	7	21	56
Lepomis macrochirus	Bluegill	2	2	2	3	0	7	2	15	21	7	54
Menidia beryllina	Inland Silverside	0	6	0	0	0	1	0	0	0	0	7
Morone americana	White Perch	14	1	40	9	24	69	62	78	145	189	442
Morone saxatilis	Striped Bass	0	0	1	0	0	0	0	0	0	0	1
Moxostoma macrolepidotum	Shorthead Redhorse	0	0	0	0	0	0	0	1	0	0	1
Notropis hudsonius	Spottail Shiner	6	0	16	14	10	16	4	15	9	13	90
Perca flavescens	Yellow Perch	1	1	4	5	8	4	0	2	1	8	26
Pomoxis nigromaculatus	Black Crappie	0	0	0	0	0	0	0	0	2	0	2
Sander vitreus	Walleye	0	0	0	0	1	0	0	0	0	0	1
Total		**60**	**30**	**80**	**94**	**131**	**125**	**79**	**181**	**232**	**275**	**1012**

Trawling collects fish that are located in the open water near the bottom. Due to the shallowness of Hunting Creek, the volume collected is a substantial part of the water column. However, in the river channel, the near bottom habitat through which the trawl moves is only a small portion of the water column. Fishes tend to concentrate near the bottom or along shorelines rather than in the upper portion of the open water.

The highest catch occurred on September 28, which was due to the high abundance of White Perch in that trawl sample (Table 6). In 2018, most catches occurred at station 3, which is similar to previous years except last year (Table 7). This was due to the high abundance of White Perch and Tessellated Darter collected at station 3. The catch at station 4 was similar to last year with 442 individuals of 13 species. At Station 3, 845 individuals were collected of 16 species.

White Perch was the dominant species as in previous years. Looking at species by dominance (Figure 59A and B) White Perch was the dominant species both at station 3 and 4 in 2018. The species distribution is slightly more even in station 3 than station 4.

Table 7. Adult and juvenile fish collected by trawling. Hunting Creek study - 2018.

Scientific Name	**Common Name**	**3**	**4**
Alosa species	unk. Alosa species	60	0
Ameiurus catus	White Bullhead	0	8
Ameiurus nebulosus	Brown Bullhead	6	5
Cyprinus carpio	Carp	0	2
Dorosoma cepedianum	Gizzard Shad	1	0
Erimyzon oblongus	Creek Chubsucker	0	1
Etheostoma olmstedi	Tessellated Darter	185	16
Fundulus diaphanus	Banded Killifish	19	0
Hybognathus regius	Eastern Silvery Minnow	2	5
Ictalurus furcatus	Blue Catfish	4	53
Ictalurus punctatus	Channel Catfish	0	2
Lepomis gibbosus	Pumpkinseed	76	1
Lepomis macrochirus	Bluegill	59	2
Menidia beryllina	Inland Silverside	7	0
Morone americana	White Perch	323	308
Morone saxatilis	Striped Bass	1	0
Moxostoma macrolepidotum	Shorthead Redhorse	0	1
Notropis hudsonius	Spottail Shiner	65	38
Perca flavescens	Yellow Perch	34	0
Pomoxis nigromaculatus	Black Crappie	2	0
Sander vitreus	Walleye	1	0
Total		**845**	**442**

White perch (*Morone americana*) is the dominant species in Hunting Creek, and continues to be an important commercial and popular game fish. Adults grow to over 30 cm long. Sexual maturity begins the second year at lengths greater than 9 cm. As juveniles they feed on zooplankton and macrobenthos, but as they get larger consume fish as well.

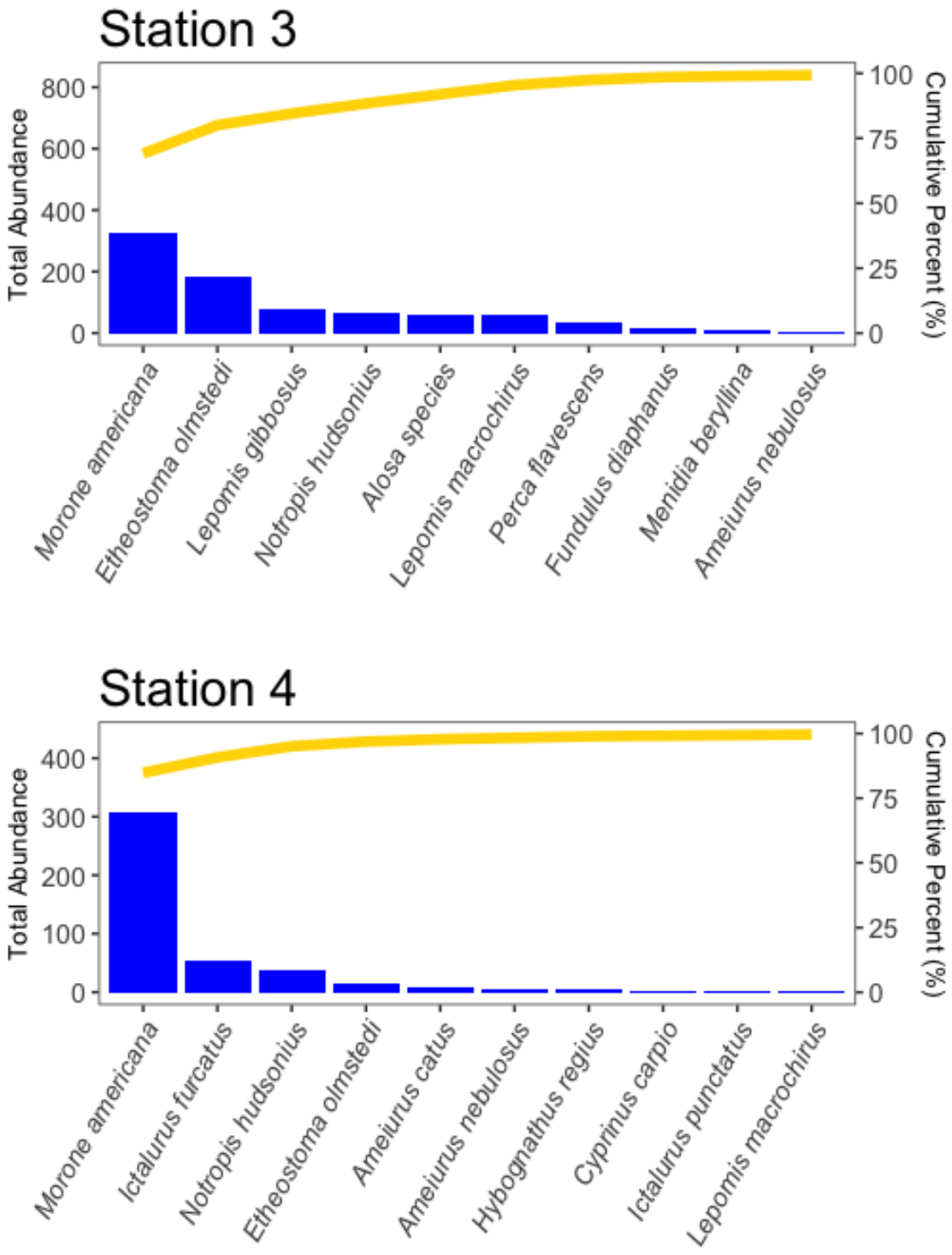

Figure 88A and B. Pareto chart of adult and juvenile fishes collected by trawling. Dominant species by station in total abundance and cumulative percentage of total for Station 3 (top) and Station 4 (bottom)

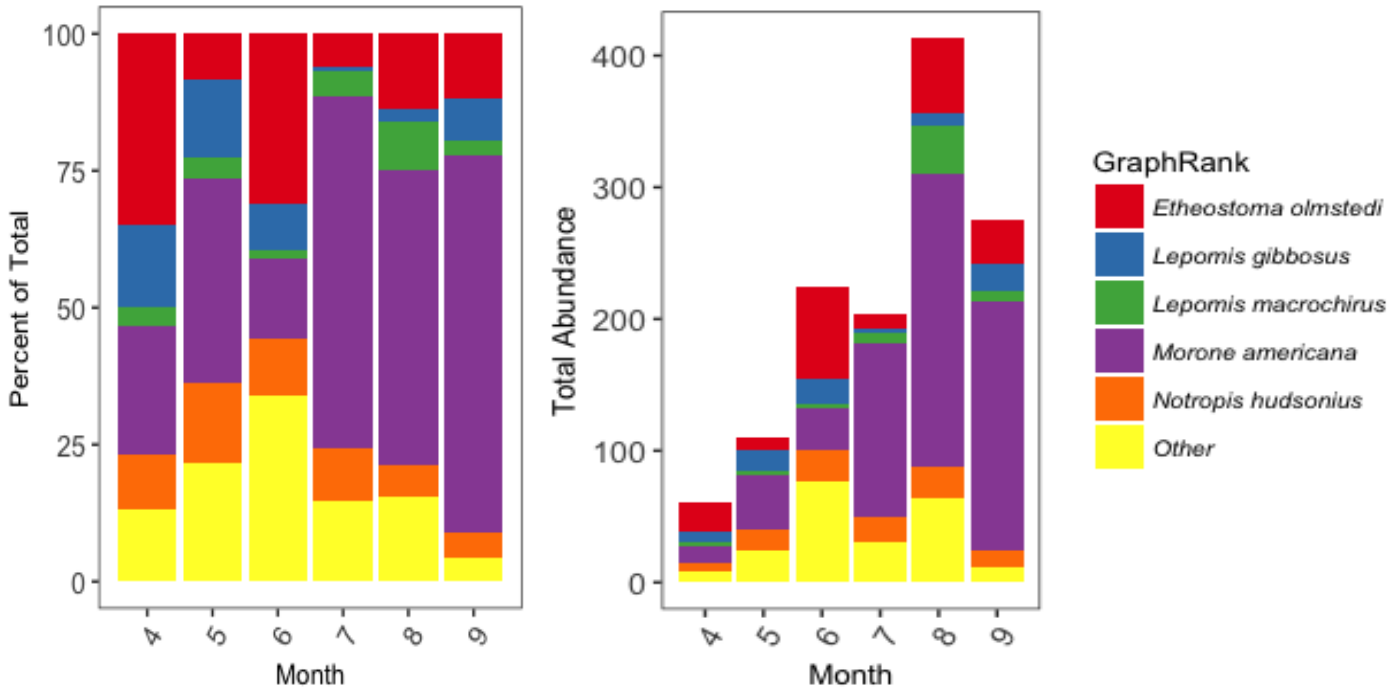

Figure 89 A&B. Adult and juvenile fishes collected by trawling. Dominant species by month in percentage of total (A) and total abundance (B).

White Perch is a dominant species in all months sampled (Figure 89 A&B). Only in April and June we found higher abundances of a different species (Tessellated Darter) than White Perch. Two species of sunfish (Bluegill and Pumpkinseed) as well as Spottail Shiner were represented throughout the sampling season as well.

Seines

Seine sampling was conducted between April 24 and September 28 at station 5 and 6. As planned, one sampling trip per month was performed in April and September, and two sampling trips per month from May to August. These two seines stations were selected as sites with shallow sloping shorelines that would enable us to tow a beach seine. The net was towed up onto the beach unless high water completely submerged the beach. In those cases, the net was towed into the boat.

A total of 20 seine samples were conducted (10 per station), comprising 1455 fishes of 22 species (Table 8). This is comparable to last year. Like previous years, the most dominant species in seine catches was banded Killifish (52.10%). Other species that were relatively abundant were species of the Alosa genus (25.64%), Inland Silverside (6.87%), Gizzard Shad (3.37%), White Perch (2.47%), Spottail Shiner (1.44%), Mummichog (1.37%), and Smallmouth Bass (1.37%). Other species occurred at low abundances (Table 8).

Banded Killifish was present from April to August, and dominant on most collections (Table 9). The most productive month was June due to the high numbers of Banded Killifish present that month. Banded Killifish were mostly collected at station 5, and wasn't the most abundant taxon at station 6, which was Alosa sp. (Table 10). The total number of specimens at station 5 was higher than station 6, because of the high abundance of Banded Killifish at station 5. Evenness distribution of abundance over multiple species was higher at station 6 than station 5, mostly due to the lower abundance of Banded Killifish in station 6 (Figure 61A&B).

Table 8. Adult and juvenile fish collected by seining. Hunting Creek- 2018.

Scientific Name	Common Name	Abundance	Percent
Fundulus diaphanus	Banded Killifish	758	52.10
Alosa species	unk. Alosa species	373	25.64
Menidia beryllina	Inland Silverside	100	6.87
Dorosoma cepedianum	Gizzard Shad	49	3.37
Morone americana	White Perch	36	2.47
Notropis hudsonius	Spottail Shiner	21	1.44
Fundulus heteroclitus	Mummichog	20	1.37
Micropterus dolomieu	Smallmouth Bass	20	1.37
Alosa pseudoharengus	Alewife	14	0.96
Lepomis gibbosus	Pumpkinseed	14	0.96
Lepomis macrochirus	Bluegill	14	0.96
Etheostoma olmstedi	Tessellated Darter	11	0.76
Hybognathus regius	Eastern Silvery Minnow	6	0.41
Notemigonus crysoleucas	Golden Shiner	5	0.34
Micropterus salmoides	Largemouth Bass	4	0.27
Perca flavescens	Yellow Perch	2	0.14
Alosa sapidissima	American Shad	2	0.14
Ameiurus nebulosus	Brown Bullhead	2	0.14
Carassius auratus	Goldfish	1	0.07
Morone saxatilis	Striped Bass	1	0.07
Pomoxis nigromaculatus	Black Crappie	1	0.07
Strongylura marina	Atlantic Needlefish	1	0.07
Total		**1455**	**100.00**

Table 9. Adult and juvenile fish collected by seining. Hunting Creek study - 2018.

Scientific Name	Common Name	4/24	5/15	5/29	6/12	6/26	7/17	7/31	8/20	8/31	9/28	Total
Alosa pseudoharengus	Alewife	14	0	0	0	0	0	0	0	0	0	14
Alosa sapidissima	American Shad	0	0	0	0	0	2	0	0	0	0	2
Alosa species	unk. Alosa species	0	0	0	0	30	63	84	15	75	106	373
Ameiurus nebulosus	Brown Bullhead	2	0	0	0	0	0	0	0	0	0	2
Carassius auratus	Goldfish	1	0	0	0	0	0	0	0	0	0	1
Dorosoma cepedianum	Gizzard Shad	0	0	0	0	0	36	11	0	0	2	49
Etheostoma olmstedi	Tessellated Darter	0	0	0	0	8	0	0	3	0	0	11
Fundulus diaphanus	Banded Killifish	13	148	38	393	128	14	7	16	1	0	758
Fundulus heteroclitus	Mummichog	0	3	0	1	11	0	0	5	0	0	20
Hybognathus regius	Eastern Silvery Minnow	0	0	0	0	0	5	0	0	0	1	6
Lepomis gibbosus	Pumpkinseed	0	1	0	1	1	0	0	10	0	1	14
Lepomis macrochirus	Bluegill	1	3	0	0	3	0	1	3	2	1	14
Menidia beryllina	Inland Silverside	0	66	8	20	1	4	0	1	0	0	100
Micropterus dolomieu	Smallmouth Bass	0	0	0	0	2	0	0	17	1	0	20
Micropterus salmoides	Largemouth Bass	1	1	0	0	1	0	1	0	0	0	4
Morone americana	White Perch	11	1	0	0	0	2	8	7	5	2	36
Morone saxatilis	Striped Bass	0	0	0	0	0	0	0	1	0	0	1
Notemigonus crysoleucas	Golden Shiner	1	2	0	0	0	2	0	0	0	0	5
Notropis hudsonius	Spottail Shiner	2	0	0	3	0	0	0	0	0	16	21
Perca flavescens	Yellow Perch	0	0	0	0	0	0	2	0	0	0	2
Pomoxis nigromaculatus	Black Crappie	0	0	0	0	0	0	0	0	1	0	1
Strongylura marina	Atlantic Needlefish	0	0	0	0	1	0	0	0	0	0	1
Total		**46**	**225**	**46**	**418**	**186**	**128**	**114**	**78**	**85**	**129**	**1455**

Table 10. Adult and juvenile fish collected by seining. Hunting Creek study – 2018.

Scientific Name	**Common Name**	**5**	**6**
Alosa pseudoharengus	Alewife	14	0
Alosa sapidissima	American Shad	2	0
Alosa species	unk. Alosa species	63	310
Ameiurus nebulosus	Brown Bullhead	0	2
Carassius auratus	Goldfish	0	1
Dorosoma cepedianum	Gizzard Shad	0	49
Etheostoma olmstedi	Tessellated Darter	6	5
Fundulus diaphanus	Banded Killifish	676	82
Fundulus heteroclitus	Mummichog	14	6
Hybognathus regius	Eastern Silvery Minnow	4	2
Lepomis gibbosus	Pumpkinseed	12	2
Lepomis macrochirus	Bluegill	11	3
Menidia beryllina	Inland Silverside	1	99
Micropterus dolomieu	Smallmouth Bass	18	2
Micropterus salmoides	Largemouth Bass	4	0
Morone americana	White Perch	12	24
Morone saxatilis	Striped Bass	0	1
Notemigonus crysoleucas	Golden Shiner	3	2
Notropis hudsonius	Spottail Shiner	17	4
Perca flavescens	Yellow Perch	2	0
Pomoxis nigromaculatus	Black Crappie	0	1
Strongylura marina	Atlantic Needlefish	0	1
Total		**859**	**596**

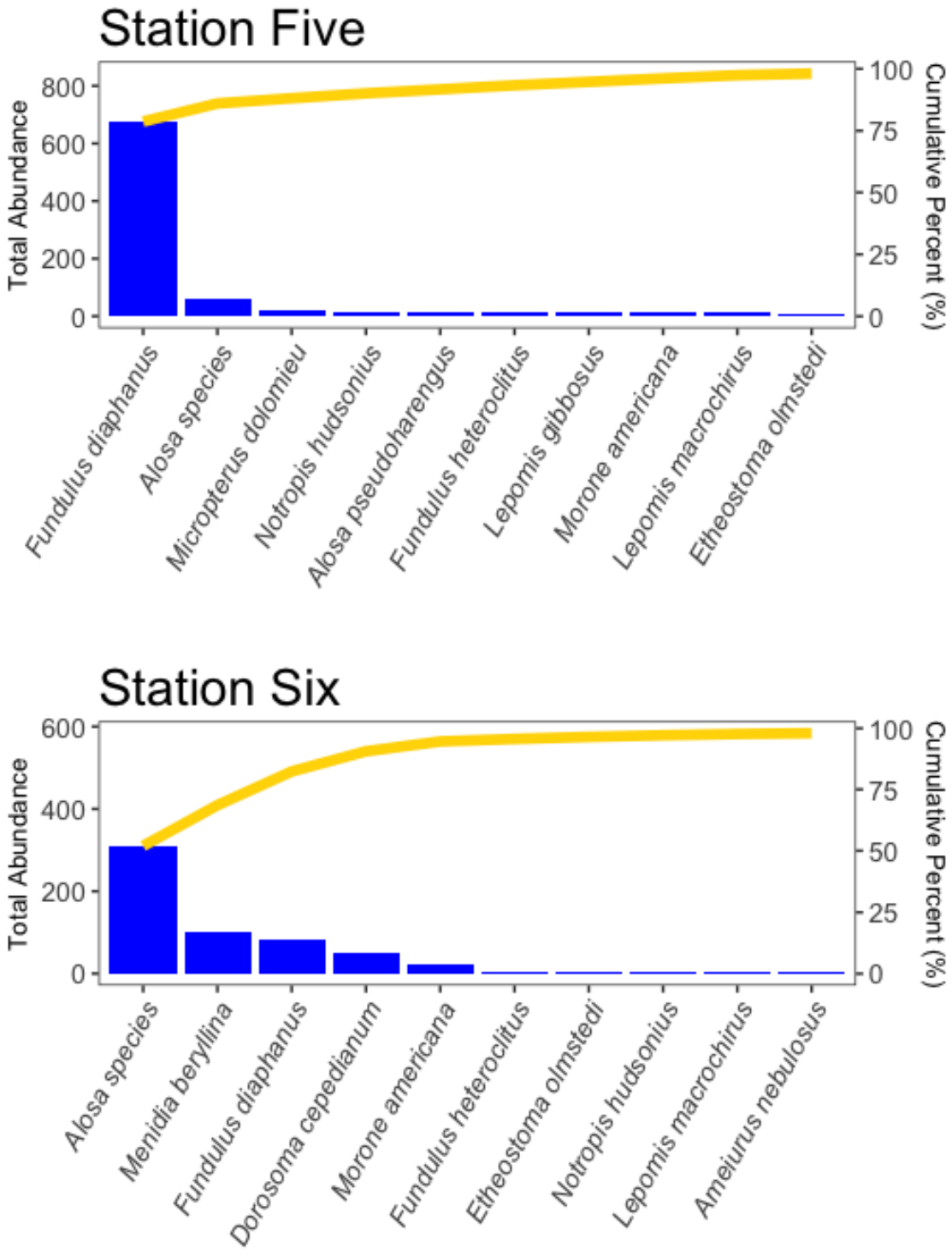

Figure 90A and B. Pareto chart of adult and juvenile fishes collected by seining. Dominant species by station in total abundance and cumulative percentage of total for Station 5 (top) and Station 6 (bottom).

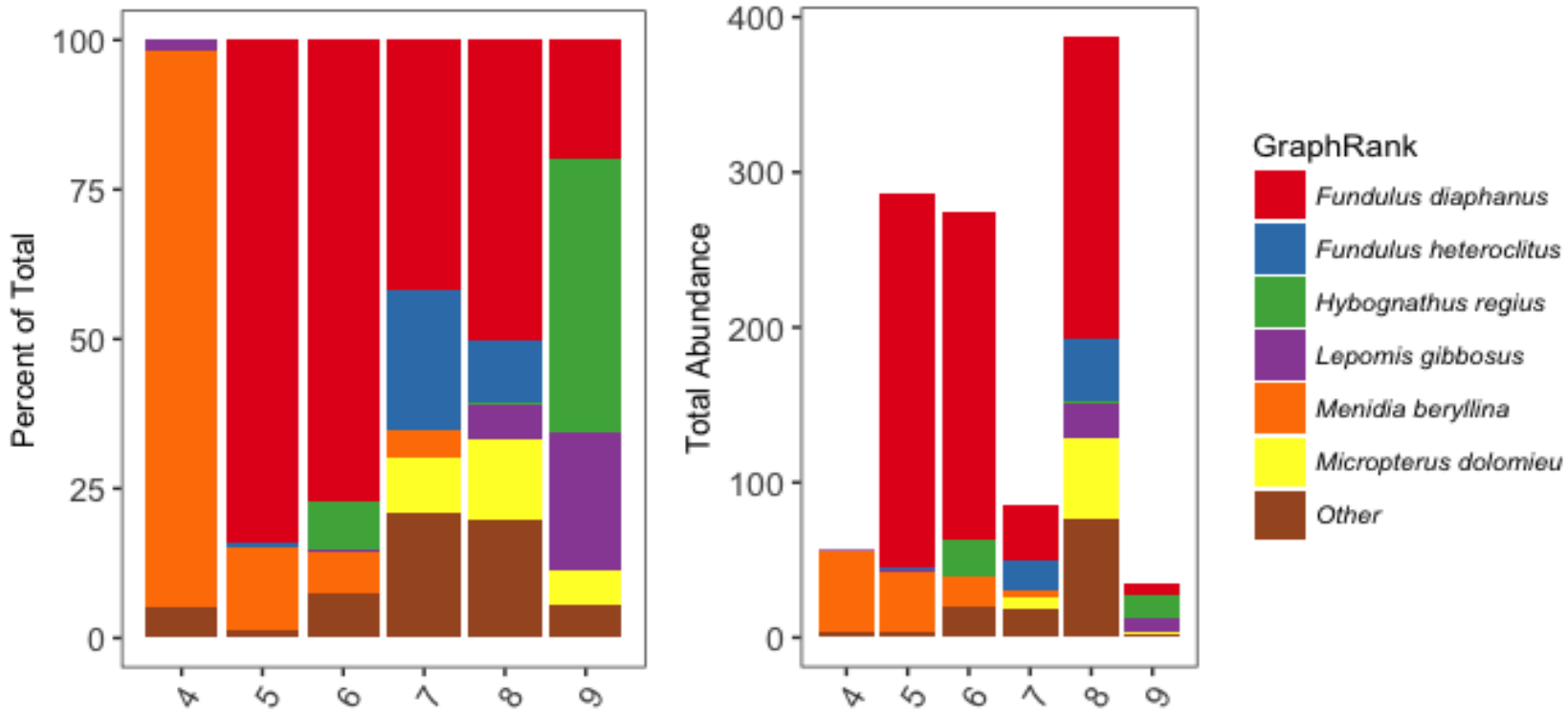

Figure 91A and B. Adult and juvenile fish collected by seining. Dominant species by month in: (a) percentage of total and (b) total abundance.

The abundance by month of dominant species shows a clear transition from Banded Killifish dominance to Alosid abundance (Figure 62A&B). Other species that were abundant but not ubiquitous in seine collections throughout the sampling season were White Perch, Inland Silverside, Spottail Shiner and Gizzard Shad.

Fyke Nets

Fyke nets were set from April 24 to September 28. Both fyke nets were set near trawl station 3 (Figure 1). In 2018 the total catch with fyke nets was much less than that with the trawl. The trade-off between trawl and fyke net catches are likely highly related to the amount of SAV present at the site. The SAV cover was low in 2018, which makes the trawl more effective resulting in a higher catch, and the fyke nest less effective because they are not hidden as well with less dense aquatic plant beds. This highlights the importance of using different gear types to accurately monitor species abundance trends. Fyke nets were very effective in 2017 when the SAV cover was much higher, with high fish abundance reflective of a diversity of species utilizing the SAV habitat. In 2018 the total catch was 52 specimens from 10 species.
Unlike previous years, Inland Silverside instead of Banded Killifish was the dominant species collected with fyke nets, representing 25.49% of the total abundance (Table 11). The percent dominance was distributed fairly evenly over the species collected in both fyke nets (Figures 63A&B). Other species with relatively high abundance were Tessellated Darter (17.65%), Pumpkinseed (17.65%), White Perch (15.69%), and Bluegill (11.76%).

Table 11. Adult and juvenile fish collected by fyke nets. Hunting Creek study – 2018.

Scientific Name	Common Name	Abundance	Percent
Menidia beryllina	Inland Silverside	13	25.49
Etheostoma olmstedi	Tessellated Darter	9	17.65
Lepomis gibbosus	Pumpkinseed	9	17.65
Morone americana	White Perch	8	15.69
Lepomis macrochirus	Bluegill	6	11.76
Lepomis species	unk. sunfish	2	3.92
Anguilla rostrata	American Eel	1	1.96
Hybognathus regius	Eastern Silvery Minnow	1	1.96
Notropis hudsonius	Spottail Shiner	1	1.96
Perca flavescens	Yellow Perch	1	1.96
Total		**51**	**100.00**

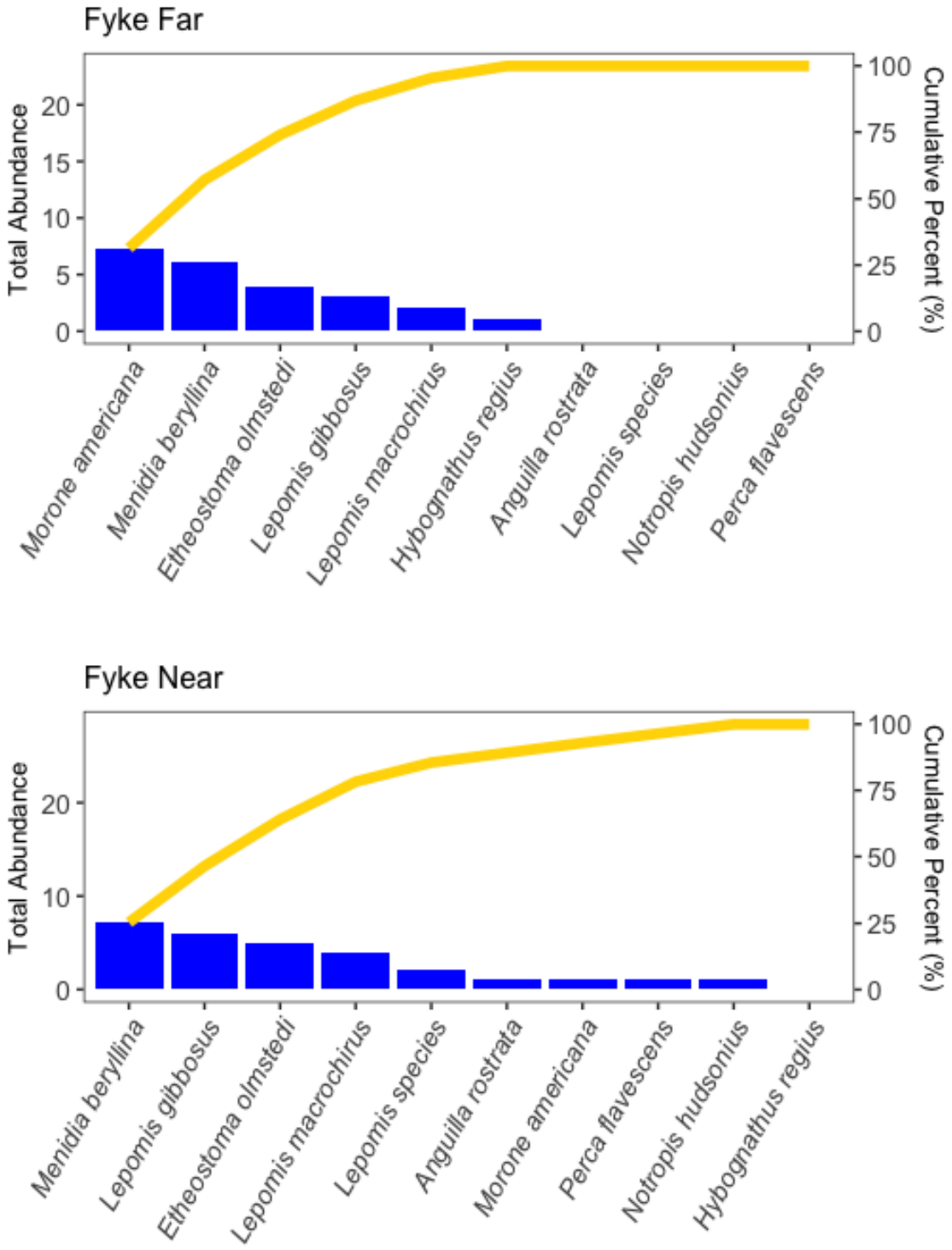

Figure 92a and b. Pareto chart of adult and juvenile fishes collected by fyke nets. Dominant species by station in total abundance and cumulative percentage of total for the Far Fyke (top) and Near Fyke (bottom).

Table 12. Adult and juvenile fish collected by fyke nets. Hunting Creek study - 2018.

Scientific Name	Common Name	4/24	5/15	5/29	6/12	6/26	7/17	7/31	8/20	8/31	9/28	Total
Anguilla rostrata	American Eel	0	1	0	0	0	0	0	0	0	0	1
Etheostoma olmstedi	Tessellated Darter	0	0	0	0	0	0	0	3	6	0	9
Hybognathus regius	Eastern Silvery Minnow	1	0	0	0	0	0	0	0	0	0	1
Lepomis gibbosus	Pumpkinseed	0	1	4	3	0	1	0	0	0	0	9
Lepomis macrochirus	Bluegill	0	0	0	0	0	4	1	0	1	0	6
Lepomis species	unk. sunfish	1	0	0	0	0	0	0	0	1	0	2
Menidia beryllina	Inland Silverside	0	4	6	1	1	0	0	0	0	1	12
Morone americana	White Perch	6	1	1	0	0	0	0	0	0	0	8
Notropis hudsonius	Spottail Shiner	0	0	0	0	0	0	0	0	0	1	1
Perca flavescens	Yellow Perch	0	0	0	0	0	0	0	1	0	0	1
Total		**8**	**7**	**11**	**4**	**1**	**5**	**1**	**4**	**8**	**2**	**51**

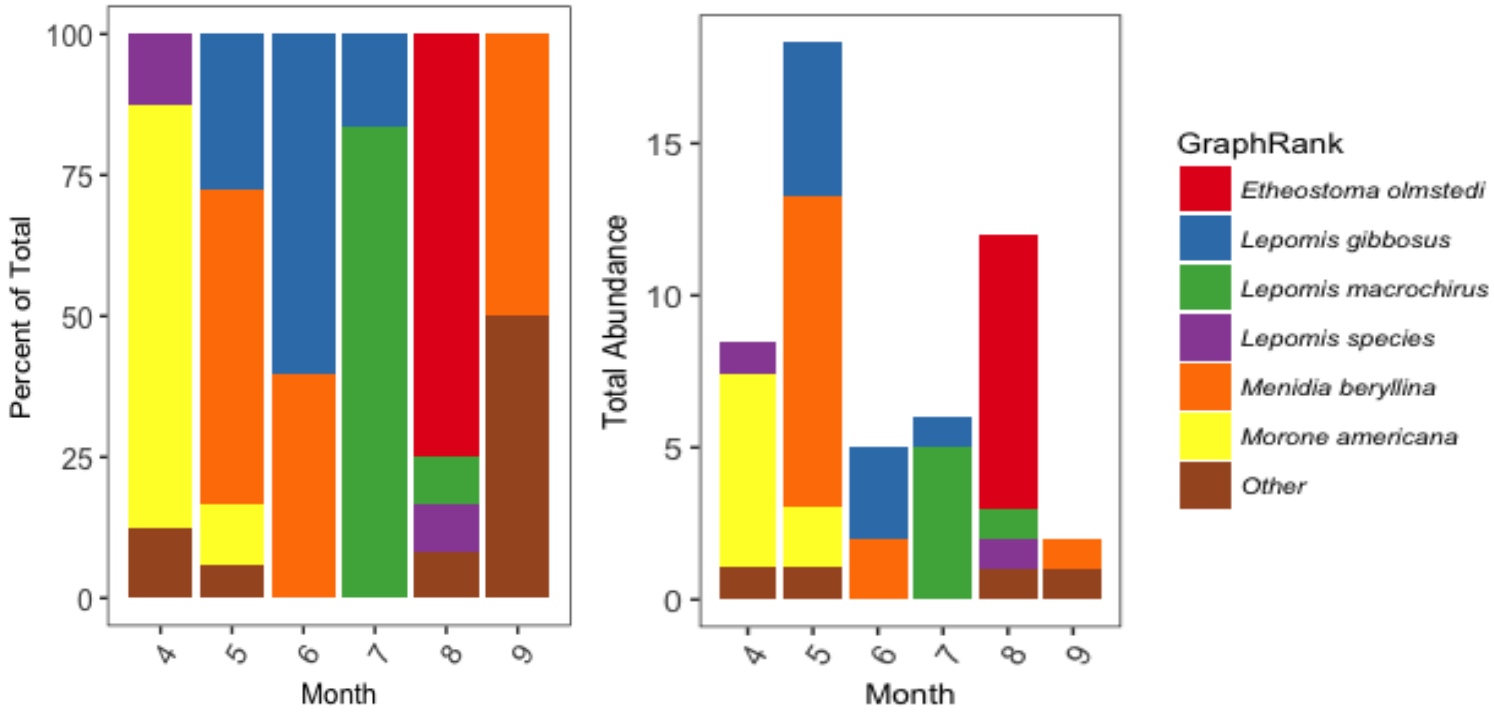

Figure 93a and b. Adult and juvenile fish collected by fyke nets. Dominant species by month in: (a) percentage of total and (b) total abundance.

The highest abundance occurred in the first half of the sampling season, with the highest catch occurring in the month of May (Table 12, Figures 64A&B). Both fyke nets collected a similarly low number of specimens (Table 13). Fyke Near collected a higher number of species, nine versus six in Fyke Far. An interesting find in Fyke Near was an American Eel, which is listed as endangered on the IUCN red list.

Table 13. Adult and juvenile fish collected by fyke nets. Hunting Creek study – 2018.

Scientific Name	**Common Name**	**Fyke Far**	**Fyke Near**
Anguilla rostrata	American Eel	0	1
Etheostoma olmstedi	Tessellated Darter	4	5
Hybognathus regius	Eastern Silvery Minnow	1	0
Lepomis gibbosus	Pumpkinseed	3	6
Lepomis macrochirus	Bluegill	2	4
Lepomis species	unk. sunfish	0	2
Menidia beryllina	Inland Silverside	6	7
Morone americana	White Perch	7	1
Notropis hudsonius	Spottail Shiner	0	1
Perca flavescens	Yellow Perch	0	1
Total		**23**	**28**

H. Submersed Aquatic Vegetation – 2018

SAV data overflights by VIMS were not conducted in 2017 as in most previous years.

As in 2017, we also assessed the relative abundance of various SAV species as part of the data mapping cruises in July and August 2018 (Table 14). All SAV taxa were greatly reduced in 2018. Coontail, a native species, which was dominant in 2017 was greatly reduced in 2018. Hydrilla, an introduced species which is considered invasive, was the most abundant on both dates in 2018, but it was also reduced as compared to 2017. Other taxa which had been quite common in 2017 were virtually absent in 2018. This is most certainly attributable to the very turbid water in 2018 which obstructed light penetration.

Table 14. Average Density of Submersed Aquatic Vegetation Species in Transects. Average included all sites with water depth less than or equal to 2 m. Comparison of 2018 with 2017. Density scale: 0 (absent) – 4 (very abundant).

		Average Density per sample by SAV Species - 2018	
Taxon Scientific Name	Taxon Common Name	July 16	August 28
Ceratophyllum demersum	Coontail	0.20	0.10
Heteranthera dubia	Water Stargrass	0.07	0
Hydrilla verticillata	Hydrilla	0.43	0.27
Najas guadalupensis	Southern Naiad	0.02	0.07
Najas minor	Spiny Naiad	0.07	0
Various	Filamentous algae	0.09	0

		Average Density per sample by SAV Species - 2017	
Taxon Scientific Name	Taxon Common Name	July 12	August 10
Ceratophyllum demersum	Coontail	1.76	1.74
Heteranthera dubia	Water Stargrass	0.19	1.19
Hydrilla verticillata	Hydrilla	0.78	0.32
Najas guadalupensis	Southern Naiad	0.20	0
Najas minor	Spiny Naiad	0.45	0.21
Various	Filamentous algae	0.03	0.43

I. Benthic Macroinvertebrates – 2018

River and Embayment Samples

Triplicate petite ponar samples were collected AR2, AR3, and AR4 monthly from May through September. Total numbers in samples collected at each station over each month are shown in Figure 94. The average number per ponar at each station by lowest taxon identified is shown in Table.15. The average number of benthic invertebrates was fairly similar across all stations.

Taxonomic Groups: Annelid worms (including Oligochaetes, Polychaetes, and Leeches) were found in high numbers at each site over all dates (Figure 94A). Overall, they accounted for 76% of all benthic organisms found. Oligochaetes were by far the dominant taxonomic annelid, being

Table 15. Taxa Identified in Hunting Creek Tidal Benthic Samples.

Taxon	Common Name	Average #/ponar		
		AR2	AR3	AR4
Platyhelminthes*	Flatworms	0	2.47	5.60
Nemertea	Ribbon worms	0	0.33	0.07
Annelida-Oligochaeta*	Oligochaete worms	107.00	68.07	73.27
Annelida-Polychaeta*	Polychaete worms	2.00	1.40	0.13
Annelida-Hirudinea*	Leeches	0.07	0	0.13
Bivalva-Corbicula*	Asiatic clams	0.80	1.67	11.27
Gastropoda-Planorbidae	Limpets	0	0	1.27
Gastropoda-Valvatidae*	Valve snails	0	0.27	0
Gastropoda-Viviparidae*	Mystery snails	0.20	3.93	0.53
Gastropoda-Pleuroceridae*	Pleurocerid snails	0	0	0.27
Hydrachnidia	Water mites	0	0	0.17
Crustacea-Isopoda-Cyathura*	Isopods	0	0.07	1.53
Crustacea-Isopoda-Chiridotea	Isopods	0	0	0.07
Crustacea-Amphipoda-Gammarus*	Amphipods	6.00	5.60	14.33
Crustacea-Amphipoda-Hyallelidae*	Amphipods	0.73	0	0.67
Collembola	Springtails	0	0	0.07
Odonata-Aeshnidae	Dragonflies	0	0	0.07
Ephemeroptera-Caenidae*	Small squaregill mayflies	0	0	0.73
Ephemeroptera-Ephemeridae	Burrowing mayflies	0	0	0.40
Ephemeroptera-Potomanthidae	Hacklegill mayflies	0	0	0.07
Coleoptera-Elmidae*	Riffle beetles	0	0	1.73
Coleoptera-Hydrophilidae	Water scavenger beetles	0	0	0.07
Trichoptera-Hydropsychidae	Hydropsychid caddisflies	0	0	0.40
Trichoptera-Leptoceridae	Long-horned caddisflies	0	0.07	0.07
Trichoptera-Polycentropidae	Tube maker caddisflies	0	0	0.07
Diptera-Chironomidae*	Midges	9.93	4.07	2.20
Diptera-Tabanidae	Horse-flies	0	0	0.07
	TOTAL	126.73	87.93	115.13

Taxa identified with an asterisk were found on 3 or more station-dates and were included in the multivariate analysis. Taxa from Collembola through Tabanidae are in the Insecta.

found in all samples in substantial number. Polychaetes were frequently found at AR2 and AR3 albeit at much lower numbers. Leeches were less common. Crustaceans (including amphipods and isopods) were the second highest group in abundance across sites and dates, accounting for 8.7% of all individuals. Gammarid amphipods (scuds) dominated this group with the isopod *Cyathura* being the second most common crustacean (Figure 94C). Insects accounted for 6.7% of the organisms sampled and more importantly for the greatest number of distinct taxa (12 taxa). Chironomids were by far the most numerous and omnipresent insect taxon. Most other insect taxa were present in only a few samples and in most cases only at AR4.

The remainder of the taxonomic groups accounted for minor components of the overall abundance and were generally most common at AR4. These included Bivalvia (4.3% of total abundance), Turbellaria (i.e., flatworms) (2.5%), and Gastropoda (2.0%). The only species found from the bivalve group was the invasive Asian clam, *Corbicula fluminea*. The gastropod (i.e., snails) group was composed of taxa from Pleuroceridae, Valvatidae, and Viviparidae. The dominant family was Viviparidae, accounting for 72% of all gastropods found. Two other groups were represented by only a few individuals: Nemertea (ribbon worms) and Hydrachnidia (water mites).

Spatial trends: The total and average abundance of organisms was highest at AR2 site over time, but this was entirely attributable to the large number of oligochaetes at that station. All three sites were dominated by Annelida, driven by high abundances of Oligochaeta (Figure 94A). Sites AR3 and AR4 had a higher diversity of taxa than the Potomac River site, with this effect most obvious at AR4. Due to their high abundance across all sites, additional analyses were conducted with all non-Annelida taxa. Flatworms and gastropods were present at AR3 and AR4, but not at AR2 and bivalves were more abundant at AR3 and AR4. When examining all non-Annelida taxa, Crustaceans were a dominant group in percent contribution across all of the sites (Figure 94C), and other taxa varied in their percent contribution by site. For example, Bivalvia were more dominant at AR4, while Insecta contributed more to AR2. Gastropoda were more prevalent at AR3 than the other two sites.

Temporal trends: Members of Annelida, composed of oligochaete, polychaetes, and leeches, were the dominant taxa recorded during all months (Figure 94B). There was a seasonal increase in crustaceans driven by Gammarid amphipods, which peaked during July most likely due to recruitment and were relatively low during the later months. Bivalve abundances, consisting only of the invasive Asian clam *Corbicula fluminea*, were highest during July at AR4. Abundance of Turbellaria were also highest during July. The lowest abundances of insect larvae across all sites occurred during August, with highest abundances in September. Gastropod abundances were highest during May and July and were driven by abundances of snails from the Viviparidae. Comparing percent contributions of all non-Annelida taxa across all of the sites, there were evident changes in the dominant taxa groups over the summer. May and June were dominated by Crustacea and Insecta became increasingly important in late summer and fall (Figure 94D). July showed the greatest evenness with no group dominant and all showing substantial contributions.

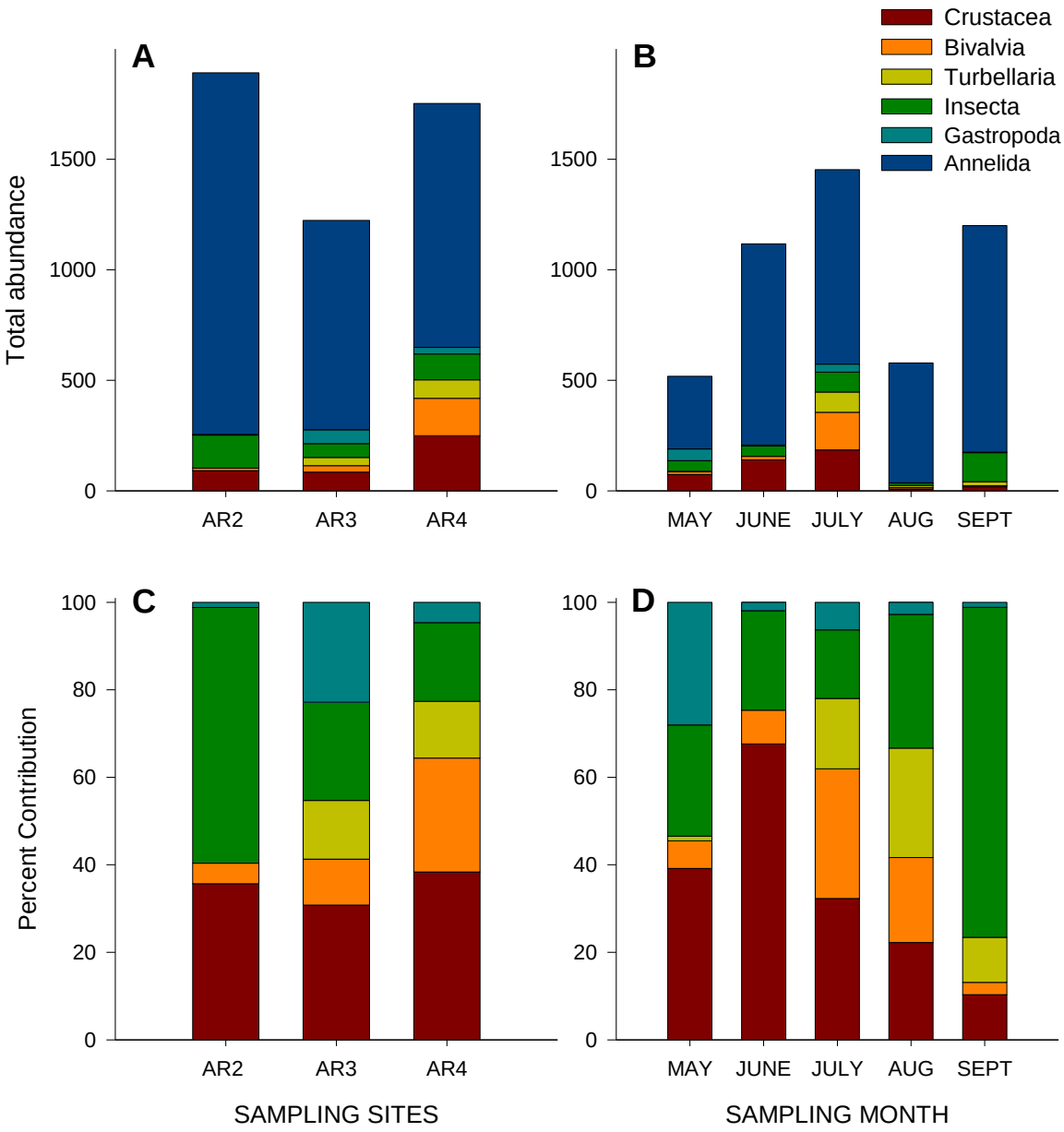

Figure 94. Total abundance of all benthic macroinvertebrate taxa (A, B) and percent contribution of all non-Annelida benthic macroinvertebrate (C, D) in petite ponar samples collected in 2018 separated by site and month.

Multivariate analyses: Due to the multispecies aspect of benthic communities, it is often useful to use multivariate analyses or ordination to examine relationships among samples. This allows multiple taxa to be considered simultaneously when assessing these relationships. In order to get the most meaningful relationships, the full macroinvertebrate sample/taxa matrix was condensed. Taxa that were present in less than three of the original replicate sample matrix were excluded. Then, the remaining, more consistently found taxa (indicated by asterisks in Table 15, were averaged over the replicates for each date and station combination. This resulted in one set of taxa values for each station on each date. This reduced matrix (15 samples x 13 taxa) was then subjected to an ordination using a technique called Non-metric Multidimensional Scaling

(nMDS). This allows relationships among samples based on their full complement of taxa to be visualized. If successful, relationships among samples can be shown on a two dimensional plot. The taxa differences responsible for the observed relationships can also be examined. The program PC-ORD was used to conduct the ordinations.

The results of an nMDS ordination using presence-absence data is shown in Figure 95. All, but one of the AR4 samples are clearly separate from the AR2 and AR3 samples which overlap completely. The AR4 samples clustered in the bottom right of the graph are the samples with the greatest number of taxa (highest taxa richness). The one AR4 sample outside of the ellipse was characterized by low taxa richness similar to that in the AR2 and AR3 samples. The higher richness at AR4 is probably due to better habitat conditions especially large and more heterogeneous sediment particle size.

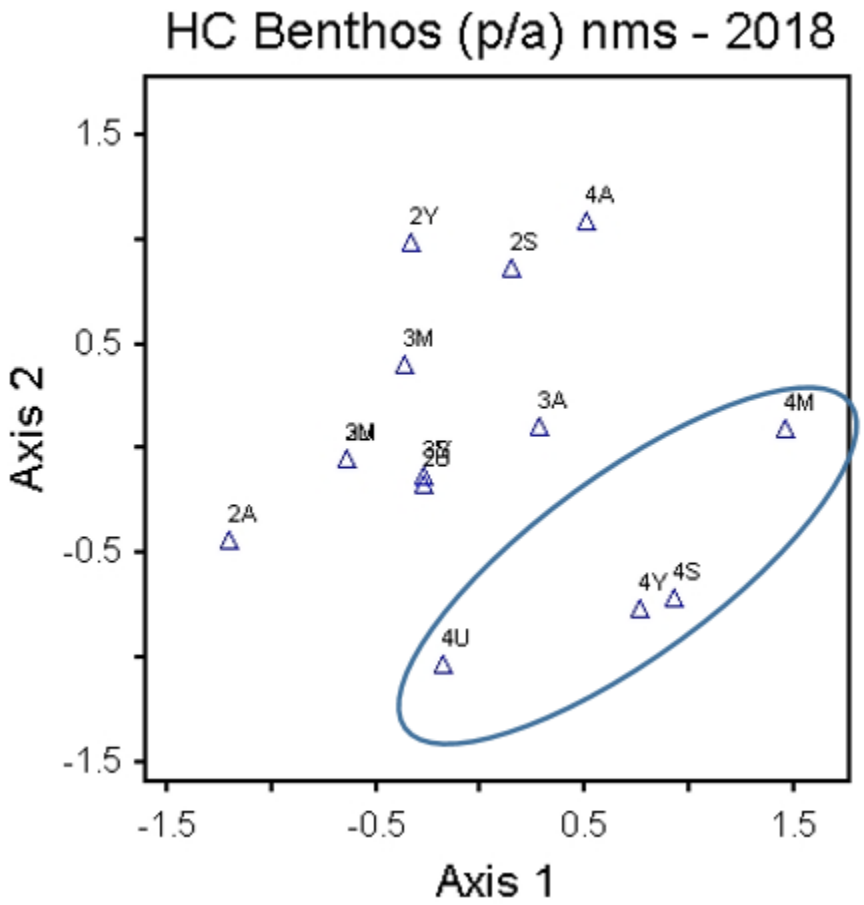

Figure 95. nMDS ordination of benthic samples from tidal stations. Numbers represent stations: 2=AR2, 3=AR3, 4=AR4. Letters represent month (M=May, U=June, Y=July, A=August, S=September). Triplicates were averaged to get a single value for each month-station combination. Data was presence/absence and distance measure was Sorensen.

Summary: Similar to previous years, the macroinvertebrate community was dominated by Annelids (including Oligochaetes, Polychaetes, and Leeches) across sites, with Oligochaetes contributing most to this group. Outside of the Annelids, Crustaceans (dominated by gammarid

amphipods) were the most abundant group at sites AR3 and AR4, while AR2 (located closer to Hunting Creek proper) was dominated by Insect larvae (midges). Abundant only at AR4 was the bivalve *Corbicula*. Comparing percent contributions of all non-Annelida taxa across all of the sites, there were evident changes in the dominant taxa groups over the summer. May and June were dominated by Crustacea and Insecta became increasingly important in late summer and fall (Figure 94D). July showed the greatest evenness with no group dominant and all showing substantial contributions. The lack of SAV in 2018 which is normally very abundant at AR2 and AR3 was at least partially responsible for the reduced diversity of communities at those stations.

Tributary Samples

Duplicate kick net samples were taken in eight tributaries of Hunting Creek during November 2018. The exact locations of the sampling sites are given in Table 16. The first 200 randomly selected individuals from each sample were identified to lowest taxonomic unit, usually genus, except for Oligochaetes (aquatic worms, subclass level) and Chironomidae (midges, family level).

Table 16. Location of Tributary Benthos Sampling Stations

Station ID	Stream	Sampling Date	Location on Stream
CR1	Cameron Run	Nov 8, 2018	Just below Metrorail bridge
BR1	Backlick Run	Nov 12, 2018	At trail bridge just upstream of the confluence with Holmes Run
TR1	Turkeycock Run	Nov 8, 2018	In Bren Mar Park just above Edsall Road
IR1	Indian Run	Nov 8, 2018	Just below Bren Mar Drive crossing
HR1	Holmes Run	Nov 12, 2018	First riffle upstream of confluence with Backlick Run
HR2	Holmes Run	Nov 8, 2018	Holmes Run Park just below pedestrian bridge at Pickett Street
TA1	Taylor Run	Nov 12, 2018	In Angel Park, underneath the trail bridge
TB1	Timber Branch	Nov 12, 2018	Just east of Ivy Hill Cemetry at W Timber Branch Parkway

Taxonomic Groups: The five most abundant taxa observed included three groups of insect larvae – Chironomidae (midges) and Trichoptera (caddisflies of the families Hydropsychidae and Philopotamidae) -- Turbellaria (i.e., flatworms) and Oligochaeta (Figure 96, top). All other taxa were significantly less abundant and included Ephemeroptera (mayflies of the family Baetidae), Crustaceas (Gammarid amphipods), Diptera (families Tipulidae and Simulidae), and the invasive Asian clam *Corbicula fluminea*. (Figure 96, bottom). Of the less abundant taxa, none of these were present at all sites.

Spatial trends: Cameron Run and Indian Run had the highest abundances of the five dominant taxa. Interestingly, dominant taxa differed by site. Hydropsychidae larvae (caddisflies) were the dominant group at 2 of the sites (i.e., Holmes Run-2 and Indian Run), and Chironomidae were dominant at Cameron Run, Backlick Run, and Taylor Run. Holmes Run-1, Turkeycock Run, and Timber Branch were dominated by Oligochaeta, with the highest values observed at Timber

Branch. Indian Run had highest numbers of Philopotamidae larvae (characterized by very low abundances of <20 at other sites). The highest abundances of Turbellaria were found at Holmes Run-2 (N=15), with all other sites had <13 total individuals of this group.

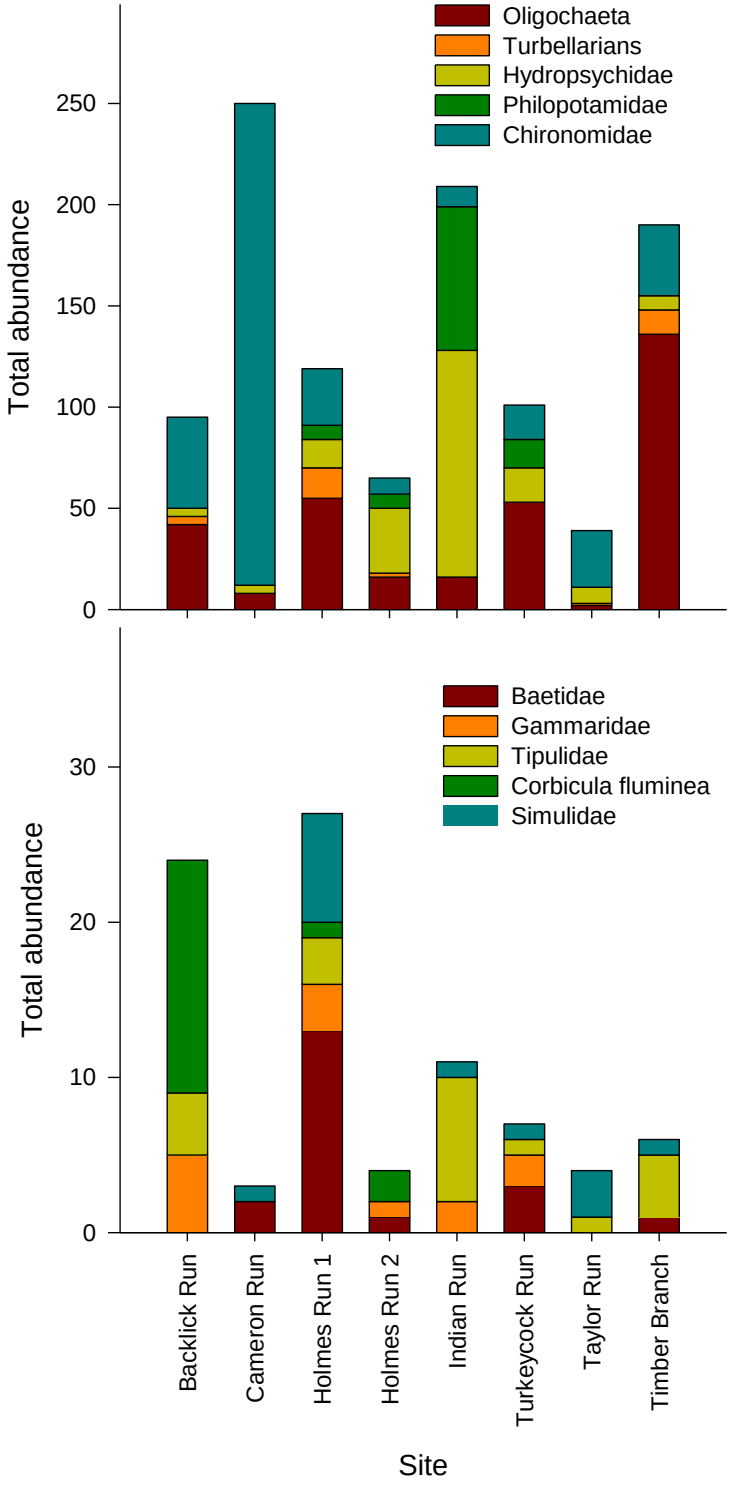

Figure 96. TOP: Total abundance of the five dominant benthic invertebrate taxa in tributary kick samples. BOTTOM: Total abundance of four less dominant benthic

invertebrate taxa in tributary kick samples. Note the different scales of the y-axes between the two graphs.

Benthic Invertebrate Community Metrics: In general, increasing taxa richness (# of taxa in a sample) reflects increasing water quality, habitat diversity, or habitat suitability. Taxa richness across all eight sites ranged from 5 to 14 taxa, with lowest richness at Cameron Run and highest richness at Timber Branch.

Table 17. Benthic invertebrate community metrics. EPT include the Insecta from Ephemeroptera, Plecoptera, and Tricoptera. % E refers to just those from the Ephemeroptera. Color shading indicates relatively good (green), moderate (yellow), or poor (red) conditions for each of the metrics and the summary statistic.

	Taxa Richness	EPT Richness	% E	Hilsenhoff Biotic Index	% Clingers	Summary Statistic
Backlick Run	9	1	0	9.76	3.31	28%
Cameron Run	5	2	0.79	9.88	1.98	28%
Holmes Run 1	13	3	8.72	7.06	19.46	44%
Holmes Run 2	10	3	1.37	5.87	54.79	60%
Indian Run	8	2	0	7.46	83.26	52%
Turkeycock Run	13	5	3.48	6.49	29.57	60%
Taylor Run	8	1	0	7.96	21.15	44%
Timber Branch	14	2	0.45	6.46	3.64	44%

A subset of abundance, EPT richness is the number of species from the generally more environmentally sensitive Insecta groups Ephemeroptera, Plecoptera, and Trichoptera. In general, if the EPT richness is ≤ 1, then conditions are poor. If between 2 and 5, then conditions are moderate. If ≥ 5, then conditions are good. EPT richness in each of the eight sampled locations was between 1 and 5, indicating that the environmental conditions are very site specific. Both Taylor Run and Backlick Run only had one species of EPT, indicating poor conditions, while five EPT species were found in Turkeycock Run, indicating good environmental conditions for these organisms.

The Insecta group Ephemeroptera is considered a particularly environmentally sensitive group. Calculating the percentage of total organisms that are Ephemeroptera provides another metric for stream condition. In this case, if the value is >40%, then conditions are good. If the value is between 20 and 40%, then conditions are moderate. If the value is < 20%, then conditions are poor. In all cases, percentage values were <20% (poor conditions).

The Hilsenhoff Biotic Index (HBI) estimates the overall tolerance of the community in a sampled area toward organic (nutrient) enrichment, weighted by the relative abundance of each taxonomic group (family, genus, etc.). Organisms are assigned a tolerance number from 0 to 10 pertaining to that group's known sensitivity to organic pollutants; 0 is most sensitive, 10 is most tolerant. Low HBI values reflect a higher abundance of sensitive groups, thus a lower level of pollution. Family-level tolerance values from USEPA (Barbour et al. 1999) were used for organisms that could not be identified to the genus level because of size or condition. Taxa with

tolerance values ≤3 were considered *intolerant*, whereas those with values ≥7 were considered *tolerant.* Low HBI (≤3.75) values reflect a higher abundance of sensitive groups, indicative of a lower level of pollution. Three locations (Turkeycock Run, Holmes Run 2 and Timber Branch) would be considered "fairly poor" with substantial organic pollution likely (values 5.76 – 6.50), while Holmes Run 1 was "poor" (values 6.51-7.25), indicating that very substantial pollution was likely. The highest scores (values 7.26 – 10) indicate "very poor" conditions indicative of severe organic pollution; high values were found for Backlick Run, Cameron Run, Indian Run and Taylor Run (Table 17).

The percent of organisms that are clingers, which are those that have fixed retreats or adaptations for attachment to surfaces in flowing water is another indicator of environmental quality. Increasing metric values indicate increasing substrate stability. In this case, if the value is >40%, then conditions are good. If the value is between 20 and 40%, then conditions are moderate. If the value is < 20%, then conditions are poor. Two locations (Holmes Run 2 and Indian Run) had values >40%, indicating good substrate stability, while four locations (Holmes Run 1, Backlick Run, Timber Branch, and Cameron Run) had poor conditions. The three other sites were considered to be moderate.

Using these five measures of biological health, we can calculate a summary statistic of relative overall health of these streams. In this case, we assign values of high (5), moderate (3), or low (1) health for each metric at each site, sum these values for each site and divide by 25 (i.e., the maximum score achievable). Streams characterized as "good" would achieve summary statistics of 90% or better of the maximum summary statistic. "Moderate" streams would be between 75 and 89%, and "poor" streams would come in at 75% of the summary statistic. Using the criteria for each metric laid out above, all of the streams scored between 44% and 68% of the maximum summary statistic. This indicates that all sampled streams are in poor condition based on these five metrics.

Water quality variables were measured on the date of benthic sampling (Table 18) and were generally supportive of aquatic life. It is important to note that all streams were at base flow conditions during the sampling period; water quality is expected to be more degraded during high flow.

Table 18. Water Quality Results from Tributary Benthos Sampling

Station	Temp (°C)	SpCond (uS/cm)	DO (mg/L)	DO (%)	pH	Turbidity YSI units
Cameron Run	14.1	260	10.06	98	8.03	6.02
Backlick Run	7.1	384	11.48	95	8.05	1.56
Turkeycock Run	12.7	251	9.53	89.8	7.87	2.32
Indian Run	12.6	306	10.26	96.7	8.02	2.20
Holmes Run 1	8.1	197	11.43	96.8	8.03	1.40
Holmes Run 2	13.8	190	10.21	98.8	8.08	2.01
Taylor Run	8.5	394	11.18	95.6	8.00	0.86
Timber Branch	8.8	352	10.76	93	7.72	1.64

Summary: In 2018, we added two new sites (Taylor Run and Timber Branch) to our list of

monitored locations. In general, the top five most abundant taxa observed across all sites stayed the same as in previous years with the exception of an increase in the Insecta family Philopotamidae and a decrease in the Insecta family Baetidae. The change was not due to the addition of the two new sites, but rather an increase in Philopotamidae at Indian Run in 2018. Cameron Run had the highest abundance of the five dominant taxa, mostly composed of the Insecta family Chironomidae. Hydropsychidae larvae (caddisflies) were the dominant group at Holmes Run-2 and Indian Run. Chironomidae were dominant at Backlick Run and Taylor Run. Holmes Run-1, Turkeycock Run, and Timber Branch were dominated by Oligochaeta. Taxa richness across all sites ranged from 5 to 14 taxa, with lowest richness at Cameron Run and highest richness at Timber Branch. Using five measures of biological health, we calculated a summary statistic of relative overall health of these streams. Using the criteria for each metric laid out above, all of the streams scored between 44% and 68% of the maximum summary statistic, indicating that all sampled streams are in poor condition.

DISCUSSION

A. 2018 Synopsis

In 2018 air temperature was below normal in March and April, but well above normal for the period May through September. August was particularly warm in 2018 with the average being 2oC higher than its long term average. Precipitation established some new records in 2018 with all months of the study period being above their long term average and May, July, and September receiving over twice their average rainfall. To better understand relationships between flow events and Hunting Creek ecology, time course graphs were constructed overlaying the sequence of precipitation, stream/river flow, and water quality/plankton sampling dates (Fig. 98a,b). During the mid-May to mid-June period and the mid-July to early August periods, Cameron Run flows were often substantially elevated due to frequent precipitation events. These would be expected to affect water quality in the study area especially AR2 and AR3. In the mainstem Potomac flows were also highly elevated May, June, and August.

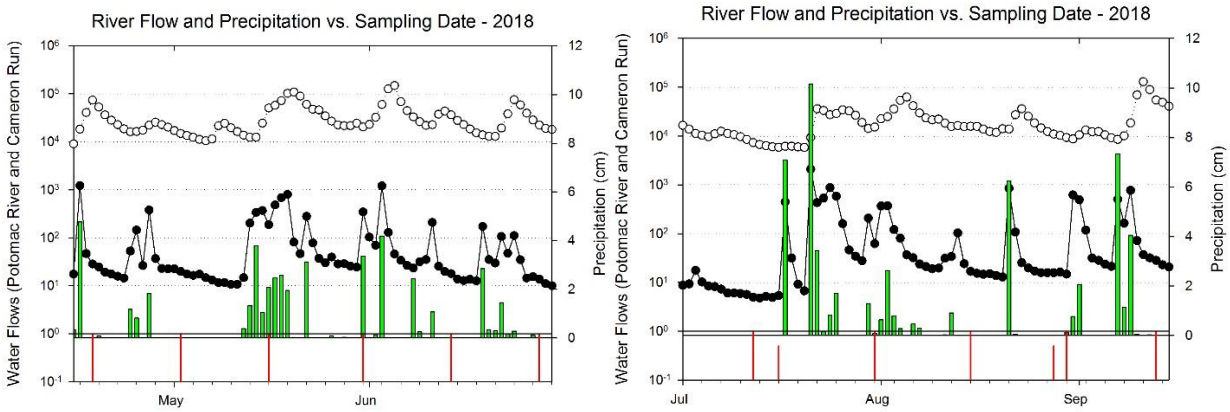

Figures 98a, b. Precipitation (green bars), Cameron Run flows (solid circles), Potomac River flows (open circles) and water quality/plankton sampling events (red lines at bottom).

Based on these graphs and the antecedent precipitation data from Table 1, it appears that May 16, May 31, July 31, and September 13 were the profile-plankton sampling dates predicted to be most strongly affected by direct water runoff from rainfall events. However, the entire year was impacted at some level due to the record precipitation and runoff in 2018.

Water temperature followed a typical seasonal pattern at all stations. A steady waring period during May was followed by a slight drop and then increase with peaks in mid-July and late August. Following a decline in early May, specific conductance remained in the 200 to 400 uS/cm range and chloride in the 10-30 mg/L range at AR2, AR3, and AR4. AR1, at the GW Parkway bridge, had elevated specific conductance and chloride through most of the year. Dissolved oxygen was generally in the 80-100 percent saturation range indicating that photosynthesis was not robust in the absence of the SAV. On the two data mapping dates, similar DO's just below 100% saturation were evident in Hunting Creek in contrast to earlier years where values above 100% were observed.. Field and lab pH was generally in the 7-8 range at all stations; in previous years with abundant SAV, pH was often higher. Total alkalinity was generally 70-120 mg/L as $CaCO_3$. Values tended to increase over the study period.

Secchi disk transparency was generally 0.3-0.7 m. Highest values were observed in May and then values declined throughout the summer which is atypical. Light attenuation coefficient also indicated the clearest water was found in May and there were many dates of high light attenuation throughout the rest of the year. Turbidity was generally in the range 10-40 NTU at all stations which is higher than typical. AR4 was generally the most turbid.

Ammonia nitrogen showed a general decrease from May through September and all values were quite low (<0.2 mg/L). In contrast to previous years, nitrate nitrogen showed no seasonal decline. This was due to lack of demand by primary producers. Nitrite was very low at all stations and did not show consistent seasonal patterns. Organic nitrogen was mostly in the range 0.2-0.7 mg/L and gradually increased from May to September. Total phosphorus was less than 0.1 mg/L but was elevated in late June and early July at all stations and in late August at AR4. N/P ratio exhibited some seasonal patterns, but remained above 7.2, consistently pointed to P limitation of primary producers. Total suspended solids was elevated compared to recent years and was generally in the range 10-40 mg/L with a few higher values at AR4. VSS values hovered around 5 mg/L.

In the tributaries, water temperature also generally followed air temperature with a steady rise in the spring and summer through late August. Specific conductance was generally 300-500 uS/cm with a gradual decline through the study period. Dissolved oxygen was generally near 100 percent saturation. AR21 was often higher and AR23 was often lower. pH values were consistently 7-8. Turbidity and YSI chlorophyll were generally low except for elevated values at AR23 which is subject to tidal inundation. Total alkalinity was fairly uniform in all of the tributaries and did not vary much seasonally. Total phosphorus and ortho-phosphorus were low on most dates and at most tributary stations. Organic nitrogen were somewhat elevated at AR23. Ammonia nitrogen was uniformly low at all stream stations throughout the year. Nitrate nitrogen showed a different pattern with elevated values at AR13 and AR23, Hoof Run and Cameron Run below Hoof Run as in previous years. TSS and VSS were low to moderate at all stations except at AR23 on most dates.

Phytoplankton biomass as indicated by chlorophyll *a* began the year in April with rather normal springtime values, but decreased dramatically during May and June to very low of 2 μg/L or less due to flushing from the frequent runoff events. By early July chlorophyll *a* began to increase and exceeded 10 μg/L. This was followed by a decline with the onset of further flushing in late July and then a further increase in August, especially at AR2 and AR3.

Phytoplankton cell density and biovolume did not show the clear patterns related to runoff flushing as was found for chlorophyll *a*. At both sites, cyanobacteria consistently dominated phytoplankton density throughout the year. *Oscillatoria* was the most important cyanobacterial genus. Phytoplankton biovolume was dominated by diatoms with *Melosira* being most important in June and July at both stations. There was a shift to discoid centric diatoms at the embayment station in early August and at the river station in late August

Rotifers showed a dramatic response to the increased runoff and flushing in 2018. Rotifer levels were very low at both stations through June. However, there was a very strong increase in mid-July to levels that were much higher than normal. This corresponds closely to the pattern in phytoplankton as indicated by chlorophyll *a*. This large pulse in rotifers led by *Brachionus* was short lived, however, and decreased abruptly by late July to levels similar to spring and early summer as more flushing occurred due to storms. There was a slight recovery in September.

Most of the crustacean zooplankton were also impacted by the runoff pulses. The small bodied cladoceran *Bosmina* was generally present at lower than normal densities, one of its modest peaks corresponding with the rotifer surge in mid-July. The larger-bodied cladoceran *Diaphanosoma* was also restricted to low numbers with peak densities of $40/m^3$ only 3% of peaks in 2017. Again, the modest peak at AR2 occurred in July. *Leptodora* was present at low levels in July. Copepod nauplii showed an impact of flushing with genrally low numbers except in mid-July. *Eurytemora* was fairly abundant in early May, but bloomed strongly in mid-July like many other zooplankters and peak values were similar to recent years. *Diaptomus* exhibited its strongest peak in mid-May while cyclopoid copepods had a peak then and in mid-July. In summary, many zooplankters showed a peak in mid-July after being suppressed during April and May by high flows. However, a few also peaked in mid-May which was during a high runoff period.

B. Correlation Analysis of Hunting Creek Data: 2013-2018

To better understand the ecological relationships in Hunting Creek and the nearby Potomac River, relationships among parameters were assessed using correlation analysis. Due to the uncertain statistical distribution of some parameters, the correlations were conducted using the Spearman rank correlation coefficient rather than the Pearson coefficient. Since all samples were collected by PEREC personnel at the same time, it was possible to pool the data on all field and lab water quality parameters at the level of depth-averages and/or surface samples. Two tables were constructed: PEREC field and lab parameters with each other, ARE lab parameters with each other.

Table 19 shows the correlations among PEREC-collected water quality parameters from the regular sampling. These reflect relationships over all six years. Indicators of photosynthesis (DOPPM, DOSAT, Field pH) were highly intercorrelated. Also, measures of particles in the water column and resultant water clarity (turbidity, TSS, Secchi disk depth, and extinction coefficient) were also highly intercorrelated. Indicators of phytoplankton abundance (CHLDI, CHLSF, YSICHL, and AFDWSF) were highly intercorrelated. Interestingly, there was a significant correlation between specific conductance and both SD and EXTCO which may related to the fact that both tend to increase seasonally.

Table 19. Spearman correlations among PEREC collected water quality parameters from regular sampling. Depth-integrated samples unless otherwise indicated. AR2, AR3, and AR4 pooled. 2013-2018. June-September. Strongest correlations (r>0.400) are have **bolded** text. Yellow: indicators of photosynthesis. Blue: indicators of water clarity. Green: indicators of phytoplankton abundance.

Spearman Correlation Matrix													
	TEMPC	SPC	DOPPM	DOSAT	FIELDPH	SECCHI	EXTCO	CHLDI	CHLSF	YSICHL	DRYWTSF	AFDWSF	YSITURB
TEMPC	1.000												
SPC	0.116	1.000											
DOPPM	-0.100	-0.230	1.000										
DOSAT	0.127	-0.222	**0.945**	1.000									
FIELDPH	0.200	-0.231	**0.658**	**0.673**	1.000								
SECCHI	0.315	**0.531**	-0.240	-0.226	-0.077	1.000							
EXTCO	0.187	**0.400**	-0.162	-0.150	0.062	**0.884**	1.000						
CHLDI	0.365	0.389	-0.032	0.071	0.005	0.141	0.006	1.000					
CHLSF	0.352	0.385	-0.091	0.010	-0.085	0.126	-0.051	**0.930**	1.000				
YSICHL	0.364	0.271	-0.096	0.000	0.067	-0.011	-0.083	**0.588**	**0.601**	1.000			
DRYWTSF	-0.249	-0.294	0.081	0.076	-0.250	**-0.749**	**-0.696**	0.207	0.230	0.022	1.000		
AFDWSF	-0.158	-0.049	0.109	0.124	-0.149	**-0.492**	**-0.532**	**0.418**	**0.427**	0.238	**0.821**	1.000	
YSITURB	-0.111	-0.274	0.123	0.119	-0.171	**-0.647**	**-0.709**	0.077	0.099	0.130	**0.776**	**0.581**	1.000

TEMP – water temperature (°C), SPC – specific conductance (µS), DOPPM – dissolved oxygen (mg/L), DOSAT – dissolved oxygen (% saturation), FLDPH – field pH,SD - secchi disk depth (m), EXTCO (light attenuation coefficient (m^{-1}), CHLDI – depth-integrated chlorophyll a (µg/L), CHLSF – surface chlorophyll a (µg/L), YSICHL – chlorophyll a (µg/L) as measured by YSI sonde *in situ.*, DRYWTSF – TSS on surface samples (mg/L), AFDWSF – VSS on surface samples (mg/L) YSITUR – Turbidity as measured by YSI sonde *in situ*, n = 81-133.

The correlation coefficients among AR lab parameters are shown in Table 20. Among the most highly correlated variables in this dataset were TSS and VSS (0.931). Total P was positively correlated with TSS and VSS. Most phosphorus is bound to particles so these correlations make sense. TP was negatively correlated with N to P ratio and this makes sense since it is in the denominator of this ratio. And TP was also correlated with nitrogen species. Lab pH was negatively correlated with ammonia nitrogen, but this may just reflect that lab pH is highest in summer when ammonia nitrogen is lowest. Other correlations were not strong.

Table 20. Correlation coefficients between AR lab parameters. AR2, AR3, and AR4 pooled. 2013-2018. June-September. Strongest correlations are bolded.

Spearman Correlation Matrix												
	PHLAB	**ALK**	**TP**	**OP**	**ON**	**NO3**	**NH4**	**NO2**	**CLD**	**TSS**	**VSS**	**NTOP**
PHLAB	1.000											
ALK	0.036	1.000										
TP	-0.225	-0.018	1.000									
OP	-0.174	-0.272	0.267	1.000								
ON	-0.150	0.023	**0.520**	-0.076	1.000							
NO3	-0.125	0.154	**0.500**	0.142	-0.019	1.000						
NH4	**-0.485**	0.032	**0.503**	0.369	0.233	0.299	1.000					
NO2	-0.064	0.040	0.094	-0.080	0.226	0.053	0.236	1.000				
CLD	0.013	0.210	-0.345	-0.127	-0.145	-0.317	-0.112	0.058	1.000			
TSS	-0.241	0.158	**0.827**	0.195	**0.447**	**0.582**	**0.549**	0.149	-0.351	1.000		
VSS	-0.192	0.159	**0.800**	0.150	**0.473**	**0.497**	**0.485**	0.155	-0.310	**0.931**	1.000	
NTOP	0.021	0.133	**-0.647**	-0.178	-0.390	0.212	-0.191	0.062	0.096	-0.358	-0.399	1.000

PHLAB – lab pH, ALK – total alkalinity (mg/L as $CaCO_3$), TP – total phosphorus (mg/L), OP – orthophosphorus (mg/L), NO3N – nitrate nitrogen (mg/L), NH4N – ammonia nitrogen (mg/L), NO2N – nitrite nitrogen (mg/L), CLD – chloride (mg/L), TSS – total suspended solids (mg/L), VSS – volatile suspended solids (mg/L), NTOP – nitrogen to phosphorus ratio by mass. n= 128-134

C. Water Quality: Comparison among Years

Since six years of data are now available for the Hunting Creek area, comparisons were made for each parameter among years. And many of the parameters vary seasonally as well as among stations. In order to assess overall patterns in the data among years and stations box plots were constructed. In a box plot, the spread of the middle 50% of the data is shown by a box with a line in the middle which is the median. Whiskers extend out to the limits of the data. In this 2018 data analysis we focused on interannual patterns. And for water quality patterns we focused on the period June through September.

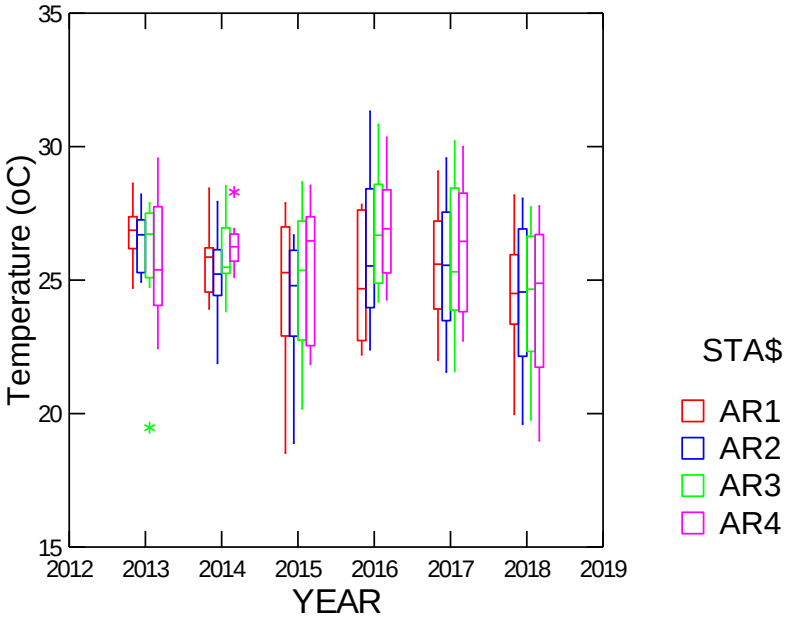

Figure 99. Box plots comparing values of Temperature between years. June through September.

Temperature did not show much difference between the years with the medians in the 24-27°C range at all sites and years (Figure 99). The 2018 medians were on the lower end of that range and varied very little between stations. Specific conductance showed clear differences among stations in most years with AR 1 consistently higher. This pattern was probably due to input from AR effluent (Figure 100). But in 2018, values were clearly lower than in previous years and there was little difference among stations. This is probably attributable to the wet summer which meant that freshwater runoff from the watershed consistently diluted the effect of the effluent and resulted in lower concentrations at all stations.

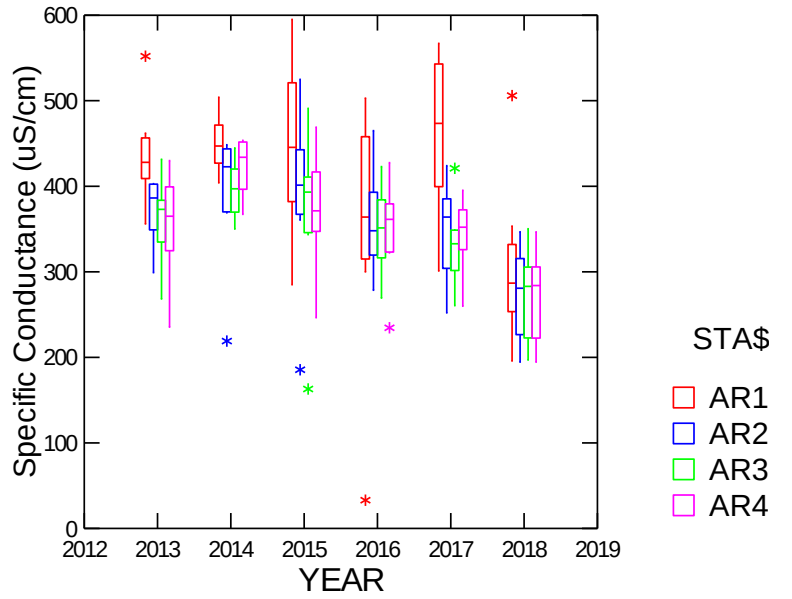

Figure 100. Box plots comparing values of Specific Conductance between years. June through September.

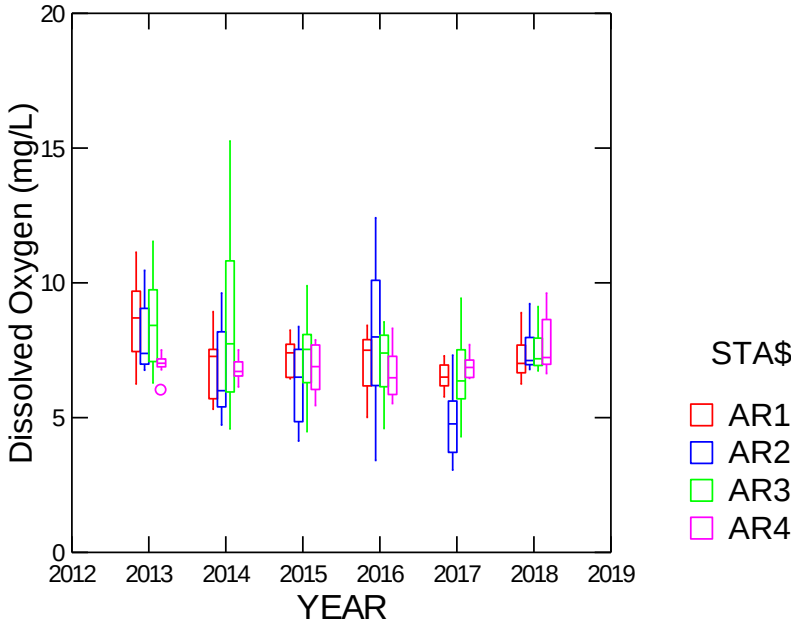

Figure 101. Box plots comparing values of dissolved oxygen as mg/L between years. June through September.

Dissolved oxygen was another variable that showed little difference among stations in 2018 compared with some marked differences in previous years (Figure 101). The interquartile range was also quite low at all stations in 2018. A similar pattern was observed in dissolved oxygen (as % saturation) (Figure 102).

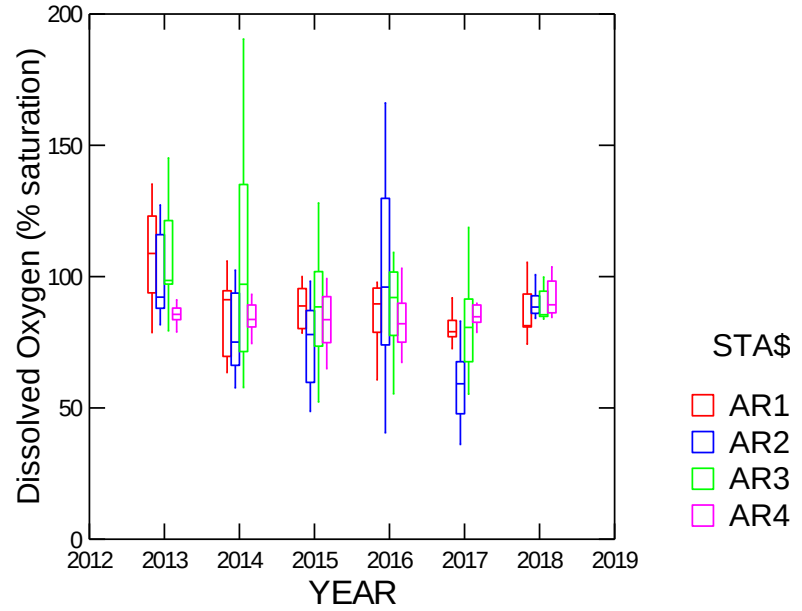

Figure 102. Box plots comparing values of dissolved oxygen as percent saturation between years. June through September.

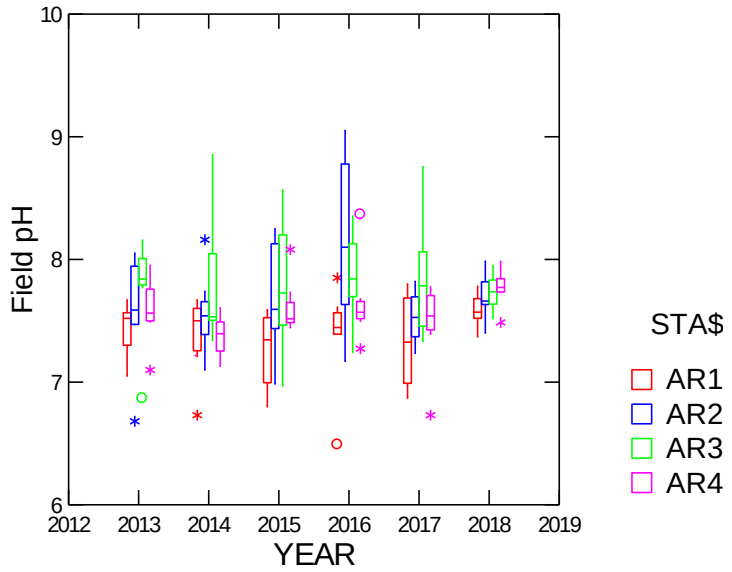

Figure 103. Box plots comparing values of field pH between years. June through September.

Field pH showed a much narrower range in 2018 than in previous years (Figure 103). In some years median values at AR2 and AR3 were much higher than at the other two stations. This was attributed to photosynthesis by SAV which tends to increase pH since the high values were observed in July and August when SAV was most abundant. This explanation works for 2018 too since SAV was very limited in 2018 and pH variation among stations was minimal.

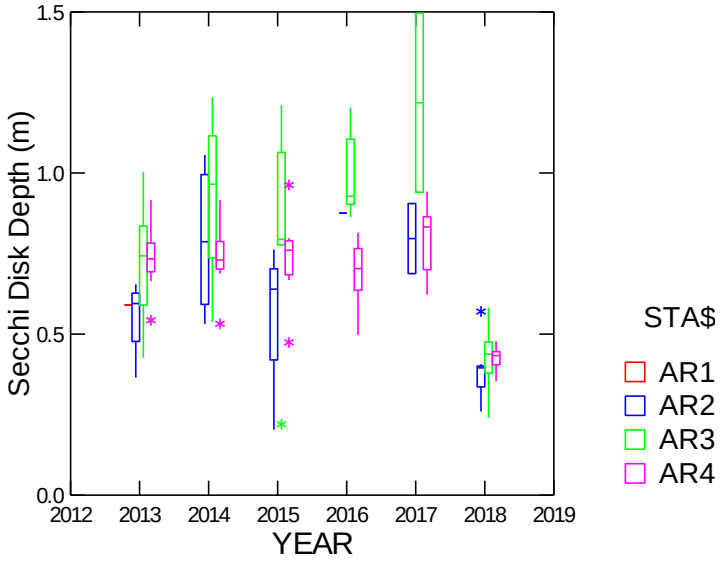

Figure 104. Box plots comparing values of Secchi disk depth between years. June through September.

Secchi disk depth (Figure 104) has generally shown major and consistent differences between stations, attributable to major differences in SAV abundance between the stations. In particular AR3 was often much higher than the other stations. However the year 2018 was quite different. There was little difference between stations and all stations were greatly reduced in Secchi depth, in other words, the water was much less transparent than normal. Again this is consistent with the lowered SAV amounts. Light attenuation coefficient is another ways of measuring water clarity: less negative values of light attenution coefficient indicate clearer water. Median values in light attenuation coefficient were similar from year to year (Figure 105). Light attenuation followed the same pattern as Secchi disk. Values in 2018 showed much less water clarity than previous years and varied little between stations.

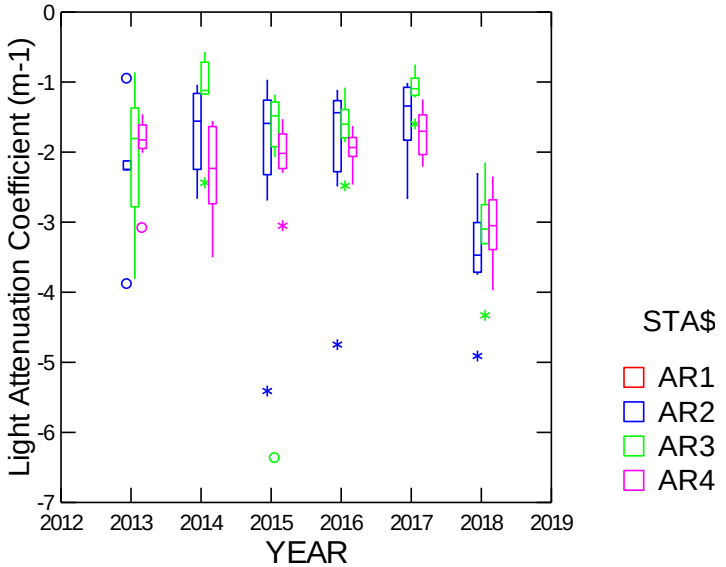

Figure 105. Box plots comparing values of Light Attenuation Coefficient between years. June through September.

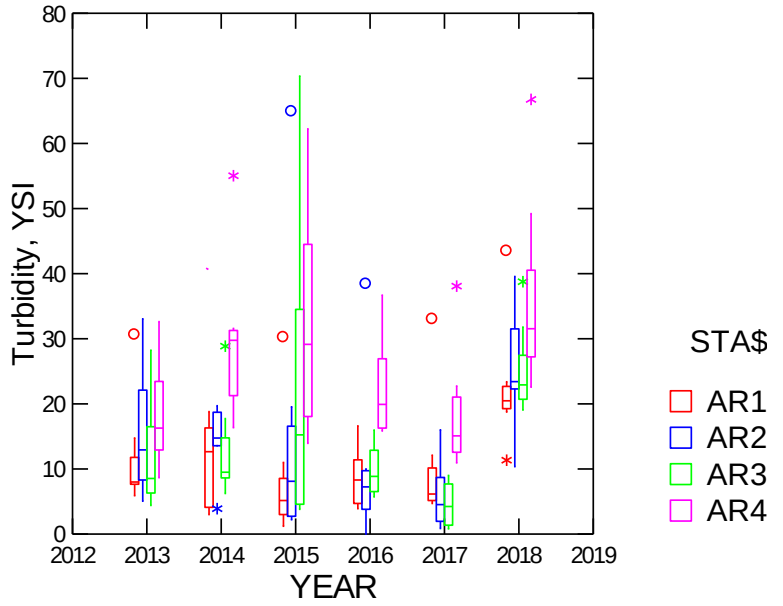

Figure 106. Box plots comparing values of Turbidity between years. June through September.

Turbidity, another measure of water clarity, exhibited much higher values at AR1, AR2, and AR3 than in previous years (Figure 106). Values at AR4 were not as different as in previous years. Total phosphorus values were generally higher in 2018 at all stations than in previous years (Figure 107). As was typical AR4 was generally the highest with AR1 as the second highest. Since total phosphorus is associated with sediments and suspended sediments were generally highest at AR 4, this is consistent.

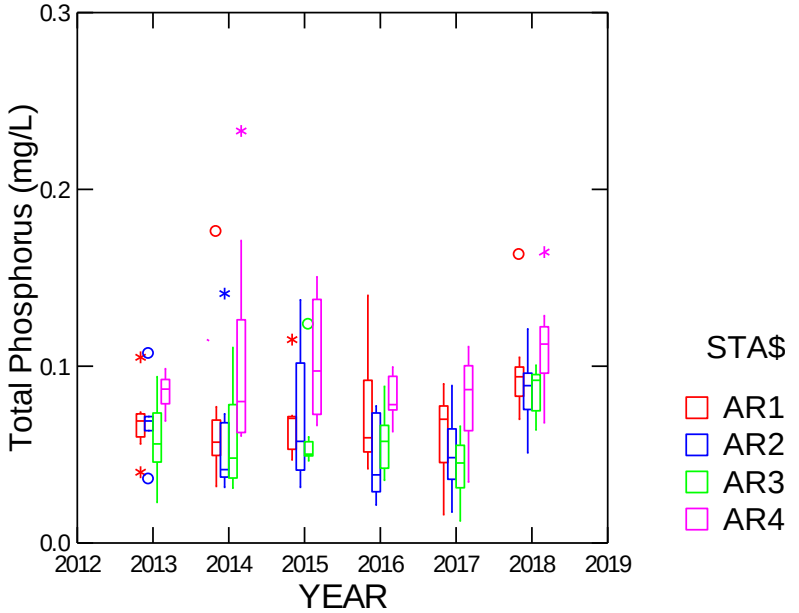

Figure 107. Box plots comparing values of Total Phosphorus between years. June through September.

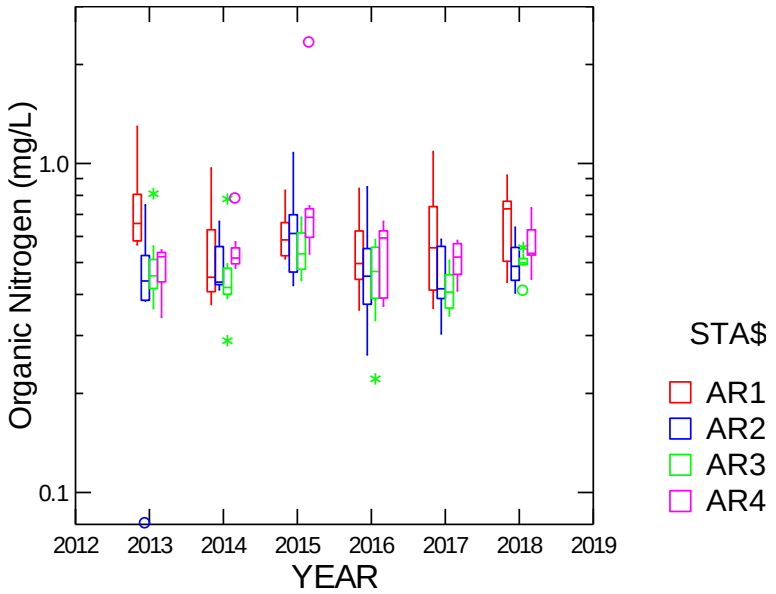

Figure 108. Box plots comparing values of Organic Nitrogen between years. June through September.

Organic nitrogen values in 2018 overlapped extensively with the ranges from previous years (Figure 108). As in previous years AR2 and AR3 were slightly lower than the other two stations. But in 2018 this effect was not strong. Nitrate nitrogen values in 2018 were consistently higher at all stations than in previous years (Figure 109). There were some values in 2018 that were equally high, but not for the whole year. The high values could be explained by two unusual features of 2018: very high flows bring in nitrate and lack of SAV taking up nitrate.

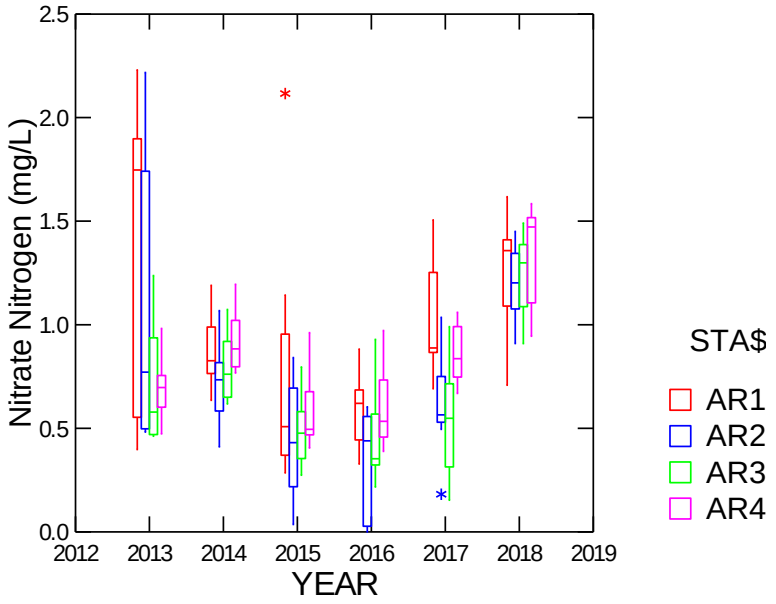

Figure 109. Box plots comparing values of Nitrate Nitrogen between years. June through September.

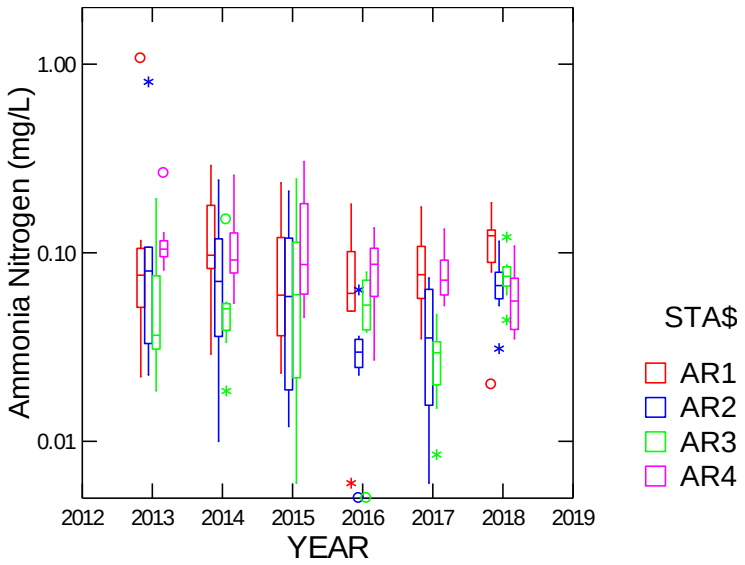

Figure 110. Box plots comparing values of Ammonia Nitrogen between years. June through September.

Ammonia nitrogen values did not show any systematic variation among the years (Figure 110). 2108 values fell within the range of previous years. There was a spatial pattern with AR1 highest and AR4 lowest. Nitrite nitrogen values in 2018 were in the middle of the range for previous years (Figure 111). Spatially, AR1 was highest and AR4 was the lowest. N to P ratio was also in the middle range of previous years and indicative of phosphorus limitation (Figure 112).

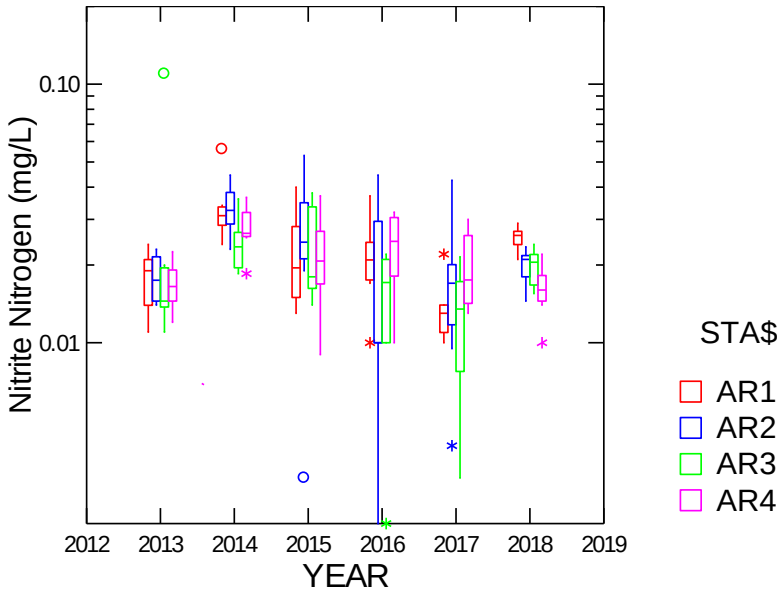

Figure 111. Box plots comparing values of Nitrite Nitrogen between years. June through September.

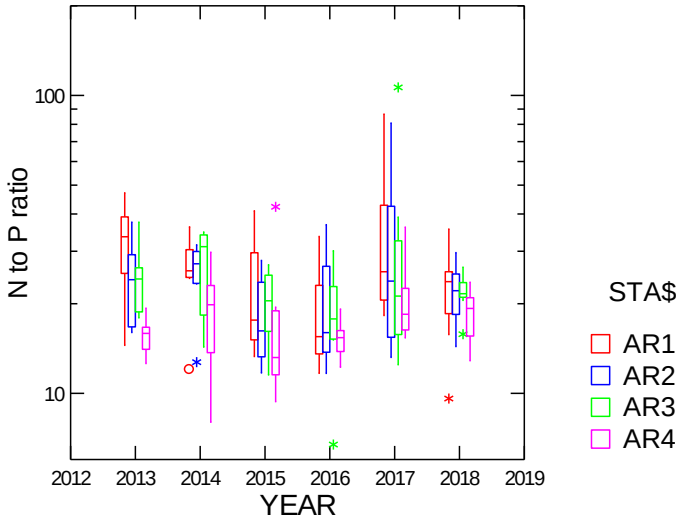

Figure 112. Box plots comparing values of N to P ratio between years. June through September.

N to P ratio for 2018 was in the lower range of values from previous years, but still well within the range indicating phosphorus limitation. AR4 had the lowest median value and AR1 had the highest as in most other years.

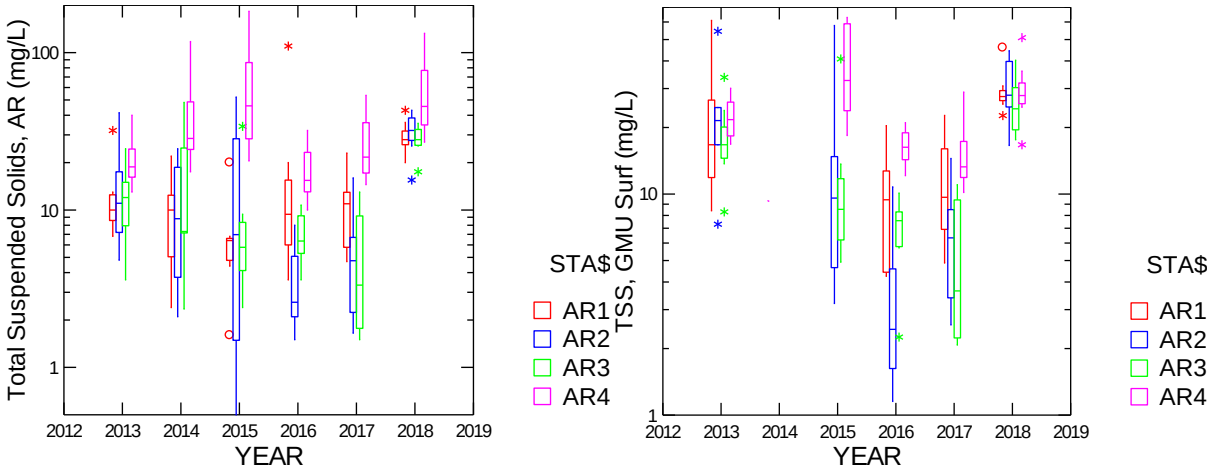

Figure 113. Box plots comparing values of Total Suspended Solids between years. Alex Renew data (a. left) and GMU data (b. right). June through September.

Total suspended solids (TSS) for most stations was substantially higher in 2018 than in any previous year (Figure 113a,b). The exception was AR4 where values have been consistently higher than at the other stations. The patterns were similar in samples analyzed by both Alex Renew and GMU. This correlates with the lower Secchi disk depths and greater light attenuation since particles are responsible for most of the degradation in water quality.Volatile suspended solids (VSS) exhibited markedly less systematic variation among years, but values were still generally on the high end in 2018 (Figure 114a,b).

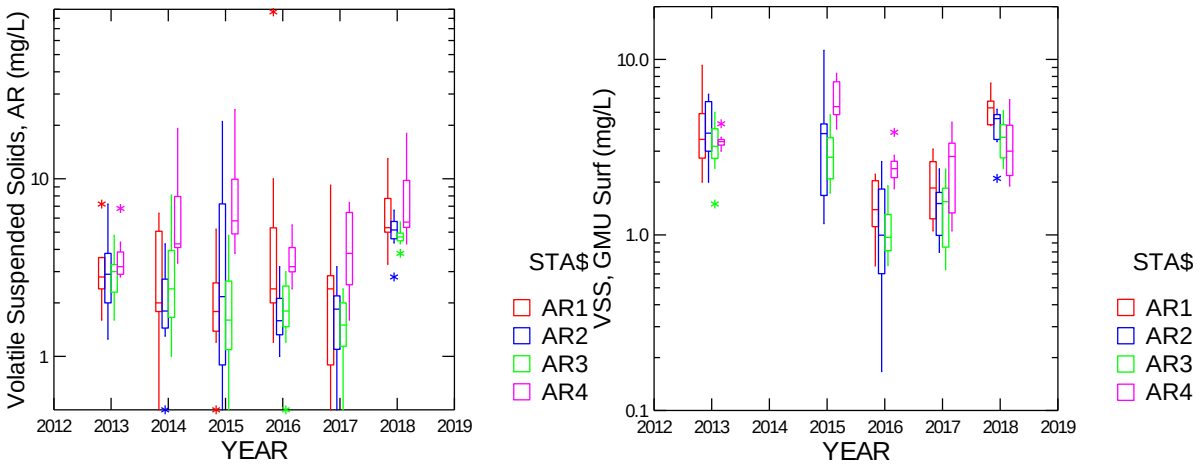

Figure 114. Box plots comparing values of Volatile Suspended Solids between years. Alex Renew Lab data (left) and GMU Lab data (right). June through September.

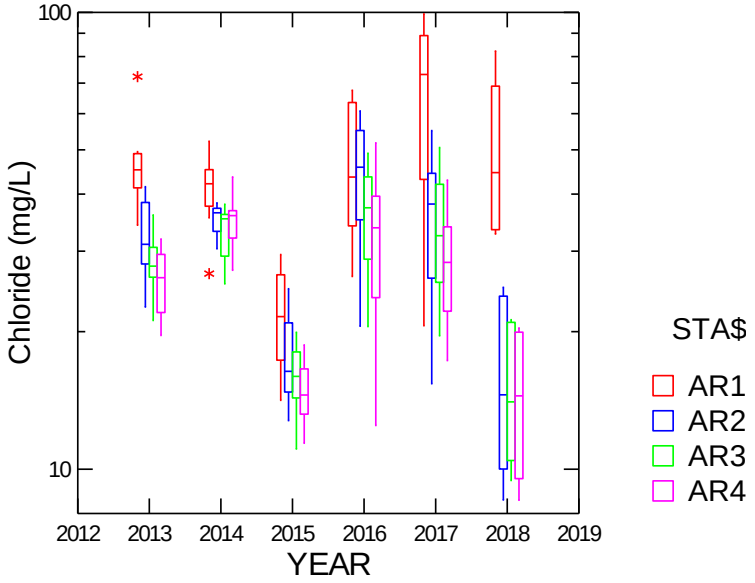

Figure 115. Box plots comparing values of Chloride between years. June through September.

Chloride levels showed a clear spatial pattern in 2018 with highest values at AR1 (Figure 115). At the other stations, chloride was much lower than in previous years with the exception of 2015. There was a surprising difference between AR1 and the other stations. The very low chloride values at AR2, AR3, and AR4 are probably related to the high rainfall and subsequent dilution and flushing with rainwater that has low chloride. Total alkalinity was slightly higher in 2018 than in previous years at AR2, AR3, and AR4, continuing an upward trend (Figure 116). In contrast to chloride, total alkalinity was actually substantially lower at AR1 than at the other stations.

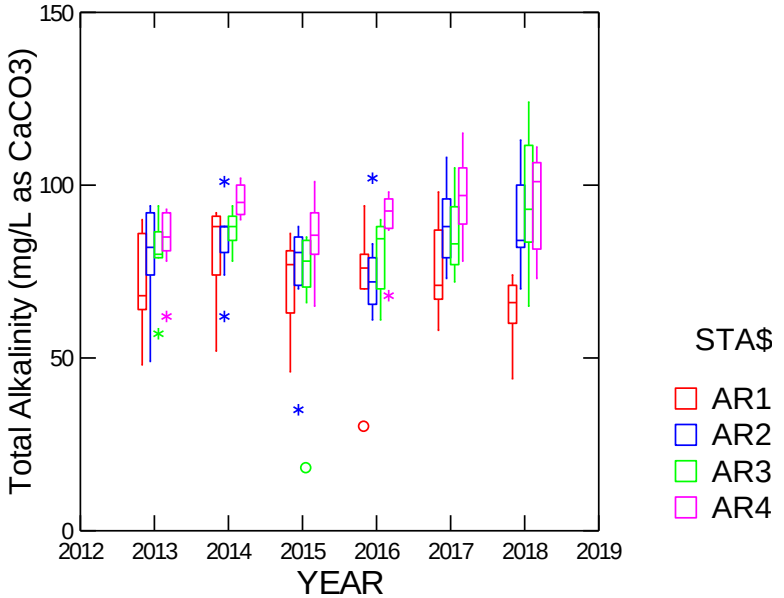

Figure 116. Box plots comparing values of Total Alkalinity between years. June through September.

D. Phytoplankton: Comparison among Years

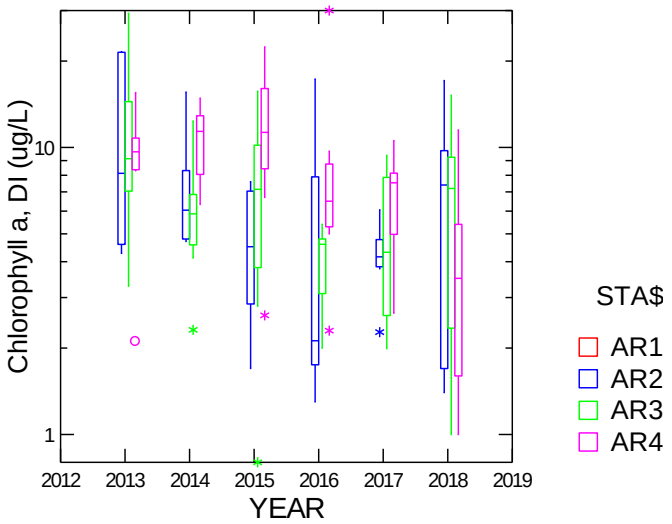

Figure 117. Box plots comparing values of depth-integrated Chlorophyll a among years. June through September.

Several things stand out in 2018 chlorophyll levels. First, values at all stations were extremely variable, especially compared to 2017 (Figure 117, 118). Second, values at AR4 were the lowest of the 5 years of study. Third, median values at AR2 and AR3 were relatively high, but some values were very low. Similar results were observed with surface chlorophyll (Figure 118a,b). Chlorophyll values in the water are a measure of phytoplankton populations which compete with SAV for light and nutrients.

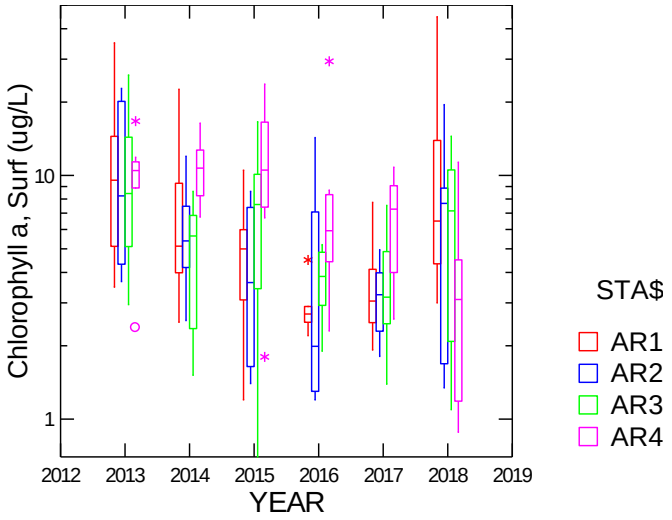

Figure 118. Box plots comparing values of surface Chlorophyll a among years. June through September.

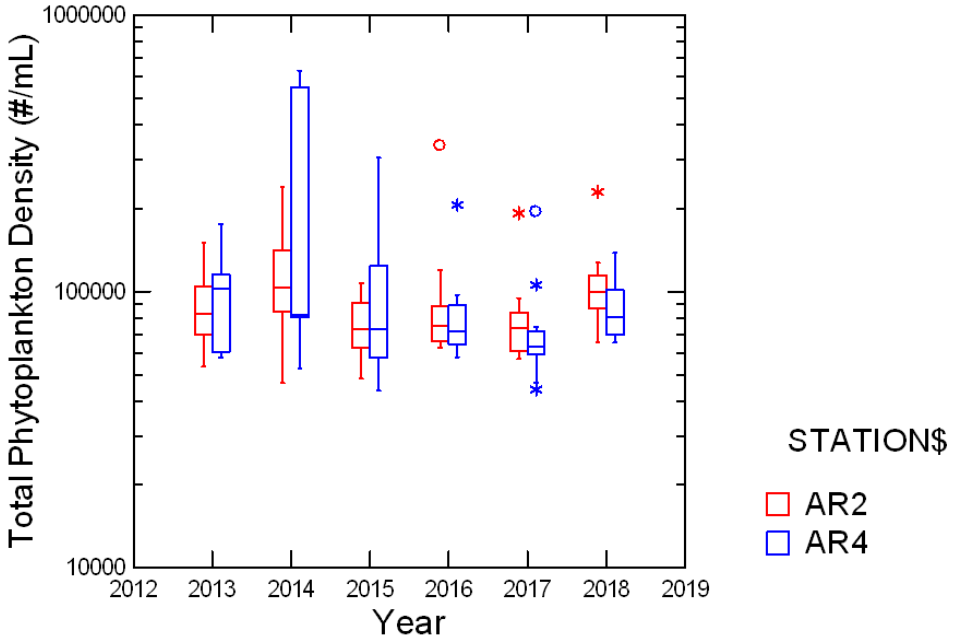

Figure 119. Box plots comparing values of Total Phytoplankton Density.

The median values for total phytoplankton cell density were similar among the six years, although there were more high values in 2015 especially at AR4 (Figure 119). Total phytoplankton cell density in 2018 was in the typical range. Total cyanobacterial cell density was clearly higher in 2014 at both stations than in the other four years (Figure 120). The main difference between the two stations was the greater variability observed at AR4 in most years. However in 2018, it was AR2 that showed greater variation. Overall though, there was not a consistent difference between the two stations in 2018.

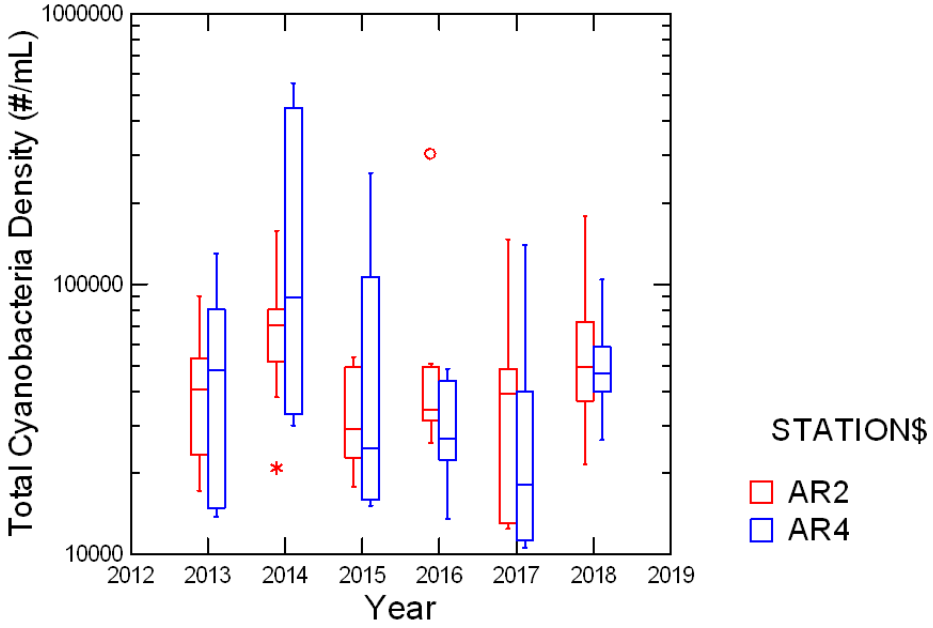

Figure 120. Box plots comparing values of Cyanobacterial Density.

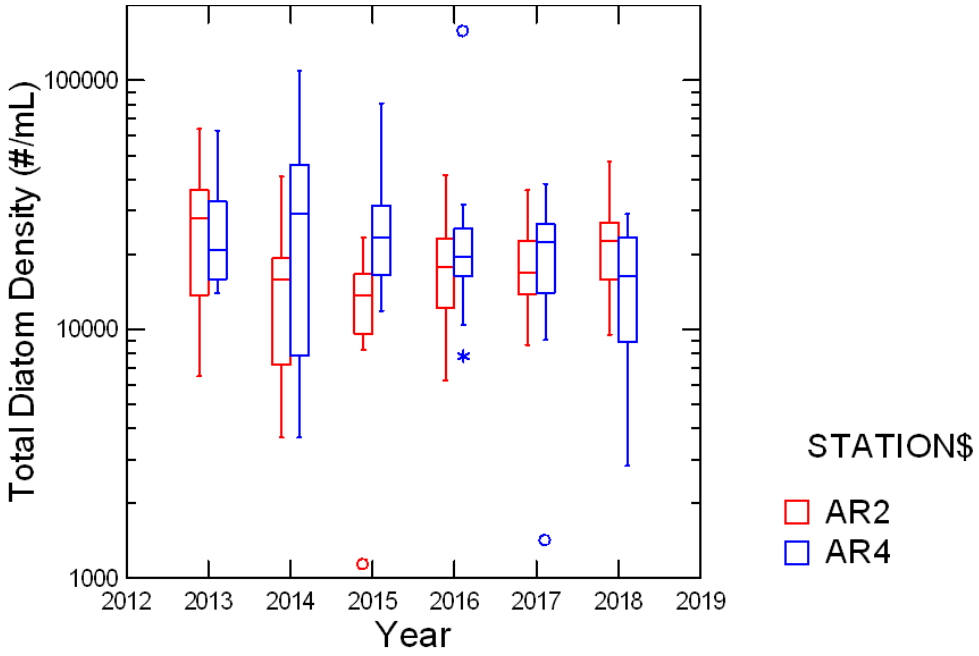

Figure 121. Box plots comparing values of Diatom Density among years.

Median diatom densities overall were fairly constant among all years at AR4 (Figure 121). At AR2, lower medians were found in 2014 and 2015 relative to the other years. Median diatom densities in 2018 were slightly higher than normal at AR2. Green algal cell densities were very similar across the five years (Figure 122). There a slight, but fairly consistent downward trend at both stations.

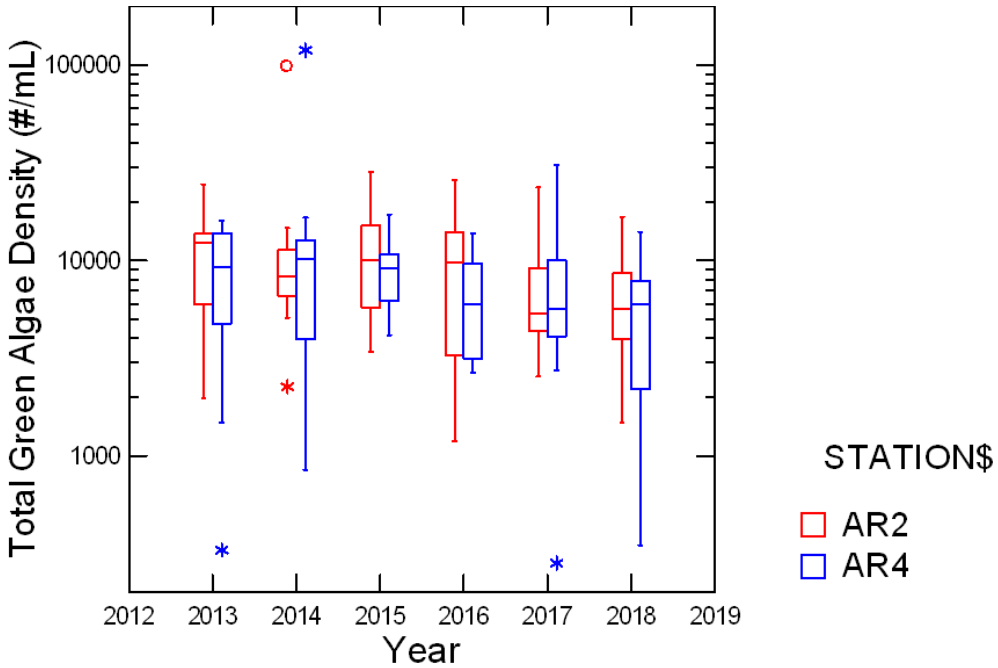

Figure 122. Box plots comparing values of Green Algal Density among years.

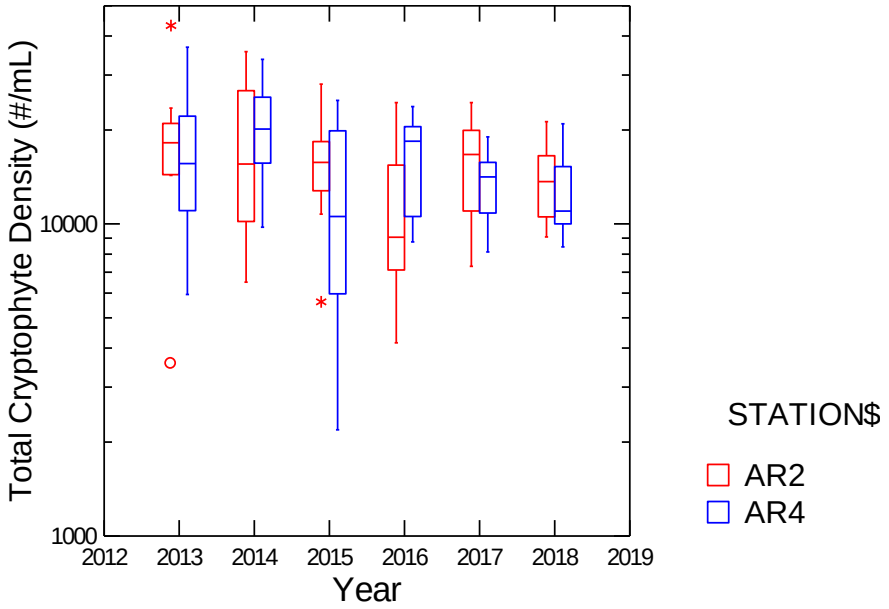

Figure 123. Box plots comparing values of Cryptophyte Density among years.

Median cryptophyte cell densities have not shown a consistent interannual pattern of the years at either station and 2018 values were well within the range of previous years (Figure 123). Miscellaneous taxa includes those species of phytoplankton in groups not tallied above. These are mainly dinoflagellates, crysophytes and euglenoids whose abundances are somewhat sporadic in the study area. This is reflected in interannual patterns which did not reveal any clear trends (Figure 124).

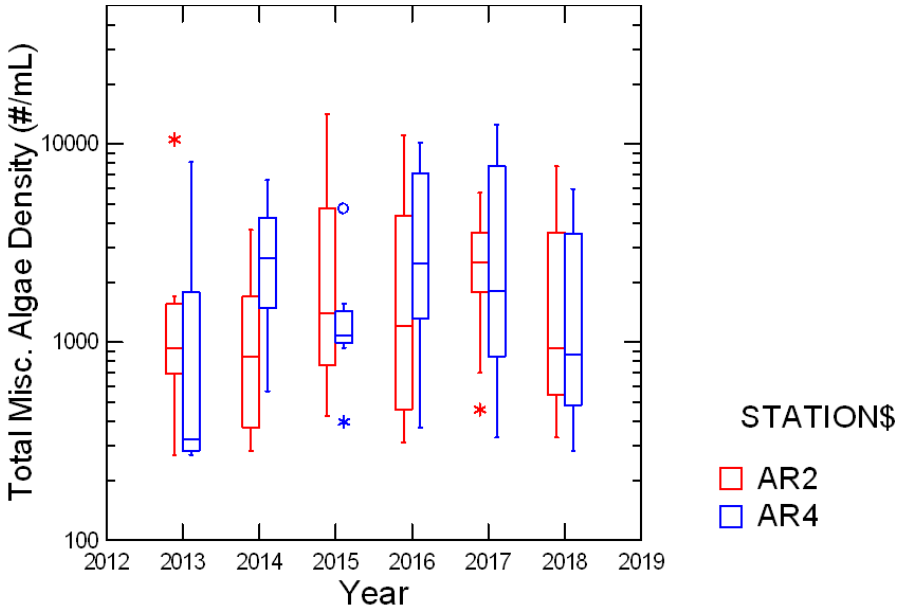

Figure 124. Box plots comparing values of Miscellaneous Taxa Density among years.

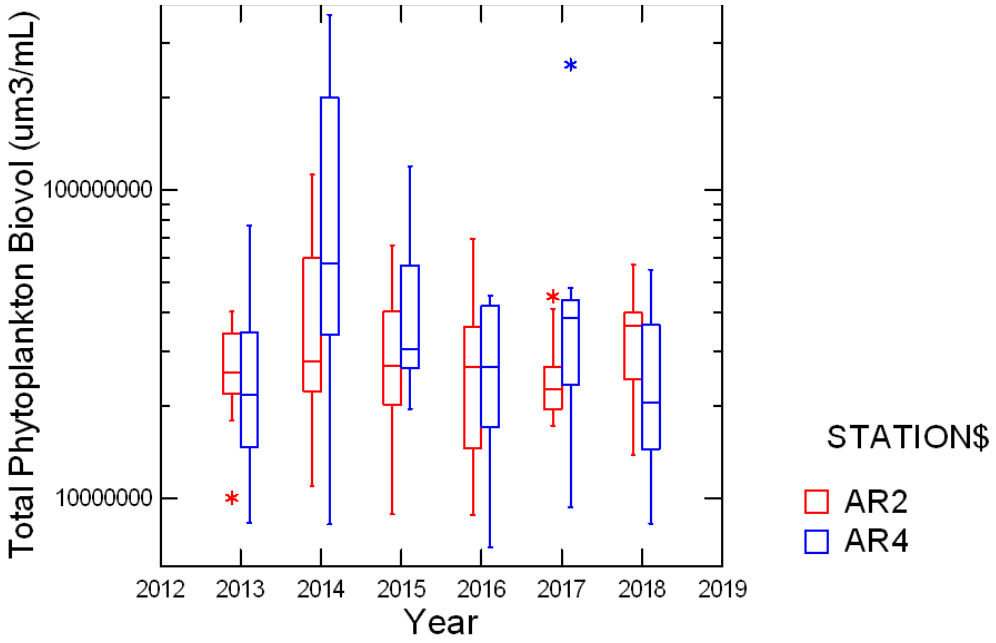

Figure 125. Box plots comparing values of Total Phytoplankton Biovolume among years.

Biovolume takes into account both the number of cells and their relative size. Median values of total phytoplankton biovolume were slightly higher in 2018 than over the previous five years at AR2 (Figure 125). At AR4 total phytoplankton biovolume in 2018 was at the lower end of yearly medians for the six years. Total cyanobacterial biovolume exhibited a steady decline in median values through 2015, but values rebounded at both stations in 2016 and 2017 and continued to increase in 2018 (Figure 126).

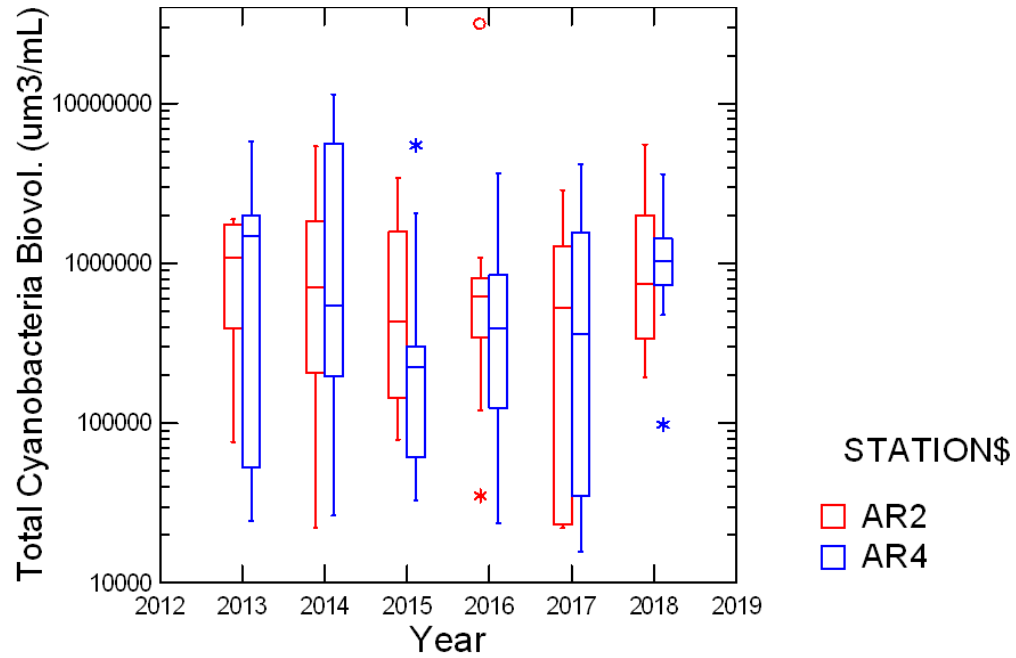

Figure 126. Box plots comparing values of Cyanobacterial Biovolume among years.

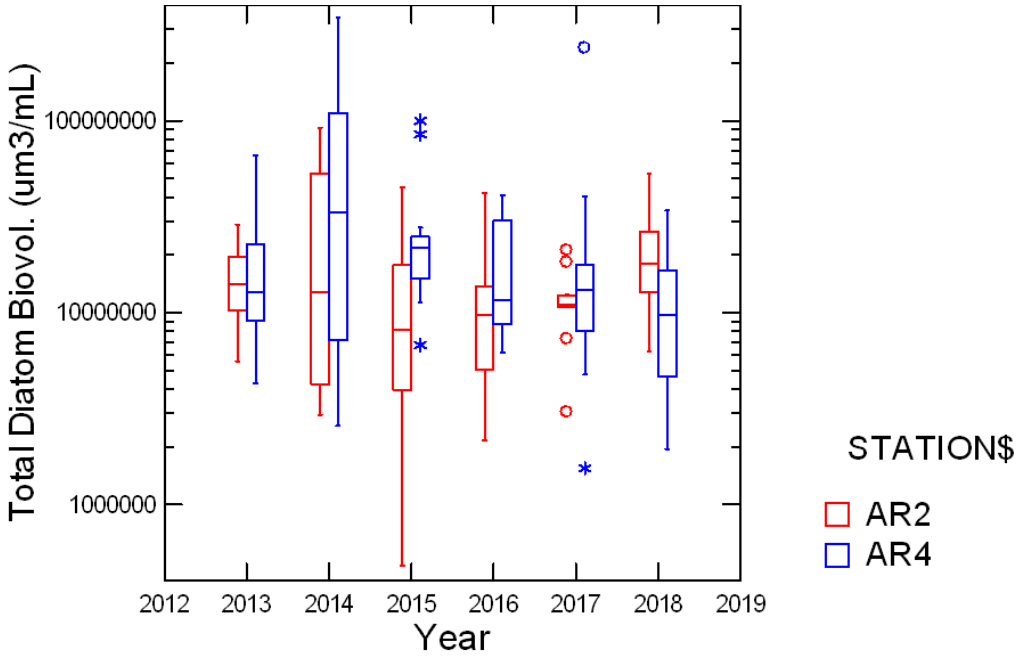

Figure 127. Box plots comparing values of Diatom Biovolume among years.

Median diatom biovolume at AR2 was generally higher than at AR4 in 2018 (Figure 127). The median values observed at AR2 were the highest of the six years while the values at AR4 were the lowest. Median values in green algal biovolume increased in 2015 and 2016, but dropped back in 2017 and 2018 (Figure 128).

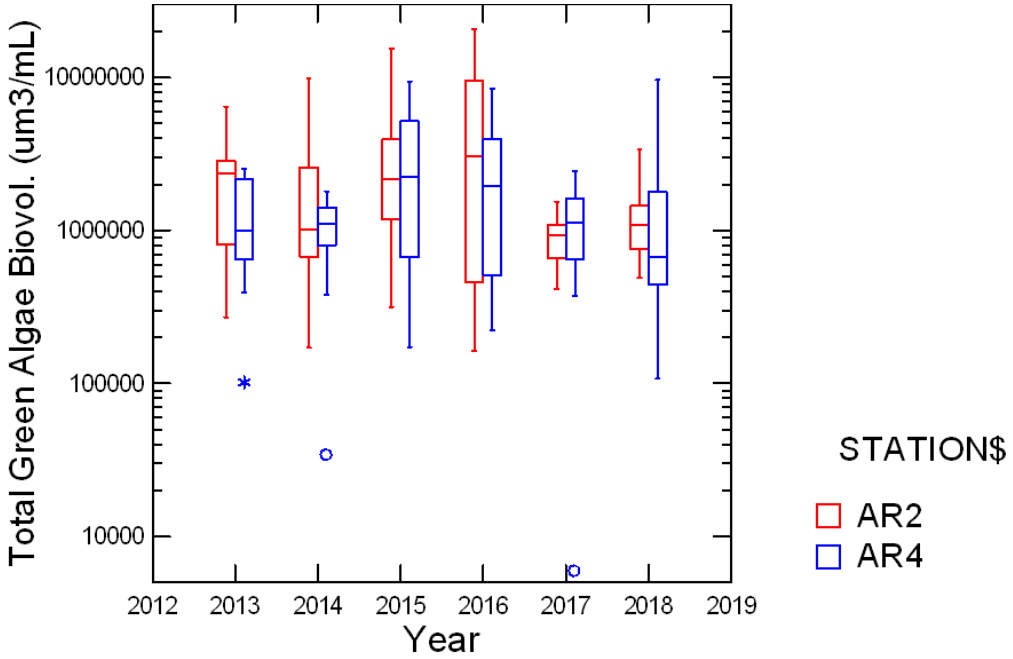

Figure 128. Box plots comparing values of Green Algal Biovolume among years.

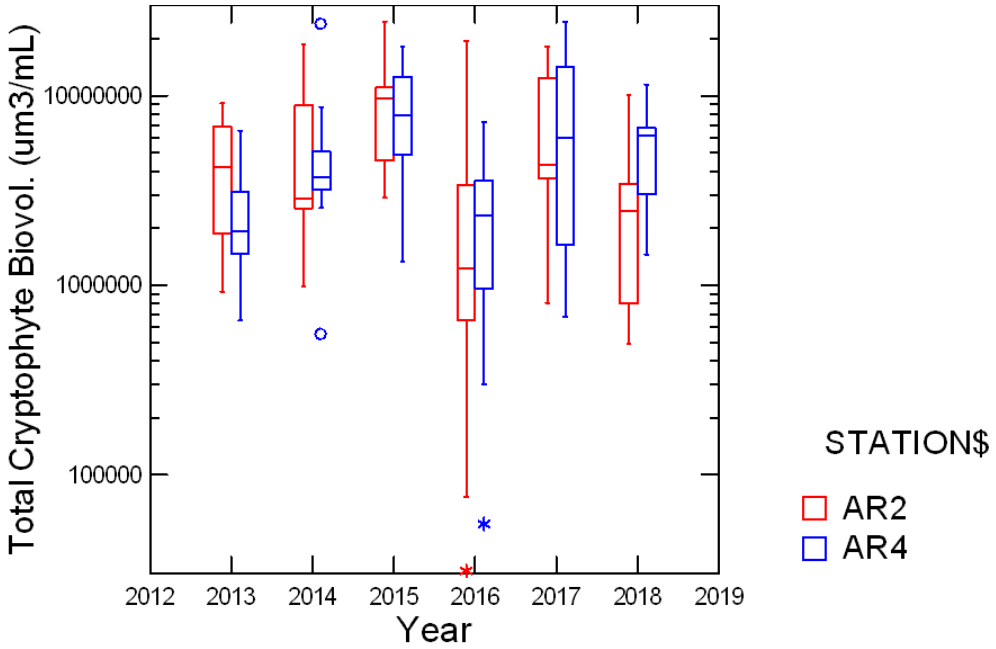

Figure 129. Box plots comparing values of Cryptophyte Biovolume among years.

Cryptophyte biovolume exhibited a clear gradual increase from 2013 through 2015 at both sites, but dropped back markedly in 2016 (Figure 129). They rebounded again in 2017. In 2018 values at AR4 remained high, but at AR2 values declined again. The patterns in Miscellaneous Taxa Biovolume were a bit sporadic and quite variable in some years (Figure 130). The median values in 2018 fell in the normal range and except for one date (outliers at the bottom of the graph), the ranges were smaller than in some years.

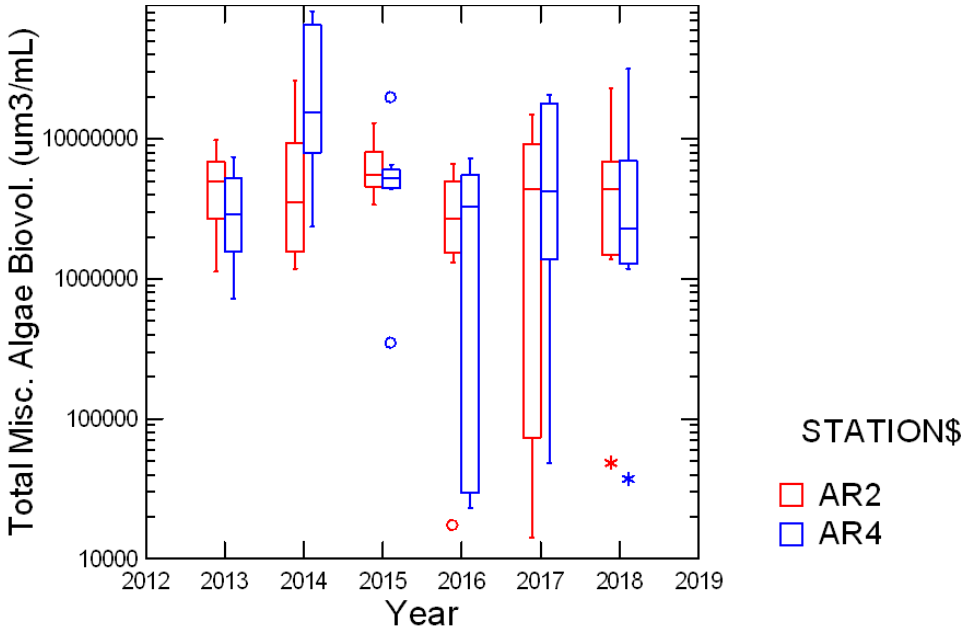

Figure 130. Box plots comparing values of Miscellaneous Biovolume among years.

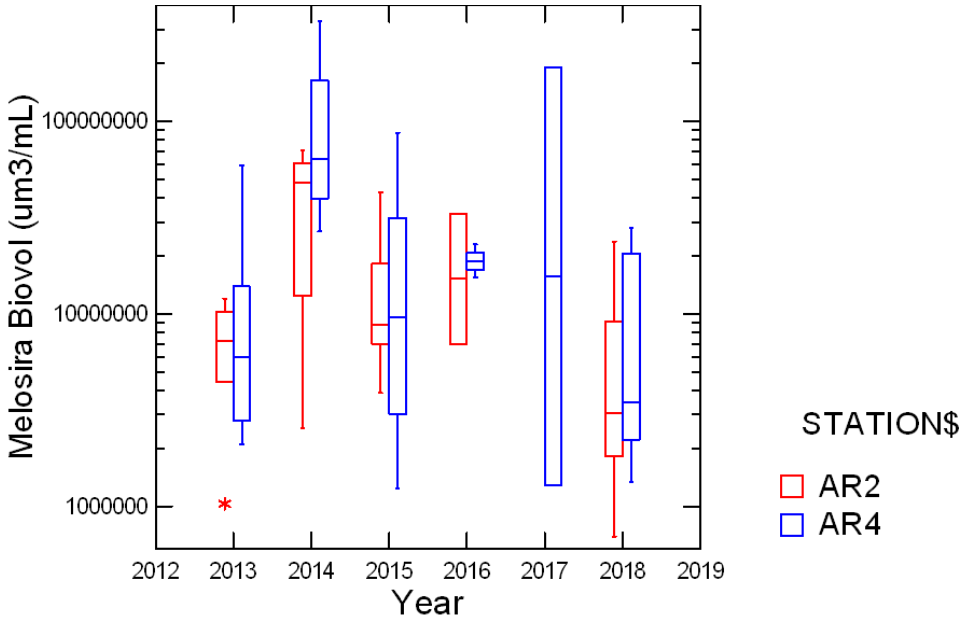

Figure 131. Box plots comparing values of *Melosira* Biovolume among years.

An analysis of interannual and seasonal effects also done for selected individual taxa. Median biovolume values of the filamentous diatom *Melosira* showed a clear peak in 2014 at both stations (Figure 131). Values of *Melosira* in 2018 were generally substantially lower than in other years except in 2017 when it was not obsereved at AR2. Discoid centric biovolume was high in 2014 and 2017 at AR4 (Figure 132a). 2018 values at AR4 ere more in the mid-range of recent years. At AR2 the year of highest median biovolume was 2013. A large range in values was observed in 2018, but the median was relatively normal.

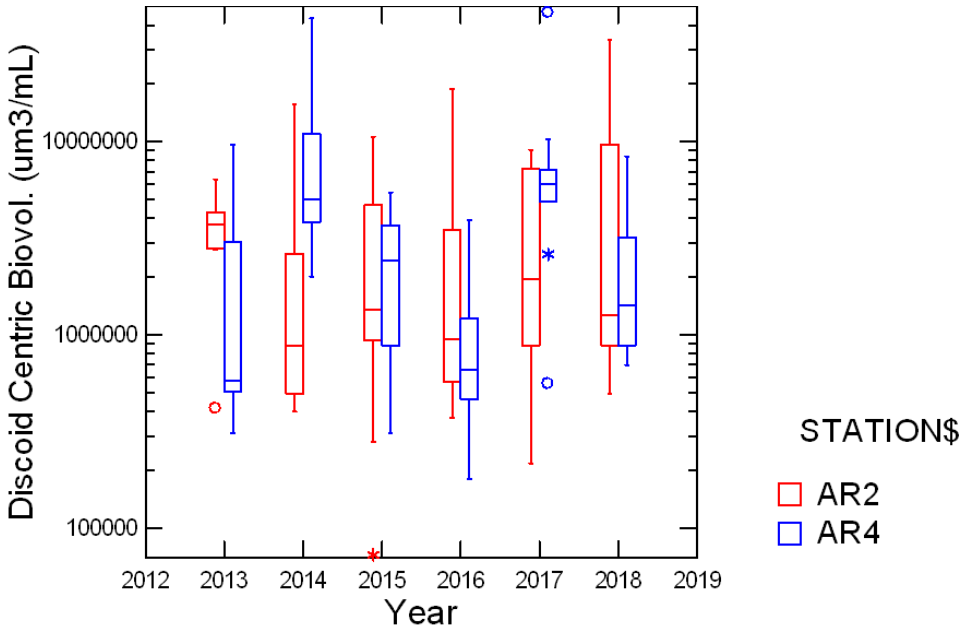

Figure 132. Box plots comparing values of Discoid Centric Diatom Biovolume among years.

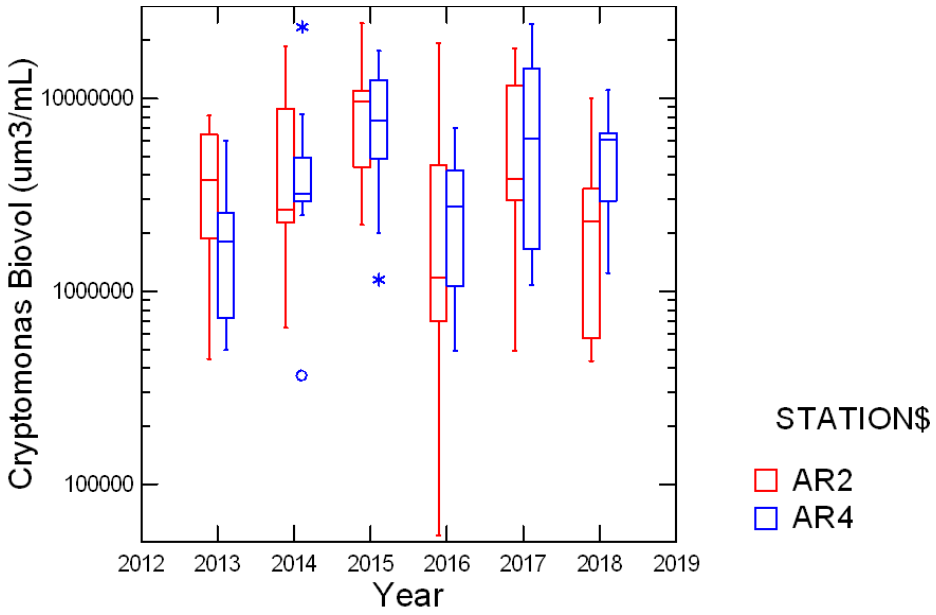

Figure 133. Box plots comparing values of *Cryptomonas* Biovolume among years.

Cryptomonas biovolume showed a general increase at both stations over the first three years of study, dropped back down in 2016, and rebounded in 2017 (Figure 133). In 2018 values remained high at AR4, but were lower at AR2 than in 2017. *Oscillatoria* is the most consistently abundant cyanobacterium in the study area. In 2014 and 2015 it was consistently more abundant at AR4. At both stations values in 2018 were in the mid range of recent years (Figure 134).

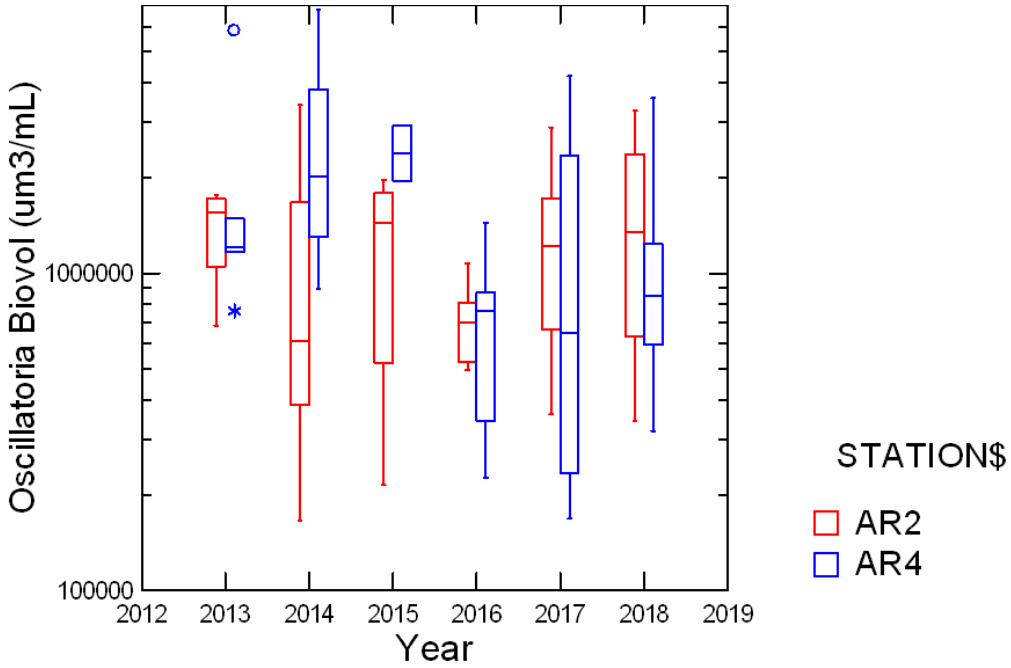

Figure 134. Box plots comparing values of *Oscillatoria* Biovolume among years.

E. Zooplankton: Comparison among Years

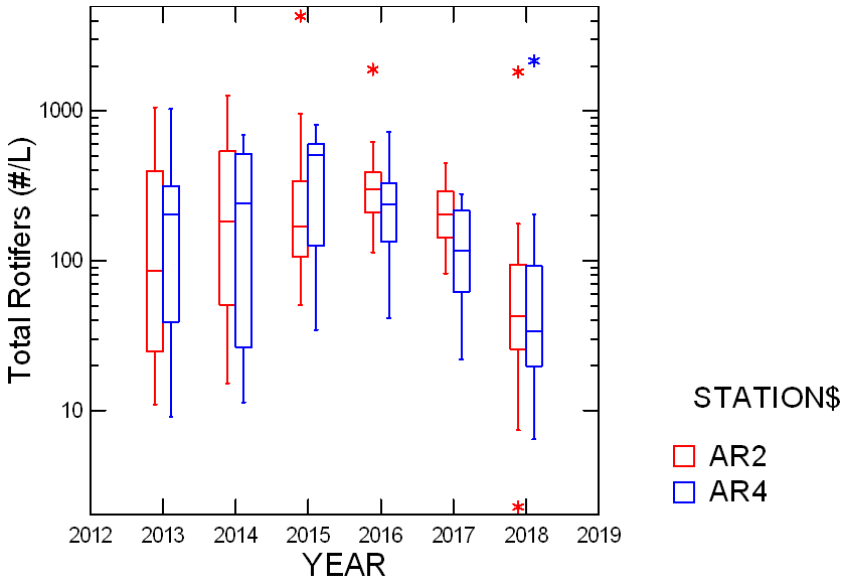

Figure 135. Box plots comparing values of Total Rotifers among years.

Median total rotifer density values did not show much of a difference between the two stations, but a trend of change over the years was observed with values increasing for the first three years and declining in the last 3 years of the study (Figure 135). 2018 had by far the lowest levels to date at both stations. These low values are probably at least partially related to the high rainfall and subsequent flushing of organisms, but may also be part of a longer term trend. The common rotifer *Brachionus* (Figure 136) displayed a similar trend as the totals with 2018 the lowest year to date and hints of a multiyear decreasing trend. *Brachionus* exhibited similar values at both station sin most years.

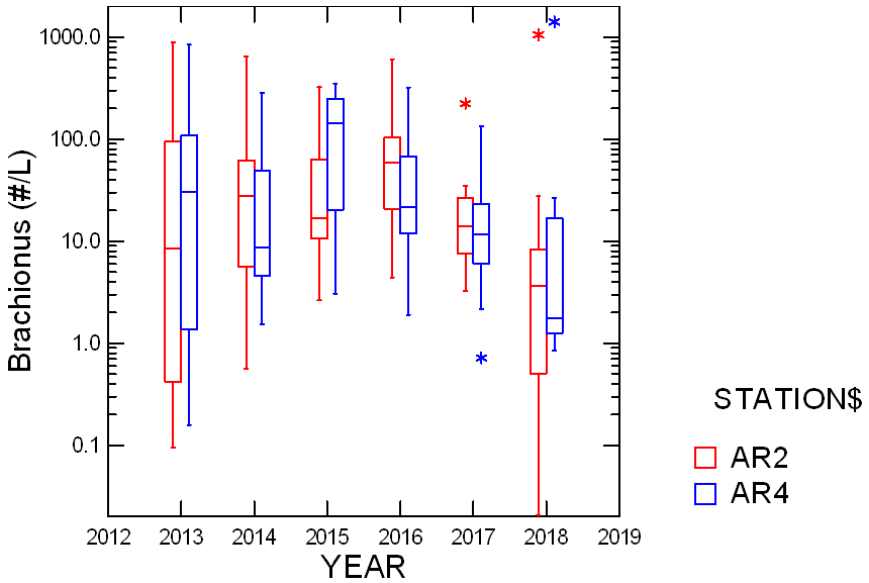

Figure 136. Box plots comparing values of *Brachionus* among years.

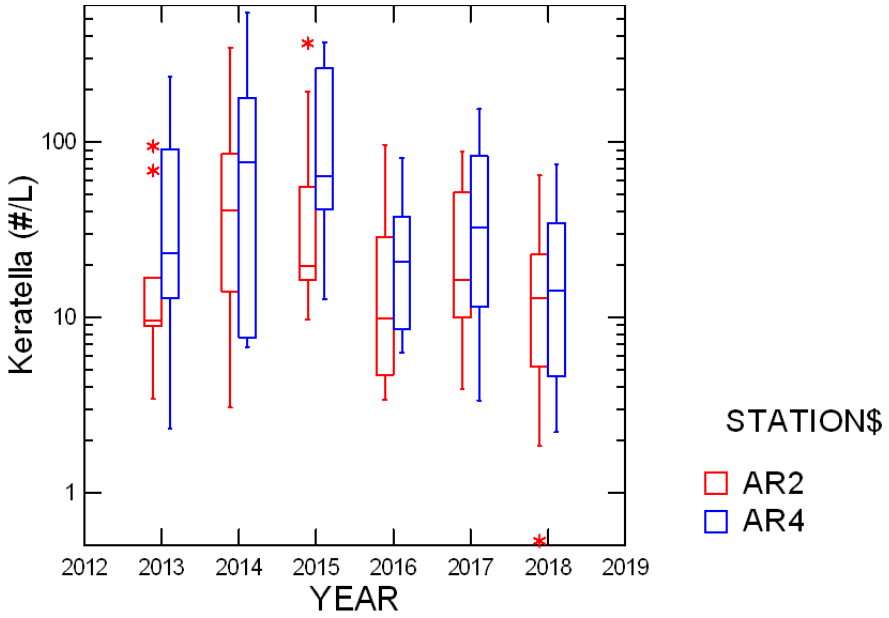

Figure 137. Box plots comparing values of *Keratella* among years.

Another common rotifer *Keratella* exhibited lower values in 2018 than in the first three years of the study but was similar to 2016 and 2017. In previous years it was clearly more abundant at AR4 than AR2, but values were similar in 2018 (Figure 137). The seasonal pattern was one of fairly consistent increase from spring through late summer at both stations (Figure 137b). *Polyarthra*, consistently observed, but less common than *Brachionus* or *Keratella*, was also lower in 2018 than in previous years and exhibited the three year decline found for total rotifers and *Brachionus* (Figure 138). It was present at similar levels at both AR2 and AR4.

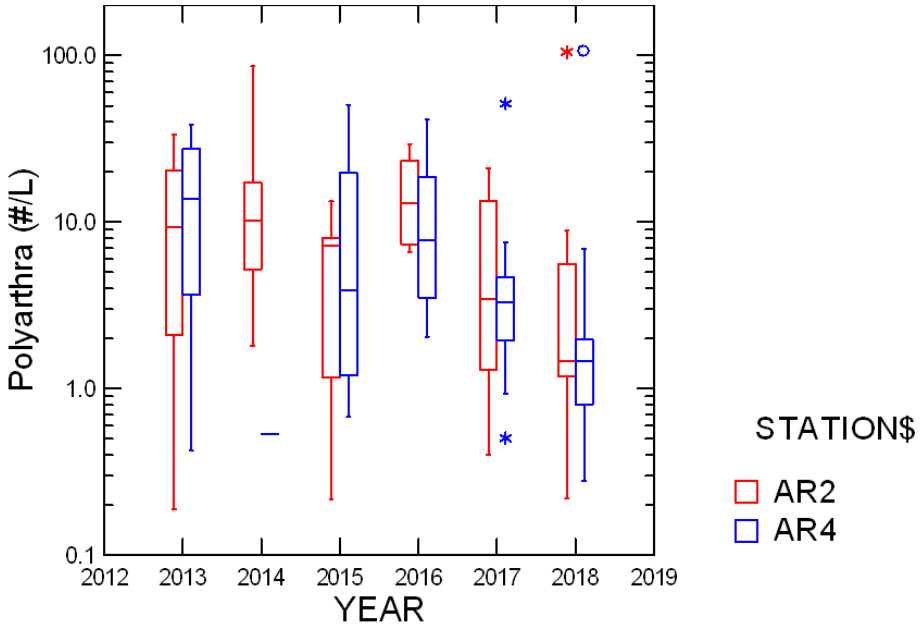

Figure 138. Box plots comparing values of *Polyarthra* among years.

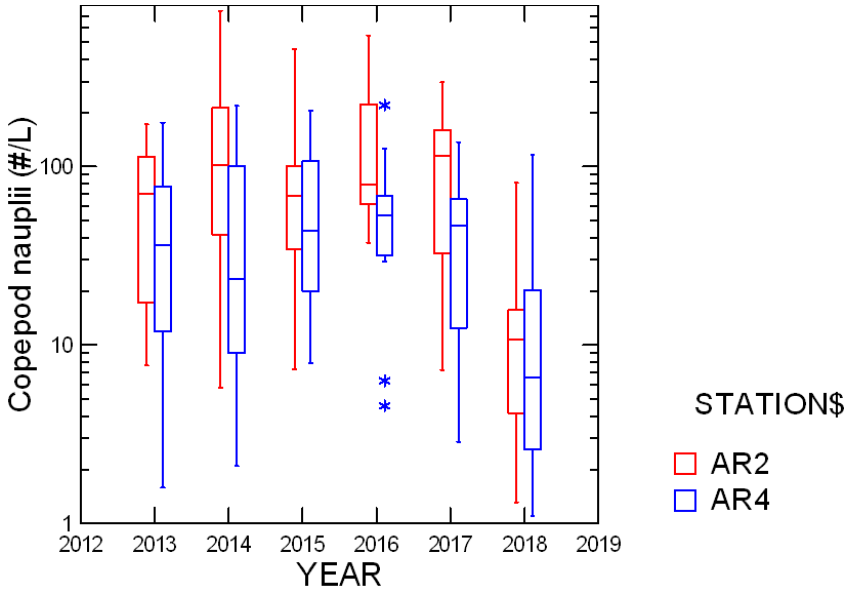

Figure 139. Box plots comparing values of Copepod Nauplii among years.

Nauplii are the juvenile stages of copepods. As such it is hard to identify them to species since they do not have mature characteristics so they have been lumped for all copepod taxa. Nauplii were strongly reduced in 2018 compared to all previous years (Figure 139). Medians were consistently an order of magnitude lower in 2018. In previous years, nauplii were consistently higher at AR2 than at AR4, but showed little difference in 2018. *Bosmina* is a small cladoceran enumerated in the 44 µm samples, but related to *Daphnia* and *Diaphanosoma* collected in the 202 µm nets. Bosmina was also sharply lower in 2018 and reduced by about an order of magnitude from previous years (Figure 140) . There was not a consistent difference in *Bosmina* levels between the two stations.

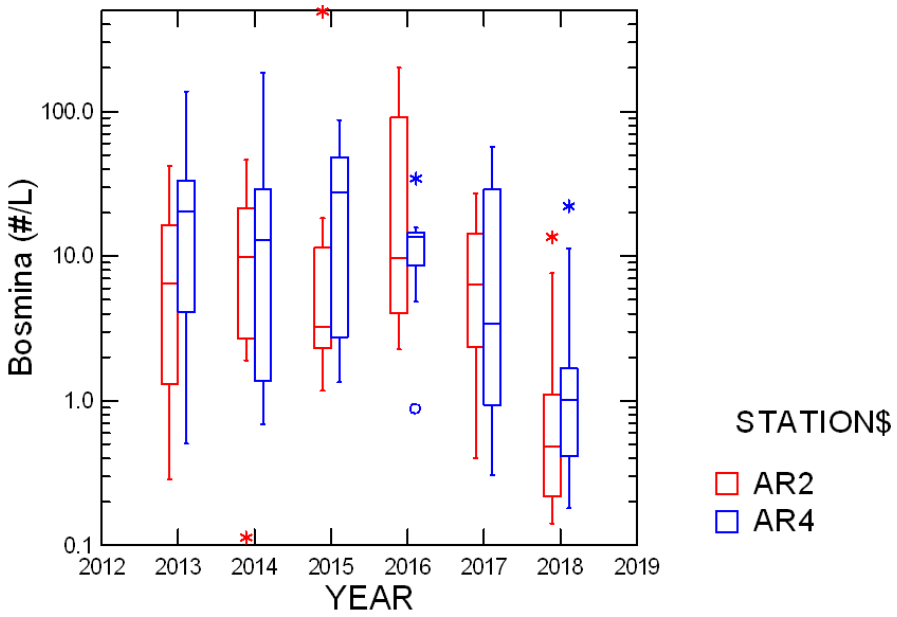

Figure 140. Box plots comparing values of *Bosmina* among years.

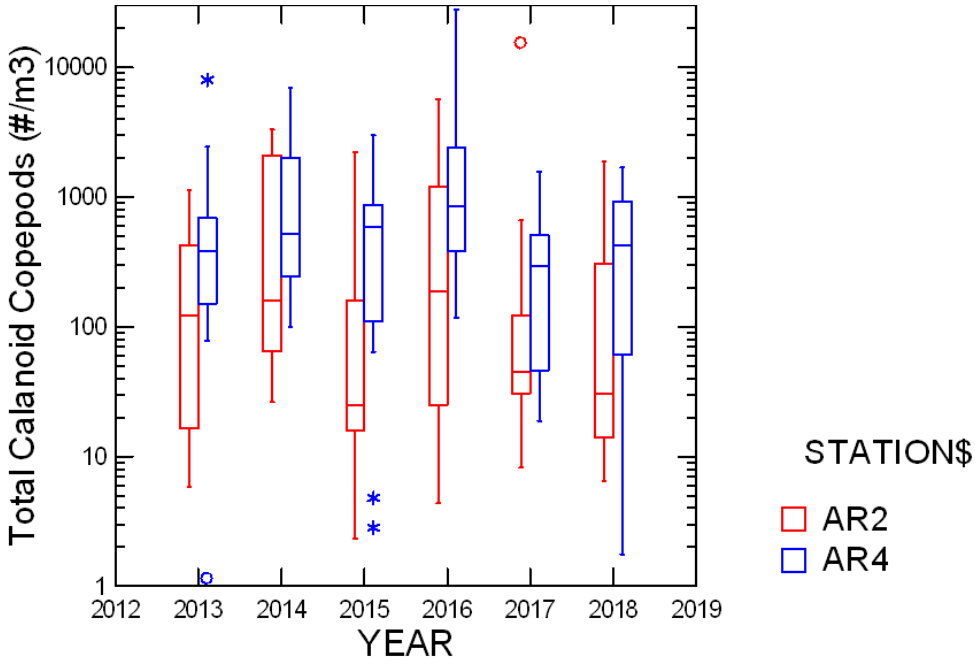

Figure 141. Box plots comparing values of Total Calanoid Copepods among years.

Median calanoid copepod densities were similar among the years at AR4 (Figure 141). At AR4 values were generally higher than at AR2. Median AR2 values in 2018 were at the low end of recent years, but medians at AR4 remained in the range from past years. *Eurytemora* is the most common calanoid copepod. Its interannual pattern was quite similar to that observed for total calanoids (Figure 142) with AR4 clearly higher than AR2 in all years except 2014.

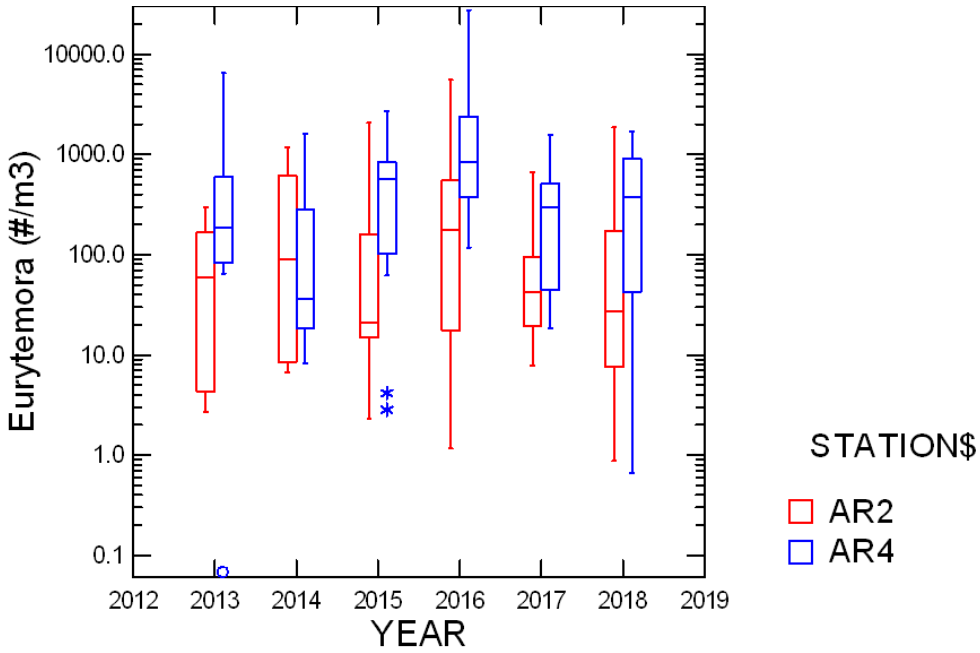

Figure 142. Box plots comparing values of *Eurytemora* among years.

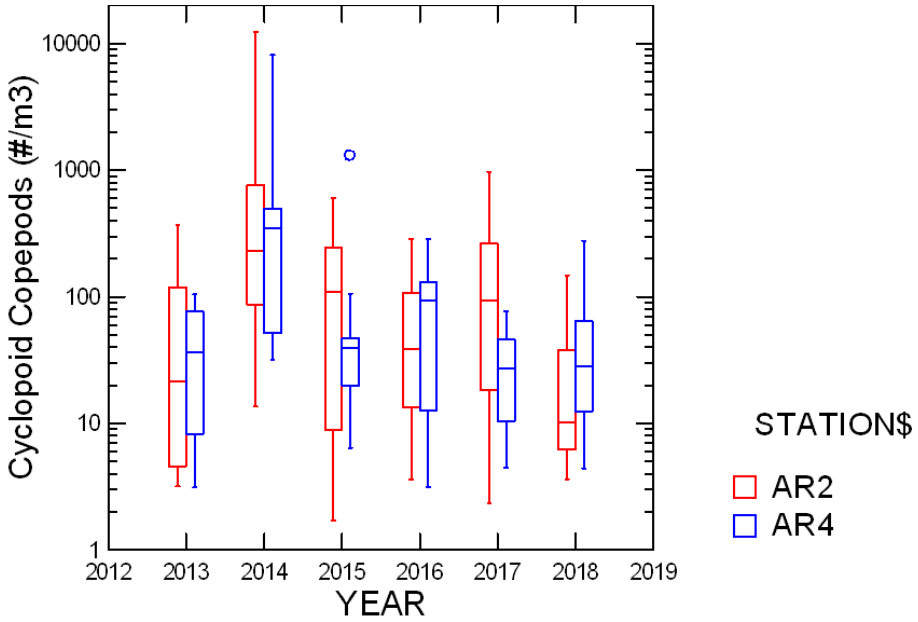

Figure 143. Box plots comparing values of Cyclopoid Copepods among years.

Cyclopoid copepods were present at similar levels in 2018 as in most previous years (Figure 143). In 2018 AR4 was consistently higher than AR2 which was different than in most previous years. *Mesocyclops* is one of the more common cyclopoid copepods. Median values of *Mesocyclops* at AR2 were lower than in the first three years of the study, but similar to 2016 and 2017 (Figure 144). Levels at AR4 were substantially higher than at AR2 and were similar to recent years.

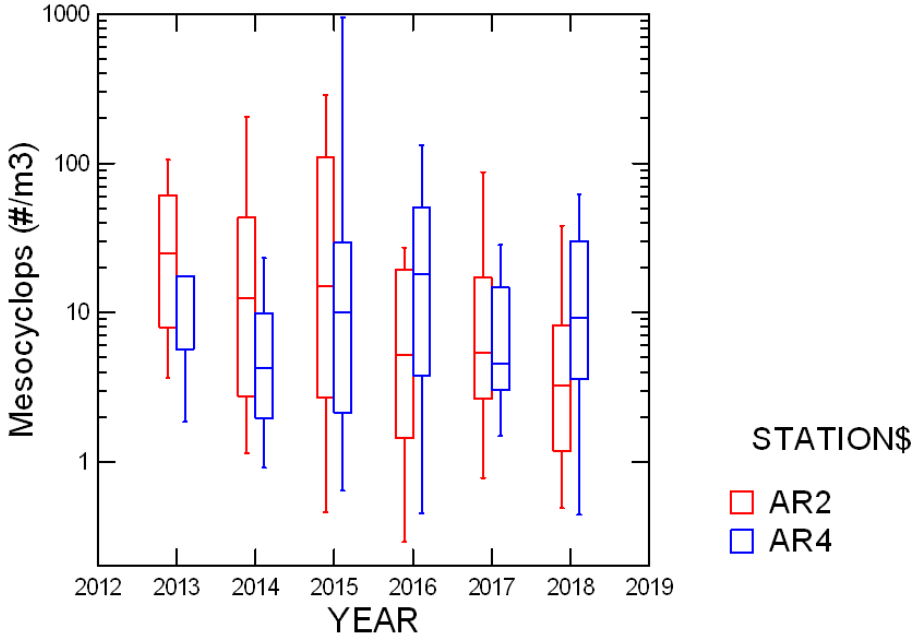

Figure 144. Box plots comparing values of *Mesocyclops* among years.

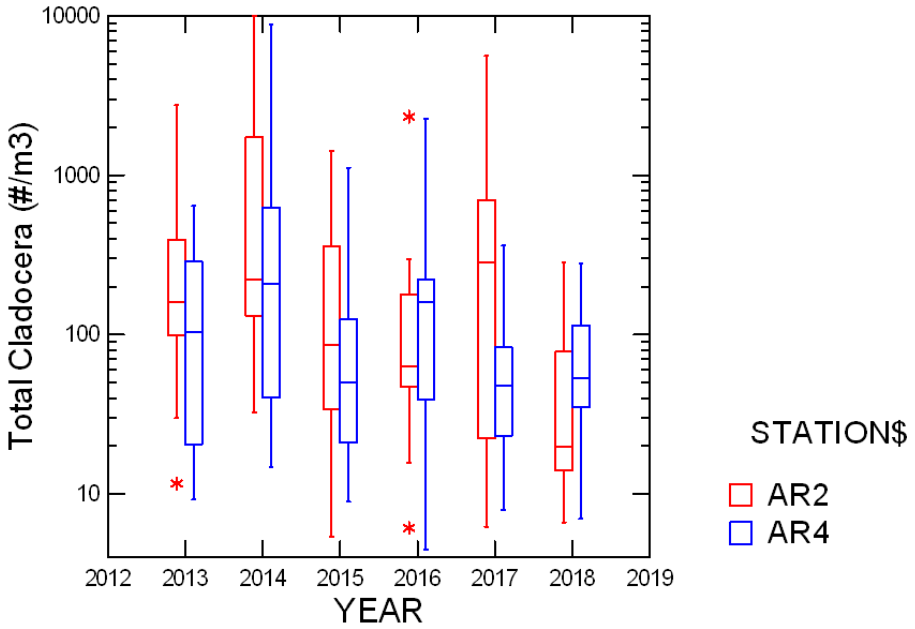

Figure 145. Box plots comparing values of Total Cladocerans among years.

Total cladoceran values (excluding *Bosmina*) at AR2 were clearly lower than in any previous year and much reduced relative to 2017 (Figure 145). Values at AR4 were much higher in 2018 than at AR2 and were similar to recent years. *Daphnia* was found at clearly higher levels in 2014 than in the other years of the study (Figure 146). Values observed in 2018 were similar at the two stations and similar to 2017 levels.

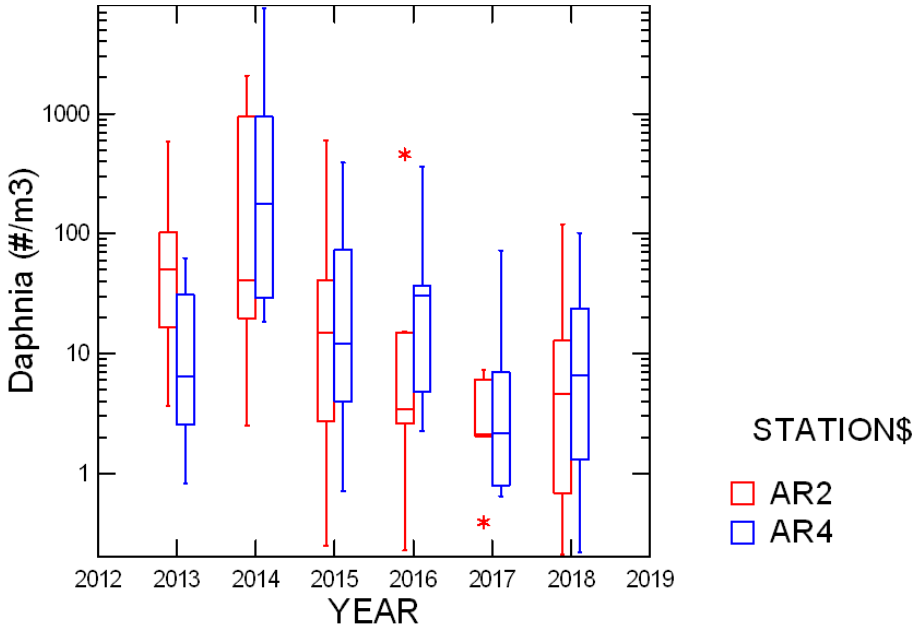

Figure 146. Box plots comparing values of *Daphnia* among years.

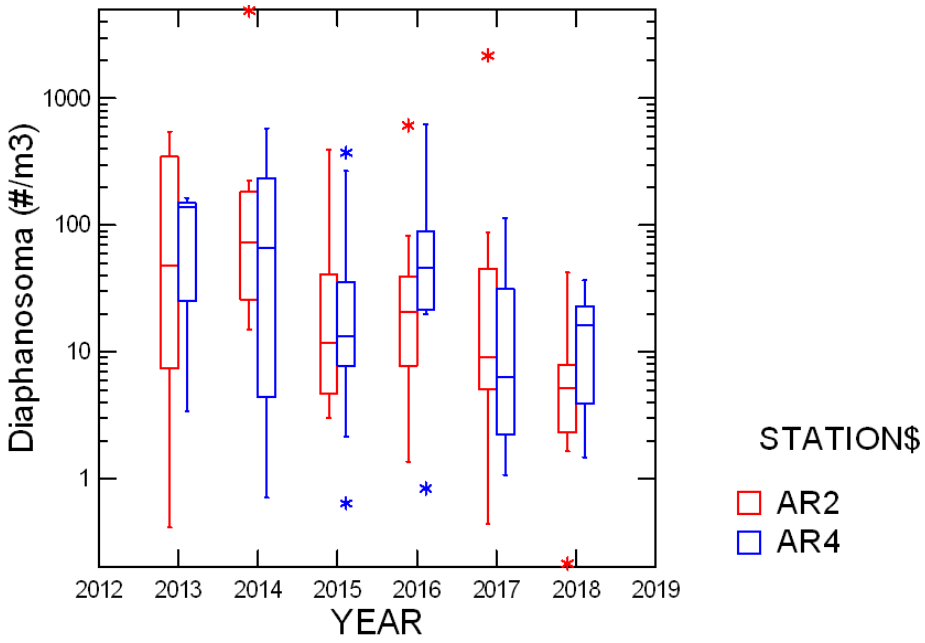

Figure 147. Box plots comparing values of *Diaphanosoma* among years.

Diaphanosoma is a very abundant cladoceran in Gunston Cove, but has proven to be less abundant in the Hunting Creek area, although still important. *Diaphanosoma* levels at AR2 were at record lows in 2018, but at AR4 they were within the range of recent years and actually higher than in 2017 (Figure 147). *Sida* was generally less abundant than *Diaphanosoma*, but has maintained its levels over time. It was also reduced in 2018 and the reduction was much stronger at AR2 (Figure 148).

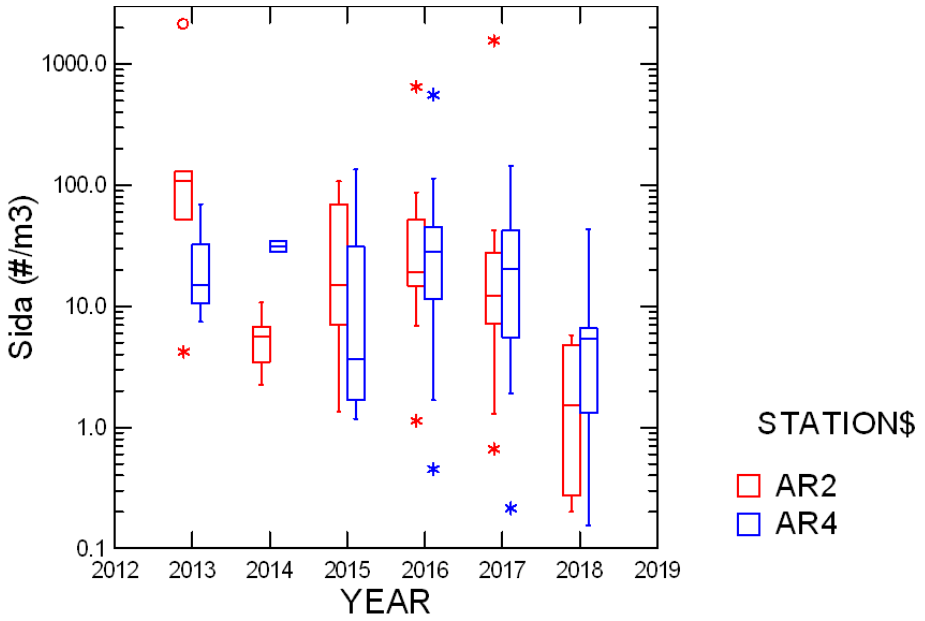

Figure 148. Box plots comparing values of *Sida* among years.

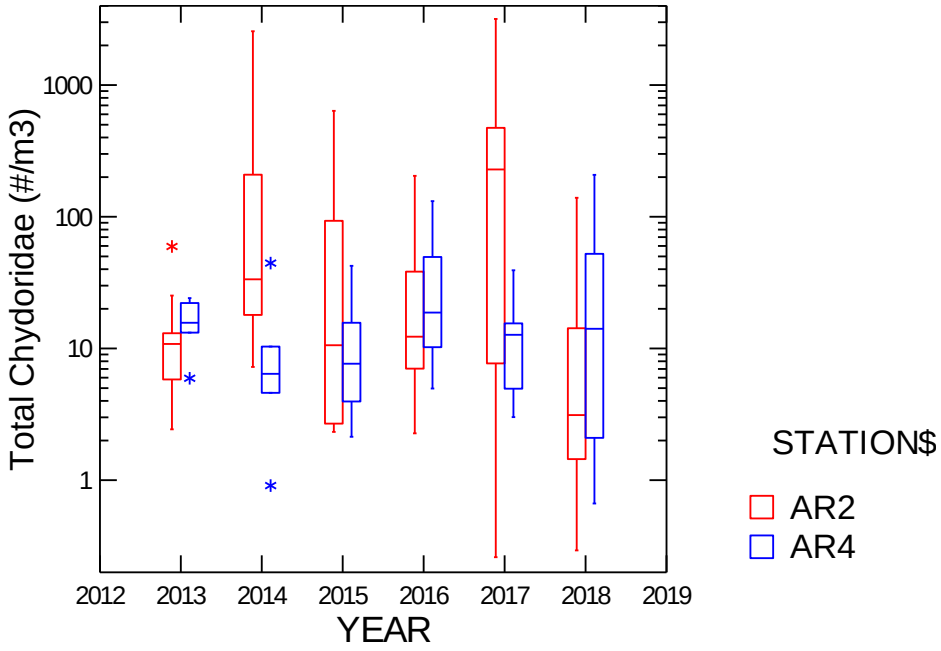

Figure 149. Box plots comparing values of Chydoridae among years.

Chydorids have generally been more abundant at AR2 than at AR4, but in 2018 they were substantially lower at AR2 (Figure 149). The lower value at AR2 was not surprising given the lack of SAV. Macrothricids, another group that likes SAV were absent from the samples in 2018 (Figure 150).

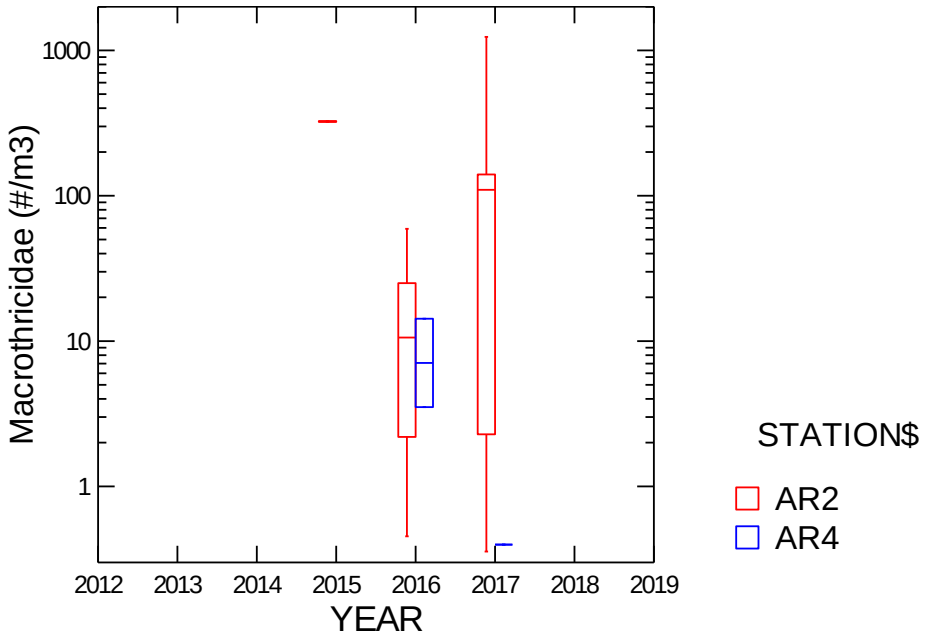

Figure 150. Box plots comparing values of Macrothricidae among years.

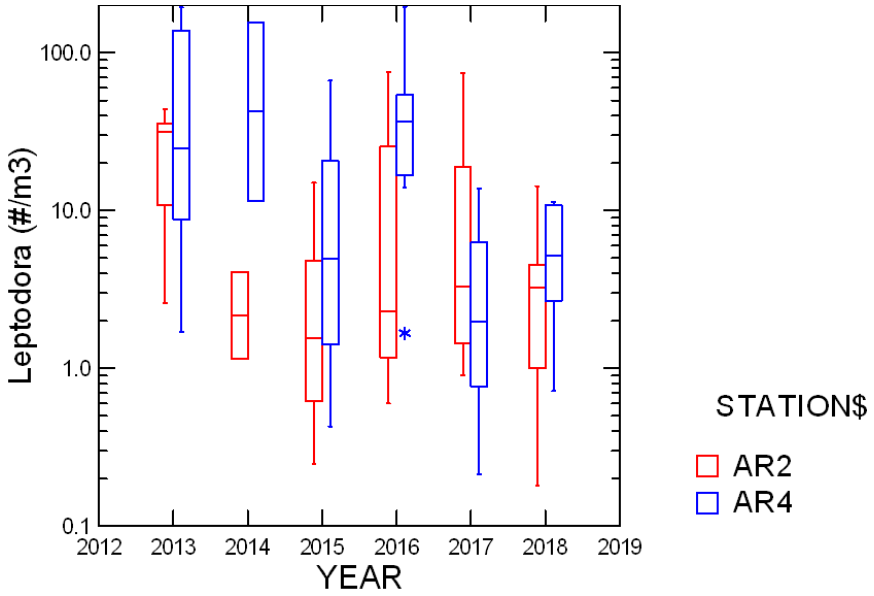

Figure 151. Box plots comparing values of *Leptodora* among years.

Leptodora is a large predacious cladoceran which occurs consistently in the study area (Figure 151). Values in 2018 were similar to those in 2017. Leptodora has been consistently higher at AR4, but not so much in 2017 and 2018. Total macrozooplankton, those collected in the 202 μm net, showed a clear interannual pattern with greatest numbers at both stations in 2014 (Figure 152). 2018 values were much reduced at AR2, but similar to recent years at AR4.

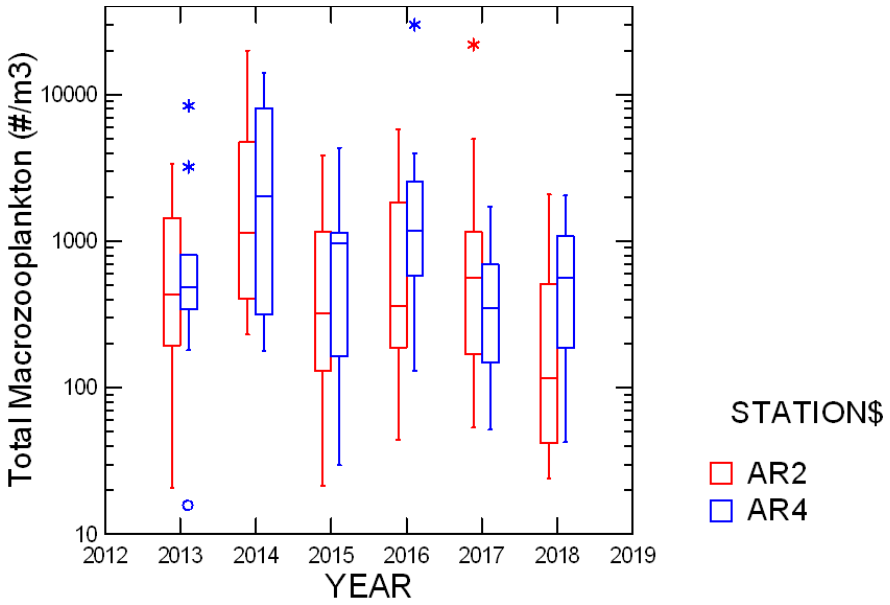

Figure 152. Box plots comparing values of Total Macrozooplankton among years.

F. Ichthyoplankton: Comparison among Years

2018 marks the sixth year of our fish collections in Hunting Creek. Both trends and inter-annual variability become apparent when comparing the years of data. In the larval data a high dominance of different species in the herring or shad family (clupeids) are consistently present, and in high densities (Table 21). These include anadromous species of concern such as Blueback Herring and Alewife, for which we also monitor the spawning populations as part of this study. Overall, larval density was lower in 2018 than in previous years.

Table 21. Density of larvae collected all years (#/10m^3).

Scientific Name	Common Name	2013	2014	2015	2016	2017	2018
Alosa aestivalis	Blueback Herring	61.69	200.36	382.05	91.54	205.29	56.54
Alosa mediocris	Hickory Shad	4.80	4.13	12.11	9.63	4.28	1.58
Alosa pseudoharengus	Alewife	139.80	57.70	265.97	78.52	81.75	38.85
Alosa sapidissima	American Shad	0.12	1.32	0.61	1.97	2.80	0.15
Alosa species	unk. Alosa species	0.00	18.49	0.00	0.00	0.00	0.00
Carassius auratus	Goldfish	56.78	0.89	0.00	0.30	7.02	0.00
Carpiodes cyprinus	Quillback	0.00	0.00	0.00	0.78	0.00	0.92
Centrarchidae	unk. centrarchidae species	0.00	0.00	0.00	0.13	0.00	0.00
Clupeidae	unk. clupeid species	422.95	781.67	444.54	175.51	193.31	129.34
Cyprinidae	unk. cyprinidae species	1.14	0.00	0.59	0.00	0.00	0.00
Cyprinus carpio	Carp	0.00	0.00	0.00	0.00	2.98	0.00
Dorosoma cepedianum	Gizzard Shad	438.39	381.85	592.25	221.54	293.50	83.18
Eggs	eggs	0.16	3.09	2.69	17.80	25.66	11.17
Enneacanthus gloriosus	Bluespotted Sunfish	0.00	0.24	0.00	0.00	0.00	0.00
Etheostoma olmstedi	Tessellated Darter	0.00	0.00	0.00	0.13	0.00	0.00
Fundulus diaphanus	Banded Killifish	0.00	0.00	0.00	0.00	0.50	0.00
Fundulus species	unk. killifish species	0.14	0.00	0.00	0.20	0.00	0.00
Hybognathus regius	Eastern Silvery Minnow	0.00	0.00	0.00	0.00	0.50	0.00
Lepisosteus osseus	Longnose Gar	0.00	0.00	0.00	0.00	0.25	0.00
Lepomis cyanellus	Green Sunfish	0.00	0.00	0.00	0.41	0.50	0.00
Lepomis gibbosus	Pumpkinseed	0.00	0.00	0.00	1.62	0.99	0.39
Lepomis macrochirus	Bluegill	0.00	0.00	0.00	0.00	0.50	0.00
Lepomis species	unk. sunfish	0.60	2.83	0.49	0.00	8.23	0.00
Menidia beryllina	Inland Silverside	2.48	3.32	1.98	20.36	60.78	0.66
Menidia species	unk. silverside species	0.00	0.00	0.00	2.60	0.00	0.00
Micropterus dolomieu	Smallmouth Bass	0.00	0.00	0.00	0.00	0.25	0.00
Morone americana	White Perch	0.00	5.90	15.93	8.59	17.54	15.48
Morone saxatilis	Striped Bass	0.00	4.02	0.00	1.09	7.71	0.00
Morone species	unk. perch/bass species	39.06	43.46	4.32	14.11	3.71	0.00
Notemigonus crysoleucas	Golden Shiner	0.00	0.84	0.00	0.00	0.00	0.00
Notropis hudsonius	Spottail Shiner	0.00	0.00	0.00	0.39	2.48	4.94
Perca flavescens	Yellow Perch	38.22	1.41	0.00	0.65	0.50	0.74
Strongylura marina	Atlantic Needlefish	0.00	0.12	0.00	0.00	0.13	0.00
Unidentified	unidentified	11.45	84.35	27.42	34.66	84.23	6.43
Total larval density		**1217.80**	**1595.98**	**1750.95**	**682.52**	**1005.38**	**350.38**

G. Adult and Juvenile Fish: Comparison among Years

The total number of adult and juvenile fishes collected in 2018 was average, with both higher and lower abundances collected in previous years (Table 22).

The SAV beds that have been increasing in cover since the start of the study are a likely contributor to the lower catches in 2016 and 2017 compared to 2013-2015; conversely the lower density of SAV in 2018 may have contributed to the increase in catch in 2018. It is important to note that the SAV growth obstructs our ability to effectively collect trawl and seine samples, therefore lower numbers with denser SAV beds likely do not represent reduced abundances; rather it reflects our reduced ability to collect representative samples. There are clear benefits to the presence of SAV, it for example provides fish habitat and helps improve water clarity. The high amount of organic matter that SAV represents is still indicative of a eutrophic system, but a system with higher functionality than a phytoplankton dominated system. There was less SAV cover in the system in 2018 than there was in previous years, which allowed for effective trawl collections all season long.

To address the problem of our reduced ability to tow nets when SAV growth is high, we have added fyke nets to our sampling gear since 2016. The extensive SAV growth makes it highly suitable gear for the location, and total catch with fyke nets actually exceeded that of the trawls in both 2016 and 2017. The fyke nets are likely the most efficient gear to sample thick SAV beds, and we recommend continued use of this gear in our surveys. In 2018, catches with the seine and trawl increased as compared to the two previous years, while the collections with the fyke nets decreased. Low SAV cover reduces the effectiveness of the fyke nets, likely because they are not well-hidden between the plants like they are in years with dense SAV beds. By having both trawls and fyke nets collecting samples at the same location, we can better evaluate true abundance changes trough time instead of erroneously assuming that SAV growth reduces fish abundance.

In 2018, the clear trend of dominance of Banded Killifish continues (Figure 153), but lower total abundance of Banded Killifish as was seen in 2017 is still the case in 2018 (Table 22). Another consistently abundant species, White Perch (*Morone americana*), was present in high abundance again in 2018. Spottail Shiner, which was found in high abundance from 2013-2015 had relatively high abundance again in 2018 after low abundance in both 2016 and 2017. Some species increased in abundance in 2018 compared to all previous years, such as Gizzard Shad, and White and Brown Bullhead. These last two are native catfishes that have generally been decreasing in numbers since the invasion of Blue Catfish. The increase of the taxon Alosa species may be a result of how many alosids we were able to identify to the species level, as for example American Shad reduced in abundance (some unidentified Alosids may be American Shad).

In 2018, 31 different species were collected, which is similar to previous years, and a sign of a healthy diversity. Now that the high abundance of Banded Killifish is reduced, and other species such as Alosids have increased in abundance, the evenness (distribution of

abundance over species) has substantially increased since 2017. The Simpson's Index of Diversity (calculated as 1-($\mathbf{\Sigma}$ $(n_i/N)^2$)) was calculated for all years based on adult and juvenile abundances (Figure 154). Note that in the 2016 report the Simpson's index (D) was reported, in which communities with higher diversity or evenness approach zero. In this report we calculated the Simpson's Index of Diversity, which is 1-D. In this index the communities with higher diversity have higher values (approaching 1) which is more intuitive to interpret. While evenness was reduced each year of sampling before 2017, 2017 showed a high Simpson's Index of Diversity value, and 2018 was even slightly higher (Figure 54). Overall, the fish species found in Hunting Creek are characteristic of Potomac River tributaries.

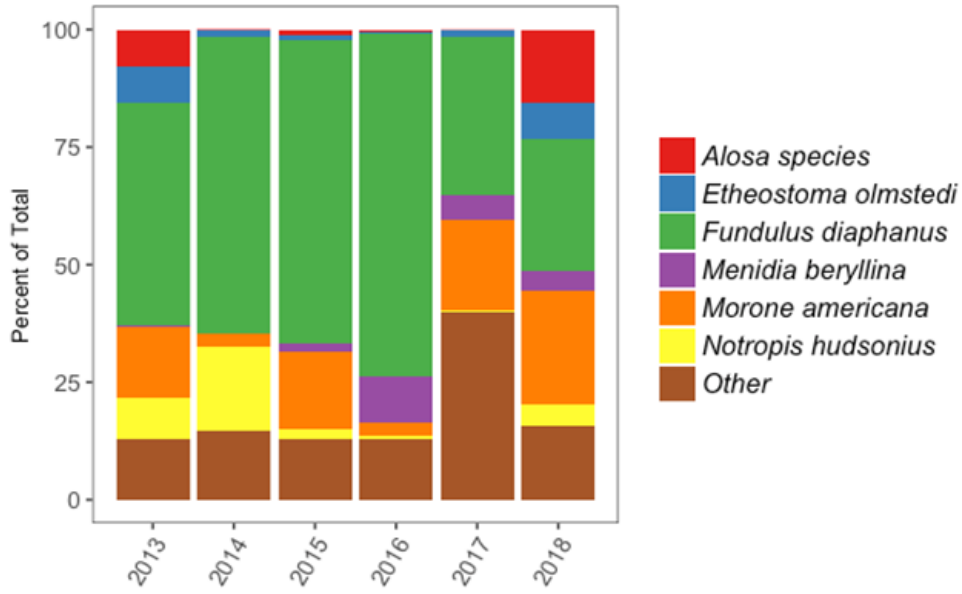

Figure 153. Percentage of total of dominant species collected in all years

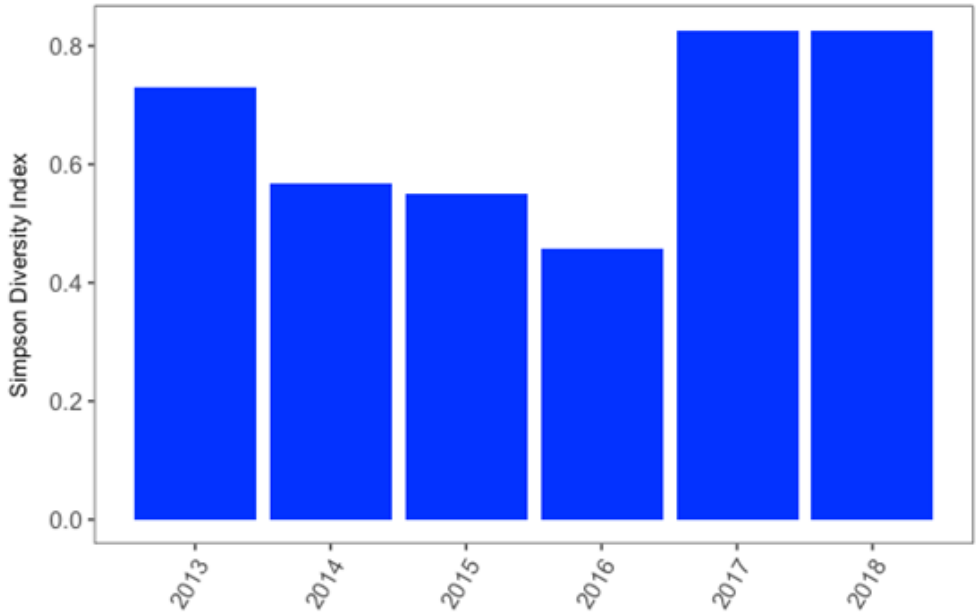

Figure 154. Simpson Diversity Index of fish species collected in Hunting Creek all years.

Table 22. Abundances of species collected all years.

Scientific Name	Common Name	2013	2014	2015	2016	2016 w/ Fyke	2017	2017 w/ Fyke	2018	2018 w/ Fyke
Alosa aestivalis	Blueback Herring	16	8	12	29	29	0	0	0	0
Alosa pseudoharengus	Alewife	6	23	28	12	12	0	0	14	14
Alosa sapidissima	American Shad	208	32	163	19	19	2	2	2	2
Alosa species	unk. Alosa species	299	8	55	11	12	3	3	433	433
Ameiurus catus	White Bullhead	0	0	0	1	2	0	0	8	8
Ameiurus nebulosus	Brown Bullhead	3	2	3	3	3	2	5	13	13
Anchoa mitchilli	Bay anchovy	69	70	7	0	0	0	0	0	0
Anguilla rostrata	American Eel	1	3	2	0	0	0	0	0	1
Carassius auratus	Goldfish	20	39	2	0	9	18	107	1	1
Carpiodes cyprinus	Quillback	9	19	2	0	0	0	0	0	0
Cyprinella spiloptera	Spotfin shiner	0	0	1	0	0	0	0	0	0
Cyprinus carpio	Carp	0	3	1	7	14	3	3	2	2
Dorosoma cepedianum	Gizzard Shad	5	1	3	0	0	0	0	50	50
Enneacanthus gloriosus	Bluespotted Sunfish	0	0	0	0	0	27	47	0	0
Erimyzon oblongus	Creek Chubsucker	0	0	0	0	0	0	0	1	1
Etheostoma olmstedi	Tessellated Darter	292	49	39	3	8	33	35	212	221
Fundulus diaphanus	Banded Killifish	1798	2382	2723	1387	1547	692	769	777	777
Fundulus heteroclitus	Mummichog	53	152	174	16	16	62	62	20	20
Gambusia holbrooki	Mosquitofish	11	69	19	0	0	1	1	0	0
Hybognathus regius	Eastern Silvery Minnow	0	6	31	2	4	40	40	13	14
Ictalurus furcatus	Blue Catfish	12	4	4	1	1	6	6	57	57
Ictalurus punctatus	Channel Catfish	0	0	2	0	0	0	0	2	2
Lepisosteus osseus	Longnose Gar	0	0	3	1	1	1	1	0	0
Lepomis auritus	Redbreast Sunfish	0	0	1	2	2	0	0	0	0
Lepomis cyanellus	Green Sunfish	0	0	2	0	0	4	7	0	0

Scientific Name	Common Name	2013	2014	2015	2016	2016 w/ Fyke	2017	2017 w/ Fyke	2018	2018 w/ Fyke
Lepomis gibbosus	Pumpkinseed	6	17	11	11	22	39	180	91	100
Lepomis macrochirus	Bluegill	12	52	21	8	20	28	188	75	81
Lepomis megalotis	Longear Sunfish	0	0	0	0	0	1	1	0	0
Lepomis microlophus	Redear Sunfish	6	11	5	2	8	0	0	0	0
Lepomis species	unk. sunfish	5	12	5	27	85	50	169	0	2
Menidia beryllina	Inland Silverside	15	6	73	209	210	114	124	107	120
Micropogonias undulatus	Atlantic Croaker	1	0	0	0	0	0	0	0	0
Micropterus dolomieu	Smallmouth Bass	5	5	9	6	6	62	70	20	20
Micropterus punctulatus	Spotted Bass	1	0	0	0	0	0	0	0	0
Micropterus salmoides	Largemouth Bass	3	7	0	5	5	2	2	4	4
Micropterus species	unk. bass species	1	0	0	0	0	0	0	0	0
Morone americana	White Perch	574	107	693	19	57	393	439	667	675
Morone saxatilis	Striped Bass	2	0	2	1	5	5	8	2	2
Morone species	unk. perch/bass species	0	1	0	0	0	0	0	0	0
Moxostoma macrolepidotum	Shorthead Redhorse	0	0	0	0	0	0	0	1	1
Notemigonus crysoleucas	Golden Shiner	2	3	13	2	2	2	2	5	5
Notropis hudsonius	Spottail Shiner	338	666	87	13	17	11	13	124	125
Perca flavescens	Yellow Perch	22	16	7	7	7	1	2	36	37
Pomoxis nigromaculatus	Black Crappie	0	0	4	0	1	0	0	3	3
Sander vitreus	Walleye	0	0	0	0	0	0	0	1	1
Strongylura marina	Atlantic Needlefish	2	4	3	0	0	9	9	1	1
Unidentified	unidentified	2	0	0	0	0	0	0	0	0
Total		**3798**	**3777**	**4210**	**1804**	**2125**	**1611**	**2294**	**2742**	**2794**

H. Submersed Aquatic Vegetation: Comparison among Years

According to annual reports of the Virginia Institute of Marine Science (VIMS) SAV Monitoring Program (http://web.vims.edu/bio/sav/maps.html), virtually the entire surface area of the Hunting Creek embayment has been covered with submersed aquatic vegetation in each of the previous years of this study (2013-2017). In 2018 there was a severe decline in SAV coverage. Furthermore, due to the frequent rainfall events and resulting poor water clarity, VIMS was unable to conduct the aircraft remote sensing so we were not able to make direct comparisons of 2018 coverage with 2016 and 2017. In 2016 and 2017 mapping of species was done via boat in association with the water quality mapping surveys and the results have been reported in the results section of these reports. In 2017 the native SAV species *Ceratophyllum demersum* was substantially more abundant than the exotic species *Hydrilla verticillata* in contrast to 2016 when they had a similar abundance. The boat transects studies in 2018 confirmed the severe dieback observed anecdotally.

I. Benthic Macroinvertebrates: Comparison among Years

River and Embayment Samples

Samples from 2018 were compared with those from 2016 and 2017. As expected, the macroinvertebrate community was dominated by annelids (including oligochaetes, polychaetes, and leeches) across sites and years (Figure 155, top). However, if Annelids are removed and we examine the other dominant taxon groups, we see a few different trends in dominant taxa between the three Hunting Creek stations across years. AR2 is the site closest to the outflow from Hunting Creek, and across years, this site is consistently dominated by Crustacea (including gammarid amphipods and isopods) and Insecta (including the larvae of Chironomidae (midges), phantom midges, riffle beetles, dragonfly nymphs, crane fly larvae, and caddisfly larvae). However, in 2018 Insecta taxa grew in dominance, outnumbering Crustacea (Figure 155, bottom). The AR4 site is the closest to the Potomac River and is consistently dominated by Crustacea and Bivalvia (mostly the invasive Asian clam, *Corbicula fluminea*), although the relative abundance of Crustacea declined in 2018 and numbers of Insecta and Gastropoda increased (Figure 155, bottom). The AR4 site receives higher water flow and movement, which many species of Bivalvia require, and may help explain why there are higher abundances of Bivalvia located closer to the Potomac River. The site with the most fluctuations in percent contributions of macroinvertebrate taxa was AR3, which is located in the middle of the embayment. In 2016, samples from AR3 were dominated by Gastropoda; in 2017, the most dominant taxa were Crustacea. In 2018, the community trended towards a more even distribution of taxa, and all taxonomic groups contributed more than 10% towards the total community. This site is probably influenced by both the Potomac River, through the daily movement of the tidal freshwater water body, and by the outfall of Hunting Creek, which moves nutrients and sediments from terrestrial sources. The relative importance of both of these waterbodies in determining benthic macroinvertebrate community structure probably varies annually, and even monthly, due to climatic events.

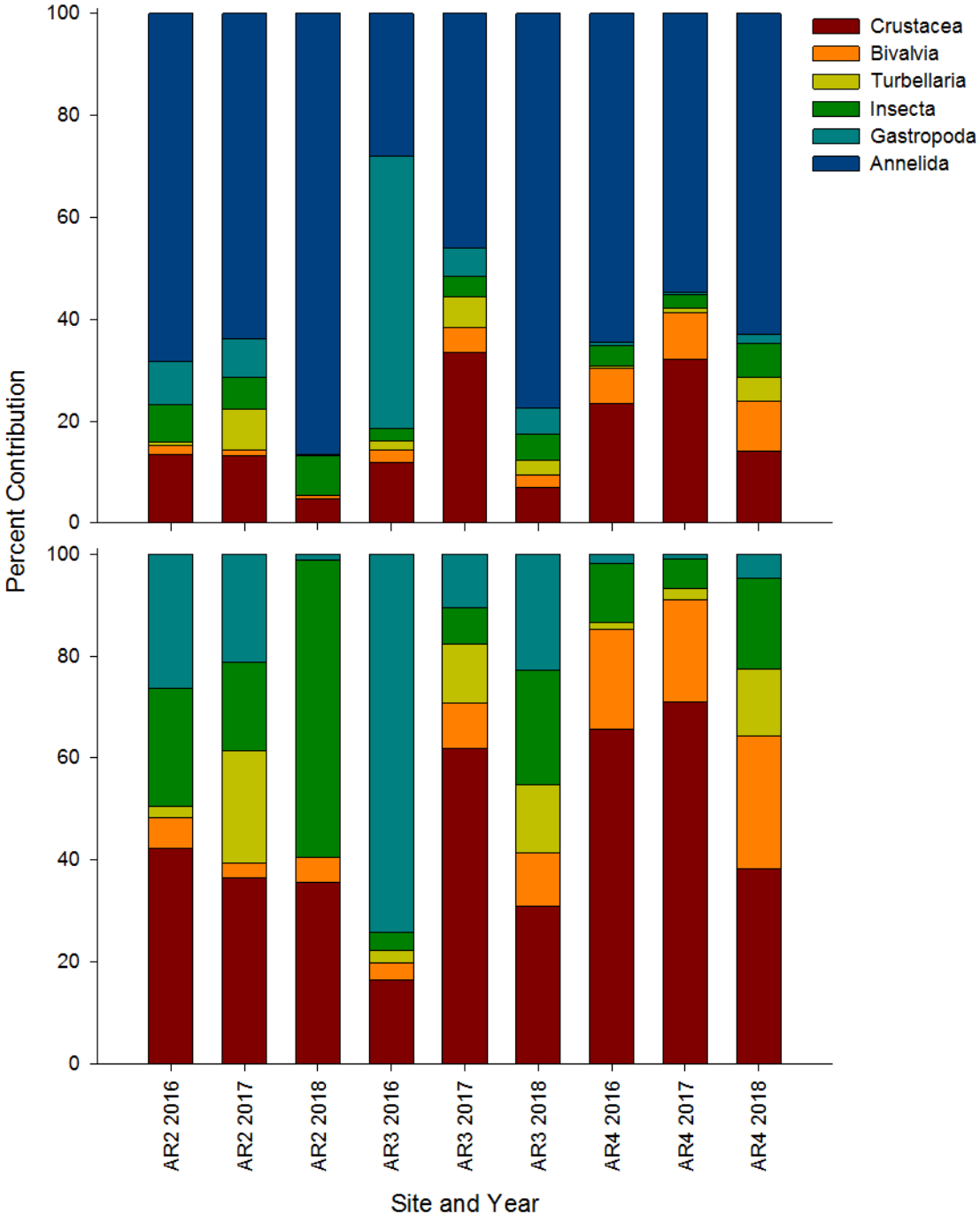

Figure 155. Percent contribution of all macroinvertebrate taxa (top) and all non-Annelida taxa (bottom) in petite ponar samples collected in 2016, 2017, and 2018 separated by site and year.

Tributary Samples

We have been collecting benthic macroinvertebrate samples from streams emptying into Hunting Creek since 2016. Because this is the first time that we have at least three years of data, we can

start to examine trends in the community over time and between the original six sites (Taylor Run and Timber Branch are excluded here, as they were first sampled in 2018). There are no trends in the dominant benthic macroinvertebrate taxa collected at these six sites, either within a site across years or across sites within a year. Looking across all sites and years, the taxa that dominates are members of the Insecta family Hydropsychidae (33% of the time, they are the most dominant group). Members within this family are netspinning caddisflies, which live in debris and under stones and spin concave silken nets that face upstream to capture floating or swimming prey. All of these sites have stones and gravel as habitat. The next most dominant group across all sites and years are members of the Insecta family Chironomidae (28%), known as midges. Chironomid larvae are filter-feeders and often live in tubes in the mud. Comparing trends within each site, both Backlick Run and Cameron Run were dominanted by Chironomdae in 2016 and 2018. Indian Run was dominated by Hydropsychidae during both 2016 and 2018. All other sites (Hunting Creek 1 and 2 and Turkeycock Run) each had a different dominant species each year of sampling. All of these sites are probably influenced by differences in the types and amounts of nutrients and sediments moving from terrestrial sources, the flow of water, and anthropogenic impacts to the system. The relative importance of a variety of abiotic factors on determining benthic macroinvertebrate community structure probably varies annually, and even monthly, due to climatic events. Therefore, site-level trends may be apparent with continued annual sampling.

LITERATURE CITED

Bigelow, H.B. and W.C.Schroeder. 1953. Fishes of the Gulf of Maine. Fishery bulletin No. 74, Vol. 53. U.S. Government Printing Office. Washinton, D.C. 577 pp.

Carter, V., P.T. Gammon, and N.C. Bartow. 1983. Submersed Aquatic Plants of the Tidal Potomac River. Geological Survey Bulletin 1543. U.S. Geological Survey. 63 pp.

Chesapeake Bay Program. 2006 Ambient water quality criteria for dissolved oxygen, water clarity, and chlorophyll *a* for the Chesapeake Bay and its tidal tributaries. 2006 Addendum. Downloaded from Bay Program website 10/13/2006.

Cummings, H.S., W.C. Purdy, and H.P. Ritter. 1916. Investigations of the pollution and sanitary conditions of the Potomac watershed. Treasury Department, U.S. Public Health Service Hygienic Laboratory Bulletin 104. 231 pp.

Dahlberg, M.D. 1975. Guide to coastal fishes of Georgia and nearby states. University of Georgia Press. Athens, GA 187 pp.

Douglass, R.R. 1999. A Field Guide to Atlantic Coast Fishes: North America (Peterson Field Guides). Houghton Mifflin Harcourt, Boston. 368 pp.

Eddy, S. and J.C. Underhill. 1978. How to know the freshwater fishes. 3rd Ed. W.C. Brown Co. Dubuque, IA. 215 pp.

Froese, R. and D. Pauly (Eds.). 2012. Fish Base. World Wide Web electronic publication. www.fishbase.org, version (04/2012).

Hildebrand and Schroeder. 1928. Fishes of the Chesapeake Bay. U.S. Bureau of Fisheries Bulletin 53, Part 1. Reprinted 1972. T.F.H. Publishing, Inc. Neptune, NJ. 388 pp.

Hogue, J.J, Jr., R.Wallus, and L.K. Kay. 1976. Preliminary guide to the identification of larval fishes in the Tennessee River. Technical Note B19. Tennessee Valley Authority. Knoxville, TN.

Islam, S. 2001. Seasonal dynamics of micro-, nanno-, and picoplankton in the tidal freshwater Potomac River in and around Gunston Cove. Ph.Dissertation. George Mason University. 127 pp.

Jenkins, R.E. and N.M. Burkhead. 1994. The freshwater fishes of Virginia. American Fisheries Society. Washington, DC. 1080 pp.

Jones, P.W., F.D. Martin, and J.D. Hardy, Jr. 1978. Development of fishes of the Mid-Atlantic bight. Volumes I-VI. Fish and Wildlife Service, U.S. Department of the Interior. FWS/OBS-78/12.

Kraus, R.T. and R.C. Jones. 2011. Fish abundances in shoreline habitats and submerged aquatic vegetation in a tidal freshwater embayment of the Potomac River. Environmental Monitoring and Assessment. Online: DOI 10.1007/s10661-011-2192-6.

Kelso, D.W., R.C. Jones, and P.L. deFur. 1985. An ecological study of Gunston Cove - 1984-85. 206 pp.

Lippson, A.J. and R.L. Moran. 1974. Manual for identification of early development stages of fishes of the Potomac River estuary. Power Plant Siting Program, Maryland Department of Natural Resources. PPSP-MP-13.

Loos, J.J., W.S. Woolcott, and N.R. Foster. 1972. An ecologist's guide to the minnows of the freshwater drainage systems of the Chesapeake Bay area. Association of Southeastern Biologists Bulletin 19: 126-138.

Lund, J.W.G., C. Kipling, and E.C. LeCren. 1958. The inverted microscope method of estimation algal numbers and the statistical basis of estimations by counting. Hydrobiologia 11: 143-170.

Mansueti, A.J. and J.D. Hardy, Jr. 1967. Development of fishes of the Chesapeake Bay region: an atlas of egg, larvae and juvenile stages: Part 1. Natural Resources Institute. University of Maryland. 202 pp.

Merritt, R.W. and K.W. Cummins. 1984. An introduction to the aquatic insects of North America. 2nd edition. Kendall/Hunt Publishing Co., Dubuque, IA. 722 pp.

Pennack, R.W. 1978. Fresh-water invertebrates of the United States. 2nd ed. Wiley-Interscience. New York, NY.

Schloesser, R.W., M.C. Fabrizio, R.J. Latour, G.C. Garman, G.C., B. Greenlee, M. Groves and J. Gartland. 2011. Ecological role of blue catfish in Chesapeake Bay communities and implications for management. American Fisheries Society Symposium 77:369-382.

Scott, W.B. and E.J. Crossman. 1973. Freshwater fishes of Canada. Bulletin 184. Fisheries Research Board of Canada. Ottawa, Canada. 966 pp.

Standard Methods for the Examination of Water and Wastewater. 1980. American Public Health Association, American Waterworks Association, Water Pollution Control Federation. 15th ed. 1134 pp.

Thorp, J.H. and A.P. Covich, eds. 1991. Ecology and classification of North American Freshwater Invertebrates. Academic Press. San Diego, CA. 911 pp.

Wetzel, R.G. 1983. Limnology. 2nd ed. Saunders. 767 pp.

Wetzel, R.G. and G.E. Likens. 1991. Limnological analyses. 2nd ed. Springer-Verlag. 391 pp.

Anadromous Fish Survey of Cameron Run – 2018

Final Report
By

Kim de Mutsert
Assistant Professor, Department of Environmental Science and Policy
Associate Director, Potomac Environmental Research and Education Center
George Mason University

Introduction

The anadromous fishes in the herring family (Clupeidae) live as adults in the coastal ocean, but return to freshwater creeks and rivers to spawn. In the mid-Atlantic region, four species are present: American Shad (*Alosa sapidissima*), Blueback Herring (*Alosa aestivalis*), Alewife (*Alosa pseudoharengus*), and Hickory Shad (*Alosa mediocris*). Two other herring family species are semi-anadromous and spawn in Potomac River tributaries. These are Gizzard Shad (*Dorosoma cepedianum*) and Threadfin Shad (*Dorosoma petenense*). Both are very similar morphologically and ecologically, but only *D. cepedianum* is found as far upriver on the Potomac River watershed as Hunting Creek/Cameron Run. Previous reports describe the history of herring populations in the Potomac River watershed (Jones et al. 2014).

The focus of the Cameron Run fish survey is river herring, the collective name of Blueback Herring and Alewife. River herring populations have declined drastically over their range, spurring conservation efforts since 1970, which have been intensified since 2005 with implementation of moratoria. Identifying all areas used as spawning habitat by Alewife and/or Blueback Herring is an important component of their conservation. Since 1988, George Mason University researchers have focused a monitoring program on the spawning of these species in other tributaries such as Pohick Creek, Accotink Creek, and, less regularly, Dogue Creek. With this study Cameron Run is added, which has not been monitored for presence of river herring or other anadromous species by either George Mason or other fisheries biologists before the start of this study in 2013 (Jim Cummins, pers. comm.). Our 2013 survey provided the first confirmation of Cameron Run as River Herring spawning habitat (Alan Weaver, VDGIF, pers. comm.). Use of Cameron Run by river herring upstream from where the effluent of Alexandria Renew Enterprises enters Cameron Run signifies that the effluent does not deter river herring from using Cameron Run as spawning habitat. In 2014 we moved the collection site approximately 500 m downstream (still above the Alexandria Renew Enterprises effluent), which increased our catches, and allows us to estimate the size of the spawning population. The new location proved successful and will remain the collection site for any subsequent surveys.

Methods

We conducted weekly sampling trips from March 16 to May 25 in 2018. During each trip (when conditions allowed it) a hoop net was set with wings blocking the complete creek (referred to as block net) to collect adults swimming upstream, and ichthyoplankton nets were set to collect larvae floating downstream. Cross-section and flow were measured to calculate discharge, and physical parameters were measured using a handheld YSI. In some occasions, the conditions were not right to complete one or more procedures, Table 1 provides the information on which procedures were completed each sampling day in 2018. The sampling location was chosen to be upstream from the Alex Renew effluent, and downstream of the first dam in Cameron Run (Figure 1).

Figure 1. Sampling location Cameron Run.

Table 1. Procedures completed each sampling date

Date	Hoop Net	Plankton Nets	Flow Profile
3/16/18	24 hr	20 mins	Yes
3/23/18		Canceled due to snow	
3/30/18	24 hr	20 mins	Yes
4/6/18	24hr	20 mins	Yes
4/13/18	Lost Net	20 mins	Yes
4/20/18	24 hr	20 mins	Yes
4/28/18		Canceled due to high flows	
5/4/18	24 hr	20 mins	Yes
5/11/18	24 hr	20 mins	Yes
5/25/18	24 hr	20 mins	Yes

Ichthyoplankton was collected by setting two conical plankton net with a mouth diameter of 0.25 m and a square mesh size of 0.333 mm in the stream current for 20 minutes. A mechanical flow meter designed for low velocity measurements was suspended in the net opening and provided estimates of water volume filtered by the net. The number of rotations of the flow meter attached to the net opening was multiplied with a factor of 0.0049 to gain volume filtered (m^3). Larval density (#/$10m^3$) per species was calculated using the following formula:

Larval density (#/$10m^3$) = 10N/(0.0049*(flow meter start reading-flow meter end reading))

Where N is the count of the larvae of one species in one sample.

We collected 2 ichthyoplankton samples per trip, and these were spaced out evenly along the stream cross-section. Coincident with plankton samples, we calculated stream discharge rate from measurements of stream cross-section area and current velocity using the following equation:

Depth (m) x Width (m) x Velocity (m/s) = Discharge (m^3/s)

Velocity was measured using a handheld digital flow meter that measures flow in cm/s, which had to be converted to m/s to calculate discharge. Both depth and current velocity were measured at 12 to 20 locations along the cross-section. At each sampling trip other physical parameters of the creek were recorded as well (water temperature, dissolved oxygen, pH, and conductivity).

The ichthyoplankton samples were preserved in 70% ethanol and transported to the GMU laboratory for identification and enumeration of fish larvae. Identification of larvae was accomplished with multiple taxonomic resources: primarily Lippson & Moran (1974), Jones et al. (1978), and Walsh et al. (2005). River herring (both species) have semi-demersal eggs (tend to sink to the bottom) that are frequently adhesive. As this situation presents a significant bias, we are not treating egg abundance in the samples as a reliable estimate of egg abundance, and this is not used in population productivity estimates. We estimate total larval production (P) during the period of sampling by multiplying the larval density (m^{-3}) with total discharge (m^3) during the spawning period, which we assume is represented with our sampling period.

The block net was deployed once each week in the morning and retrieved the following morning (see Figure 2). Fish in the block net were identified, enumerated, and measured.

Since the net was set 24 hours per week during the spawning season, and the spawning season is estimated to last 10 weeks, we approximated total abundance of spawning river herring during the time of collection by extrapolating the mean catch per hour per species during the time the creeks were blocked over the total collection period as follows:

Average catch/24 hours * 1680 hours = total abundance of spawners

Our total collection period is assumed to be a good approximation of the total time of the spawning run of Alewife.

In response to problems with animals tearing holes in our nets in previous sampling experiences, we used a fence device in front of the mouth of the net that significantly reduces this problem. The device effectively excluded wildlife such as otters and turtles, while it has slots that allowed up-running fish to be captured.

Figure 2. Block net (hoop net with deer fencing attached to block the creek) deployed in Cameron Run. The hedging is angled downstream in order to funnel up-migrating herring into the opening of the net.

Results and Discussion

During the sampling period, we caught fourty-five adult Alewife, and several non river herring species (Table 2). The abundance of river herring collected in 2018 was higher than previous years, which signifies the consistent use of Cameron Run as spawning ground. The net is set in such a way that fishes need to swim upstream into Cameron Run to be caught in the net, which is a behavior associated with spawning. We did not find adult Blueback Herring specimens in our collections, of which we have only collected one in 2014. We did positively identify Blueback Herring among the larvae collected, of which we only found a few in previous years. Since the spawning populations is small and sampling variability high (for larval density, a small portion of the water column is sampled for 20 minutes per week), sampling over multiple years will provide us with increasingly better estimates of the spawning population of Alewife and Blueback Herring in Cameron Run.

The high ichthyoplankton density in 2018 was unprecedented. In the ichthyoplankton samples we could positively identify 1248 Alewife larvae, and 60 Blueback Herring larvae (Table 3). The unidentified larvae (78) and especially the unidentified clupeids (2762)

could potentially include more Alewife and/or Blueback Herring larvae. We found 2156 Gizzard Shad (*Dorosoma cepedianum*) larvae, which is a clupeid as well, and makes it the most abundant clupeid in the samples. A few larvae of other species were present in the samples as well, including Spottail Shiner (*Notropis hudsonius*), Common Carp (*Cyprinus carpio*), inland silverside (*Menidia beryllina*), and White Perch (*Morone americana*; Table 3).

Table 2. Species collected in Cameron Run with hoop net during weekly sampling from 3/16/18-5/25/18. River herring are indicated by bold font.

Date	Scientific Name	Common Name	Count
3/30/18	***Alosa pseudoharengus***	**Alewife**	**19**
3/30/18	*Carassius auratus*	Goldfish	3
3/30/18	*Micropterus salmoides*	Largemouth Bass	1
4/13/18	*Micropterus salmoides*	Largemouth Bass	1
4/20/18	***Alosa pseudoharengus***	**Alewife**	**16**
5/11/18	*Carassius auratus*	Goldfish	5
5/11/18	*Lepomis auritus*	Redbreast Sunfish	1
5/11/18	*Lepomis macrochirus*	Bluegill	2
5/11/18	*Micropterus salmoides*	Largemouth Bass	3
5/25/18	*Lepomis macrochirus*	Bluegill	6
5/25/18	*Micropterus salmoides*	Largemouth Bass	4
5/4/18	***Alosa pseudoharengus***	**Alewife**	**10**
5/4/18	*Carassius auratus*	Goldfish	2
5/4/18	*Dorosoma cepedianum*	Gizzard Shad	1
5/4/18	*Lepomis macrochirus*	Bluegill	1
Total			75

We measured creek discharge and other physical parameters at the same location and times where ichthyoplankton samples were taken, which was about 100 m downstream from the block net (Table 4). Mean creek discharge was lower than last year but comparable to previous years. Mean discharge in 2018 was 0.216 $m^3 s^{-1}$, ranging from 0.097 $m^3 s^{-1}$ to 0.441 $m^3 s^{-1}$, while mean discharge in 2017 was 1.12 $m^3 s^{-1}$, ranging from 0.12 $m^3 s^{-1}$ to 3.62 $m^3 s^{-1}$. There was one date when discharge could not be calculated because the flow was so low that the flow meter did not function properly. Therefore the lowest flow recorder is even an underestimate. Water temperature (Temp) was under 10 °C the first sampling day, which is too low for river herring spawning. The first sampling date where we found Alewife (larvae) was April 6, when temperature was 9.6 °C (close to

10), but had already reached 16.62 before that. Dissolved oxygen (DO), and pH were in the benign range for occurrence of river herring throughout the sampling period (Table 4).

During the sampling period of 10 weeks, the total discharge was estimated to be on the order of 1.3 million cubic meters (Table 5). This is very low as compared to last year. Given the observed mean densities of larvae, the total production of river herring larvae was estimated at approximately 25 thousand for Cameron Run (Table 5). Note that the estimate is based on a small sample (0.0002 % of the total discharge). With 45 adult Alewife collected, and extrapolating over period of the spawning run as explained in the methods, this could mean that the Alewife spawning population in 2017 was the size of 315 individuals (123 last year).

Table 3. Larvae collected in Cameron Run. Herring larvae (river herring and other clupeids) are in bold. Fish larvae too damaged for identification to species level were identified at the highest level possible.

Date	Scientific	Count	Volume	AveDensity
3/30/18	Eggs	192	22.682	67.129
4/6/18	***Alosa pseudoharengus***	**8**	**0.103**	*****
4/6/18	**Clupeidae**	**1**	**0.103**	*****
4/6/18	Eggs	43	0.103	*
4/6/18	Unidentified	1	0.103	*
4/13/18	***Alosa pseudoharengus***	**9**	**24.765**	******
4/13/18	**Clupeidae**	**1**	**24.765**	******
4/13/18	Eggs	92	24.765	**
4/13/18	Unidentified	3	24.765	**
4/20/18	Eggs	137	37.108	41.979
4/20/18	Unidentified	1	37.108	0.188
5/4/18	Eggs	41	0.030	*
5/11/18	***Alosa pseudoharengus***	**14**	**37.235**	**3.598**
5/11/18	**Clupeidae**	**3**	**37.235**	**0.970**
5/11/18	*Cyprinus carpio*	2	37.235	0.414
5/11/18	***Dorosoma cepedianum***	**1**	**37.235**	**0.382**
5/11/18	Eggs	68	37.235	19.838
5/11/18	*Menidia beryllina*	3	37.235	0.796
5/11/18	*Notropis hudsonius*	1	37.235	0.208
5/11/18	Unidentified	1	37.235	0.382
5/25/18	***Alosa aestivalis***	**60**	**87.367**	**8.424**
5/25/18	***Alosa pseudoharengus***	**1217**	**87.367**	**140.596**

5/25/18	**Clupeidae**	**2757**	**87.367**	**324.362**
5/25/18	***Dorosoma cepedianum***	**2155**	**87.367**	**270.512**
5/25/18	Eggs	291	87.367	36.693
5/25/18	*Morone americana*	2	87.367	0.240
5/25/18	*Notropis hudsonius*	5	87.367	0.470
5/25/18	Unidentified	72	87.367	8.235

*The flow velocity in Cameron Run was too low at this date for the flow meter to function properly; therefore, volume sampled is likely an underestimate, and larval density not calculated. **The flow velocity in one plankton tow was abnormally low, indicating gear malfunction.

Table 4. Physical parameters measured at Cameron Run during each sampling week. ND = no data as a result of very low flow. SpCond = specific conductivity.

Date	Discharge (m^3 s^{-1})	Temp (°C)	SpCond (mS cm^{-1})	DO (mg l^{-1})	pH
3/16/18	0.097	4.54	0.646	16.11	7.62
3/30/18	0.371	16.62	1.13	12.91	8.03
4/6/18	ND	9.6	0.811	13.88	7.67
4/13/18	0.102	18.7	0.723	13.36	7.82
4/20/18	0.320	11.12	0.615	8.44	7.87
5/4/18	0.223	23.84	0.566	7.56	7.59
5/11/18	0.172	24.17	0.575	9.65	7.75
5/25/18	0.441	23.9	0.434	9.43	7.56

Table 5. Estimation of river herring (alewife and blueback herring) larval production and spawner abundance from Cameron Run during spring 2018.

Parameter	Cameron Run
Mean discharge (m^3 s^{-1})	0.216
Total discharge (m^3)	1,305,787.000
Total volume sampled (m^3)	235.348
Mean Alosa larvae density ($10m^3$)	19.077
Total river herring production (# larvae)	24,910.499
Total adult river herring (#)	315.000

Conclusions

After finding that Cameron Run is used as river herring spawning habitat with just one adult river herring and seven larvae in 2013, we were able to confirm this finding by collecting more river herring adults and larvae from 2014-2018 (Figure 3). By moving our sampling site approximately 500 m downstream in 2014 we have found a better sampling location. Even further downstream Cameron Run becomes too deep and wide for our sampling strategy.

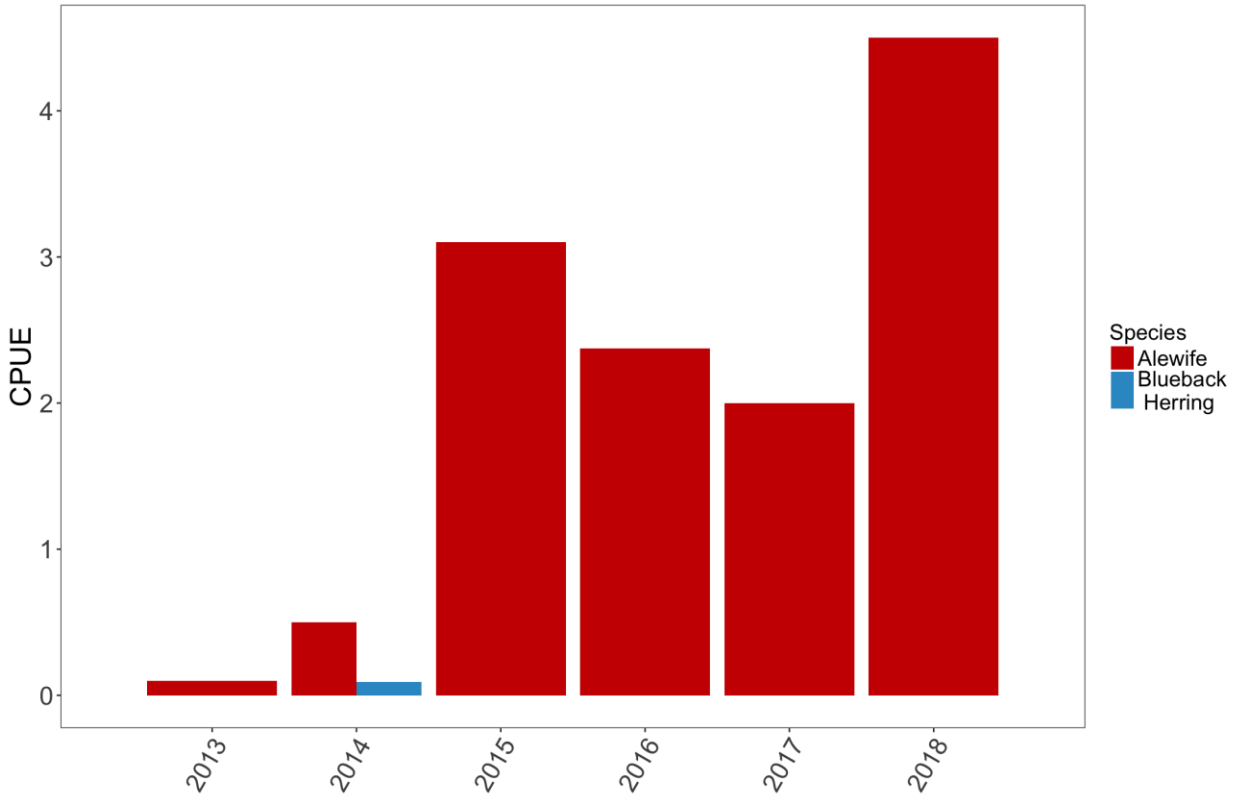

Figure 3. Catch per Unit Effort of Alewife and Blueback Herring (number of individuals per block net) collected with the block net in each year.

The finding of river herring adults and larvae in an area above the outflow of the Alexandria Renew Enterprises wastewater reclamation facility signifies that the water of Cameron Run is clean enough to use as spawning habitat for these species of concern. These finding will not affect AlexRenew, but will affect the terms of construction permits in and around Cameron Run (i.e. some construction activities may be restricted by the Virginia Department of Game and Inland Fisheries (VDGIF) during the annual spawning period (mid-March to mid-May) of river herring (Alan Weaver, VDGIF, pers. comm.).

Although the current evidence suggests that the importance of Cameron Run may be marginal to Alewife and Blueback Herring populations, it is important to recognize that marginal habitats may sustain fish populations during periods of declining abundance and low recruitment (Kraus and Secor 2005). Due to the moratorium on river herring set in place bay-wide in 2012, annual estimation of spawner abundance should be a continued priority for annual monitoring of this and other Potomac River tributaries. The peak in abundance in 2015 was 3 years after the 2012 moratorium, which is about the time it takes for Alewife to grown to adulthood and return to their spawning grounds. This peak has been seen in other tributaries to the Potomac River as well (Jones and De Mutsert 2016) and could signify the effect of the release from the fishery. This effect was not seen throughout Virginia however (Alan Weaver, VDGIF, pers. comm.), and was not maintained to the same level in the subsequent years (2016 and 2017). Anadromous fishes typically exhibit strong year-class fluctuations, and we expected a high return of river herring in 2018 if the offspring of the successful 2015 year-class was able to return. We indeed saw even higher numbers return in 2018, which is a sign that the high abundance in 2015 may have given a lasting boost to the population. Additional years of data collection (at least through 2 generation lengths ~ a decade) will allows us to see if this cycle continues into the future and helps with the slow built-up of river herring populations.

Literature cited

Jones, P. W., F. D. Martin, and J. D. Hardy, Jr. 1978. Development of fishes of the Mid-Atlantic Bight: an atlas of egg, larval, and juvenile stages, volume 1. Acipenseridae through Ictaluridae. U.S. Fish and Wildlife Service, FWS/OBS-78/12.

Jones, R. C., De Mutsert, K., and G. D. Foster. 2014. An Ecological Study of Hunting Creek-2013. Final report to Alexandria Renew Enterprises, Alexandria, VA. 123 p.

Jones, R. C. and De Mutsert, K. 2016. An Ecological Study of Gunston Cove-2015. Final report. Potomac Environmental research and education Center, Fairfax, VA.

Kraus, R. T. and D. H. Secor. 2005. Application of the nursery-role hypothesis to an estuarine fish. Marine Ecology Progress Series 290:301-305.

Lippson, A. J., and R. L. Moran. 1974. Manual for the identification of early developmental stages of fishes of the Potomac River estuary. Maryland Department of Natural Resources, Baltimore.

Walsh H.J., L.R Settle, and D.S. Peters. 2005. Early life history of blueback herring and alewife in the lower Roanoke River, North Carolina. Transactions of the American Fisheries Society 134:910-926.

ESCHERICHIA COLI ABUNDANCES IN HUNTING CREEK/CAMERON RUN AND ADJACENT POTOMAC RIVER - 2018

Final Report
By

Benoit Van Aken
Associate Professor, Department of Chemistry & Biochemistry
George Mason University

Introduction

Again during 2018, in connection with examination of ecological and chemical parameters, a study of *Escherichia coli* in waters in the areas of Hunting Creek/Cameron Run and adjacent waters of the Potomac River was continued with samples being collected at 10 sites. The 12 sites sampled in the prior years (2016 - 2017) included AR1, AR2, AR3, AR4, AR10, AR11, AR12, AR13, AR21, AR22, AR23, and AR30. However, two of these sites, AR11 and AR22, were not accessible for sampling in 2018 due to existence of large-scale construction projects including renovations at Lake Cook (AR11) and earthwork along the stream bank of Huntington Park (AR22).

This work provides current microbiological water quality information in these aquatic ecosystems adjacent to and receiving water from the wastewater reclamation facility operated by Alexandria Renew Enterprises (Alex Renew). The research continues to determine if these waters are impaired under the Clean Water Act in terms of their uses as designated by the Commonwealth of Virginia.

The text of the Virginia Water Quality Standards (9 VAC 25-260-10) is as follows:

"All state waters, including wetlands, are designated for the following uses: recreational uses, e.g., swimming and boating; the propagation and growth of a balanced, indigenous population of aquatic life, including game fish, which might reasonably be expected to inhabit them; wildlife; and the production of edible and marketable natural resources, e.g., fish and shellfish." (VSWCB 2011)

Section 9VAC25-260-170 of the Virginia Water Quality Standards (amended as of January 2011) specifies the bacteriological criteria for *E. coli* that apply to primary contact recreational use surface waters:

1. "*E.coli* bacteria shall not exceed a monthly geometric mean of **126 CFU/100 mL** in freshwater […]."

2. "Geometric means shall be calculated using all data collected during any calendar month with a minimum of four weekly samples."

3. "If there are insufficient data to calculate monthly geometric means in freshwater, no more than 10% of the total samples in the assessment period shall exceed **235 *E.coli* CFU/100 mL** […]."

5. "For beach advisories or closures, a single sample maximum of **235 *E.coli* CFU/100 mL** in freshwater […] shall apply." (VSWCB 2011b)

Of all of the conditions in rivers and streams which can lead to a listing of 'impaired water', the one criterion that, more than any other, results in such a listing is coliform bacteria or *E. coli* abundances (USEPA 2014). Both Hunting Creek and Cameron Run were listed as impaired under the Clean Water Act for exceedances of Virginia's water quality criterion for *E. coli* bacteria (VADEQ, 2012), although the earlier impairment listing of Hunting Creek was based on the then applicable fecal coliform criterion (VADEQ 2010). The fecal coliform criterion was subsequently changed to *E. coli* based on the understanding that this subset of fecal coliforms is more specifically associated with fecal material from humans and other warm-blooded animals. The U.S. EPA (USEPA 2012) recommended and the Commonwealth of Virginia accepted *E. coli* as the better indicator of health risk related to recreational water contact. That is the current microbiological water quality criterion.

Due to this impairment, total maximum daily load (TMDL) allocations for *E. coli* were developed for both of these watersheds in late 2010 (VADEQ 2010). The City of Alexandria is working toward achieving the bacteriological criteria for these waters through a variety of programs including a storm water program, minimizing combined storm water sewer system overflows and eventually eliminating those discharges, reductions in pet waste sources, and discovery of illegal discharges. Because the sources of *E. coli* to water systems are many and varied, including wildlife sources which are generally not controlled unless at a nuisance level, continued monitoring of *E. coli* in these waterways is an important aspect of maintaining and improving water quality. The results reported here add to the understanding of the microbiological quality of these systems.

Methods

Sampling Regime

Samples were collected on 11 dates from 18 April 2018 to 13 September 2018 (**Table EC1**). The approach was to sample on a bimonthly basis in May through September with one sample in April. Water samples were collected at 10 stations on each sampling day. Station identifiers and locations are shown in **Table EC2** (the map of EC sample station is provided in Appendix A, **Figure A1**). Samples were collected in clean, steam sterilized (autoclaved), 4-liter, wide-mouth polypropylene bottles. Eight of the stations were approached from the shore and 4 were sampled from a small, outboard powered research vessel. Stations AR21, AR23, and AR30 were sampled from the shore without wading into the stream. At station AR1, samples were collected remotely using a sterilized, 4-liter round, polypropylene wide-mouth bottle fitted with a harness and nylon

line. The sample bottle was deployed from atop the George Washington Parkway Bridge over Hunting Creek on the downstream side approximately at mid-span. In all cases, the bottles were rinsed twice with sample water and then the final sample was collected. Collection of two shore-approached samples required wading in the streams. At AR12, we waded into the water downstream of the collection site, waited for the current to carry away any disturbed sediment and then collected the sample by submerging the 4-liter bottle upstream of the sample collector. At AR 13, the bottom of the stream at the approach site is paved with concrete. At this site, we waded to approximately midstream and to the edge of the concrete paved segment. After waiting for any disturbed sediment to be washed away, the sampled was collected again by submerging the sterile 4-liter bottle in the stream. Boat-approached sites were sampled by submerging the collection bottles over the side of the research vessel as the vessel coasted on final approach to the station.

Immediately after collection, samples were placed in dark, insulated containers, and packed with ice. Samples were returned to the George Mason University at the Potomac Science Center, where they were processed within about 5 hours of collection.

Analytical Method

Determination of the abundance of *E. coli* was performed following the EPA Method 1603 (*Escherichia coli* in Water by Membrane Filtration Using Modified Membrane-Thermotolerant *Escherichia coli* Agar–Modified mTEC). This is an EPA-approved method for determining abundance of *E. coli* in fresh water. It is a one-step modification of the EPA Method 1103.1. It is based on *E. coli* production of β-D-glucuronidase and the consequent metabolism of 5-bromo-6-chloro-3-indolyl-β-D-glucuronide in the medium to glucuronic acid and a red- or magenta-colored product (USEPA 2009).

Table EC1. Sampling Dates

Date	Date Code for Figures
18-Apr-18	20180418
2-May-18	20180502
16-May-18	20180516
31-May-18	20180531
14-Jun-18	20180614
28-Jun-18	20180628
12-Jul-18	20180712
31-Jul-18	20180731
15-Aug-18	20180815
30-Aug-18	20180830
13-Sep-18	20180913

Table EC2. Station identifiers, locations and access type

Station ID	Access Type	Location Description	Latitude	Longitude
AR 1	Shore	Hunting Cr just above GW Parkway Bridge	38º 47.40' N	77º 03.09' W
AR 2	Boat	Northern portion of Hunting Cr.	38º 47.10' N	77º 02.95' W
AR 3	Boat	Southern portion of Hunting Cr.	38º 46.93' N	77º 02.89' W
AR 4	Boat	Potomac River Channel off Hunting Cr.	38º 46.88' N	77º 02.04' W
AR 10	Boat	Potomac River North of Wilson Bridge	38º 47.65' N	77º 02.34' W
AR 11	Shore	Outlet of Lake Cook – NOT SAMPLED in 2018	38º 48.26' N	77º 05.85' W
AR 12	Shore	Last Riffle of Cameron Run near Beltway crossing	38º 48.11' N	77º 05.07' W
AR 13	Shore	Hoff's Run upstream of Alex renew outfall	38º 48.17' N	77º 03.50' W
AR 21	Shore	South side of Cameron Run downstream from Lake Cook drain	38º 48.19' N	77º 05.73' W
AR 22	Shore	South side of Cameron Run at north end of Fenwick Dr. – NOT SAMPLED in 2018	38º 47.87' N	77º 04.26' W
AR 23	Shore	South side of Cameron Run across from AlexRenew outfall	38º 47.62' N	77º 03.58' W
AR 30	Shore	Cameron Run upstream near metro rail bridge	38º 48.32' N	77º 06.44' W

For this work, mTEC medium (Fisher) was prepared in our laboratory at George Mason University (Potomac Science Center) shortly before each sampling trip. The medium was prepared as per package directions, and ~5 mL of the molten medium was placed aseptically into sterile, 50-mm Petri dishes with tight fitting lids. Prepared medium was stored at 4°C in the dark until use. Phosphate buffered saline (PBS) was prepared as per Method 1603 and autoclave sterilized. PBS was added to smaller samples (1.0 mL and 10 mL) to make volumes up to at least 20 mL before filtration. This aids in distributing bacteria uniformly across the membrane surface. The PBS was also used for blank controls.

Upon return to the laboratory, samples were processed immediately. Sterile, gridded, 0.45 µm membrane filters were aseptically positioned, grid side up, on the base of a sterile, polycarbonate filter holder, and the filter tower was placed in position on a vacuum flask over the filter and base. Samples were shaken vigorously to assure complete mixing and appropriate volumes (1.0 mL, 10.0 mL, and 100.0 mL) of sample were added to each of three replicate filter systems. Before adding the two smaller volume aliquots to the filter funnels, sufficient PBS was added to make the final volume approximately 20 mL. Samples were then filtered with vacuum (approximately 10 in. Hg). Each filter was then removed from the filter holder base aseptically with sterile,

blunt-tipped forceps and placed onto the surface of the mTEC agar without trapping any air bubbles beneath the filter. After replacing the Petri dish tops the plates were incubated in a 35°C incubator for 2 ± 0.5 hours. They were then removed, placed in tightly closed double, zipper-locked plastic bags and submerged in a water bath at 44.5°C ± 0.2°C for 22 ± 2 hours. Blank controls consisting of 100 mL of PBS were checked each time samples were processed. Generally, no *E. coli* were detected in these blank controls, although occasionally controls had one or two presumptive *E. coli* colonies. The data were not corrected for this low background as it was generally far less than 1 percent of the abundances on countable plates.

After the water bath incubation, samples were retrieved and observed immediately for typical red or magenta *E. coli* colonies. All Petri dishes (3 volumes x 3 replicates = 9 Petri dishes per sample) were observed. Although only dilutions yielding colony counts between 20 and 80 needed to be enumerated, we generally recorded colonies for each countable dilution. Often, however, when *E. coli* were abundant, the higher volume samples were not countable due to overgrowth. Calculation of final *E. coli* abundances followed the procedures described in Appendix B of the EPA Method 1603 (USEPA 2009). Since there were triplicate analyses of each dilution, the colony count per Petri dish was separately converted to *E. coli* abundance per 100 mL and then the triplicates were averaged. If no dilution gave individual counts between 20 and 80, the nearest count was selected and used for the final calculation as described in appendix B of the EPA Method 1603.

Results & Discussion

Typical *E. coli* colonies were observed in some dilution in every sample tested. Therefore there is a point estimate of *E. coli* per 100 mL for each. *E. coli* abundances grouped by station are shown in **Figure EC1** and *E. coli* abundances grouped by sampling date are shown in **Figure EC3** (tabular data is in Appendix A, **Table A1** and **A2**).

Since there was no situation in which 4 weekly samples were collected in a calendar month, the 235 per 100 mL (more than 10%) criterion is applicable in determining impairment.

Data Grouped by Station

In 2018, thermotolerant *E. coli* abundances grouped by station exceed the 235 per 100 mL 'impaired water' criterion *at all stations* sometime during the sampling period, as they did in 2015, 2016, and 2017 (**Figure EC1**). This is in contrast to observations made in a prior monitoring campaigns, 2014, when, at 4 of the 8 stations sampled (AR3, AR4, AR10, and AR11), *E. coli* abundances never exceeded 235 per 100 mL. In addition, the majority of the stations sampled throughout the spring and summer 2018 showed exceedance of 325 per 100 mL the majority of the time (8 to 10 of the 11 sampling times): AR1 (9 times), AR12 (9 times), AR13 (10 times), AR21 (9 times), AR23 (9 times), and AR30 (8 times). On the other hand, 4 stations exceeded that value only a

few times (3 to 5 of the 11 sampling times): AR2 (5 times), AR3 (4 times), AR4 (3 times), and AR10 (3 times).

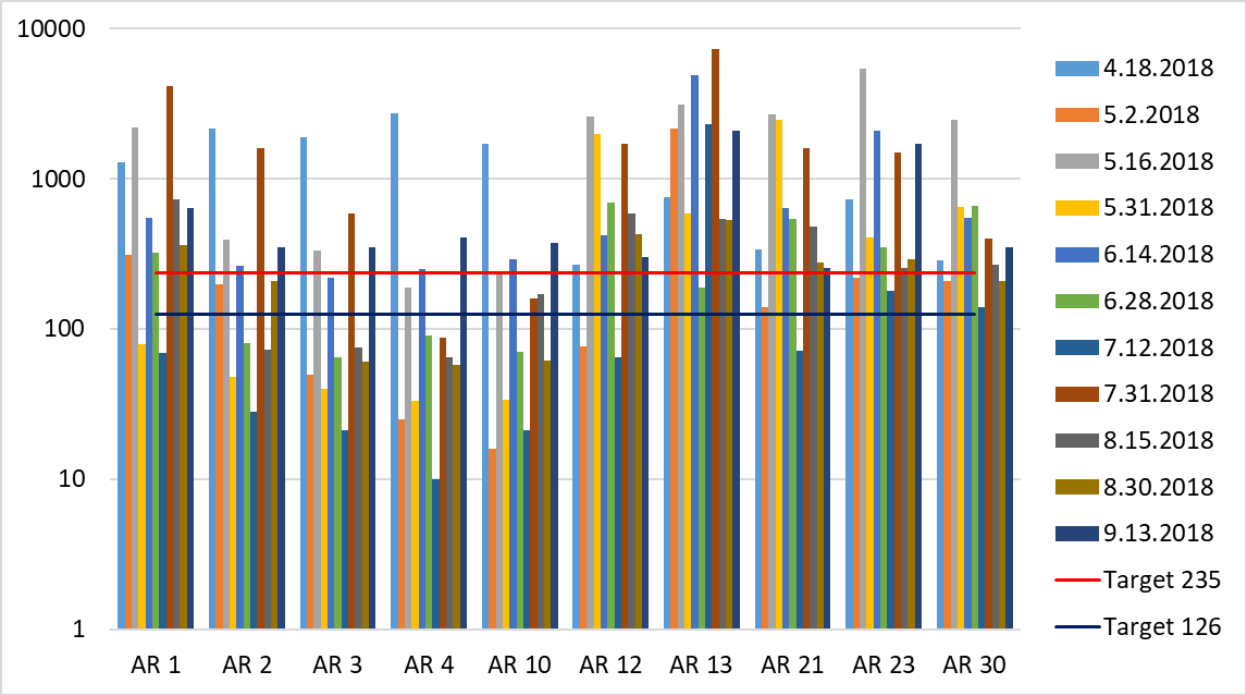

Figure EC1. *E. coli* abundance per 100 mL in Cameron Run, Hunting Creek, and the adjacent Potomac River grouped by stations from April to September 2018. The blue horizontal line represents the *E. coli* criterion for the geometric monthly mean allowable abundance (126 per 100 mL), and the red line represents the criterion for allowable abundance in the absence of four monthly samples (235 per 100 mL).

E. coli abundance at station AR13, Hoff's Run, which exceeded 235 per 100 mL on all 11 dates from April through September in 2015, 2016, and 2017, showed exceedance on 10 dates out the 11 sampled in 2018. *E. coli* abundance at station AR13 averaged 2,230 counts per 100 mL and had a maximum of 7,350 counts per 100 mL on July 31, 2018.

Figure EC2 shows the box plots of *E. coli* numbers per 100 mL as arrayed by site. AR1 is Hunting Creek at the GW Parkway Bridge. AR2 to AR 10 are off-shore stations in the Potomac River (Figure A1): AR2 and AR3 are in the Hunting Creek embayment. AR4 is in the Potomac River channel just east of the Hunting Creek embayment. AR10 is a Potomac River site upstream of the Wilson Bridge. AR21 and AR23 are in tidal Cameron Run, AR 12 and AR30 are in the flowing part of Cameron Run.AR13 is in Hoff's Run, a tributary of Cameron Run, **Figure EC2** reveals the large variability of the numbers recorded at each station, with extremes spanning several orders of magnitude. As in 2018, the highest *E. coli* numbers on average were observed in AR13, Hoff's Run. The lowest numbers were the off-shore stations in the Potomac River, AR2, AR3, AR4, and AR10. Values at AR1 and AR23, which were both directly impacted by the AlexRenew outfall showed the second highest numbers. Interestingly AR21, which was above tidal influence, had rather high numbers as well, perhaps due to runoff from the

Lake Cook area. The farthest upstream station, AR30, was relatively low but somewhat higher than the embayment-river stations.

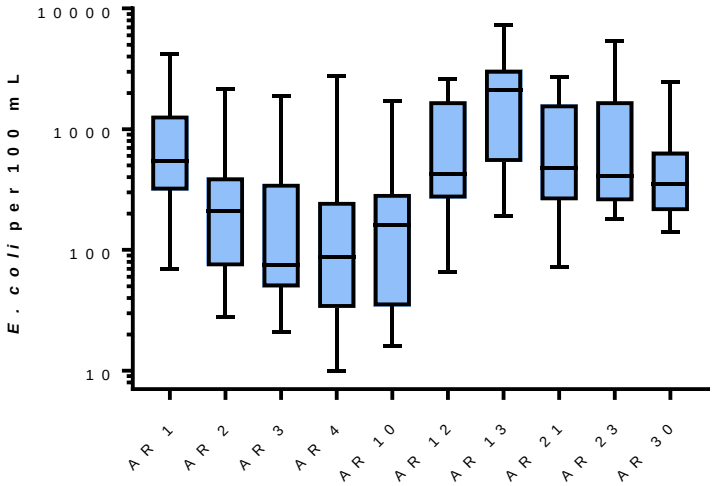

Figure EC2. Box plots of *E. coli* abundance per 100 mL for each site in Cameron Run, Hunting Creek, and the adjacent Potomac River over the sampling period. The bars show the minimum and maximum counts, the boxes show the 25 and 75-percentile, and the median.

Data Grouped by Date

E. coli abundance grouped by dates showed that environmental and/or climatic conditions may have played on important role on some sampling dates, resulting in exceedance of the 235 per 100 mL at the large majority of stations (8 to 10 of the 10 sampling stations, **Figure EC3**): April 18 (10 stations), May 16 (9 stations), June 14 (9 stations), July 31 (8 stations), and September 13 (10 stations). These are also the dates when the average precipitation exceeded 0.4 cm (an exception is May 31, where the precipitation was 0.5 cm with exceedance at only 4 stations). The two dates with the highest flow (> 0.7 cm), April 18 and September 13 were also the only ones where exceedances were observed at all 10 stations. In fact, a good correlation (Pearson's correlation coefficient, r = 0.77) was observed between precipitation and average *E. coli* abundance at all sites (**Figure EC4**). The same pattern can be seen from the box plots of *E. coli* numbers per 100 mL arrayed by date (**Figure EC5**).

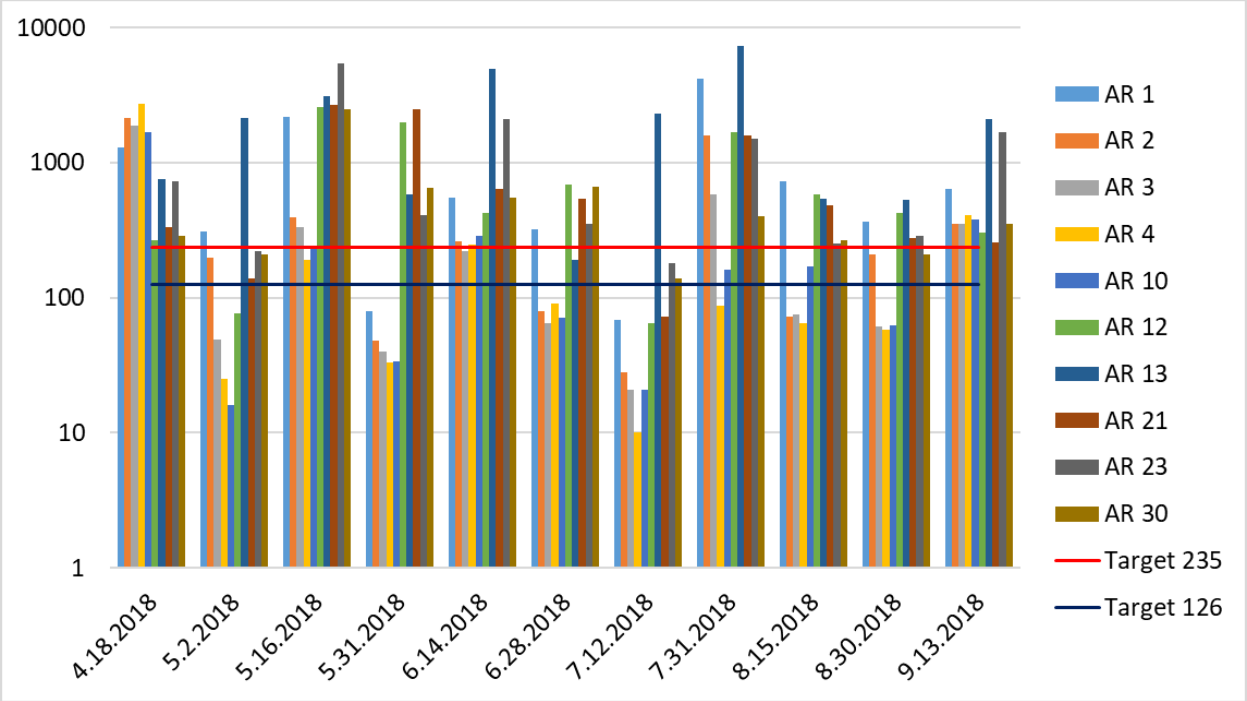

Figure EC3. *E. coli* abundance per 100 mL in Cameron Run, Hunting Creek, and the adjacent Potomac River grouped by sampling dates for all stations. The blue horizontal line represents the *E. coli* criterion for the geometric monthly mean allowable abundance (126 per 100 mL), and the red line represents the criterion for allowable abundance in the absence of four monthly samples (235 per 100 mL).

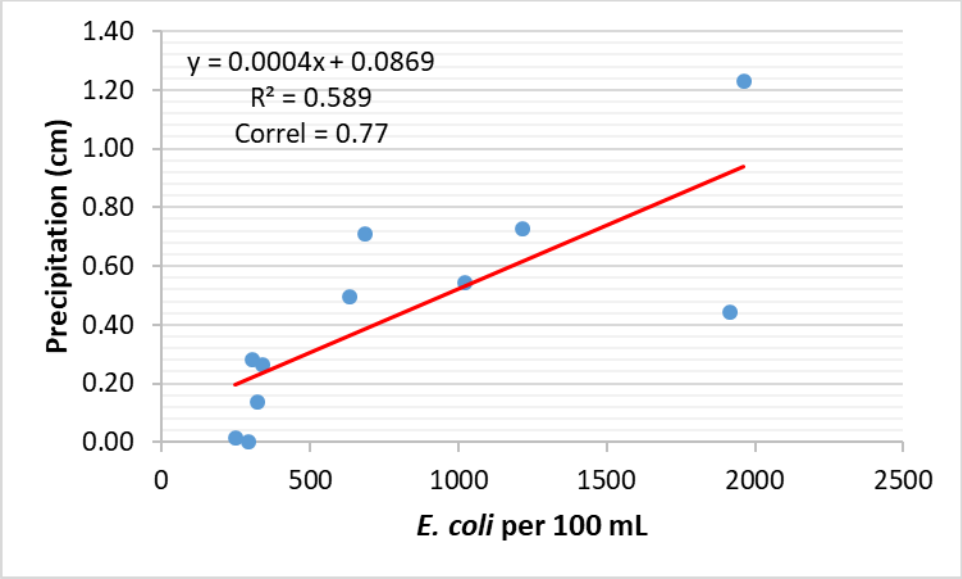

Figure EC4. Relationship between the mean *E. coli* per 100 mL and the precipitation for each sampling date in Cameron Run, Hunting Creek, and the adjacent Potomac River.

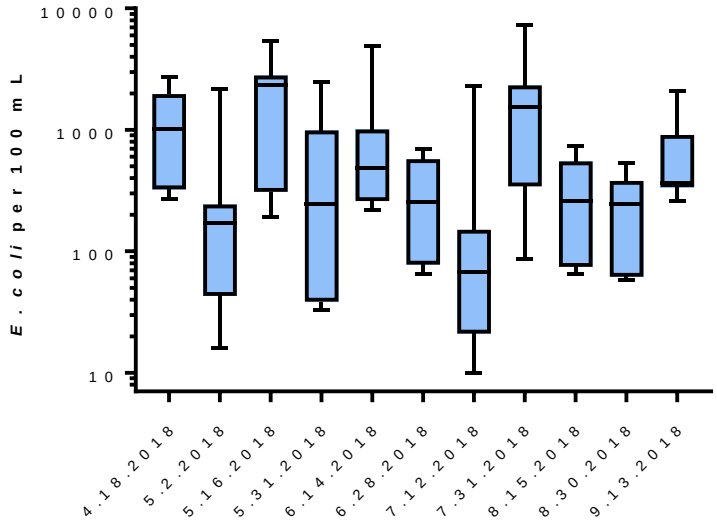

Figure EC5. Box plots of *E. coli* abundance per 100 mL for each site in Cameron Run, Hunting Creek, and the adjacent Potomac River over the sampling period. The bars show the minimum and maximum values, the boxes show the 25 and 75-percentile, and the median.

Temporal Trends

Although the number of stations and sampling events have increased since 2014 (8 sites and 6 sampling times in 2014, 8 sites and 11 sampling times in 2015, 12 sites and 11 sampling times in 2016 and 2017, and 10 sites and 11 sampling times in 2018), we present here a timeline of changes in the percentage of samples that exceeded the 235 per 100 mL standard (**Figure EC6**). Even though over the period 2014 – 2017, this trend globally suggested increasing exceedances of the 235 per 100 mL standard (as mentioned in the 2017 Final Report), examination of the *E. coli* abundances per 100 mL over the period 2014 – 2018 does not indicate any worsening of the conditions (**Figure EC7**).

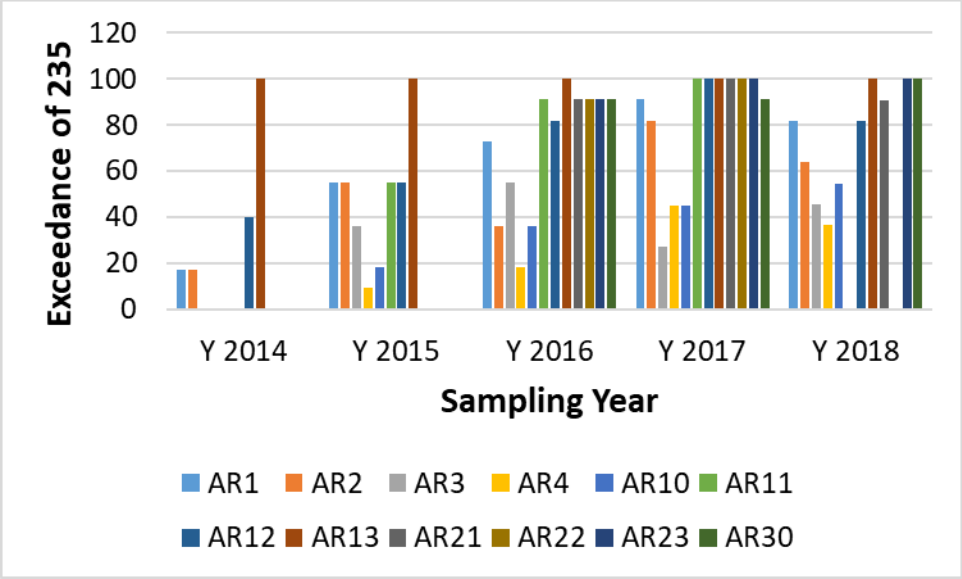

Figure EC6: Percentage of sample event when *E. coli* abundances exceeded 235 per 100 mL in year 2014, 2015, 2016, 2017, and 2018. Samples were collected 6 times during 2014, whereas in each of the subsequent years, samples were collected 11 times.

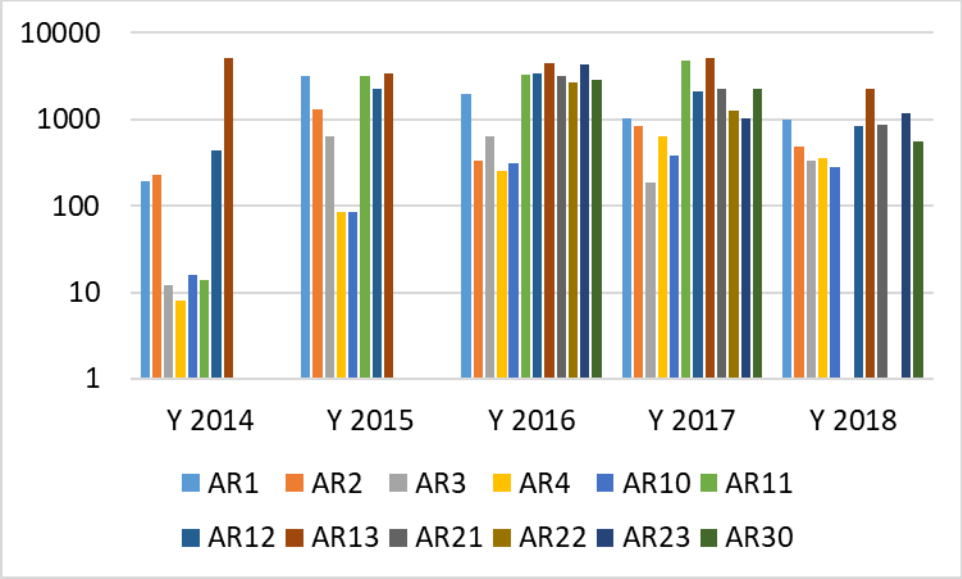

Figure EC7: *E. coli* abundances per 100 mL in year 2014, 2015, 2016, 2017, and 2018. Samples were collected 6 times during 2014, whereas in each of the subsequent years, samples were collected 11 times.

CONCLUSIONS:

The data continue to support a conclusion that the entire area sampled, including the mainstem of the Potomac River (AR4), is impaired for the bacteriological water quality criterion (*E. coli*) content under Section 9VAC25-260-170 of the Virginia Water Quality Standards that applies to primary contact recreational use surface waters. Although our

data showed an increase of the *E. coli* abundance and percent exceedance of the 235 criterion from 2014 to 2016, these numbers seemed to have peaked in 2016 – 2017 and even showed a slight decrease in 2018.

It is noteworthy that the large geographical and temporal variability that we observed during the sampling events prevent to draw clear conclusion on the trend of water quality impairment.

Finally, the highest counts in 2018 were observed in April and September (the highest counts in 2017 were observed in June and July), revealing no clear seasonal trend in the data. High counts were shown to reflect rainfall data instead of a seasonal trend.

Literature Cited

U.S. Environmental Protection Agency (USEPA). 2009. Method 1603: *Escherichia coli* (*E. coli*) in Water by Membrane Filtration Using Modified membrane-Thermotolerant *Escherichia coli* Agar (Modified mTEC). Available at: < http://water.epa.gov/scitech/methods/cwa/bioindicators/> search Method 1603, December 2009.

U.S. Environmental Protection Agency (USEPA). 2012. Water: Monitoring & Assessment: 5.11 Fecal Bacteria. Available at: http://water.epa.gov/type/rsl/monitoring/vms511.cfm

U.S. Environmental Protection Agency (USEPA). 2014. National Water Quality Assessment Report, water Quality Assessment and Total Maximum Daily Loads Information. Available at: <http://ofmpub.epa.gov/waters10/attains_index.control>

Virginia Department of Environmental Quality (VADEQ). 2010. Bacteria TMDLs for the Hunting Creek, Cameron Run, and Holmes Run Watersheds. Available at: <deq.state.va.us>

Virginia Department of Environmental Quality (VADEQ). 2012. 2012 Impaired Waters: Category 4 & 5 by Basin and Stream Name, Potomac and Shenandoah River Basins, Cause Group Code: A13R-03-BAC - Cameron Run/Hunting Creek. Available at: <http://www.deq.virginia.gov/Programs/Water/WaterQualityInformationTMDLs/WaterQualityAssessments.aspx>

Virginia. *State Water Control Board* (VSWCB). 2011. 9 VAC 25-260-10 Designation of uses. Virginia Water Quality Standards. Available at: <http://lis.virginia.gov/cgi-bin/legp604.exe?000+reg+9VAC25-260-10>

Virginia. *State Water Control Board* (VSWCB). 2011b. 9 VAC 25-260-170 Bacteria; other recreational waters. Virginia Water Quality Standards. Available at:

<http://lis.virginia.gov/cgi-bin/legp604.exe?000+reg+9VAC25-260-170>

Appendix A

Figure A1. Maps of sample sites

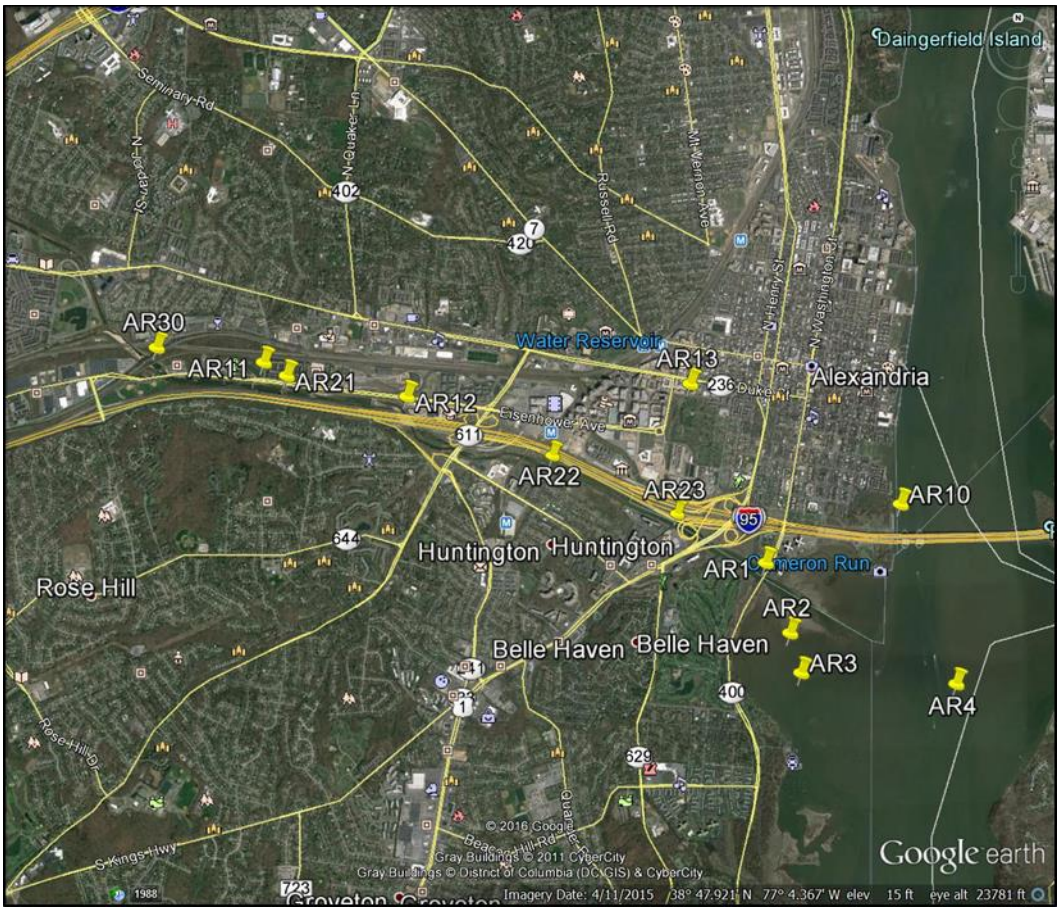

Table A1. 2018 *E. coli* abundances per 100 mL for all station, all sampling dates.

Date	Sites	E. coli per 100 mL	Date	Sites	E. coli per 100 mL	Date	Sites	E. coli per 100 mL
4/18/2018	AR1	1300	6/14/2018	AR1	547	8/15/2018	AR1	730
	AR2	2150		AR2	263		AR2	73
	AR3	1900		AR3	220		AR3	75
	AR4	2750		AR4	250		AR4	65
	AR10	1700		AR10	290		AR10	170
	AR11	No data		AR11			AR11	
	AR12	267		AR12	423		AR12	585
	AR13	750		AR13	4933		AR13	537
	AR21	337		AR21	640		AR21	480
	AR22	No data		AR22			AR22	
	AR23	725		AR23	2100		AR23	253
	AR30	285		AR30	550		AR30	267
	Control	1		Control	2		Control	0
5/2/2018	AR1	310	6/28/2018	AR1	323	8/30/2018	AR1	363
	AR2	200		AR2	80		AR2	210
	AR3	49		AR3	65		AR3	61
	AR4	25		AR4	90		AR4	58
	AR10	16		AR10	71		AR10	62
	AR11	No data		AR11			AR11	
	AR12	77		AR12	693		AR12	427
	AR13	2150		AR13	190		AR13	530
	AR21	140		AR21	540		AR21	277
	AR22	No data		AR22			AR22	
	AR23	220		AR23	350		AR23	290
	AR30	210		AR30	663		AR30	210
	Control	1		Control	0		Control	0
5/16/2018	AR1	2200	7/12/2018	AR1	69	9/13/2018	AR1	640
	AR2	397		AR2	28		AR2	350
	AR3	333		AR3	21		AR3	353
	AR4	190		AR4	10		AR4	410
	AR10	233		AR10	21		AR10	377
	AR11			AR11			AR11	
	AR12	2600		AR12	65		AR12	303
	AR13	3100		AR13	2300		AR13	2100
	AR21	2700		AR21	72		AR21	257
	AR22			AR22			AR22	
	AR23	5400		AR23	180		AR23	1700
	AR30	2467		AR30	140		AR30	353
	Control	1		Control	0		Control	1
5/31/2018	AR1	79	7/31/2018	AR1	4167			
	AR2	48		AR2	1600			
	AR3	40		AR3	587			
	AR4	33		AR4	87			
	AR10	34		AR10	160			
	AR11			AR11				
	AR12	2000		AR12	1700			
	AR13	587		AR13	7350			
	AR21	2467		AR21	1600			
	AR22			AR22				
	AR23	410		AR23	1500			
	AR30	650		AR30	403			
	Control	1		Control	0			

Table A2. Mean of *E. coli* abundances per 100 mL, seasonal means and standard deviations and percent exceedances of 235 criteria.

Station	Seasonal Mean	Seasonal St. Dev.	Percent Exceedance 126	Percent Exceedance 235
AR1	975	1225	82	82
AR2	491	706	64	64
AR3	337	549	45	45
AR4	361	801	36	36
AR10	285	484	55	55
AR11				
AR12	831	861	82	82
AR13	2230	2216	100	100
AR21	864	945	91	91
AR22				
AR23	1193	1552	100	100
AR30	563	656	100	100